

Ventricular arrhythmogenesis in the genetically-susceptible heart

Citation for published version (APA):

ter Bekke, R. M. A. (2018). *Ventricular arrhythmogenesis in the genetically-susceptible heart: time to change concepts of mechanisms and management*. [Doctoral Thesis, Maastricht University]. <https://doi.org/10.26481/dis.20180622rb>

Document status and date:

Published: 01/01/2018

DOI:

[10.26481/dis.20180622rb](https://doi.org/10.26481/dis.20180622rb)

Document Version:

Publisher's PDF, also known as Version of record

Please check the document version of this publication:

- A submitted manuscript is the version of the article upon submission and before peer-review. There can be important differences between the submitted version and the official published version of record. People interested in the research are advised to contact the author for the final version of the publication, or visit the DOI to the publisher's website.
- The final author version and the galley proof are versions of the publication after peer review.
- The final published version features the final layout of the paper including the volume, issue and page numbers.

[Link to publication](#)

General rights

Copyright and moral rights for the publications made accessible in the public portal are retained by the authors and/or other copyright owners and it is a condition of accessing publications that users recognise and abide by the legal requirements associated with these rights.

- Users may download and print one copy of any publication from the public portal for the purpose of private study or research.
- You may not further distribute the material or use it for any profit-making activity or commercial gain
- You may freely distribute the URL identifying the publication in the public portal.

If the publication is distributed under the terms of Article 25fa of the Dutch Copyright Act, indicated by the "Taverne" license above, please follow below link for the End User Agreement:

www.umlib.nl/taverne-license

Take down policy

If you believe that this document breaches copyright please contact us at:

repository@maastrichtuniversity.nl

providing details and we will investigate your claim.

Ventricular Arrhythmogenesis in the Genetically-Susceptible Heart:

Time to Change Concepts of Mechanisms and Management



Rachel ter Bekke

VENTRICULAR ARRHYTHMOGENESIS IN THE GENETICALLY-SUSCEPTIBLE HEART:

TIME TO CHANGE CONCEPTS OF
MECHANISMS AND MANAGEMENT

PROEFSCHRIFT

ter verkrijging van de graad van doctor
aan de Universiteit Maastricht,
op gezag van de Rector Magnificus,
Prof. dr. Rianne M. Letschert
volgens het besluit van het College van Decanen,
in het openbaar te verdedigen
op vrijdag 22 juni 2018 om 14.00 uur

door

Rachel Mariet Anouk ter Bekke

Promotor

Prof. dr. P.G.A. Volders

Beoordelingscommissie

Prof. dr. H.J.G.M. Crijns (voorzitter)

Prof. dr. C.R. Bezzina (Universiteit van Amsterdam)

Prof. dr. F.W. Prinzen

Prof. dr. P.J. Schwartz (IRCCS Istituto Auxologico Italiano, Milaan, Italië)

Prof. dr. H.J.J. Wellens

The research in this thesis was supported by a grant of the Dutch Heart Foundation/ The Netherlands CardioVascular Research Initiative (CVON-PREDICT). Additional research support by the Health Foundation Limburg is gratefully acknowledged. The Dutch Heart Foundation also contributed to the printing costs of this thesis. I also thank the Stichting Hartsvrienden RESCAR for a financial contribution the publication of this thesis.

© Rachel M.A. ter Bekke, 2018

ISBN 978-94-6159-821-9



Cover art and design: Claudia Volders and Rachel ter Bekke

*For all families including mine:
Jade, Myrthe, Inez, Marga, Frans, and Esther*

CONTENTS

CHAPTER 1		1
	Introduction.	
CHAPTER 2		21
	Arrhythmogenic Mechano-Electric Heterogeneity in the Long-QT Syndrome. Rachel M.A. ter Bekke, Paul G.A. Volders <i>Prog Biophys Mol Biol</i> 2012;110:347-358	
CHAPTER 3		41
	Electromechanical Window Negativity in Genotyped Long-QT Syndrome Patients: Relation to Arrhythmia Risk. Rachel M.A. ter Bekke, Kristina H. Haugaa, Arthur van den Wijngaard, J. Martijn Bos, Michael J. Ackerman, Thor Edvardsen, Paul G.A. Volders <i>Eur Heart J</i> 2015;36:179-186	
	Editorial	59
	Vox Clamantis in Deserto. We Spoke but Nobody was Listening: Echocardiography can help Risk Stratification of the Long-QT Syndrome. Gaetano M. De Ferrari, Peter J. Schwartz <i>Eur Heart J</i> 2015;36:148-150	
CHAPTER 4		65
	Proarrhythmic Proclivity of Left-Stellate Ganglion Stimulation in a Canine Model of Drug-Induced Long-QT Syndrome Type 1. Manuscript submitted, 2018	
CHAPTER 5		83
	Heritability in a <i>SCN5A</i> -Mutation Founder Population with Female Susceptibility to Non-Nocturnal Ventricular Tachyarrhythmia and Sudden Cardiac Death. Rachel M.A. ter Bekke, Aaron Isaacs, Andrei Barysenka, Marije B. Hoos, Jan D.H. Jongbloed, Jan C.A. Hoorntje, Alfons S.M. Patelski, Apollonia T.J.M. Helderma-van den Enden, Arthur van den Wijngaard, Monika Stoll, Paul G.A. Volders <i>Heart Rhythm</i> 2017;14:1873-1881	

Editorial	103
Founder Populations with Channelopathies and Church Records Reveal All Sorts of Interesting Secrets: Some are Scientifically Relevant. Peter J. Schwartz and Lia Crotti <i>Heart Rhythm</i> 2017;14:1882-1883	
CHAPTER 6	107
Beauty and the Beat: A Complicated Case of Multifocal Ectopic Purkinje-Related Premature Contractions. Manuscript accepted for publication in <i>Heart Rhythm Case Reports</i>	
CHAPTER 7	119
Life-Threatening Ventricular Arrhythmias in the Genetically-Susceptible Heart: Time to Change Concepts.	
CHAPTER 8	141
HeArt Project. Rachel M.A. ter Bekke, Claudia A.A. Volders Manuscript accepted for publication in <i>Tijdschrift voor Gezondheidswetenschappen</i>	
SUMMARY/SAMENVATTING	153
VALORIZATION	157
REFERENCES	163
GENEALOGICAL SOURCES	195
LIST OF ABBREVIATIONS	203
ACKNOWLEDGEMENTS/DANKWOORD	207
CURRICULUM VITAE	213



"Le cœur a ses raisons que la raison ne connaît pas"

1

INTRODUCTION

CONTENTS

GENETIC PREDISPOSITION TO SUDDEN CARDIAC DEATH	2
Genetic Susceptibility to Sudden Cardiac Death	3
Infarct-Related Ventricular Fibrillation	4
Inherited Arrhythmia Syndromes	5
Drug-Induced Repolarization Prolongation	6
Genetic Modulators of Disease Variability	6
ARRHYTHMIA MECHANISMS	7
LQTS: A Purely Electrical Disease?	7
Arrhythmogenic Role of Purkinje Fibers	9
Brugada Syndrome: Depolarization or Repolarization?	10
VENTRICULAR ARRHYTHMOGENESIS AND THE AUTONOMIC NERVOUS SYSTEM	10
THERAPEUTIC AVENUES	12
Antiarrhythmic Drugs	12
Interventional Modalities	13
AIMS AND STRUCTURE OF THIS THESIS	14

GENETIC PREDISPOSITION TO SUDDEN CARDIAC DEATH

One early morning in June 2017, in a home nearby Maastricht, The Netherlands, a father heard a snoring sound in the corridor while traversing to the bathroom. Startled by this peculiar noise, but still somewhat drowsy, he checked on his sleeping daughter, who was well. Two hours later his other child, the apparently healthy 29-year-old son, was found dead in his bed. A stilling “why” is what remains amongst the relatives, and a deafening call to health-care providers concerned with the topic of sudden cardiac death.

As exemplified by this case, sudden death is defined as an unexpected, non-traumatic fatal event occurring within one hour of the onset of symptoms in an apparently healthy subject.¹ A cardiac origin is suspected if a potentially fatal cardiac condition was known to be present, when autopsy has indicated a cardiac anomaly as the probable cause of the event or no obvious extra-cardiac causes have been identified by post-mortem examinations with fatal arrhythmia being the likely cause of death.¹

Sudden cardiac death (SCD) imposes a sizable socioeconomic and psychosocial burden, claiming almost a million deaths annually in Western Europe and the United States. It accounts for 15-20% of all natural deaths and up to 50% of all cardiovascular deaths.^{2,3} Out-of-hospital SCD occurs with a yearly incidence of 39-100 per 100,000 individuals aged 20-75 years in the Netherlands.^{4,5} In the Dutch province of Limburg SCA affects approximately 15 individuals per week.⁶ Once SCA ensues, the victim’s survival rate declines at a rapid pace (8-10% per minute),⁷ prompting urgent attempts to rescue the subject by cardiopulmonary resuscitation, preferably with community-available automated external defibrillators (AEDs) utilized by trained volunteers.

Ventricular fibrillation (VF) mostly underlies SCD and usually occurs in the setting of coronary heart disease and myocardial ischemia (~75%).^{3,8,9} However, SCD is the first manifestation of heart disease in approximately 45% of cases.⁴ Inherited arrhythmia syndromes predispose to VF, accounting for 5-10% of total VF victims, relatively often in the young.¹⁰ These primary electrical arrhythmia syndromes comprise of the long-QT syndrome (LQTS), Brugada syndrome, catecholaminergic polymorphic ventricular tachycardia (CPVT), short-QT syndrome (SQTS), short-coupled torsades de pointes (TdP), early-repolarization syndrome (ERS), and other rare conditions. In <5% of VF cases no cardiac structural or electrical abnormalities can be ascertained; this is referred to as “idiopathic VF”.

In this thesis, I will focus on life-threatening ventricular tachyarrhythmias, including VF, in the structurally-normal, but electrically-compromised heart. I will investigate genotype-phenotype relations, assess novel SCD risk indicators, evaluate triggers of arrhythmia, and discuss antiarrhythmic treatment. Special emphasis will be put on electromechanical interrelations and the influence of the autonomic nervous system. These aspects are examined mainly in the long-QT syndrome, Brugada syndrome, and multifocal ectopic Purkinje-related ectopy. The gained insights into ventricular arrhythmogenesis and treatment will ultimately also benefit patients with scar-related ventricular arrhythmia, which is typically characterized by a more heterogeneous structural substrate.

GENETIC SUSCEPTIBILITY TO SUDDEN CARDIAC DEATH

SCD has a complex, multifactorial nature and usually depends on a combination of acquired (e.g., myocardial ischemia or scar formation) and heritable components, modified by external/environmental factors. The segregation of SCD in families¹¹ implicates the importance of heritable factors for the development of life-threatening ventricular arrhythmia, both in primary arrhythmia syndromes and in the presence of myocardial ischemia. Generally, the younger the SCD victim, the higher the contribution of genetic components (**Figure 1.1**). Besides genetic variation, phenotypic expression can be modified by DNA phosphorylation, glycosylation, or lipidation. However, such epigenetic or posttranslational modifications are rarely addressed clinically. Lifestyle and environmental modulators of disease expressivity, e.g., smoking, obesity, sedentary habitus, and dietary intake, are of great importance but fall beyond the scope of this dissertation.

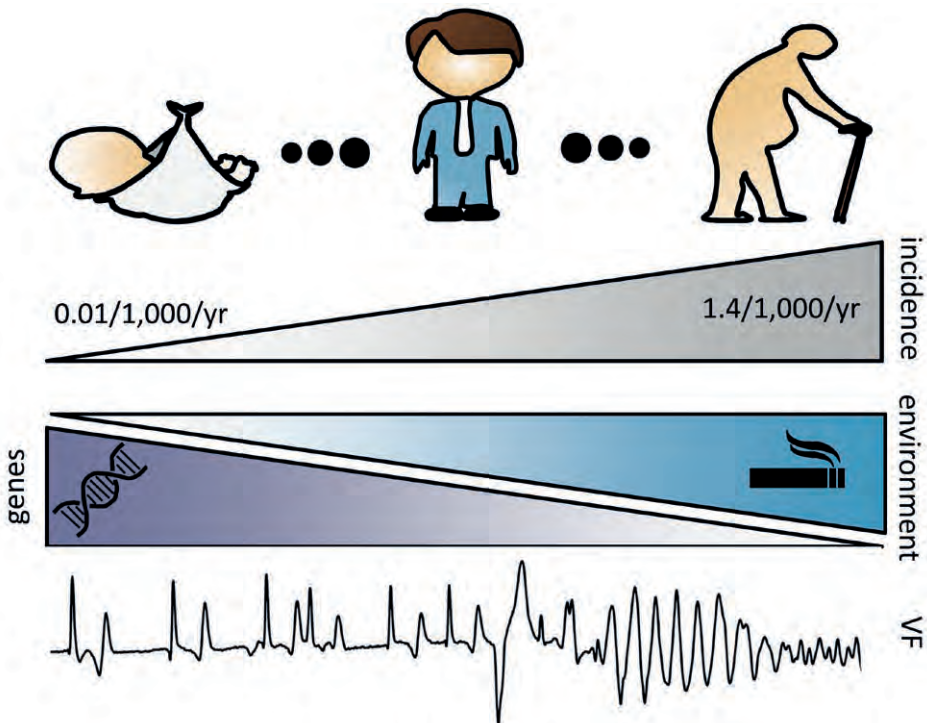


Figure 1.1 Schematic representation of the relative contribution of genetic and environmental risk factors to the vulnerability to VF over a person's life span.

Primary electrical arrhythmia syndromes are typically characterized by an autosomal dominant inheritance pattern. Rare genetic variants with large effect size can be encountered. The annotation “disease-causing genetic variants” applies here. Oligogenic modes of inheritance are recognized in Brugada syndrome,¹² with causal *SCN5A* mutations

implicated in only a quarter of patients. Even more complex inheritance patterns are suggested to contribute to SCD susceptibility in (late onset) coronary-artery disease associated VF,¹³ where common allelic variation only exerts a moderate effect size.¹⁴ Analytical approaches to unmask these different genetic variants should be adapted accordingly: linkage analysis and exome/genome sequencing, combined with smart bioinformatics, are suitable approaches for common and rare diseases related to rare genetic variants. Common genetic variants are currently identified using genome-wide association studies (GWAS) on large numbers of patients.¹⁵

The identification of genetic contributors is important for diagnostic purposes, risk stratification of the index patients and their relatives, elucidation of molecular pathways, and to find potential therapeutic targets. Unfortunately, limited sample sizes of representative populations, heterogeneity of the arrhythmogenic substrate, and the difficulty of obtaining phenotypic information after cardiac arrest complicate scientific progress in this field. Founder populations with increased SCD susceptibility that share an identical-by-descent mutation are gold mines for identification of genetic modifiers¹⁶ as they are robust to false-positive findings due to the population substructure, they typically share a large proportion of environmental factors, and they may be enriched for rare variants that are difficult to study in the general population.

INFARCT-RELATED VENTRICULAR FIBRILLATION

The strong familial component to SCD risk in the presence of coronary artery disease^{8, 11, 17, 18} has sparked several groups to investigate associations between postulated electrocardiographic markers of augmented SCD risk (e.g., QTc, QRS width) and common genetic variants using GWAS in large populations. As QTc prolongation constitutes a higher arrhythmic risk in acute coronary syndromes^{19, 20} and heritability of QT/QTc approximates 35%,²¹⁻²⁶ it was postulated that genetic variants affecting QT are associated with ischemia-related SCD.

Genome-wide association signals were found between prolonged cardiac repolarization and variants in *NOS1AP*, a gene that encodes the nitric oxide synthase 1 adaptor protein.^{27, 28} These variants were associated with SCD in Caucasian US adults,²⁹ findings that were confirmed by the Rotterdam study.³⁰ Also, a polymorphism in the *KCNH2* gene (p.(Lys897Thr), rs1805123), encoding the alpha subunit of the rapidly-activating delayed-rectifier potassium current (I_{Kr}) and affecting QTc duration,³¹ has been associated with polymorphic ventricular tachycardia (VT) in the subacute phase of myocardial infarction.³² Furthermore, a common genetic variant in the *SCN5A* gene (p.(Ser1101Tyr), rs7626962) has been associated with arrhythmia risk in African-Americans (OR = 8.7; 95% C.I. 3.2–23.9; $P=0.001$), especially if co-occurring with additional arrhythmia risk factors.³³ Other rare *SCN5A* mutations were identified exclusively in women with SCD in two large prospective cohorts (Nurses' Health Study and Health Professional Follow-Up Study).³⁴ And finally, a genome-wide significant signal was found at 2q24.2 (rs4665058) near the *BAZ2B* gene, which almost doubled the SCD risk (OR = 1.92, 95% C.I. 1.57-2.34, $P=1.8 \times 10^{-10}$).³⁵

Alternatively, but more tediously, attempts have been made to directly associate genetic loci to infarct-related primary VF in well-defined SCD cohorts. The Arrhythmia Genetics in the Netherlands Study (AGNES) identified a common genetic variant at 21q21 (rs2824292) near the *CXADR* gene that was associated with primary VF (OR = 1.78, 95% C.I. 1.47-2.13, $P=3.3 \times 10^{-10}$).³⁶ The *CXADR* gene encodes the coxsackie- and adenovirus receptor and has been implicated in reduced cardiac conduction properties and increased arrhythmia vulnerability during ischemia in *CXADR* haploinsufficient mice.³⁷ Clinical replication studies, however, failed to confirm the association of rs2824292 with VF in first infarct patients.^{38, 39} In the Genetics Causes of Ventricular Arrhythmias in Patients with First ST-elevation Myocardial Infarction (GEVAMI) cohort, a single nucleotide polymorphism (SNP) at chromosome 3 (rs11720524) in intron 1 of the *SCN5A* gene was significantly associated with arrhythmic events (OR = 1.87, 95% C.I. 1.12-3.12, $P=0.017$).⁴⁰ In conclusion, the inherited susceptibility to VF in the setting of myocardial ischemia/infarction justifies the quest for risk loci, but is not yet ready for clinical implementation.

INHERITED ARRHYTHMIA SYNDROMES

Numerous gene variants have been related to the primary arrhythmia syndromes like LQTS, Brugada syndrome, ERS, CPVT, short-coupled TdP and idiopathic VF. Inheritance is usually Mendelian and genetic approaches mostly rely on family-based studies. Although recently, GWAS meta-analysis identified 35 common variant QT-associated SNPs in genetically elusive LQTS subjects.²⁸ This provides exciting novel insights into arrhythmogenesis and brings forward new candidate genes for ventricular arrhythmias.²⁸

The long-QT syndrome constitutes the most paradigmatic example of inherited arrhythmia diseases. Prolonged and dispersed ventricular repolarization predisposes to torsades-de-pointes arrhythmias. Since the first association of LQTS with the Harvey *ras-1* locus to in 1991,⁴¹ allelic variants in at least 15 LQTS-susceptibility genes have been described (**Table 1.1**). Three major causative LQTS-susceptibility genes encoding ion-channel alpha subunits explain approximately 75% of clinically-diagnosed LQTS cases:¹ *KCNQ1*, encoding the alpha subunit of the slowly-activating delayed-rectifier potassium current (I_{Ks}) was recognized for LQT1;⁴² *KCNH2* encoding for I_{Kr} for LQT2;⁴³ *SCN5A* encoding for pore-forming alpha subunit of the cardiac sodium channel ($Na_v1.5$) for LQT3.⁴⁴ Other minor LQTS-associated genes encode for 1) the alpha subunit of G protein-activated inward rectifier potassium current 4, *KCNJ5*, which is implicated in LQT13,⁴⁵ 2) for cardiac potassium- or sodium-channel interacting proteins: *KCNE1* (LQT5),⁴⁶ *KCNE2* (LQT6),⁴⁷ *AKAP9* (LQT11),⁴⁸ and *CAV3* (LQT9),⁴⁹ *SCN4B* (LQT10),⁵⁰ and *SNTA1* (LQT12),⁵¹ respectively. Finally, 3) calmodulin-associated LQT syndrome allocated to the *CALM1* (LQT14) or the *CALM2* gene (LQT15).⁵² Other multisystem disorders displaying concomitant repolarization prolongation and ventricular arrhythmia were linked to *ANKB* (ankyrin-B syndrome previously LQT4),^{53, 54} *KCNJ2* (Andersen-Tawil syndrome previously LQT7),⁵⁵ and *CACNA1C* (Timothy syndrome previously LQT8).⁵⁶

Prominent phenotypic heterogeneity including SCD susceptibility has been observed among LQTS patients sharing an identical-by-descent mutation. Low disease penetrance (~25%), differential expressivity, and non-genetic factors such as age, gender, and the use of medication⁵⁷⁻⁶⁰ have been postulated to contribute to this phenotypic variability. Furthermore, compound heterozygosity is present in ~8% of LQTS cases, hinting towards a more complex genetic architecture.⁶¹

The *SCN5A* gene encodes the pore-forming alpha subunit of the cardiac sodium channel. Loss-of-function mutations in the *SCN5A* gene resulting in a reduced sodium current (I_{Na}) have been causally related to Brugada syndrome in ~20-25% of cases (**Table 1.2**).⁶² Although the Brugada syndrome is considered to be a monogenic disorder by some, with an autosomal dominant mode of inheritance, disease penetrance is considerably low⁶³ and sometimes the causative *SCN5A* mutation does not segregate in affected family members with the syndrome,⁶⁴ indicating a more complex genetic architecture. The unraveling of such complex architecture in a familial cohort with a *SCN5A* founder mutation and excess sudden arrhythmic death will be one of my PhD studies. In other conditions, like Purkinje-related ectopy, atrial fibrillation, sick-sinus syndrome, dilated cardiomyopathy, and cardiac conduction disease, *SCN5A* mutations have also been implicated.

Idiopathic VF is a rare SCD entity where fibrillation occurs in the absence of an identifiable cause despite extensive cardiac work-up.⁶⁵ A familial history of sudden cardiac death or resuscitated arrest is noted in ~20% of cases, suggesting a genetic substrate in some.⁶⁶ **Table 1.3** summarizes genes and risk haplotypes involved in idiopathic VF, as currently known. Also mentioned are the reported genes associated with short-coupled TdP: *CALM1* (c.268T>C, p.(Phe90Leu), rs730882253)⁶⁷ and *RyR2*.⁶⁸ Allelic variants associated with the short-QT syndrome, CPVT, and ERS are listed in **Table 1.4**.

DRUG-INDUCED REPOLARIZATION PROLONGATION

Genetic susceptibility to drug-induced LQTS, potentially leading to TdP, can be identified in 5-19% of patients with acquired QT prolongation.^{69, 70} Mostly, genetic variants of known arrhythmia genes play a role in this.⁶⁹⁻⁷² For example, the variant in *KCNE1*, p.(Asp85Asn) rs1805128, increases the risk of drug-induced TdP nearly 9-fold (95% C.I. 3.26–24.17; $P=1.95 \times 10^{-5}$).⁷³ The mean allelic frequency of *KCNE1*-p.(Asp85Asn) is approximately 1-2% in healthy Caucasians^{69, 73} but this variant is enriched in LQTS probands (4%).⁷⁴ In addition, common variants in the *NOS1AP* gene have been associated with QT prolongation during treatment with verapamil, sotalol, amiodarone, and diuretics.^{75, 76} GWAS analysis of sotalol-, amiodarone-, and quinidine-induced TdP, however, failed to identify common variants with large enough effect sizes.⁷⁷

GENETIC MODULATORS OF DISEASE VARIABILITY

Phenotypic diversity (including SCD susceptibility) among carriers of identical-by-descent mutations is often remarkable.⁵⁷ Common genetic variants other than the high-impact familial mutation, also termed ‘modifier genes’, can modulate disease variability. Multiple

LQTS-associated modifier genes have been identified: *KCNQ1* (rs8234, rs10798, rs199473403),^{78, 79} 3' untranslated region of *KCNQ1* (rs2519184, rs8234, and rs10798),⁸⁰ *KCNH2* (rs1805123),³¹ *SCN5A* (rs1805124),⁸¹ *KCNE1* (rs1805128),⁸² *NOS1AP* (rs12143842, rs16847548, rs4657139),^{78, 83} and adrenergic receptor gene polymorphisms *ADRA2C*-del322-325 and *ADRB1*-R389.⁸⁴ In contrast to these disease-aggravating variants, the *KCNQ1* modifier polymorphism rs2074238 lowers arrhythmogenic risk in LQTS patients.⁸¹ Disease-modifying SNPs associated with the sick-sinus and Brugada syndrome have been identified in the *SCN5A*,⁸⁵ *SCN10A*, and *HEY2* genes.⁸⁶ Thus far, these associations could not be replicated in other cohorts.⁸⁷

The mechanisms underlying variable expressivity and phenotypic diversity remain largely elusive due to the complexity of the genetic architecture. Here, family cohorts provide substantial benefits.

ARRHYTHMIA MECHANISMS

Throughout an average person's life span and generally about 2.5 billion times, tiny electrical impulses generated by sinu-atrial myocytes travel down the specialized conduction system to coordinate contraction. Ventricular excitation-contraction coupling proceeds from endocardium to epicardium and from the apical to basal regions. Ventricular depolarization and contraction are followed by repolarization and relaxation. Importantly, but often disregarded, cardiac mechanics feed back on electrical properties mostly via mechanosensitive ion channels, to maintain electromechanical homeostasis. Cardiac arrhythmias can arise if individual elements of these delicately balanced processes are deranged.

LQTS: A PURELY ELECTRICAL DISEASE?

In the last decades, ample research has been performed to decipher the molecular-biophysical basis of congenital repolarization defects and the electrophysiological mechanisms of TdP in the long-QT syndrome. Cellular experiments, ventricular wedge preparations, and Langendorff-perfused heart set-ups have contributed substantially to this mechanistic insight. Intact large-animal experiments and human investigations in LQTS, however, are scarce, which limits the advancement of the understanding of arrhythmia mechanisms and optimal management in patients.

Acute repolarization prolongation modulates myocardial contraction⁸⁸⁻⁹¹ through altered myocyte Ca^{2+} loading. Conditions that promote myocyte Ca^{2+} overload (e.g., rapid pacing, paroxysmal tachycardia, high blood plasma $[\text{Ca}^{2+}]$ or low $[\text{K}^+]$, cardiac glycosides, beta-adrenergic receptor stimulation⁹²), can evoke $[\text{Ca}^{2+}]_{\text{cyt}}$ oscillations due to spontaneous Ca^{2+} release from the sarcoplasmic reticulum (SR).^{93, 94} These $[\text{Ca}^{2+}]_{\text{cyt}}$ oscillations may also occur in the case of inherited SR dysfunction, e.g., in the presence of calsequestrin or ryanodine-receptor gene mutations.⁹⁵ Spontaneous SR Ca^{2+} release, when occurring during late repolarization (i.e., early Ca^{2+} aftertransients), can activate inward $\text{Na}^+/\text{Ca}^{2+}$ exchanger

current (I_{Na-Ca}), which delays repolarization, thus contributing to the “conditioning phase” of early afterdepolarizations (EADs). EAD upstrokes may then be carried by the reactivation of the L-type calcium current (I_{CaL}).⁹² Diastolic spontaneous SR Ca^{2+} release during beta-adrenergic receptor stimulation results in I_{Na-Ca} -induced (and I_{Cl} -induced⁹⁶) delayed afterdepolarizations (DADs). Such delayed Ca^{2+} aftertransients (which typically occur late in diastole) deplete the SR and cause prolongation of the subsequent action-potential duration (APD) through reduced SR Ca^{2+} -release dependent inactivation of the L-type calcium current.⁹⁷ This holds particularly during conditions with reduced I_{Ks} , such as in drug-induced LQT1. Beta-adrenergic EADs coincide with early aftercontractions based on Ca^{2+} aftertransients. In fact, these aftercontractions often commence earlier than the upstroke of their accompanying EAD, often even without frank EADs, but never without a concomitant delay in repolarization.⁹⁸ The resultant spatiotemporal repolarization heterogeneities will be further exaggerated by regional heterogeneities in ion-channel^{99, 100} and Ca^{2+} -cycling protein expression¹⁰¹⁻¹⁰⁵ or myocardial conduction properties. Ca^{2+} -dependent inward currents thus facilitate EAD- and DAD-induced abnormal impulse formation and reentrant excitation by enhancing regional dispersion of repolarization and causing functional conduction block.

Short-long-short RR sequences mostly precede arrhythmias in conditions with inherited or acquired I_{Kr} defects.¹⁰⁶ The presence of a pause allows larger amounts of Ca^{2+} to accumulate in the SR, eliciting a larger Ca^{2+} -induced Ca^{2+} transient.¹⁰⁷ The post-pause Ca^{2+} transient rapidly inactivates I_{CaL} , resulting in a smaller I_{CaL} during the AP plateau. On the other hand, it enhances the inward mode of the sodium-calcium exchanger, and I_{Ks} is reduced (by prolonged I_{Ks} deactivation). The net effect is AP prolongation of the post-pause beat. This allows for the inactivated I_{CaL} to recover and generate pause-dependent EADs.¹⁰⁷ In $\Delta KPQ-SCN5A$ myocytes from mice with LQT3,¹⁰⁸ it was found that besides AP effects, the altered Na^+ channels contributed to pause-dependent spontaneous diastolic activity in the setting of increased $[Ca^{2+}]_{SR}$, spontaneous Ca^{2+} waves, and transient inward current (I_{ti}) induction.^{109, 110} Combined, pharmacological inhibition and congenital mutations in LQTS-associated genes will amplify repolarization disparity, facilitate triggered activity and provoke functional reentrant excitation under specific conditions.¹¹¹

Intact large animal experiments^{112, 113} and human investigations in LQT1¹¹⁴ have provided crucial novel mechanistic insights into the role of mechanoelectric feedback to prolonged-repolarization-dependent arrhythmogenesis. In a drug-induced LQT1 canine model, Gallacher and colleagues noted a marked electromechanical window (EMW: $QLVP_{end}$ minus QT) negativity that preceded TdP onset during beta-adrenergic provocation.^{112, 113} Within this EMW negativity, and before EAD generation, sizeable postsystolic aftercontractions occurred. These mechanical eruptions mounted substantially to amplitudes of approximately 25 mm Hg (and sometimes much higher) in the final beats before TdP. Subsequent reinduction of TdP was prevented by verapamil, esmolol and atenolol, which significantly increased the EMW to less negative values and eliminated the

aftercontractions. Clinical data obtained within our team reinforce the notion that ventricular mechano-electric interactions may conspire to induce ventricular ectopy, nonsustained VT and even TdP in the presence of a profoundly negative and very dynamic EMW.¹¹⁴ Combined, these data allude to the arrhythmogenic role of mechano-electric feedback loops under conditions of non-uniform repolarization prolongation and sympathetic stress. Mechano-electric arrhythmogenesis, although new to the field of inherited arrhythmia syndromes, is well-recognized in commotio cordis,¹¹⁵ stretch-induced arrhythmias in ischemia,¹¹⁶ and volume-overload ventricular tachyarrhythmias in heart failure.¹¹⁷

ARRHYTHMOGENIC ROLE OF PURKINJE FIBERS

Subendocardial Purkinje fibers are specialized for rapid electrical propagation, and they are structurally and functionally different from adjacent ventricular cardiomyocytes. Purkinje cell APs have a longer duration, exhibit a prominent phase 1 of repolarization and have a faster AP upstroke.¹¹⁸ These unique AP properties are determined by Purkinje-specific ion-channel compositions. Contrary to what is known for ventricular (working) cardiomyocytes, the Purkinje-cell I_{Na} contains an important non-inactivating and TTX-sensitive component that contributes significantly to APD.¹¹⁹ Purkinje cells contain both L-type and T-type calcium channels, have functionally different transient outward currents (I_{to}),¹¹⁸⁻¹²⁰ and have a sizeable inward rectifier potassium current (I_{K1}).¹¹⁸ Furthermore, the absence of an intricate t-tubular system drives Ca^{2+} -induced Ca^{2+} release from the corbular and junctional SR. This typical intracellular Ca^{2+} handling of Purkinje cells makes them susceptible to cytosolic Ca^{2+} overload, DADs and EADs^{121, 122} and triggered APs.^{123, 124} Combined, these features may contribute to the participation of Purkinje fibers in the initiation and maintenance of ventricular arrhythmias in inherited arrhythmia syndromes, myocardial infarction and congestive heart failure.¹²⁰

In the syndrome of short-coupled TdP, characterized by polymorphic VT,¹²⁵ triggering premature ventricular contractions (PVCs) originate in the Purkinje system in ~86%.¹²⁶ Proposed arrhythmia mechanisms include 1) regenerative Ca^{2+} -release events in Purkinje cells or adjacent cardiomyocytes,¹²³ 2) phase-2 reentry in electrically coupled Purkinje-muscle junctions, and 3) substantial conduction slowing of pathological Purkinje fibers.¹²⁴

In 2009, linkage analysis in three genealogically-linked Dutch families with idiopathic VF and SCD identified a shared locus at chromosome 7q36.¹²⁷ This haplotype contains the *DPP6* gene that encodes dipeptidyl peptase-like protein-6, the putative beta-subunit of I_{to} with a predominant expression in Purkinje fibers.¹²⁰ Overexpression of *DPP6*, as is found in idiopathic VF patients with the 7q36 risk haplotype, accentuates the Purkinje-cell I_{to} resulting in localized repolarization shortening, steep repolarization gradients, and the likelihood of phase-2-reentrant excitation. Overall, this electropathological profile corresponds with the clinically-observed short-coupled Purkinje-related ectopy that can trigger VF in the absence of detectable abnormalities on the 12-lead ECG.¹²⁸

Mounting evidence has implicated a triggering role for Purkinje-fiber ectopy in LQTS.¹²⁹ Likewise, hyperexcitability of the His-Purkinje network (resulting in the syndrome of multifocal ectopic Purkinje-related premature contractions) is caused by a *SCN5A* channelopathy.¹³⁰ Besides multifocal Purkinje-related ectopy, this syndrome can be associated with cardiomyopathy and SCD. Typically, no signs of LQTS or Brugada syndrome are found here.

BRUGADA SYNDROME: DEPOLARIZATION OR REPOLARIZATION?

The pathophysiological underpinnings of Brugada syndrome are still debated but two leading hypotheses have been postulated: the depolarization and repolarization hypothesis.¹³¹ The former argues that delayed and discontinuous right-ventricular depolarization is conveyed by a reduced I_{Na} ^{62, 132} and microscopic structural abnormalities in the RV outflow tract.^{133, 134} Shortened APs in the RV outflow tract are believed to result from hampered conduction and electrotonic interaction at structural discontinuities leading to excitation failure.¹³⁵ On the other hand, the “repolarization theory” claims that repolarization gradients exist secondary to the combination of reduced I_{Na} and differential I_{to} expressivity. In the epicardium, this results in an accentuated epicardial notch.¹³⁶ Both wedge preparations¹³⁷ and human data¹³⁸ demonstrate the prominent RV epicardial spike-and-dome AP morphology in relation to a coved-type Brugada ECG phenotype. Dispersion of repolarization develops if epicardial AP domes are heterogeneously attenuated, favoring (concealed) phase-2-reentrant excitation, and functional reentrant arrhythmias.

The majority of Brugada patients experience arrhythmic events between 18h00 and 06h00, while resting or sleeping.¹³⁹ Heart-rate spectral analysis showed brisk increases in parasympathetic activity prior to VF.¹⁴⁰ Edrophonium, a parasympathomimetic agent, aggravates type-1-Brugada ECG whereas beta-adrenoreceptor agonists ameliorate this phenotypic feature.¹⁴¹ Besides the influence of vagally-mediated heart-rate slowing, internal and external influences impacting on the arrhythmogenic substrate remain largely unknown.

VENTRICULAR ARRHYTHMOGENESIS AND THE AUTONOMIC NERVOUS SYSTEM

Cardiac autonomic innervation comprises efferent and afferent neural pathways that intricately govern cardiac inotropy, chronotropy, dromotropy, and lusitropy on a beat-to-beat and longer-term basis via feedback loops between the intrinsic cardiac nervous system, extracardiac-intrathoracic ganglia, and higher brain centers (**Figure 1.2**).¹⁴²

Sympathoexcitation impinges on ventricular electrophysiological properties exaggerating dispersion of refractoriness,¹⁴³ facilitating triggered activity,⁹² and reducing VF threshold.¹⁴⁴ On the other hand, there is mounting evidence of rich parasympathetic postganglionic ventricular innervation across species. Functionally, vagal-nerve stimulation operates mostly by antagonizing cardiac sympathetic actions and, thus, it prolongs the effective refractory period of canine ventricular cardiomyocytes via cholinergic-muscarinic pathways,^{145, 146}



increases VF threshold (via neural nitric oxide synthase (nNOS) mediated NO release),¹⁴⁵ and increases the variability of the dominant VF frequency.¹⁴⁷ Intriguingly, vigorous and simultaneous excitation of both limbs of the autonomic nervous system is implicated in a wide range of arrhythmias, including TdP, in susceptible hearts.¹⁴⁸

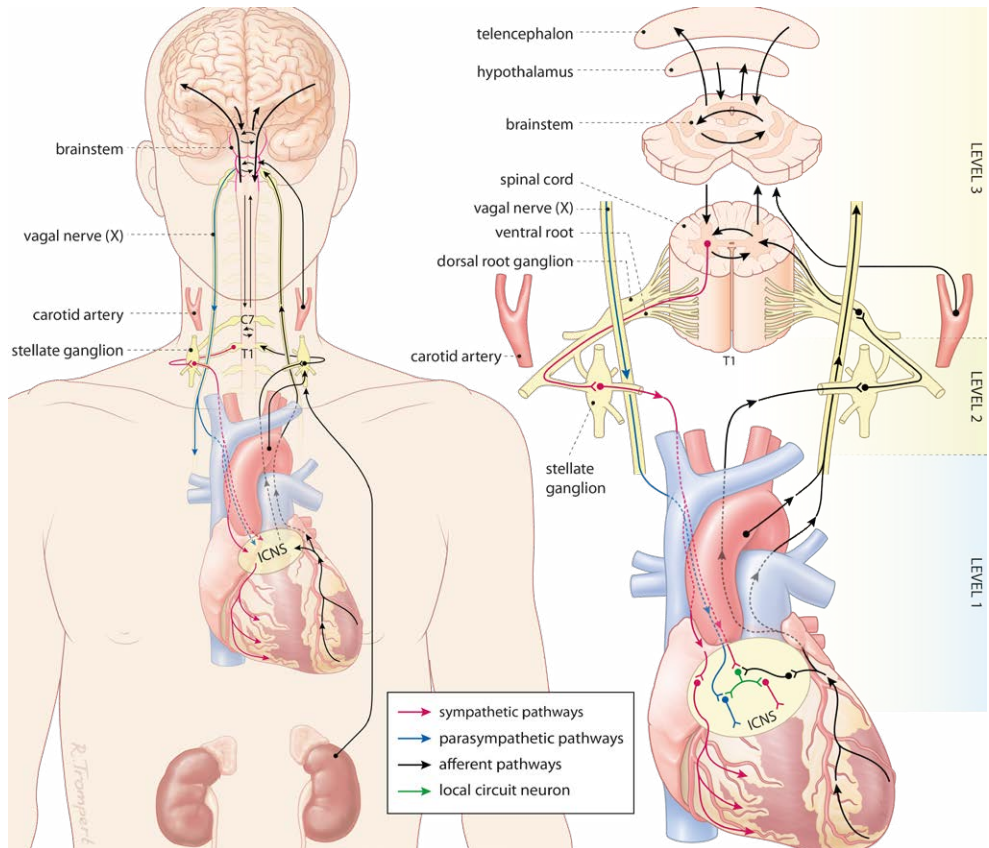


Figure 1.2 Schematic illustration of autonomic innervation of the heart. ICNS indicates intrinsic cardiac nervous system. Multiple reflex loops provide feedback: cardiocardiac (level 1), intrathoracic (level 2), spinal and brainstem reflexes (level 3). Furthermore, additional control is imposed by higher braincentres like the hypothalamic and forebrain region. [Modified from^{142, 149, 150} with permission].

In LQT1, it has been shown that arrhythmic events were mainly provoked by exercise or emotional stress (~88%) and during swimming.¹⁵¹ The potassium current I_{Ks} is normally upregulated during beta-adrenoceptor stimulation and at shorter cycle lengths to ensure repolarization shortening under circumstances of stress. Deficient I_{Ks} fails to do so, which can cause AP prolongation, dispersion of repolarization, beta-adrenergic afterdepolarizations, triggered activity and functional reentry. Interestingly, a distinctive

arrhythmic trigger in LQT1 is cold-water diving and swimming, which strongly drives sympathetic and parasympathetic nerve activity.¹⁵¹⁻¹⁵³ This hints towards a more complex vago-sympathetic interaction, fueling ventricular arrhythmogenesis in LQT1. The potential contribution of the parasympathetic limb is further supported by the notion that higher vagal reflexes, specifically after a stress test, confer higher arrhythmic risks in *KCNQ1*-p.(Ala341Val) patients.¹⁵⁴ In these patients, heart-rate variability analysis indicated that a higher sympathetic control of the QT interval and a reduced vagal activity of heart rate are associated with less arrhythmic events.¹⁵⁵

In contrast to the circadian arrhythmia patterns observed in congenital LQT1, arrhythmic events in LQT3 and Brugada syndrome occur mostly during resting conditions.^{139, 151} LQT3 patients exhibit longer QT intervals at slower heart rates,¹⁵⁶ and show QT shortening upon at rate acceleration. This clinical observation was confirmed experimentally in a drug-induced LQT3 model.¹⁵⁷ Documentation of LQT3-associated arrhythmia initiation is scarce in patients, but a predominant non-pause dependency has been described.¹⁰⁶ Bradycardia-related ventricular arrhythmias were prevented by preferential atrial pacing in a subset of *SCN5A*-p.(1795InsAsp) patients.¹⁵⁸ Cholinergic stimulation in a mouse model of LQT3 with the knock-in *SCN5A* deletion of three amino acids (Δ KPQ: Lys-1505, Pro-1506, Gln-1507) provoked sinus bradycardia, QT prolongation and TdP, underscoring the proarrhythmic propensity of parasympathetic hyperactivity during augmented late sodium current ($I_{Na,L}$).¹⁵⁹ It is currently unclear if this effect is exclusively mediated by bradycardia-induced $I_{Na,L}$ enhancement or whether a direct impact of muscarinic stimulation on ion channels plays a significant role here.^{144, 159, 160}

THERAPEUTIC AVENUES

ANTIARRHYTHMIC DRUGS

Beta-blockers are the cornerstone of pharmacological treatment for ventricular tachycardia in the setting of inherited arrhythmia syndromes and acquired heart disease. They operate mainly by interfering with beta-adrenergic receptors, but also impose sinus-rate slowing and possibly affect cellular Ca^{2+} handling through *RyR2* inhibition.¹⁶¹ Carvedilol also suppresses spontaneous SR Ca^{2+} release¹⁶¹ and $I_{Na,L}$.¹⁶² According to the ESC Guidelines, beta-blockers are recommended in LQTS patients with a prolonged QTc (class I, level of evidence B) and should be considered in subjects with a causative LQTS-associated mutation and normal QTc (class IIa, level of evidence B).¹

Metoprolol, nadolol, propranolol, and atenolol were equally effective as preventive therapy in asymptomatic LQT1 and LQT2 patients,^{163, 164} with nadolol conferring a significant risk reduction in LQT2.¹⁶³ Propranolol provoked additional QTc shortening in LQTS by concomitant $I_{Na,L}$ inhibition.¹⁶² Although beta-blockers effectively suppress arrhythmic events in LQT1 and LQT2, breakthrough events still occur in 20-30%,¹⁶⁵⁻¹⁶⁷ especially in patients with a history of cardiac events.¹⁶⁸ Retrospective analyses yielded conflicting results



on the efficacy of various beta-blockers when comparing the suppression of breakthrough events.^{163, 164} In this high-risk group, propranolol appeared the least effective drug.¹⁶³ Nadolol reduced the risk of breakthrough events in symptomatic LQT1 and LQT2 patients, whereas metoprolol led to an increased risk with OR = 3.95 (95% C.I. 1.2-13.1; $P=0.025$).¹⁶⁴

As LQT3 patients typically have slower basal heart rates and experience lethal events at rest, the use of beta-blockers is still somewhat of a debate,^{151, 165, 169} despite being recommended by the ECS Guidelines.¹ Based on the results of a large cohort of 406 LQT3 patients, chronic beta-blocker therapy was associated with an 83%-reduction of cardiac events in female patients.¹⁷⁰ The type of beta-blocker was not reported. Ranolazine preferentially inhibits $I_{Na,L}$ ^{109, 171, 172} besides I_{Ti} , and it reduces $[Ca^{2+}]_{SR}$ load.¹¹⁰ This compound has proven efficacy in LQT3 patients, either as monotherapy^{173, 174} or combined with a beta-blocker.¹⁷⁵ Ranolazine may be considered in LQT3 patients with a $QTc > 500$ ms as add-on therapy according to the ESC Guidelines (class IIb, level of evidence C).¹ Mexiletine¹⁵⁶ or flecainide¹⁷⁶ are useful alternatives in this condition.

Amiodarone, with Vaughan-Williams class I, II, III, and IV antiarrhythmic properties, has complex electropharmacological actions, targeting multiple ion channels (K^+ , Na^+ , and Ca^{2+}),¹⁷⁷ besides its beta-blocking action, and is highly effective in suppressing ventricular arrhythmias through effects on reentrant pathways and abnormal impulse formation. This drug induces differential repolarization prolongation leading to reduced transmural repolarization dispersion.^{178, 179} It is considered unsuitable for arrhythmia management in LQTS patients.

INTERVENTIONAL MODALITIES

Invasive treatment of life-threatening arrhythmias in patients without noticeable structural abnormalities has developed considerably in the recent years. In selected cases, radiofrequency catheter ablation of VF-triggering Purkinje-related PVCs can (at least temporarily) prevent VF to occur.^{126, 129, 180, 181} In the case of a genetic mechanism for VF, the arrhythmogenic propensity of Purkinje fibers is not confined to a particular endocardial area, and VF triggers may arise distant from the site of ablation. As such, these patients should be treated with an implantable cardioverter defibrillator (ICD) besides antiarrhythmic drug therapy, whereas a dominant focal trigger may additionally be ablated.

Neuraxial modulation through left cardiac sympathetic denervation (LCSd) was first successfully employed in a patient with therapy-refractory angina pectoris and ventricular arrhythmias by Thomas Jonnesco in 1916.¹⁸² Some fifty years later, cardiac sympathetic denervation was occasionally performed in sporadic idiopathic VT/VF and LQTS cases,^{183, 184} and, by now, has established as adjuvant treatment for large numbers of patients with suspected sympathetic-induced VTs.¹⁸⁵⁻¹⁸⁷ Currently, LCSd or bilateral sympathetic denervation¹⁸⁸ entail important treatment modalities in patients with refractory VT in whom medicinal is ineffective or contra-indicated, if ICD therapy is unsuited, or if breakthrough events occur despite beta-blocker therapy requiring ICD shocks.¹

AIMS AND STRUCTURE OF THIS THESIS

The aims of this PhD thesis are captured as follows:

1. To investigate the modulatory role of mechano-electric heterogeneities besides non-uniform repolarization prolongation in the arrhythmogenic deterioration of congenital LQTS.
2. To refine risk stratification in LQTS patients taking electromechanical parameters into account.
3. To unravel potential genotype-specific determinants of electromechanical disparity in patients LQT1, LQT2, or LQT3.
4. To explore the proarrhythmic proclivity of unilateral sympathetic stimulation in an in-vivo canine model of drug-induced LQT1.
5. To investigate ventricular electromechanical heterogeneities provoked by increased autonomic tone in drug-induced LQT1.
6. To study genotype-phenotype relationships in high-risk patients guiding personalized arrhythmia treatment.
7. To pave the way for the identification of genetic modifiers in a *SCN5A* founder population with phenotypic overlap and excess SCD using unbiased whole-exome and targeted genome sequencing.

This thesis is structured following these aims. A critical appraisal of the contemporary knowledge of non-uniform repolarization prolongation, associated altered cellular Ca^{2+} handling, and mechano-electric disparity in the setting of LQTS is described in **Chapter 2**. Furthermore, preliminary results are provided on the non-invasive assessment of EMW negativity in LQTS patients under basal conditions and EMW dynamicity during instances of electrical instability preceding TdP. These pilot data inspired us to investigate the discriminatory role of EMW negativity in a multicenter cohort of 244 genotyped symptomatic and asymptomatic LQTS patients (**Chapter 3**). Next, we investigated repolarization instability, electromechanical interplay, and LQT1-associated ventricular arrhythmogenesis during unilateral stimulation of the (intact) stellate ganglion in a canine model (**Chapter 4**). With the intention to improve understanding of individual genotype-phenotype correlations the following two chapters, **Chapter 5** and **Chapter 6**, are written. **Chapter 5** illustrates the novel insights in arrhythmia patterns and divergent phenotypes obtained after meticulous cardiac phenotyping of a large kindred segregating the deletion of phenylalanine at position 1617 of the *SCN5A* gene. This founder population allows complex family-based statistical analyses to assess residual heritability besides a shared pathogenic mutation and paves the way for the unambiguous identification of additional disease-modifying variants. In **Chapter 6**, at an individual patient level, genetic profiling adds to the mechanistic understanding of life-threatening arrhythmias, unraveling novel arrhythmia mechanisms, and even guiding personalized anti-arrhythmic therapy. **Chapter 7** discusses these different layers of complexity important for ventricular arrhythmogenesis and provides prospective for future research.



Finally, I take the opportunity to share with the reader the HeArt Project (**Chapter 8**), an art-based intervention that paralleled this dissertation, aiming to promote the synergy between artistic and scientific creativity. Artistic perspectives are provided to translate complex scientific content to the general public.

Table 1.1 Genetic variants associated with LQTS.

Syndrome	Chromosome	Gene	Protein	Functional effect	Freq.	Ref.
Long-QT syndrome (major)						
LQT1	11p15.5	<i>KCNQ1</i>	K _V 7.1	Reduced I _{Ks}	30-35%	41, 42
LQT2	7q35-46	<i>KCNH2</i>	K _v 11.1	Reduced I _{Kr}	25-30%	43
LQT3	3p21-p24	<i>SCN5A</i>	Na _v 1.5	Increased I _{Na}	5-10%	44
Long-QT syndrome (minor)						
LQT4	4q25-q27	<i>ANKB</i>	Ankyrin B	Ab. ion chan./transp.	Rare	53, 54
LQT5	21q22.1	<i>KCNE1</i>	MinK	Reduced I _{Ks}	Rare	46, 189
LQT6	21q22.1	<i>KCNE2</i>	MiRP1	Reduced I _{Kr}	Rare	47, 190
LQT7	17q23	<i>KCNJ2</i>	Kir2.1	Reduced I _{K1}	Rare	55
LQT8	12p13.3	<i>CACNA1C</i>	Ca _v 1.2	Increased I _{CaL}	Rare	56
LQT9	3q25	<i>CAV3</i>	Caveolin 3	Increased I _{Na}	Rare	49
LQT10	11q23.3	<i>SCN4B</i>	Na _v β4	Increased I _{Na}	Rare	50
LQT11	7q21-q22	<i>AKAP9</i>	Yotiao	Reduced I _{Ks}	Rare	48
LQT12	20q11.2	<i>SNTA1</i>	Syntrophin-α1	Increased I _{Na}	Rare	51
LQT13	11q24.3	<i>KCNJ5</i>	Kir3.4	Reduced I _{K,Ach}	Rare	45
LQT14	14q32.11	<i>CALM1</i>	Calmodulin 1	Dysfunct. Ca ²⁺ sign.	Rare	52
LQT15	2p21.1-p21.3	<i>CALM2</i>	Calmodulin 2	Dysfunct. Ca ²⁺ sign.	Rare	52
Jervell and Lange-Nielsen syndrome						
JLNS1	11p15.5	<i>KCNQ1</i>	K _V 7.1	Reduced I _{Ks}	Rare	189
JLNS2	21q22.1	<i>KCNE1</i>	MinK	Reduced I _{Ks}	Rare	191

In chronological order of publication.

Table 1.2 Genetic variants associated with Brugada syndrome.

Syndrome	Chromosome	Gene	Protein	Function. effect	Freq.	Ref.
Brugada syndrome (major)						
BrS1	3p21-p24	<i>SCN5A</i>	Na _v 1.5	Reduced I _{Na}	20-30%	62
Brugada syndrome (minor)						
BrS2	3p22.3	<i>GPD1L</i>	<i>GPD1L</i>	Reduced I _{Na}	Rare	192
BrS3	12p13.3	<i>CACNA1C</i>	Ca _v 1.2	Reduced I _{CaL}	6.6%	193
BrS4	10p12	<i>CACNB2</i>	Ca _v β2b	Reduced I _{CaL}	5%	194
BrS5	19q13.1	<i>SCN1B</i>	Na _v β1	Reduced I _{Na}	1-2%	195
BrS6	11q13.4	<i>KCNE3</i>	MiRP2	Increased I _{to}	<1%	196
BrS7	11q24.1	<i>SCN3B</i>	Na _v β3	Reduced I _{Na}	Rare	197
BrS8	7q35	<i>KCNH2</i>	K _v 11.1	Increased I _{Kr}	Rare	198
BrS9	12p12.1	<i>KCNJ8</i>	Kir6.1	Increased I _{K,ATP}	Rare	199
BrS10	7q21-q22	<i>CACNA2D1</i>	Ca _v α2/δ1	Reduced I _{CaL}	Rare	200
BrS11	17p13.1	<i>RANGRF</i>	MOG1	Reduced I _{Na}	Rare	201
BrS12	Xq22.3	<i>KCNE5</i>	MiRP4	Increased I _{to} /I _{Ks}	Rare	202
BrS13	1p13.2	<i>KCND3</i>	K _v 4.3	Increased I _{to}	Rare	203
BrS14	15q24.1	<i>HCN4</i>	HCN4	Reduced I _f	Rare	51, 204
BrS15	3q14.3	<i>SLMAP</i>	SLMAP	Reduced I _{Na}	Rare	205
BrS16	19q13	<i>TRPM4</i>	NSC _{Ca}	Reduced I _{Na}	8%	206
BrS17	11q23.2	<i>SCN2B</i>	Na _v β2	Reduced I _{Na}	Rare	207
BrS18	12p12.1	<i>ABCC9</i>	SUR2A	Increased I _{K,ATP}	4-5%	208
BrS19	3p22.2	<i>SCN10A</i>	Na _v 1.8	Reduced I _{Na}	2.5-16%	209
BrS20	12p11.21	<i>PKP2</i>	Plakophilin-2	Reduced I _{Na}	2.5%	210
BrS22	7q21.11	<i>SEMA3A</i>	Semaphorin 3A	Increased I _{to}	?	211

In chronological order of publication.



Table 1.3 Chromosomal loci/genetic variants associated with idiopathic VF and short-coupled TdP.

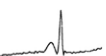
Syndrome	Chromosome	Gene	Protein	Functional effect	Freq.	Ref.
Short-coupled TdP						
sc-TdP	14q32.11	<i>CALM1</i>	Calmodulin 1	Dysfunct. Ca ²⁺ sign.	?	67
sc-TdP	1q43	<i>RYR2</i>	Ryanodine rec 2	Dysfunct. Ca ²⁺ sign.	?	68
Idiopathic ventricular fibrillation						
iVF	7q36	<i>DPP6</i>	Dipeptidyl peptase-like protein-6	Increased I _{to}	?	127
iVF	16q12.2	<i>IRX3</i>	Iroquois homeobox protein 3	Enhanced HP conduction	?	212
iVF	6p24.3	<i>DSP</i>	Desmoplakin	?	?	213
iVF	12p13.33	<i>CACNA1C</i>	Ca _v 1.2	?	?	213
iVF	14q11.2	<i>MYH7</i>	Myosin heavy chain 7	?	?	213
iVF	2q31.2	<i>TTN</i>	Titine	?	?	213
iVF	10q22.2	<i>VCL</i>	Vinculine	?	?	213
iVF	12p11.21	<i>PKP2</i>	Plakophilin	?	?	213
iVF	19q13	<i>TRPM4</i>	TRPM4/NSCCa	?	?	214
iVF	11q24.1	<i>SCN3B</i>	Na _v β3	Reduced I _{Na}	?	215

In chronological order of publication.

Table 1.4 Genetic variants associated with SQTS, ERS, and CPVT.

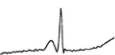
Syndrome	Chromosome	Gene	Protein	Functional effect	Freq.	Ref.
Short-QT syndrome						
SQT1	7q36.1	<i>KCNH2</i>	K _v 11.1	Increased I _{Kr}	<5%	216
SQT2	11p15.5	<i>KCNQ1</i>	K _v 7.1	Increased I _{Ks}	<5%	217
SQT3	17q24.3	<i>KCNJ2</i>	Kir2.1	Increased I _{K1}	<5%	218
SQT4	12p13.3	<i>CACNA1C</i>	Ca _v 1.2	Reduced I _{CaL}	Rare	193
SQT5	10p12.33	<i>CACNB2b</i>	Ca _v β2b	Reduced I _{CaL}	Rare	193
SQT6	7q21.11	<i>CACN2D1</i>	Ca _v α2/δ1	Reduced I _{CaL}	Rare	219
SQT7	2q35	<i>SLC4A3</i>	H,HCO ₃ -exch.	High pH _i	Rare	220
Early repolarization syndrome						
ERS1	12p11.23	<i>KCNJ8</i>	Kir6.1	Increased I _{K,ATP}	?	221
ERS2	12p13.3	<i>CACNA1C</i>	Ca _v 1.2	Reduced I _{CaL}	4%	200
ERS3	10p12.33	<i>CACNB2b</i>	Ca _v β2b	Reduced I _{CaL}	8%	200
ERS4	7q21.11	<i>CACNA2D1</i>	Ca _v α2/δ1	Reduced I _{CaL}	4%	200
ERS5	3p21	<i>SCN5A</i>	Na _v 1.5	Reduced I _{Na}	?	222
ERS6	12p12.1	<i>ABCC9</i>	SUR2A	Increased I _{K,ATP}	?	208
Catecholaminergic polymorphic ventricular tachycardia						
CPVT1	1q42.1-q43	<i>RYR2</i>	Ryanodine rec 2	Dysfunct. Ca ²⁺ sign.	50-60%	223
CPVT2	1q13.3	<i>CASQ2</i>	Calsequestrin 2	Dysfunct. Ca ²⁺ sign.	1-2%	224
CPVT3	4q25-q27	<i>ANKB</i>	Ankyrin-B	Ab. ion chan./transp.	Rare	225
CPVT4	17q23	<i>KCNJ2</i>	Kir2.1	Increased I _{K1}	Rare	226, 227
CPVT5	14q32.11	<i>CALM1</i>	Calmodulin 1	Dysfunct. Ca ²⁺ sign.	Rare	228
CPVT6	6q22.31	<i>TRDN</i>	Triadin	Dysfunct. Ca ²⁺ sign.	Rare	229
CPVT7	2p21.1-p21.3	<i>CALM2</i>	Calmodulin 2	Dysfunct. Ca ²⁺ sign.	Rare	230
CPVT8	19q13.2-13.3	<i>CALM3</i>	Calmodulin 3	Dysfunct. Ca ²⁺ sign.	Rare	231

In chronological order of publication.





*"Een HeArt verwarmend, kunstzinnig
en innovatief idee"*



2

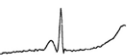
ARRHYTHMOGENIC MECHANO-ELECTRIC HETEROGENEITY IN THE LONG-QT SYNDROME

Rachel M.A. ter Bekke, Paul G.A. Volders

Prog Biophys Mol Biol 2012;110:347-358

ABSTRACT

Since the first linkage of the long-QT syndrome to the Harvey *ras-1* gene in 1991 ample research has been performed to decipher the molecular-biophysical basis of congenital repolarization defects and the electrophysiological mechanisms of torsades-de-pointes arrhythmias in this condition. Mechanistic knowledge is mostly derived from cellular experiments (cardiac myocytes, cultured cells), ventricular tissue (including arterially-perfused wedge) preparations and Langendorff-perfused hearts, with relatively little information from in-vivo animal models, and even more scant intact human-heart investigations. Until now, much emphasis has been put on purely membrane-related pathways of arrhythmia initiation with a prominent role for spatiotemporal dispersion of repolarization, early afterdepolarizations and reentrant excitation. Here, we review additional factors that influence the onset of torsades de pointes, notably myocardial Ca^{2+} (over)loading and spontaneous SR Ca^{2+} release, occurring particularly during intense sympathetic nervous stimulation and dynamic cycle-length changes. Recent tissue and in-vivo data suggest that spontaneous SR Ca^{2+} release, underlying aftercontractions in the isolated myocyte, may organize to local myocardial Ca^{2+} waves and aftercontractions in the intact heart. In the setting of prolonged repolarization and a negative electromechanical window, these spontaneous $[\text{Ca}^{2+}]_{\text{cyt}}$ -based events (which often arise during early diastole) may exaggerate repolarization instability via $[\text{Ca}^{2+}]_{\text{cyt}}$ -activated inward membrane currents and, as we postulate, via mechano-sensitive ion currents. Future long-QT research should focus on the intact beating heart with preserved autonomic input to examine these arrhythmogenic mechanisms.



INTRODUCTION

Intrinsic electromechanical heterogeneity is present in the normal beating heart. Differences in action-potential morphology and duration exist between various regions of the ventricular myocardium under physiological conditions.^{100, 232} Likewise, spatial gradients of contraction and relaxation exist, e.g., between the endo- and epicardium, apex and base, left (LV) and right ventricular, and at the circumferential diameter.²³³ Differential expressions of transmembrane ion currents, and Ca^{2+} -transport and storage mechanisms underlie these non-uniformities.

In patients with the congenital long-QT syndrome, electromechanical heterogeneity of the ventricles is often increased. The various LQTS that have been identified to date are caused by genetic mutations in ion-channel subunits or ion-channel-associated proteins. Mutation carriers may remain asymptomatic during their entire life, but severe cases are susceptible to syncope or sudden death due to torsades de pointes and ventricular fibrillation. Although these syndromes are considered “primary electrical cardiomyopathies”, LQT patients may exhibit mechanical wall abnormalities under basal conditions. One initial echocardiographic study revealed a rapid early contraction and a very prolonged phase of wall thickening before rapid relaxation in more than half of referred patients, who had an averaged QTc interval of approximately 500 ms.²³⁴ In some of these, a peculiar double-peak pattern of later thickening was observed. Similar results were obtained by other groups using M-mode²³⁵ and tissue-Doppler imaging techniques.²³⁶ Mechanical wall abnormalities were normalized by intravenous treatment with the Ca^{2+} -channel blocker verapamil.²³⁷ More recently, strain-imaging studies revealed that contraction duration was longer in the subendocardium than midmyocardium of symptomatic LQT mutation carriers, but not of asymptomatic or healthy individuals, indicating transmural mechanical dispersion in the former group.²³⁸ Prolonged contraction duration and augmented longitudinal mechanical dispersion were superior to QTc for arrhythmia-risk assessment.

While these clinical data hint to an association between increased mechanical heterogeneity and the occurrence of arrhythmias in susceptible LQT patients, a mechanistic link remains elusive. This applies particularly to the dynamic beat-to-beat instabilities of the heart just prior to the onset of TdP when sympathetic activity is often enhanced. Does mechano-electric coupling contribute to arrhythmogenesis at these very instances? And if so, how?

In the present article, we review the literature on arrhythmia mechanisms in the setting of congenitally prolonged and/or dispersed ventricular repolarization, focusing mainly on the role of altered myocardial Ca^{2+} handling, spontaneous sarcoplasmic reticulum Ca^{2+} release and the generation of afterdepolarizations, aftercontractions, and premature ectopic beats. The concept of the “electromechanical window” will be discussed. We will argue that in the intact beating heart, besides $[\text{Ca}^{2+}]_{\text{cyt}}$ -dependent pathways, mechano-sensitive activation of ion channels can participate in torsadogenesis when

electromechanical heterogeneity exaggerates and systolic and/or diastolic occur. As much as possible, we will seek in-vivo confirmation of cellular mechanisms.

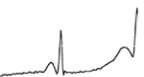
CELLULAR Ca^{2+} OVERLOAD AND SPONTANEOUS SR Ca^{2+} RELEASE DURING PROLONGED REPOLARIZATION

Ca^{2+} HANDLING AND Ca^{2+} ACCUMULATION IN CARDIAC MYOCYTES

Thorough insight into myocyte Ca^{2+} handling is essential for the understanding of arrhythmogenesis in a broad variety of cardiac diseases, including the LQTS.⁹² Under normal conditions, Ca^{2+} -induced Ca^{2+} release from the SR is triggered by sarcolemmal Ca^{2+} influx mainly through L-type Ca^{2+} channels (**Figure 2.1A**).^{239, 240} A rise in subsarcolemmal $[\text{Ca}^{2+}]$ by L-type Ca^{2+} -channel influx and/or Ca^{2+} diffusion from nearby ryanodine receptors (RyR) can activate these RyRs to release much more Ca^{2+} from the SR. Both subsarcolemmal $[\text{Ca}^{2+}]$ and intra-SR $[\text{Ca}^{2+}]$ influence RyR-channel gating properties.²⁴¹ Multiple local Ca^{2+} -release events summate into a propagating whole-cell Ca^{2+} transient that activates the contractile apparatus via Ca^{2+} binding to the myofilament protein troponin C. Changes in the size of the Ca^{2+} transient feed back on transsarcolemmal Ca^{2+} fluxes, adjusting the SR Ca^{2+} content such that the size of the Ca^{2+} transient returns to its basal level.

It has long been recognized that Ca^{2+} can also be released from the SR without a preceding membrane depolarization. This process, referred to as spontaneous Ca^{2+} release, can occur under conditions of myocyte Ca^{2+} overload when $[\text{Ca}^{2+}]_{\text{SR}}$ is abnormally high.²⁴²⁻²⁴⁵ Protein-kinase-A (PKA)-dependent phosphorylation of I_{CaL} and PKA- and Ca^{2+} /Calmodulin-kinase II (CaMKII)-dependent modulation of SR Ca^{2+} uptake (via SERCA2a and phospholamban) have a large impact on SR Ca^{2+} levels and the incidence of spontaneous Ca^{2+} release.²⁴⁶ The functional consequences of RyR phosphorylation (by PKA and/or CaMKII) are still debated.²⁴⁷ Several conditions promote $[\text{Ca}^{2+}]_{\text{SR}}$ accumulation and spontaneous SR Ca^{2+} release with self-propagating Ca^{2+} waves, including beta-adrenergic receptor stimulation, rapid electrical stimulation, digitalis intoxication, and elevated extracellular $[\text{Ca}^{2+}]$.^{245, 248}

The $\text{Na}^+/\text{Ca}^{2+}$ exchanger (NCX) is the main Ca^{2+} -extrusion protein for the beat-to-beat regulation of contraction and relaxation in cardiac myocytes. Because of a predominant stoichiometry of 3 Na^+ ions : 1 Ca^{2+} ion inward $I_{\text{Na-Ca}}$ is generated when Ca^{2+} is extruded from the cell and outward $I_{\text{Na-Ca}}$ is generated when Ca^{2+} enters via this transporter. The direction and magnitude of NCX are dependent on the membrane potential and the intra- and extracellular $[\text{Na}^+]$ and $[\text{Ca}^{2+}]$ in the direct vicinity of the NCX protein. The dynamics of the AP and the resultant local Na^+ and Ca^{2+} signals change the NCX-reversal potential on a continuous basis. Under normal conditions, it functions predominantly in the inward mode during the decay phase of the Ca^{2+} transient generating inward current during most of the repolarization. This increases the APD.



ALTERED MYOCARDIAL Ca^{2+} HANDLING DURING PROLONGED REPOLARIZATION

It is well established that AP amplitude and/or duration per se are important regulators of contraction,^{88, 89} mainly by changing the amount of Ca^{2+} released from the SR.⁹³ A prolonged AP-plateau phase contributes to incomplete inactivation of voltage-dependent L-type Ca^{2+} current resulting in cellular Ca^{2+} loading.²⁴⁹

In addition, pharmacological modulation of repolarization can profoundly alter myocardial Ca^{2+} handling even in the absence of beta-adrenergic stimulation. Drug-induced AP prolongation with the selective I_{Kr} blocker almokalant caused a positive inotropic effect in isolated human ventricular muscle strips (steady-state pacing cycle length 1000 ms),⁹¹ consistent with earlier data.⁹⁰ In canine ventricular M-cell preparations pretreated with the I_{Kr} blocker E-4031, sudden rate acceleration or a single premature beat could induce or facilitate transient AP prolongation and the generation of early afterdepolarizations via a mechanism linked to Ca^{2+} loading,²⁵⁰ in line with model data.¹⁰⁷ Furthermore, optical-mapping experiments in dofetilide-treated Langendorff-perfused rabbit hearts revealed discernible $[Ca^{2+}]_{cyt}$ oscillations that preceded EAD generation by minutes, indicating that they could arise from spontaneous SR Ca^{2+} release rather than Ca^{2+} -induced Ca^{2+} release through I_{CaL} reactivation.⁹⁴ Thapsigargin and ryanodine, by suppressing SR Ca^{2+} uptake and release, successfully prevented the occurrence of EADs. In another study on Langendorff-perfused rabbit hearts treated with sotalol or veratridine, the NCX inhibitor SEA0400 was effective in preventing TdP by suppressing EADs.²⁵¹ Collectively, these data support that acute (drug-induced) repolarization prolongation causes myocardial Ca^{2+} loading, potentially leading to overload and $[Ca^{2+}]_{cyt}$ oscillations owing to spontaneous SR release. If occurring during systole, these $[Ca^{2+}]_{cyt}$ oscillations can activate inward I_{Na-Ca} to delay repolarization (together with inactivating I_{CaL}), thus allowing for reactivating I_{CaL} to generate EAD upstrokes. Besides these electrogenic effects $[Ca^{2+}]_{cyt}$ increments will also activate the mechanical machinery and dictate myocyte contraction. At least on theoretical grounds and depending on their timing, local spontaneous contractile events or aftercontractions could activate mechano-sensitive non-selective stretch-activated cation (I_{SAC}) channels to contribute to the initial repolarization delay and EAD formation (**Figure 2.1**).

Virtually nothing is known about Ca^{2+} handling in native ventricular myocytes from LQT patients. In a transgenic mouse model of the LQTS type 3 (LQT3; gain-of-function mutations of *SCN5A*) sudden accelerations in heart rate or premature beats cause AP prolongation with EADs and triggered arrhythmias.¹⁰⁸ Mutation-altered Na^+ entry contributes to the occurrence of pause-dependent spontaneous diastolic activity¹⁰⁹ caused by Ca^{2+} -dependent transient inward current in the setting of elevated $[Ca^{2+}]_{SR}$ and spontaneous Ca^{2+} waves. Ranolazine, at concentrations that preferentially target late I_{Na} during prolonged depolarization, inhibits these spontaneous events by decreasing $[Ca^{2+}]_{SR}$.¹¹⁰ Irregularities of Ca^{2+} handling may also underlie prolonged and unstable repolarization at increasing rates. These are corrected with verapamil.²⁵² To the best of our knowledge, detailed studies of myocyte Ca^{2+} handling in mouse and rabbit models of LQT1 and LQT2 are lacking.

SERCA2a, SR Ca^{2+} ATPase; CASQ, calsequestrin; SAC_{NS} , non-selective stretch-activated cation channels; SAC_{K} , K^+ -selective stretch-activated channels. **(B) Left**, diastolic Ca^{2+} aftertransient causing aftercontraction and DAD carried by $[\text{Ca}^{2+}]_{\text{cyt}}$ -dependent $I_{\text{Na-Ca}}$ and $I_{\text{Cl(Ca)}}$. Based on known reversal potentials for SAC_{NS} and SAC_{K} , mechano-dependent inward I_{SAC} could contribute to DAD during aftercontraction. **Right**, systolic Ca^{2+} aftertransient (*) underlying aftercontraction and initial repolarization delay (EAD-conditioning phase by $[\text{Ca}^{2+}]_{\text{cyt}}$ -dependent $I_{\text{Na-Ca}}$ and inactivating I_{CaL}) versus the EAD upstroke (reactivating I_{CaL} and/or I_{Na}). Based on known reversal potentials for SAC_{NS} and SAC_{K} , mechano-dependent inward I_{SAC} can be present throughout both EAD-conditioning and upstroke phase when aftercontraction occurs.

ARRHYTHMOGENIC CONSEQUENCES OF SPONTANEOUS Ca^{2+} RELEASE

Spontaneous SR Ca^{2+} release of sizeable magnitude can alter the membrane potential via two, mutually inclusive, mechanisms: $[\text{Ca}^{2+}]_{\text{cyt}}$ -dependent I_{ti} and mechano-dependent inward ion currents activated by aftercontractions.

$[\text{Ca}^{2+}]_{\text{cyt}}$ -DEPENDENT I_{ti}

Spontaneous Ca^{2+} aftertransients can activate Ca^{2+} -sensitive I_{ti} to generate delayed afterdepolarizations²⁵³ and/or the “conditioning phase” of EADs, particularly during beta-adrenergic stimulation⁹⁸, depending on the phase in the cardiac cycle at which they occur (**Figure 2.1B**).

For DADs, several $[\text{Ca}^{2+}]_{\text{cyt}}$ -dependent inward currents are implicated: $I_{\text{Na-Ca}}$, Ca^{2+} -activated Cl^- current ($I_{\text{Cl(Ca)}}$)⁹⁶ and the non-selective cation current.²⁵⁴ The latter may be carried by transient receptor potential M4 (TRPM4) channels.²⁵⁵

For EADs, the ionic mechanisms are complex and diverse, depending on the cell type and conditions in which they occur. Different ionic mechanisms can contribute to the conditioning phase, i.e., the initial repolarization delay that sets the stage for EAD upstrokes. In the case of proarrhythmic I_{Kr} blockade (in the absence of beta-adrenergic stimulation) AP prolongation and EADs are caused by decreased repolarizing K^+ currents in combination with reduced inactivation and subsequent reactivation of I_{CaL} .⁹² This is in line with experiments with the I_{CaL} agonist Bay K 8644 by January and coworkers, who observed a concentration-dependent AP lengthening followed by the generation of EADs at a non-physiological 0.2-Hz stimulation frequency.²⁵⁶

By contrast, EADs generated during intense beta-adrenergic receptor stimulation often appear jointly with DADs and are fast-rate dependent, suggesting that $[\text{Ca}^{2+}]_{\text{cyt}}$ overload and spontaneous Ca^{2+} aftertransients underlie both.^{98, 257, 258} I_{Ks} blockade potentiates the occurrence of these beta-adrenergic EADs that are almost always accompanied by DADs in the preceding diastole.²⁵⁹ Beta-adrenergic EADs coincide with early aftercontractions based on Ca^{2+} aftertransients. In fact, these aftercontractions commence approximately 30 ms earlier than the upstroke of their accompanying EAD and they arise often without EADs, but never without a concomitant delay in repolarization. In experiments with Ni^{2+} , a non-specific inhibitor of NCX, early and delayed aftercontractions persisted despite complete inhibition of EADs and DADs.⁹⁸ Others have shown (1) similar results using alternative NCX blockers,²⁶⁰

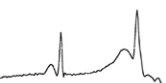
²⁶¹ (2) that the photolysis of caged intracellular Ca^{2+} during or after a stimulated action potential can elicit an EAD or DAD, respectively,²⁶⁰ and (3) that early and delayed Ca^{2+} aftertransients persist in myocytes even when switching from current-clamp (stimulated action potentials with EADs and DADs) to voltage-clamp mode (applying action-potential command waveforms without EADs and DADs).²⁶¹ Taken together, these observations strongly imply that beta-adrenergic-elicited early Ca^{2+} aftertransients are due to spontaneous SR Ca^{2+} release, and that these primary events drive Ca^{2+} -dependent inward $I_{\text{Na-Ca}}$ to delay repolarization during the conditioning phase prior to the actual EAD. Besides $I_{\text{Na-Ca}}$, beta-adrenergic-enhanced window I_{CaL} also contributes to this phase (**Figure 2.1B**).²⁶² Actual EAD upstrokes are carried by reactivating I_{CaL} . In-vivo observations in a canine model of drug-induced LQT1 and beta-adrenergic receptor stimulation¹¹² are consistent with these cellular mechanisms, confirming their relevance in the beating heart.

Of course, in LQT3-mimicking conditions the importance of (late) I_{Na} is more prominent. This applies also to Purkinje cells in which (late) I_{Na} is intrinsically larger than in ventricular myocytes. As an important side note, Ca^{2+} -activated TRPM4 channels, which are permeable to monovalent cations such as Na^+ and K^+ ,^{263, 264} have also been implicated in EAD (and DAD) generation, particularly during cardiac hypertrophy.²⁶⁵

MECHANO-DEPENDENT INWARD CURRENTS: ROLE FOR STRETCH-ACTIVATED CHANNELS

The notion that mechanical forces imposed on the myocardium can induce electrical responses is not new. In 1876, Nélaton reported a case of sudden death after a non-penetrating mechanical impact to the precordium.²⁶⁶ Since then it has become increasingly clear that the heart has intrinsic mechano-sensory properties that can exhibit profound effects on membrane excitation, repolarization, abnormal impulse formation and conduction, and arrhythmia, as exemplified in the following section.

In isolated, chronically-infarcted canine hearts, acute volume loading increased dispersion of refractoriness and ventricular arrhythmias.²⁶⁷ Likewise, in isolated blood-perfused canine hearts, an additional volume of 15 ± 1.6 mL on top of a holding volume of 20 mL (end-diastolic pressure 5.3 ± 5.2 mm Hg) evoked a 50% probability of stretch-induced ventricular arrhythmia.²⁶⁸ The temporal delay between peak stretch volume and ventricular premature depolarization was approximately 38 ms. Electrophysiological responses are not only determined by the magnitude of the imposed mechanical stress, but are also reliant on myocardial wall compliance and spatiotemporal mechanical heterogeneity. The strain-electric response relationship of myocardial tissue was elegantly demonstrated by Seo and co-workers using optical voltage mapping coupled to tissue-marker tracking techniques in the rabbit RV wall and in whole-heart preparations.²⁶⁹ Medium-sized (10-15%) stretch induced focal excitation that could develop into reentrant arrhythmias. Counterintuitively, when enlarging the mechanical stimulus the likelihood of arrhythmia induction decreased due to synchronous excitation of larger myocardial regions. This stretch-induced excitation was suppressed by 71% after pharmacological non-selective inhibition of stretch-activated channels with Gd^{3+} . They observed predilection sites of focal activity in thin-walled regions



probably reflecting the heterogeneity in strain distribution due to complex ventricular geometry.²⁶⁹ This may relate to the observation that TdP in humans originates preferentially from the LV- and/or RV-outflow tract regions, which are thin-walled and often richly innervated.²⁷⁰

To elucidate the biophysical basis of mechano-electric coupling and arrhythmogenesis, extensive research has been done in various species, including mouse, rat, canine, lamb and human.^{268, 271-275} Stretch-activated channels (SACs) are the most likely candidates for mechano-electric transduction as these channels open their pores in response to mechanical deformation. SACs are ubiquitous in various organs including the heart where they are localized in T-tubules,²⁷⁶ in caveolae, and in intracellular membrane compartments.²⁷⁷ Since the discovery of SACs in embryonic chick skeletal muscle in 1984,²⁷⁸ a broad diversity of mechano-sensitive channels has been reported. Some of these have been linked to myocardial stretch-evoked arrhythmogenic effects: of the canonical TRP subfamily, TRPC1²⁷⁹ and TRPC6,²⁸⁰ and of the melastatin TRP subfamily, mainly $[Ca^{2+}]_{cyt}$ -activated TRPM4.²⁶³ Of note, various ion channels primarily operated by voltage-gated mechanisms, also exhibit mechano-sensitive properties, including the I_{CaL} channel,²⁸¹ I_{Ks} channel,²⁸² I_{Na} channel,²⁸³ and the Na^+/H^+ exchanger.²⁸⁴ Recently, it has been shown that the $Na_v1.5$ antagonist ranolazine also effectively inhibits the mechano-sensitivity of the Na^+ channel decreasing the pressure-induced window current and late current.²⁸⁵ The I_{Ks} channel is upregulated by hypotonic-induced myocyte stretch (besides stretch-induced increased Cl^- current) causing action-potential shortening in guinea pig myocytes. Interestingly, a human stretch-sensitive *KCNQ1* mutation (R14C) has been reported that is associated with shortened APD (in computer models) and familial atrial fibrillation upon atrial dilation.²⁸⁶ To the best of our knowledge, there is no evidence for stretch-induced modulation of the I_{Kr} channel.

At least two main classifications of SACs have been distinguished based on their ion selectivity: (1) cation non-selective stretch-activated channels (SAC_{NS}) that are permeable to a variety of cations including Na^+ , K^+ , and Ca^{2+} , and can be inhibited by GsMtx-4 a small peptide found in the venom of the tarantula *Grammostola spatulata*,²⁸⁷ (2) K^+ selective stretch-activated channels (SAC_K).^{278, 288} As is depicted in **Figure 2.1B**, SAC_{NS} have a reversal potential around 0 to -20 mV (AP-plateau level; current of approximately 25 pS), whereas SAC_K have a reversal potential at -90 to -95 mV (well below the cardiac myocyte resting membrane potential; 100 pS).^{276, 289, 290}

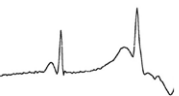
SAC activation can either lengthen or shorten the APD, depending on the timing of the mechanical trigger during the AP.^{268, 280} A depolarizing current can be evoked when a transient stretch is applied near the end of the AP at voltages more negative than the SAC_{NS} reversal potential evolving into frank EADs under conditions of oxidative stress.²⁷² However, although there is considerable evidence that SAC activation can alter AP amplitude, duration and resting potential, there is still a giant leap of understanding between cellular findings and clinical arrhythmias, especially regarding LQTS-associated arrhythmias. Based on (1) the

known reversal potentials of non-selective stretch-activated cation channels and K^+ -selective stretch-activated channels, (2) the finding that stretch-activated inward currents promote EADs in myocytes under oxidative stress, (3) the involvement of stretch-activated membrane excitation and arrhythmias in canine and rabbit whole-heart preparations, and (4) the temporal relation between aftercontractions (as potential stretch activators), EAD upstrokes and T-wave deflections, we believe that such role is likely under specific torsadogenic conditions. We argue that fluctuating mechanical impact changes electrical characteristics,²⁹¹ and if electrical properties are regionally heterogeneous, as in the congenital LQTS, or if tissue mechanosensitivity is inhomogeneous, then spontaneous mechanical events such as aftercontractions can elicit electrical responses that may trigger arrhythmia (see **Figure 2.2**).

REGIONAL MOLECULAR AND CELLULAR HETEROGENEITY: EFFECTS ON MYOCARDIAL Ca^{2+} HANDLING, REPOLARIZATION AND ARRHYTHMOGENESIS

Across the LV-transmural wall, distinct morphologies of AP, cell shortening and intracellular Ca^{2+} transient are found, at least in cellular and tissue experiments. Epicardial APs have the most pronounced spike-and-dome morphology. The hallmark of midmyocardial APs is their ability to prolong with slowing of the pacing rate with much more accentuation than at the epi- and endocardium, although the extent to which this will happen in situ is a matter of ongoing debate.²⁹² Epi- and midmyocardial cells express a shorter latency in the onset and time to peak of cell shortening than endocardial myocytes. The relaxation of cell shortening and Ca^{2+} transient lasts significantly longer in endo- than epicardial myocytes. As a possible consequence, Ca^{2+} -transient alternans and increased diastolic levels of intracellular Ca^{2+} may occur preferentially closer to the endocardial surface. In line with this, pharmacological studies have shown that Ca^{2+} -dependent DADs and EADs, as well as triggered activity, develop much more readily in tissues from the subendocardial/midmyocardial region than at the epicardium.¹⁰²

Non-uniform expression of ion channels and other transporters underlies physiological transmural, interventricular, anteroposterior and apicobasal electric heterogeneity necessary for optimal excitation-contraction coupling.^{99, 100} Transmural molecular expression of NCX is found to be the largest in epi- and midmyocardium compared to endocardium^{103, 293} which is confirmed by prominent mRNA expression in epicardium.²⁹⁴ In non-failing myocardium, mRNA expression of the ryanodine receptor gene is largest in the midmyocardium¹⁰⁵ and much lower at the endocardium.^{105, 295} mRNA expression of SERCA is significantly lower in the endocardial compared to the subepicardial region.^{101, 104, 295} These spatial heterogeneities in molecular expression of Ca^{2+} -cycling proteins result (at least partly) in a lower peak of Ca^{2+} amplitude (-32%), a 16% longer rise time and slower Ca^{2+} reuptake, with a 24% larger Ca^{2+} decay time constant and 9% longer Ca^{2+} transient duration in endocardium versus epicardium. These transmural differences in Ca^{2+} cycling likely contribute to the heterogeneous APD characteristics of the myocardial layers and can be



important for arrhythmogenesis. Under conditions of enhanced Ca^{2+} entry such as during I_{Ks} blockade, beta-adrenergic stimulation and rapid pacing, $[\text{Ca}^{2+}]_{\text{cyt}}$ increased more at the endocardium than at the epicardium.¹⁰² Spontaneous SR Ca^{2+} release occurred predominantly at the endocardium (earliest onset, largest amplitude) rendering this layer the most vulnerable for DAD- and EAD-mediated triggered activity.

Besides spatial heterogeneous expression and function of Ca^{2+} -cycling proteins, there is physiological non-uniformity in the distribution of repolarizing potassium currents. The density of I_{Ks} is found lowest in the midmyocardium compared with the subepicardium and subendocardium.²⁹⁶ Also, I_{Ks} is more prevalent in basal than in apical regions.²⁹⁷ Finally, there is an interventricular difference with a 50% larger density of I_{Ks} in RV midmyocardium compared with LV midmyocardium.²⁹⁸ In ferret, ERG transcript and protein expression was most abundant in the epicardial cell layers throughout the ventricle, with the exception of the basal regions.²⁹⁹ Pharmacological inhibition and congenital defects (mutations in *KCNQ1*, *KCNH2* or *KCNE* family) of I_{Kr} or I_{Ks} exaggerate this innate repolarization disparity facilitating arrhythmia under specific conditions.

MECHANICAL DISPERSION IN HETEROGENEOUS REPOLARIZATION

LQTS is often considered to be a “primary electrical” cardiomyopathy without deviant mechanical characteristics. However, if one considers the marked spatiotemporal heterogeneous repolarization and non-uniform regional Ca^{2+} transients with sporadic local Ca^{2+} releasing events, it would be highly unlikely that myocardial mechanical performance is unaffected, particularly during the dynamic beat-to-beat alterations prior to TdP.

In 1991, Schwartz and colleagues reported for the first time discrete aberrant mechanical behavior in symptomatic LQTS patients²³⁴ assessed by echographic M-mode imaging. Ventricular wall motion abnormalities, primarily located in, but not restricted to, the LV posterior wall, were characterized by faster early contraction kinetics and a protracted contraction plateau phase prior to rapid relaxation. These mechanical abnormalities were more prevalent in symptomatic than in asymptomatic LQTS patients (77% versus 19%), and were associated with a higher risk of cardiac arrhythmic events thus bearing prognostic value. In 55% of LQTS patients the late systolic phase harbored a secondary inward motion, or contraction, of the LV-endocardium, termed a ‘double-peaked’ pattern. This was even more strongly correlated with cardiac events as it was present in 91% of symptomatic subjects. Notched T waves were present in 88% of patients with mechanical abnormalities as opposed to 27% of the individuals with normal mechanics. Moreover, 92% of patients with the double-peaked pattern displayed T-wave notching. This suggests that altered mechanical dynamics influence cardiac repolarization via mechano-electric coupling. Whereas human sympathetic modulation via beta-adrenergic receptor blocker or left cardiac stellate denervation did not significantly influence the two mechanical indices, Ca^{2+} -channel blockade (verapamil 10 mg) had impressive effects on aberrant mechanical behavior, completely normalizing it.²³⁷ In addition, verapamil significantly reduced the QTc

interval in LQTS patients, again supporting a relationship between electrical activity and underlying mechanics. More evidence for the antiarrhythmic effects of Ca^{2+} -blockade comes from a case report of a LQT2 patient in whom verapamil combined with permanent pacing prevented TdP.³⁰⁰ These findings suggest that altered cellular Ca^{2+} handling contributes to the contraction abnormalities in LQTS patients.

Recently, Haugaa and coworkers examined mechanical abnormalities in LQTS-mutation carriers using tissue-Doppler imaging (TDI).³⁰¹ Myocardial contraction duration, as assessed by myocardial velocity or strain traces from Q onset on ECG to zero-crossing of the TDI velocity curve, was significantly longer in symptomatic LQTS mutation carriers than in asymptomatic carriers or healthy controls (460 ± 60 ms versus 400 ± 60 ms versus 360 ± 40 ms, respectively). In LQTS, myocardial contraction exceeded the time to aortic valve closure and often a significantly pronounced post-ejection velocity was observed, defined as a post-ejection peak after closure of the aortic valve. The latter was predominantly distributed in the posteroseptal region, but also in the anteroseptal, anterior and lateral wall. Importantly, receiver-operating-characteristic (ROC) curve analysis revealed that myocardial contraction duration identified genotyped symptomatic LQTS patients better than QTc interval. Also, in all symptomatic mutation carriers with a normal QTc interval, contraction duration was still prolonged. Mechanical dispersion, assessed as the standard deviation of contraction duration, was significantly greater in symptomatic than asymptomatic single-mutation carriers. Speckle-tracking enabled to non-invasively discriminate between subendocardial (or longitudinal) and midmyocardial (or circumferential) fiber mechanics. LQTS mutation carriers, either symptomatic or asymptomatic, demonstrated more pronounced transmural mechanical dispersion in the interventricular septum and anterior LV wall.³⁰² In symptomatic patients the mean longitudinal contraction duration was longer than the circumferential (460 ± 45 ms versus 445 ± 45 ms), indicative of transmural mechanical dispersion. On the contrary, in healthy controls and asymptomatic carriers transmural mechanical inhomogeneity was negligible. This mechanical dispersion in LQTS likely reflects differences in repolarization and Ca^{2+} handling between adjacent myocardial regions.

THE ELECTROMECHANICAL WINDOW

In healthy subjects the duration of cardiac electrical and mechanical activity are closely matched. The electrical systole (equivalent to the QT interval) ends earlier than the completion of contractile relaxation, creating a positive electromechanical window. The EMW (in ms) can be measured invasively (end of LV pressure (LVP_{end}) minus T_{end}) or non-invasively by the time lag between T_{end} and the second heart sound (QS_2 minus T_{end} ; albeit without a final phase of relaxation), with mean values of 26 ± 13 ms.³⁰³ A negative EMW, formerly referred to as inverted QT/ QS_2 ratio or 'QT> QS_2 Syndrome', occurs if either LV-contraction duration shortens or if the QT-interval prolongs (or a combination of both). A negative EMW has been linked to increased mortality risk in various cardiac diseases, such as prolonged QT in the setting of coronary artery disease³⁰³ and mitral-valve prolapse,³⁰⁴



and can be pronounced during an increased autonomic tone.^{305, 306} Vincent and coworkers were the first to report on an increased baseline QT/QS₂ ratio in an ungenotyped Romano-Ward family.³⁰⁷ This ratio further augmented upon exercise. Recently, a markedly negative EMW preceding TdP onset was demonstrated in a canine model of drug-induced LQT1 and beta-adrenergic provocation (**Figure 2.2**).^{112, 113} Here, the temporal relationship of a negative EMW and the generation of late EADs is demonstrated. The EMW (highlighted in pink in **Figure 2.2**) was negative enough (reaching levels of -100 to -200 ms) to allow the occurrence of LV aftercontractions well before the end of repolarization. As such, we believe that the EMW, and particularly the occurrence of aftercontractions, could contribute to arrhythmogenesis via stretch-activated membrane excitation, at least on theoretical grounds. Obviously, more experimental work is necessary to examine this further. In the LQT1 model, the induction of TdP was prevented by verapamil, esmolol and atenolol, significantly increasing the EMW to less negative values and eliminating the aftercontractions. Recent clinical data obtained within our team reinforce the notion that ventricular mechano-electric interactions may conspire to induce TdP in the presence of a profoundly negative and very dynamic EMW (**Figure 2.3**).

As opposed to this dynamicity of the EMW during beat-to-beat instability prior to TdP onset, we have found in LQTS patients in stable clinical conditions and during sinus rhythm that the aortic valve closes on average 60 ms earlier than the end of the T wave. We assessed ventricular electromechanical disparity in 53 genotyped LQTS patients compared to 25.³⁰⁸ In the LQTS group, 31 carriers experienced ≥ 1 arrhythmic event, compared to 22 event-free individuals and/or asymptomatic carriers. Mean EMW was significantly more negative in the LQTS-mutation carriers than in controls (-60 ± 59 ms versus 4 ± 27 ms), and was even more negative in symptomatic than in asymptomatic mutation carriers (-75 ± 68 ms versus -39 ± 36 ms). Subgroup analysis of LQT1 and LQT2 mutation carriers did not show statistically different EMW values.

In summary, these findings strongly imply that a negative EMW *per se* is not the *primum movens* but it renders the intact heart vulnerable to additional arrhythmogenic impact such as aftercontractions elicited by sympathetic nervous stimulation. As such, the dynamicity of the EMW is a potentially important proarrhythmic parameter, but causal mechano-electric relations remain to be elucidated.

SYMPATHETIC STIMULI OF TdP IN LQTS

It is well-known that sudden or tonic sympathetic stimulation can provoke ventricular tachyarrhythmias, notably TdP, in congenital LQTS. Differential responsiveness to sympathetic stimuli by various triggers has been observed in LQT1 versus LQT2.

In LQT1 due to loss-of-function mutations in *KCNQ1* encoding the alpha-subunit of I_{Ks}, 68% of the lethal arrhythmias were encountered during episodes of exercise, 26% during emotion and only 3% during rest/sleep.¹⁵¹ I_{Ks} contributes trivially to repolarization under basal conditions, but is of paramount importance for repolarization shortening in setting of

sympathetic-mediated rate acceleration and through direct stimulatory effects.³⁰⁹ Maladaptive I_{Ks} by a loss-of-function mutation fails to accommodate APD adequately and allows for the overriding of Ca^{2+} -dependent inward currents, which facilitates EAD- and DAD-induced abnormal impulse formation and reentrant excitation by regional dispersion of repolarization. Increasing the outward current with nicorandil, an $I_{K,ATP}$ opener, improved repolarization abnormalities, abolished EADs and prevented ventricular premature complexes during epinephrine infusion in genotyped LQT1 patients with previous syncope, TdP and/or palpitations.³¹⁰ Shimizu and coworkers provoked beta-adrenergic-EADs in LQTS patients, which prolonged monophasic action potentials (MAPs) and were accompanied by de-novo secondary T-wave components and arrhythmia.^{311, 312} Verapamil and propranolol effectively suppressed these arrhythmogenic responses. Unfortunately, no pressure recordings were obtained to examine mechanical events that might have accompanied the EADs.

By contrast, in LQT2 due to loss-of-function mutations of *KCNH2* encoding the alpha-subunit of I_{Kr} lethal arrhythmias occurred during exercise in only 13% of cases, during emotion in 43% and at rest/sleep in 29%.¹⁵¹ LQT2 patients were particularly vulnerable to auditory stimuli³¹³ and this may differentiate them from LQT1 patients.³¹⁴ Due to its rapid activation kinetics I_{Kr} contributes prominently to repolarization under basal conditions. When it is defective, even slight decreases of $[K^+]_o$ or bradycardia can dramatically prolong the APD and generates EADs.³¹⁵ Additional sympathetic stimulation (such as during auditory stimuli) may provoke EADs due to predominant PKA-dependent upregulation of I_{CaL} rather than I_{Ks} in the first seconds of response. This is a particularly vulnerable window for arrhythmogenesis.

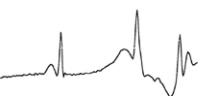
In the case of LQT3, triggers of cardiac events occurred mostly during sleep or (39%), but exercise, emotion and other triggers were still accountable in a significant number of cases.¹⁵¹

IN-VIVO OCCURRENCE OF AFTERCONTRACTIONS

CANINE LQT1 MODEL

In 2007, Gallacher and coworkers¹¹² described an in-vivo anesthetized dog model of drug-induced LQT1 by selective I_{Ks} blockade with HMR1556 (**Figure 2.2**). Beta-adrenergic receptor stimulation on top of I_{Ks} blockade evoked paradoxical QT and LV-endocardial repolarization prolongation during heart-rate acceleration, beat-to-beat endocardial repolarization instability, and TdP in 94% of the animals. Of note, neither programmed electrical stimulation nor electrical remodeling was required for TdP induction under these conditions.

Sizeable aftercontractions (black arrow heads in **Figure 2.2**) emerged during isoproterenol infusion, consistently preceding TdP in a crescendo manner. Aftercontraction amplitudes averaged peak pressures of 25 ± 6 mm Hg (17% of 'normal' AP-evoked



contractions, with incidental examples of even higher amplitudes). Of note, these contractile eruptions appeared only in the LV, not in the RV. In MAP recordings, concomitant late EADs appeared on the endocardial surface of the LV, not on the LV epicardium or in the RV. These in-vivo findings match well with the results reported by Katra and Laurita¹⁰² of a predominant endocardial origin of triggered activity in a canine LV-wedge model of drug-induced LQT1 syndrome. In **Figure 2.2**, note the marked disparity (shaded pink areas) between the end of the electrical systole and the end of relaxation, appearing as a negative EMW, during I_{Ks} blockade and beta-adrenergic provocation compared to a completely different interrelation during I_{Ks} blockade alone (shaded green area). Focusing on temporal relationships, one should note that the initiation of LV aftercontractions preceded the MAP EADs by tens of ms (dashed black line), occurring even without EADs in some cases (data not shown). Interestingly, the de-novo secondary T wave components on the surface ECG (indicated by the diagonal black arrows in **Figure 2.2**) also appeared secondary to the initiation aftercontractions.

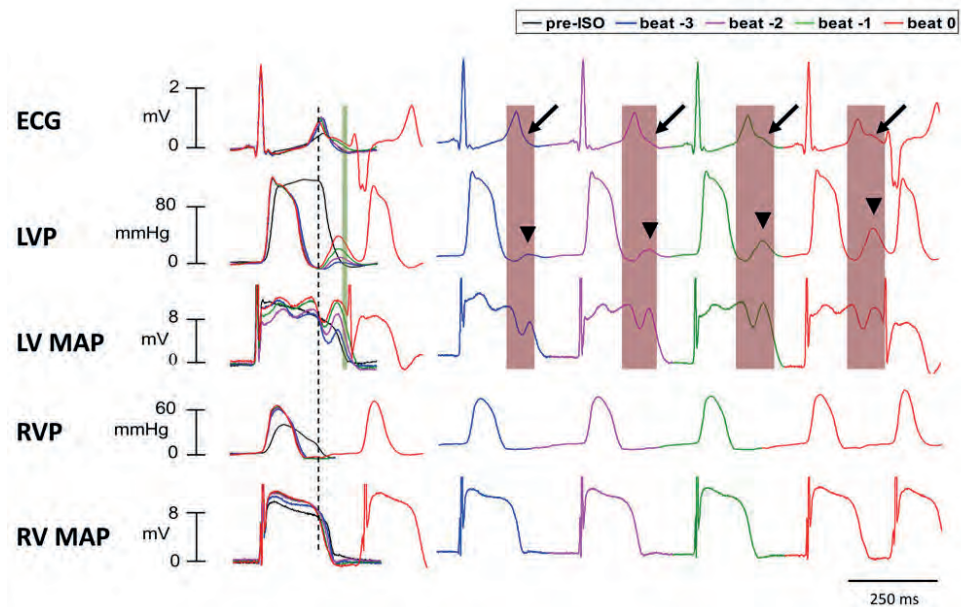


Figure 2.2 In-vivo recordings of electromechanical heterogeneity in the final sinus beats prior to TdP onset (right most beat) in a canine model of drug-induced LQTS type 1 and isoproterenol challenge. Pink columns highlight a markedly negative EMW with crescendo aftercontractions emerging from the LVP signal (black arrow heads). By contrast, the narrow grey column at the left indicates a minimal positive EMW during I_{Ks} inhibition prior to isoproterenol. Dashed vertical black line, timing of events in relation to the initiation of LV aftercontractions. The black arrowheads in the LVP recording appoint emerging aftercontractions. The black arrows on the ECG point at the rising of a secondary component of the T wave that parallels the mounting amplitude of aftercontraction. LVP left ventricular pressure; LV MAP left ventricular monophasic action

potential; RVP right ventricular pressure; RV MAP right ventricular monophasic action potential. [Reproduced and modified with permission from¹¹²].

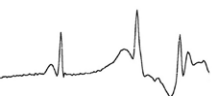
These in-vivo findings are in accordance with the temporal coincidence found in canine ventricular myocytes by Volders and coworkers,⁹⁸ suggesting a common primary role for spontaneous regenerative SR Ca²⁺ release in delaying repolarization (conditioning phase). It is obvious that the electromechanical properties of a single myocyte are only a pale shadow of the complex biophysics of the intact beating heart, in which many additional factors such as spatial and temporal dispersion of myocardial repolarization, sympathetic nerve activity and regional nerve arborization, local electrolytes and electromechanical and mechano-electric coupling are crucial for arrhythmogenesis.

MECHANO-ELECTRIC HETEROGENEITY AND TdP IN HUMAN LQTS

The first report on the clinical relevance of human mechano-electric arrhythmogenesis was recently described by Moers and Volders.¹¹⁴ A 51-year old patient with a prolonged resting QT interval of 600 ms and unexplained syncope was examined. Programmed electrical stimulation during invasive electrophysiological study failed to induce ventricular tachycardia, after which beta-adrenergic provocation testing with isoproterenol was performed. Upon isoproterenol, pseudonormalization of deviant T-wave morphology, inappropriate QT-interval accommodation and a substantially negative EMW of -50 to -100 ms were noted. Interestingly, intracardiac pressure signals revealed LV (but not RV) aftercontractions during relaxation, frequently preceding ectopic impulse formation or non-sustained ventricular tachycardia. These aftercontractions could reach impressive peak amplitudes up to 100 mm Hg (mean amplitudes of 29 mm Hg). Prolonged diastolic intervals, i.e. after pacing trains or premature ventricular beats, preceded the aftercontractions in a consistent manner. Infusion of esmolol or verapamil prevented the LV-systolic aftercontraction and related ventricular arrhythmia, in spite of preserved augmented inotropic and chronotropic state. These findings strongly suggest a prominent role for increased myocardial Ca²⁺ loading for mechano-electric events. The patient was treated with metoprolol and during 3 years of follow-up, no syncope occurred and no cardiac arrhythmic events were documented. To this date, no mutations in LQTS or catecholaminergic-polymorphic VT genes have been found yet.

We also assessed the complex interplay between mechanics and electrics in a 38-year-old female, with LQT3 (*SCN5A* p.(Phe1617del)), admitted to our hospital because of electrical storm due to recurrent TdP (**Figure 2.3**).

Her baseline ECG showed marked QTc prolongation of 585 ms with biphasic T-waves. During isoproterenol infusion her heart rate increased to 90 bpm, shortening ventricular repolarization and preventing TdP. Within a few minutes after cessation of isoproterenol, short-long-short cycle-length sequences recurred, followed by TdP. Exactly at that moment, by coincidence, TDI signals were recorded from the basal anterolateral wall during echocardiography, which later allowed a critical analysis of the electrical and mechanical



phenomena prior to arrhythmic deterioration. **Figure 2.3** shows these data, indicating the evident discrepancy between the duration of electrical (in green) and mechanical systole (in pink). Here, the EMW approximated -160 ms. In this vulnerable window one can appreciate sizeable secondary positive velocity increments (asterisks) after the initial descent in the velocity curve. As the vertical white lines indicate, the timing of these secondary mechanical contractions (asterisks) approximated or even preceded the corresponding ventricular premature beats. We propose that these are tissue-Doppler velocity derivatives of arrhythmogenic LV aftercontractions during a negative EMW. If these aftercontractions activated SACs, the resultant change in membrane excitation could evoke abnormal impulses, potentially triggering TdP.²⁸⁹

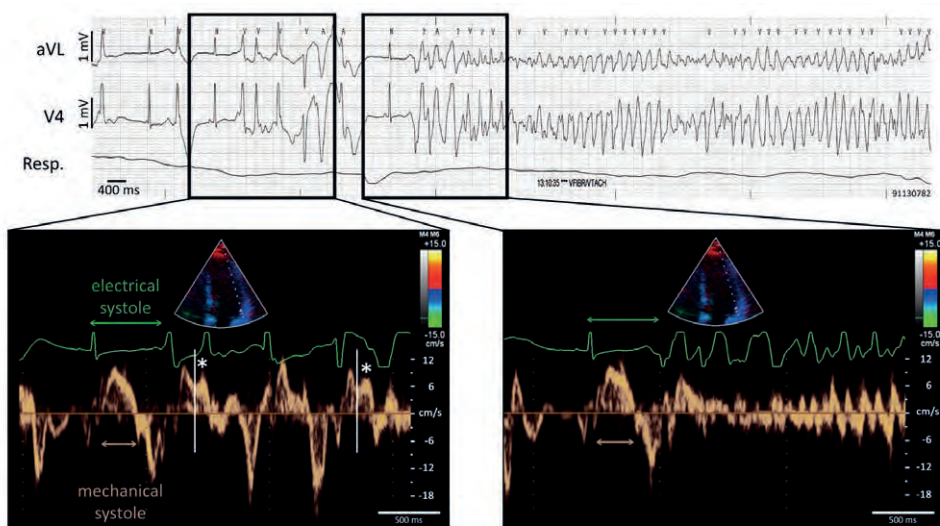


Figure 2.3 Recordings of electromechanical instability in a patient with LQT3 (F; 38 yr) who suffered from recurrent TdP. The TdP shown here occurred shortly after the attempted withdrawal of antiarrhythmic β -sympathomimetic therapy. The upper panel (ECG leads aVL and V4, and respiration signal (Resp.)) shows sinus rhythm with ventricular ectopic beats having mostly narrow QRS complexes with coupling intervals from 300 to 650 ms. A classical short-long-short sequence ignites TdP. The lower panels display simultaneous TDI signals obtained from the basal lateral LV wall. The time sequence for excitation-contraction coupling is normal in the sinus beats. The duration of the mechanical systole (pink double arrow) is profoundly shorter than the electrical systole (green double arrow), rendering an electromechanical window of -190 ms. Two aftercontractions (*) are noted that start *prior* to the initiation of associated ventricular ectopic complexes (white lines). Both have a markedly short coupling interval of 300 ms. [Courtesy of Bas L.J.H. Kietselaer, MD, PhD and Dirk W. Donker, MD, PhD, Department of Cardiology, Maastricht University Medical Centre, The Netherlands].

CONCLUDING REMARKS

In present article, we reviewed the complex and dynamic interplay of electromechanical, mechano-electric, and sympathetic factors conspiring to torsadogenesis in the LQTS. The most important aspects are summarized in **Figure 2.4**. Intrinsic spatiotemporal dispersion of myocardial repolarization, Ca^{2+} handling and mechanics, present under normal conditions, is generally larger in LQTS. Cycle-length dependent amplification of repolarization dispersion and the generation of EADs promote reentrant excitation by causing functional block.³¹⁶ This prolonged repolarization-dependent reexcitation³¹⁷ fuels the arrhythmogenic substrate, although cell-to-cell coupling smoothens disparities in the intact heart. Altered Ca^{2+} transients determined (at least partly) by prolonged APD impose an “inotropic”-like effect.

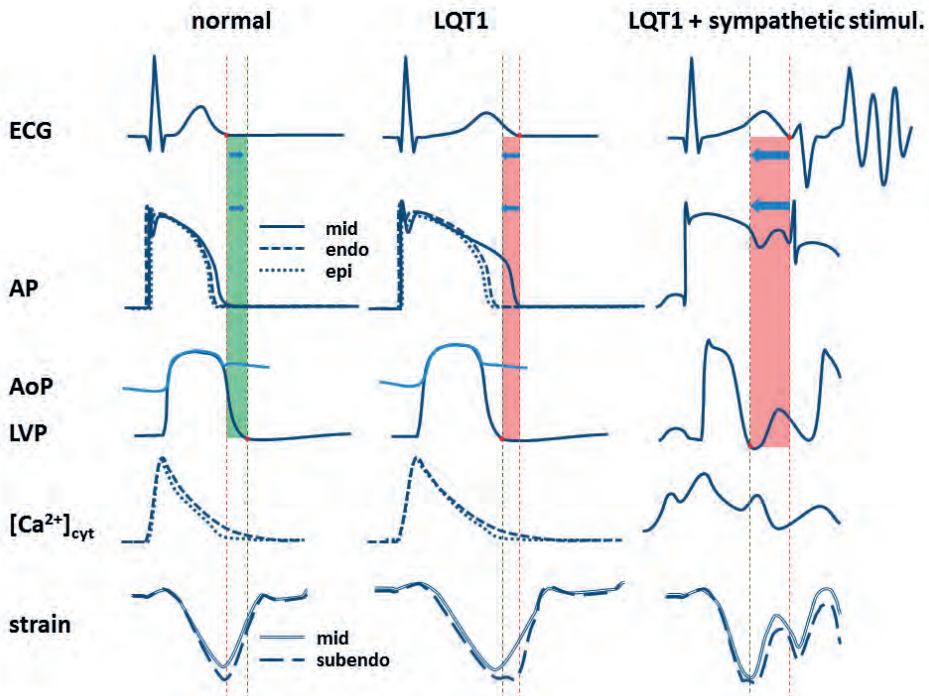
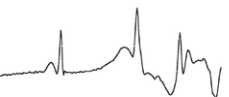


Figure 2.4 Schematic of the central theme of this paper: mechano-electric heterogeneity, altered myocyte Ca^{2+} handling and spontaneous SR Ca^{2+} release conspiring to abnormal ventricular impulse formation and TdP in LQTS. Left, in normal individuals (**normal**) there is only modest transmural dispersion of repolarization, a small positive EMW (green column), a short time-to-peak strain, and simultaneous strain peaks of the transmural layers. Middle panels, in LQTS type 1 (**LQT1**), marked dispersion of repolarization, a prolonged Ca^{2+} transient with a longer time constant of relaxation at the endocardium than at the epicardium, and a negative EMW (pink column) are observed. Strain imaging displays the longest contraction duration at the subendocardium (subendo). Right panels, upon the addition of intense sympathetic stimulation (**LQT1 + sympathetic stim.**), myocardial Ca^{2+} loading occurs that increases the probability of spontaneous SR Ca^{2+} release and the generation of DADs, EADs and aftercontractions during a profoundly negative EMW (pink column). These events promote abnormal ventricular impulse formation and the initiation of TdP via $[\text{Ca}^{2+}]_{\text{cyt}}$ - and mechano-



dependent pathways, and reentrant mechanisms (latter not shown). The LV-strain traces in the right lower panel are inferred by the authors. AP indicates action potential; AoP, aortic pressure; LVP, left-ventricular pressure; $[Ca^{2+}]_{\text{cyt}}$, cytoplasmic Ca^{2+} concentration, Ca^{2+} transient.

In LQT1, sympathetic stimulation fails to upregulate I_{Ks} sufficiently, but promotes $[Ca^{2+}]_{\text{cyt}}$ accumulation and enhanced lusitropy. Hence, the EMW decreases to negative values and ventricular repolarization dispersion increases (**Figure 2.4**). Spontaneous SR Ca^{2+} release underlies beta-adrenergic EADs and DADs, which may trigger abnormal impulses, and aftercontractions. The latter have been demonstrated in the intact beating heart.

After thorough review of the literature and analysis of original electromechanical recordings in experimental animals and humans, we argue that mechano-sensitive (besides $[Ca^{2+}]_{\text{cyt}}$ -dependent) ion-channel activation contributes to torsadogenesis in LQTS, particularly if sizeable systolic and/or diastolic aftercontractions emerge in the presence of a negative EMW such as during enhanced sympathetic nerve activity. Here, mechano-dependent proarrhythmia is very probable, an argument that is strengthened by (1) the known reversal potentials of SAC_{NS} and SAC_K , (2) the observation of stretch-induced EADs in myocytes under oxidative stress, (3) the documentation of stretch-activated membrane excitation and arrhythmias in whole-heart preparations, and (4) the temporal relation between aftercontractions (as potential stretch activators), EAD upstrokes and T-wave deflections just prior to TdP.

More than 20 years after Zipes' referral to the Rosetta Stone for the understanding of sympathetic-induced ventricular tachyarrhythmias in the LQTS,³¹⁸ we propose that "mechano-electric coupling" constitutes one of the proarrhythmic complexities of torsadogenesis.

EDITORS' NOTE

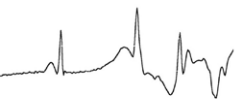
Please see also related communications in this issue by Hales³¹⁹ and Blazeski.³²⁰

ACKNOWLEDGEMENTS

RMAAtB is supported by the Foundation "Sint Annadal", Maastricht, The Netherlands, and PGAV by a Vidi grant from the Netherlands Organization for Scientific Research (ZonMw 91710365). Roel L.H.M.G. Spätjens, BSc, Department of Cardiology, Cardiovascular Research Institute Maastricht, The Netherlands assisted in the making of the figures.



“Ogen geven aan de patiënt is belangrijk, maar om de mens met zijn vragen te begrijpen is het belangrijk dat de arts zijn ogen ook zelf gebruikt om echt te willen en kunnen zien wie de patiënt is, en niet alleen vanuit aannames te blijven zenden!”



3

ELECTROMECHANICAL WINDOW NEGATIVITY IN GENOTYPED LONG-QT SYNDROME PATIENTS: RELATION TO ARRHYTHMIA RISK

Rachel M.A. ter Bekke, Kristina H. Haugaa, Arthur van den Wijngaard, J. Martijn Bos,
Michael J. Ackerman, Thor Edvardsen, Paul G.A. Volders

Eur Heart J 2015;36:179-186

ABSTRACT**AIMS**

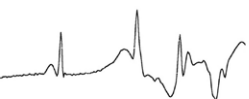
Prolonged and dispersed left-ventricular contraction is present in patients with long-QT syndrome. Electrical and mechanical abnormalities appear most pronounced in symptomatic individuals. We focus on the “electromechanical window” (duration of LV-mechanical systole minus QT interval) in patients with genotyped LQTS. Profound EMW negativity heralds torsades de pointes in animal models of drug-induced LQTS.

METHODS AND RESULTS

We included 244 LQTS patients from three centres, of whom 97 had experienced arrhythmic events. Seventy-six matched healthy individuals served as controls. QT interval was subtracted from duration of Q-onset to aortic-valve closure midline assessed noninvasively by continuous-wave echocardiography, measured in the same beat. EMW was positive in controls but negative in LQTS patients (22 ± 19 versus -43 ± 46 ms; $P < 0.0001$), being even more negative in symptomatic than event-free patients (-67 ± 42 versus -27 ± 41 ms; $P < 0.0001$). QT, QTc, and QAoC were longer in LQTS subjects (451 ± 57 , 465 ± 50 , and 408 ± 37 ms, $P < 0.0001$). EMW was a better discriminator of patients with previous arrhythmic events than resting QTc (AUC 0.77 (95% CI, 0.71-0.83) and 0.71 (95% CI, 0.65-0.78); $P = 0.03$). In multivariate analysis, EMW predicted arrhythmic events independently of QTc (odds ratio 1.25; 95% CI, 1.11-1.40; $P = 0.001$). Adding EMW to QTc for risk assessment led to a net reclassification improvement of 13.3% ($P = 0.03$). No EMW differences were found between the three major LQTS genotypes.

CONCLUSIONS

Patients with genotype-positive LQTS express EMW negativity, which is most pronounced in patients with documented arrhythmic events.



INTRODUCTION

The congenital long-QT syndromes are caused by mutations in genes encoding for cardiac ion-channel subunits or ion-channel-associated proteins. To date, at least 15 different genes have been causally implicated.³²¹ LQTS-related ion-channel defects predispose to cardiac action-potential prolongation and accentuate regional and temporal dispersion of repolarization. Genotype-specific proarrhythmic conditions can exacerbate repolarization dispersion and lead to the occurrence of afterdepolarizations, premature ventricular ectopic beats and reentrant excitation. These mechanisms can precipitate torsades de pointes in susceptible LQTS patients, but their exact contribution to arrhythmogenesis remains often obscure. Additional mechanisms, including mechano-electrical triggers, appear relevant, but remain to be fully elucidated.³²²

There have been reports of altered ventricular mechanics in (subsets of) LQTS patients. Using M-mode, Nador *et al*²³⁴ demonstrated rapid early contraction and an extended phase of LV-wall thickening before rapid relaxation in 55% of LQTS patients, being most overt in symptomatic individuals. In some, mostly symptomatic, patients a peculiar double-peak pattern of LV-wall thickening was observed, possibly the mechanical correlate of early afterdepolarizations.²³⁴ These LQTS-related mechanical abnormalities were normalized by Ca²⁺-channel blocker treatment.²³⁷ Similar results were obtained using tissue-Doppler imaging techniques.^{236, 301} Strain-imaging revealed longer contraction duration in the subendocardium than midmyocardium of symptomatic LQTS-mutation carriers (but less so of asymptomatic or healthy individuals), indicating accentuated transmural mechanical dispersion in the former.³⁰¹ Prolonged contraction duration and augmented longitudinal mechanical dispersion were superior to QTc for arrhythmia-risk assessment.^{301, 302}

Only few studies have addressed indices of electromechanical coupling in LQTS patients to assess arrhythmia risk. In 1991, Vincent *et al*³⁰⁷ reported on the ratio of electrical to mechanical systole in an ungenotyped Romano-Ward family. By measuring QT interval and time from Q wave to second heart sound (QS₂), they demonstrated a prolonged QT/QS₂ ratio in rest increasing during exercise (1.12 to 1.45) in Romano-Ward patients with a resting QTc of 490 ms. In controls, QT/QS₂ increased only modestly from a rest ratio of <1.0. The relation of QT/QS₂ to major arrhythmic events was not examined.³⁰⁷

Experimentally, Gallacher *et al*^{112, 113} demonstrated in anesthetized dogs that under baseline conditions the LV-pressure duration outlasts both QT interval and LV-endocardial monophasic-action-potential duration, thus creating a positive so-called “electromechanical window”.¹¹³ EMW turned very negative during pharmacological I_{Ks} block just prior to the induction of TdP by beta-adrenergic stimulation.^{112, 113} Within this negative EMW, sizeable LV aftercontractions arose consistently if TdP ensued.

This led us to investigate EMW in a large population of LQTS probands and their asymptomatic genotype-positive family members, under clinically stable conditions. We compared LQTS patients with healthy controls, with and without beta-blocking therapy. All underwent echocardiography with simultaneous standard 3-lead ECG recording to

determine the EMW noninvasively. We hypothesized that EMW is more negative in LQTS patients than in healthy controls, and that profound EMW negativity correlates significantly with major arrhythmic events.

METHODS

This study was carried out in accordance with the ethical guidelines of the Declaration of Helsinki. Patients gave written informed consent for DNA diagnostics and echocardiographic research. IRB approval for the retrospective analysis of genotype and echocardiographic phenotype data was provided for the patients evaluated at Mayo Clinic.

STUDY POPULATION

In this case-control, multicentre study, 244 genotype-positive LQTS index cases and asymptomatic family members, and 76 healthy controls were included. A heterozygous *KCNQ1* mutation was present in 107 individuals (LQT1), a *KCNH2* mutation in 84 (LQT2), a *SCN5A* mutation in 41 (LQT3), a *KCNE1* mutation in 8 (LQT5), a *KCNE2* mutation in 1 (LQT6), and double heterozygous mutations (*KCNQ1* + *KCNH2*) in 2 patients. The remaining patient was double heterozygote for *KCNQ1* mutations with clinical features of Jervell and Lange-Nielsen syndrome. Mutations were considered “pathogenic” or “variants of uncertain significance” (VUS) based on literature reports and molecular-genetic assessment. Class-3 VUS-positive patients were included after exclusion of other causative gene mutations.

In all probands, the clinical diagnosis of LQTS was made using the Schwartz criteria.³²³ Arrhythmic events were scored as syncope, documented ventricular tachyarrhythmia, aborted cardiac arrest, and/or sudden death. We included subjects older than 10 years. The use of antiarrhythmic drugs and history of ICD or pacemaker implantation at the time of echocardiography were noted. If possible, EMW measurements were made prior to the initiation of antiarrhythmic therapy.

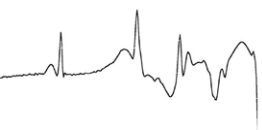
The healthy control group consisted of seventy-six age- and gender-matched individuals, who underwent 12-lead ECG recording and echocardiography because of unexplained dyspnea, palpitations or atypical chest complaints, but with normal findings. None were using QT-prolonging medication. Furthermore, we included 18 individuals, temporarily treated with beta-blockers for suspected angina pectoris, ahead of elective coronary angiography, but with non-significant findings.

ECHOCARDIOGRAPHY

Echocardiographic examinations were performed on a Vivid 7 (General Electric Healthcare, Horten, Norway) or IE33 system (Philips, Eindhoven, The Netherlands) and data were analyzed by R.M.A.t.B. and K.H.H., blinded to the patient’s diagnosis.

EMW CALCULATION

Continuous-wave Doppler images in the apical long-axis view assessing the aortic-valve flow and concurrent 3-lead ECG tracings were used for EMW calculations (**Figure 3.1**). We



measured (1) the interval from QRS onset to the aortic-valve closure midline (QAoC interval), (2) QT interval in lead II, *for the same beat*. The EMW (ms) was calculated by subtracting QT from the QAoC interval. QAoC incorporates the LV-excitation contraction coupling delay, isovolumetric contraction, and ejection time and is taken as an arbitrary derivative of the duration of LV-mechanical systole.³⁰⁶ It is generally accepted to measure the QT interval in ECG lead II or any longest QT time at the precordium. Here, we assessed lead II because this is also available in commercial ultrasound systems, whereas precordial ECG recordings are normally not. Hypothetically, a longer precordially-derived QT would lead to more profound EMW negativity when QAoC remains unaltered. In 6% of our subjects, the 3-lead-echo-related QT interval could not be determined accurately. Instead, contiguous 12-lead ECG-derived QT was obtained at an equivalent RR interval (≤ 25 ms difference). Bazett's formula was used to correct QT for heart rate.

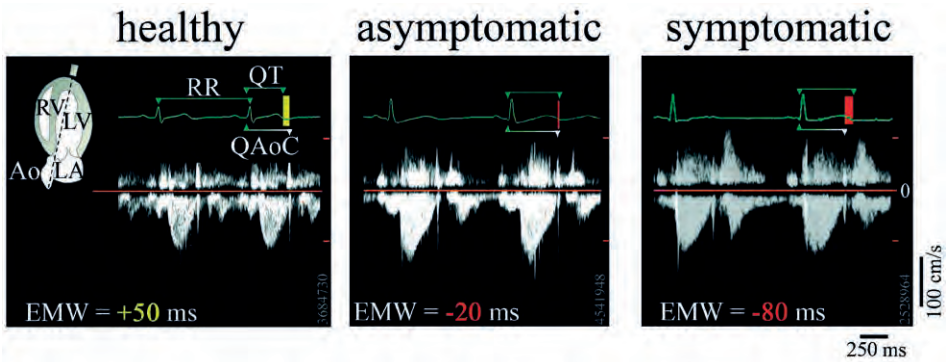


Figure 3.1 Representative EMW calculations in the same beat during continuous-wave Doppler echocardiography of the LV-outflow tract. **Left panel**, EMW positivity (yellow bar) in a healthy individual. **Middle panel**, EMW negativity (red bar) in an asymptomatic LQTS subject. **Right panel**, Profound EMW negativity in a symptomatic patient. QAoC, interval from initiation of QRS to aortic-valve closure; EMW, electromechanical window; RV, right ventricle; LV, left ventricle; LA, left atrium; Ao, ascending aorta.

STATISTICAL ANALYSIS

Continuous data were tested for normality of distribution and depicted as mean \pm SD. Comparison of means in Gaussian-distributed groups was performed by unpaired Student's *t* testing. For nonparametric methods the Mann-Whitney U test was used. For multiple comparisons, one-way ANOVA was applied. ROC curve and logistic regression analysis were established to assess predictive accuracy. The optimal cut-off value for EMW at highest accuracy, sensitivity, and specificity for the optimal cut-off value was determined. The area under the curve (AUC) and 95%-confidence interval (CI) were determined for EMW/QTc/QT. Comparison of ROC curves was performed using the DeLong and DeLong method. The net reclassification improvement (NRI) was calculated using the following risk categories for arrhythmic events: low probability of arrhythmic events (<20%), intermediate (20-60%), high (>60%). The number of patients correctly reclassified when EMW was added to the

QTc-based model was determined and from that the NRI was calculated. *P* values presented were two-sided and considered significant if <0.05 .

RESULTS

CLINICAL CHARACTERISTICS

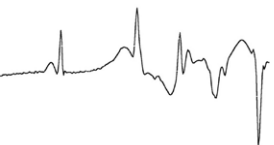
Clinical characteristics of the LQTS population and healthy controls are illustrated in **Table 3.1**. Of the LQTS population 163 (67%) were female and 97 (40%) were classified as “symptomatic”, with 31 having cardiac arrest (documented TdP/VF in 23; mean TdP/VF episodes per patient 2.8 ± 5.9 ; electrical storm in six), resulting in death in two. The remaining 66 patients experienced at least one syncopal event, with documented nonsustained (polymorphic) VT in nine. LQTS patients had lower mean heart rates (66 ± 13 versus 73 ± 14 bpm in controls; $P<0.0001$).

Table 3.1 Characteristics of healthy individuals and LQTS patients

	Healthy individuals (n=76)	LQTS patients (n=244)	<i>P</i> value
Age, y	37 ± 12	38 ± 16	0.57
Female sex, n (%)	51 (67)	163 (67)	0.97
Antiarrhythmic drug at time of echocardiogram			
beta-blocker, n (%)	0	100 (41)	
mexiletine, n (%)	0	6 (2)	
<i>ECG</i>			
RR interval, ms	845 ± 157	950 ± 182	<0.0001
QT interval, ms	357 ± 29	451 ± 57	<0.0001
QTc, ms	391 ± 27	465 ± 50	<0.0001
<i>Echocardiogram</i>			
LV-ejection fraction, %	63 ± 7	63 ± 5	0.83
QAoC interval, ms	379 ± 31	408 ± 37	<0.0001
EMW, ms	22 ± 19	-43 ± 46	<0.0001

LQTS, long-QT syndrome; LV, left ventricular; QAoC, interval from QRS-onset to aortic-valve closure; EMW, electromechanical window.

Forty-one percent of patients were on beta-blocker therapy at the time of echocardiography (for EMW calculation), 23% had been implanted with an ICD, 2% with a pacemaker, and 1 individual had undergone left-cardiac sympathetic denervation. None of the patients were ventricularly paced at the time of investigation. Seventy-five percent harbored a pathogenic mutation in one or more LQTS-related genes, whereas 25% had a VUS, being equally present in symptomatic and event-free subjects. LQTS patients had longer QT intervals and QTc compared to controls (QT: 451 ± 57 versus 357 ± 29 ms; QTc:



465 ± 50 versus 391 ± 27 ms; $P < 0.0001$), with less exaggerated QTc because of inclusion of asymptomatic mutation-positive relatives (i.e., a representative population at the Cardiogenetics Clinic). QAOc was significantly longer in LQTS patients (408 ± 37 versus 379 ± 31 ms; $P < 0.0001$). Combined, these parameters led to negative EMWs in LQTS patients as opposed to positive values in controls (-43 ± 46 versus 22 ± 19 ms; $P < 0.0001$; **Figure 3.2**).

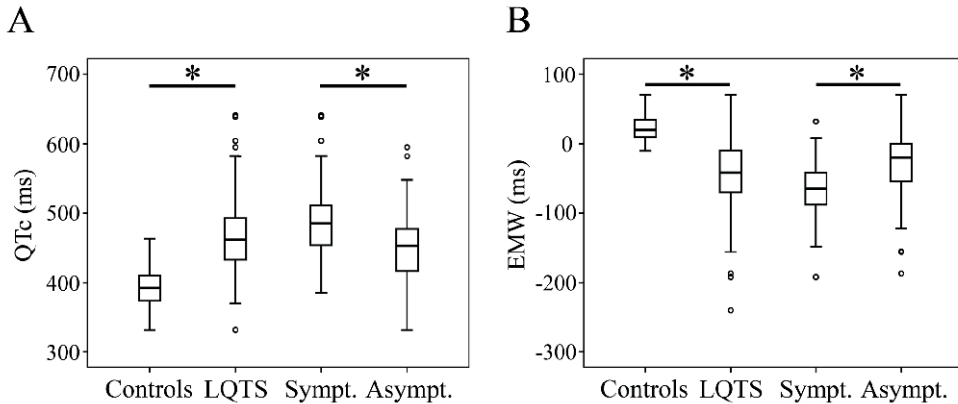


Figure 3.2 Boxplots illustrating the interquartile range and outliers of (A) QTc and (B) EMW in controls and LQTS patients with and without arrhythmic events, ** $P < 0.0001$.

Patients (n=16) with double LQTS mutations, a history of pacemaker implantation or stelletomy, or on mexiletine treatment did not influence the general outcomes of this study. The inter- and intra-observer variability of EMW measurements had a correlation coefficient of 0.91 (95% CI, 0.65-0.98) and 0.99 (95% CI, 0.97-1.0). Serial EMW measurements were similar in 25 clinically-stable patients, after a mean of 48 ± 37 months (-30 ± 49 versus -24 ± 30 ms; $P = 0.33$). There was no difference between echocardiogram-related and standard-ECG lead-II-derived QT and RR intervals (QT: 450 ± 57 versus 459 ± 59 ms, $P = 0.76$; RR: 949 ± 181 versus 973 ± 185 ms; $P = 0.15$). Subgroup analysis of 76 patients with concealed LQTS (i.e., QTc < 440 ms, being on average 412 ± 23 ms) yielded an EMW of -8 ± 32 ms ($P < 0.0001$ versus controls), which was most pronounced in symptomatic individuals (**Figure 3.2**).

EMW AND ARRHYTHMIC EVENTS

Age, gender and genetic diagnosis were similar for symptomatic and asymptomatic LQTS patients (61 versus 28% beta-blocker therapy, respectively, at the time of echocardiography; **Table 3.2**). QT and QTc were longer in the former (QT: 479 ± 56 versus 432 ± 49 ms; QTc: 488 ± 50 versus 450 ± 44 ms; $P < 0.0001$). QAOcs were similar in both groups. Consequently, symptomatic LQTS patients had a more negative EMW: -67 ± 42 versus -27 ± 41 ms ($P < 0.0001$; **Table 3.2**, **Figure 3.2**). Interestingly, when plotting EMW

against QTc (**Figure 3.3**), symptomatic and asymptomatic LQTS patients had more negative EMWs for any given QTc than control subjects, which coincided with a more negative slope of the linear relation and a leftward shift of its crossing of the abscissa.

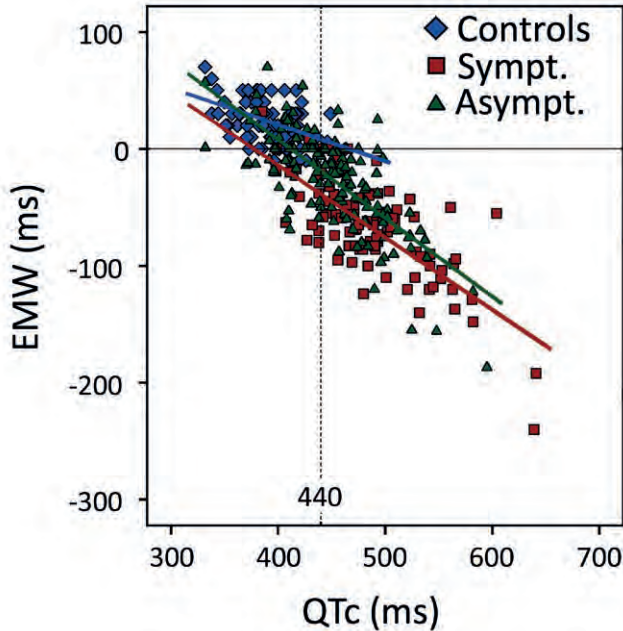
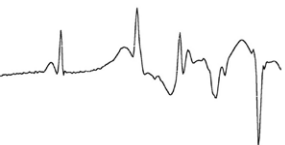


Figure 3.3 EMW as a function of QTc for controls (blue) and LQTS patients with (red) and without (green) previous arrhythmic events. Dotted line indicates QTc 440 ms.

By ROC analysis, EMW proved a better discriminator for arrhythmic events than QTc, with an AUC_{EMW} 0.77 (95% CI, 0.71-0.83), AUC_{QTc} 0.71 (95% CI, 0.65-0.78) and AUC_{QT} 0.74 (95% CI, 0.68-0.81; $P=0.03$; **Figure 3.4**). The optimal cut-off value for EMW with 72% accuracy was -62 ms, identifying symptomatic patients with 84% sensitivity and 54% specificity. Logistic regression analysis identified EMW, QTc, and beta-blocker therapy as univariate predictors of arrhythmic events (**Table 3.3**). After multivariate analysis, EMW (but not QTc) remained an independent predictor (odds ratio for 10-ms EMW decrease 1.25 (95% CI, 1.11-1.40; $P=0.001$)). Adding EMW to QTc in LQTS risk assessment resulted in 12 individuals being correctly reclassified into a higher risk category, as compared to a model without EMW. Seven subjects were incorrectly reclassified into a lower risk category. Similarly, 25 asymptomatic individuals were correctly reclassified into a lower risk category, whereas 13 were incorrectly reclassified into a higher risk category. The net reclassification improvement was 13.3% ($P=0.03$) when adding EMW.



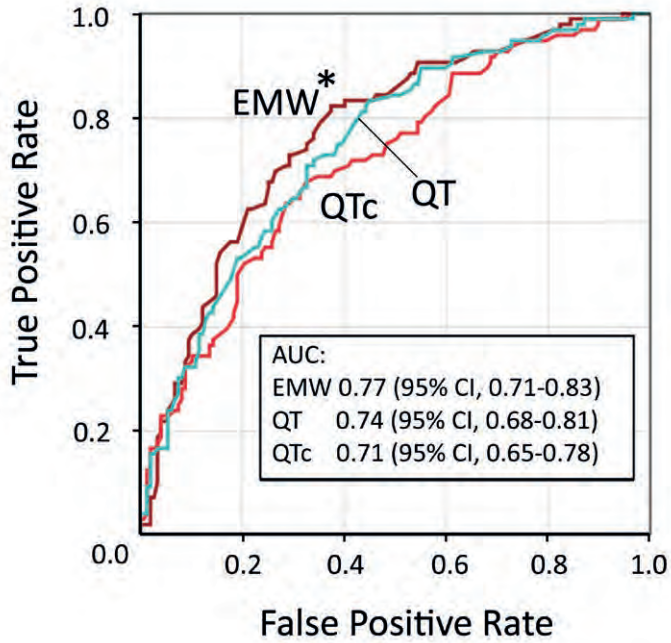


Figure 3.4 ROC curves of EMW/QTc/QT for arrhythmic events in LQTS. EMW has a better discriminatory power than QTc, * $P=0.03$.

Table 3.2 Characteristics of LQTS patients according to previous arrhythmic events (n=244)

	Asymptomatic (n=147)	Symptomatic (n=97)	P value
Age, y	39 ± 16	37 ± 17	0.37
Female sex, n (%)	92 (63)	71 (73)	0.15
<i>Genotypic characteristics</i>			
<i>KCNQ1</i> (LQT1), n (%)	69 (47)	38 (39)	0.30
<i>KCNH2</i> (LQT2), n (%)	42 (28)	42 (43)	0.05
<i>SCN5A</i> (LQT3), n (%)	31 (21)	10 (10)	0.14
<i>KCNE1</i> (LQT5), n (%)	5 (3)	3 (3)	
<i>KCNE2</i> (LQT6), n (%)	0	1 (1)	
Double heterozygous carriers/JLNS, n (%)	0	3 (3)	
Pathogenic mutation, n (%)	108 (73)	73 (75)	0.86
Variant of unknown significance, n (%)	39 (27)	24 (25)	0.66
<i>Antiarrhythmic drug at time of echocardiogr.</i>			
beta-blocker, n (%)	41 (28)	59 (61)	<0.0001
mexiletine, n (%)	6 (4)	0	
<i>ECG</i>			
RR interval, ms	931 ± 175	976 ± 189	0.06
QT interval, ms	432 ± 49	479 ± 56	<0.0001
QTc, ms	450 ± 44	488 ± 50	<0.0001
<i>Echocardiogram</i>			
QAoC interval, ms	405 ± 33	412 ± 42	0.16
EMW, ms	-27 ± 41	-67 ± 42	<0.0001

Abbreviations as in Table 3.1.

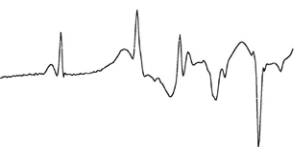


Table 3.3 Predictors of arrhythmic events

	Univariate				Multivariate			
	B	SE	OR (95% CI)	Wald	B	SE	OR (95% CI)	Wald
EMW per 10 ms decr.	0.24	0.04	1.27 (1.17-1.37)*	36	0.22	0.06	1.25 (1.11-1.40)*	13
QTc per 10 ms increase	0.18	0.03	1.19 (1.12-1.27)*	29	0.02	0.05	1.02 (0.92-1.13)	0.1
QAoC per 10 ms decr.	-0.05	0.04	0.95 (0.88-1.02)	2	-0.06	0.04	0.94 (0.86-1.03)	2
QT per 10 ms increase	0.18	0.03	1.20 (1.13-1.28)*	33	redundant			
Beta-blocker	1.39	0.28	4.01 (2.33-6.92)*	25	1.26	0.32	3.53 (1.89-6.61)*	16
Age	-0.01	0.01	1.00 (0.98-1.01)	0.5	-0.01	0.01	0.99 (0.97-1.01)	0.8
Gender	0.49	0.29	1.63 (0.93-2.86)	3	0.32	0.35	1.38 (0.69-2.74)	0.8

EMW, electromechanical window; B, exponential component; SE, standard error; OR, odds ratio; CI, confidence interval. * $P < 0.05$.

BETA-BLOCKER THERAPY

In healthy individuals, beta-blocker treatment was associated with longer QAoC despite similar QT/QTc (QAoC: 413 ± 42 versus 379 ± 31 ms; $P < 0.01$; QT: 371 ± 42 versus 357 ± 29 ms; $P = 0.20$; QTc: 377 ± 34 versus 391 ± 27 ms; $P = 0.06$). Consequently, their EMW increased to 43 ± 25 ms ($P < 0.01$). For beta-blocker-treated LQTS subjects, both QT and QAoC were longer than in untreated patients (QT: 470 ± 57 versus 437 ± 52 ms; QAoC: 416 ± 33 versus 400 ± 32 ms; $P < 0.001$ for both), rendering the EMW more negative (-54 ± 51 versus -36 ± 41 ms; $P = 0.004$). Also, QTc was longer (478 ± 53 versus 457 ± 46 ms; $P = 0.002$). In 26 symptomatic patients, beta-blocker therapy was initiated directly after echocardiography. In 15 of these, mostly LQT1 and LQT5 patients, repeat echocardiography confirmed preferential QAoC (over QT) prolongation by the addition of therapy, resulting in a trend towards reduced EMW negativity (EMW_{preBB} -32 ± 33 versus EMW_{postBB} -19 ± 33 ms; $P = 0.06$). In total, 88% of the symptomatic patients of this study were ultimately treated with beta-blockers.

GENOTYPE SUBGROUP ANALYSIS

For 107 LQT1, 84 LQT2, and 41 LQT3, averaged QTc was similar (467 ± 55 , 467 ± 47 , and 462 ± 45 ms; 40%, 51%, 7% beta-blocker therapy, respectively), **Table 3.4**. QAoC was slightly shorter in LQT3 (LQT3: 394 ± 37 , LQT1: 413 ± 40 , LQT2: 409 ± 33 ms; $P = 0.02$), which may be related to shorter RR and QT intervals in this subgroup. Altered I_{Ks}/I_{Kr} -dependent pacemaker activity³²⁴ and imbalanced negative chronotropic therapy may have contributed to this. EMW negativity was similar for LQT1, LQT2, and LQT3, (-43 ± 47 , -47 ± 44 , and -37 ± 47 ms) with longer QTc and unaltered QAoC in symptomatics, resulting in more profound EMW negativity (**Table 3.4**). Exclusion of the mexiletine-treated LQT3 patients did not alter these findings significantly.

The double-mutation and Jervell and Lange-Nielsen (JLNS) patients had the most profound EMW negativity: -91 ± 46 ms ($n=3$, all symptomatic). For the remaining 8 *KCNE1* (LQT5) and 1 *KCNE2* (LQT6)-mutation positive patients, an EMW of -16 ± 34 ms was found.

Table 3.4 Genotype subgroup analysis

	LQT1 (n=107)	LQT2 (n=84)	LQT3 (n=41)	P value
Age, y	40 ± 16	38 ± 16	35 ± 18	0.21
Female sex, n (%)	68 (64)	57 (68)	28 (68)	0.77
<i>Antiarrhythmic drug at echo</i>				
beta-blocker, n (%)	43 (40)	43 (51)	8 (7)	0.003
mexiletine, n (%)	0 (0)	0 (0)	6 (19)	
<i>ECG</i>				
RR interval, ms	964 ± 179	961 ± 182	888 ± 178	0.05
QT interval, ms	456 ± 59	456 ± 56	431 ± 47	0.04
QTc, ms	467 ± 55	467 ± 47	462 ± 45	0.80
<i>Echocardiogram</i>				
QAoC interval, ms	413 ± 40	409 ± 33	394 ± 37	0.02
EMW, ms	-43 ± 47	-47 ± 44	-37 ± 47	0.57

QAoC, interval from QRS-onset to aortic-valve closure; LQT, long QT; EMW, electromechanical window.

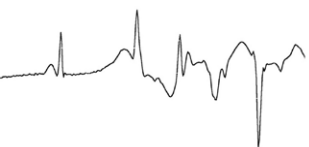


Table 3.5 Genotype subgroup analysis

	LQT1			LQT2			LQT3		
	Asymptomatic (n=69)	Symptomatic (n=38)	Asymptomatic (n=42)	Symptomatic (n=42)	Asymptomatic (n=31)	Symptomatic (n=10)			
Age, y	44 ± 15	34 ± 17*	37 ± 15	39 ± 17	32 ± 18	45 ± 13*			
Female sex, n (%)	42 (61)	26 (68)	26 (62)	31 (74)	19 (61)	9 (90)			
<i>Antiarrhythmic drug at time of echocardiogram</i>									
beta-blocker, n (%)	22 (32)	21 (55)*	14 (33)	29 (69)*	0 (0)	8 (80)			
mexiletine, n (%)	0	0	0	0	6 (19)	0			
<i>ECG (-mexiletine)</i>									
RR interval, ms	943 ± 173	1001 ± 186	943 ± 182	980 ± 184	897 ± 177 (883 ± 168)	861 ± 182§			
QT interval, ms	438 ± 52	488 ± 58*	431 ± 45	481 ± 55*	425 ± 47 (427 ± 48)	451 ± 43			
QTc, ms	454 ± 51	491 ± 54*	446 ± 33	489 ± 50*	452 ± 42 (458 ± 44)	491 ± 43*			
<i>Echocardiogram (-mexiletine)</i>									
QAOc interval, ms	409 ± 33	420 ± 50	404 ± 34	413 ± 31	398 ± 32 (396 ± 30)	381 ± 49			
EMW, ms	-29 ± 46	-68 ± 37*	-26 ± 34	-68 ± 43*	-27 ± 42 (-31 ± 45)	-70 ± 49*			

Abbreviations as in Table 3.1 *sympt. vs asympt.; §LQT3 vs LQT1; ||Sympt. LQT3 vs LQT1 and LQT2; P<0.05.

EMW DYNAMICITY IN A LQTS PATIENT WITH ELECTRICAL STORM

In a *SCN5A*-mutation-positive female (c.4850-4852delTCT; p.(Phe1617del)), we determined the EMW serially by means of tissue- and continuous-wave Doppler imaging during a phase with electrical storm, and after clinical stabilization (**Figure 3.5**). Acute TdP suppression was achieved by β -sympathomimetic treatment with isoproterenol, increasing her heart rate to 87 bpm. At that moment, EMW was -83 ms (after 27-ms correction for TDI-derived timing of aortic-valve closure,³²⁵ QTc 538 ms). After interruption of isoproterenol, EMW values deteriorated further to -163 ms within minutes (QTc 505 ms), followed by the recurrence of TdP. During these very negative EMWs, just prior to TdP, premature ventricular beats arose with mechanical activity initiating earlier than the measurable start of QRS, suggesting a mechanism other than excitation-contraction coupling.³²² The patient was restabilized with isoproterenol and permanent right-atrial pacing after ICD implantation. In the months thereafter her EMW during intrinsic sinus rhythm markedly increased to -50 ms (QTc 508 ms) and no ventricular arrhythmias occurred.

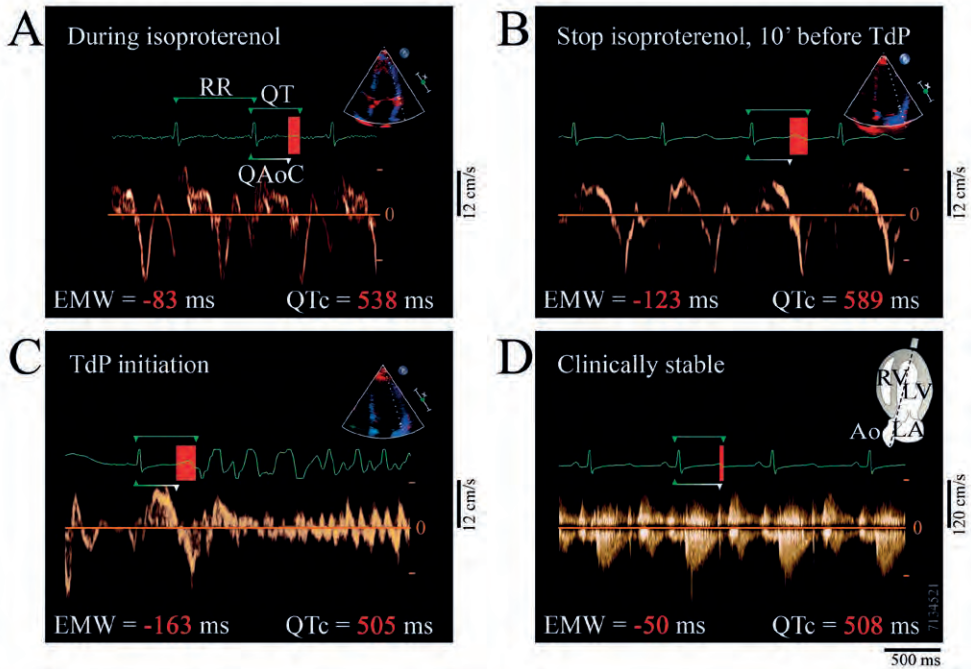


Figure 3.5 Serial EMW measurements in a LQTS patient during different stages of treatment for recurrent TdP, and after clinical stabilization. (A) Beta-sympathomimetic therapy with isoproterenol resulted in marked EMW negativity without TdP. (B) Interruption of isoproterenol with progressive EMW negativity. (C) During extreme EMW negativity TdP recurred. (D) “Normalized”, non-paced EMW values after clinical stabilization.

DISCUSSION

The present study focuses on electromechanical coupling in genotyped LQTS patients, particularly the EMW, in relation to major arrhythmic events. Our results demonstrate that the physiological LV electromechanical sequence, in which aortic-valve closure occurs after T-wave completion, is reversed in LQTS. The consequent negative EMW occurs primarily by a prolonged QT interval in the absence of a correspondingly increased QAOc. Interestingly, in LQTS the EMW is more negative for any QTc suggesting repolarization-independent influences.

EMW negativity was most pronounced in patients with documented arrhythmic events and those with double heterozygous mutations (two *KCNQ1* + *KCNH2*; one *JLNS*). Moreover, it appeared a better and independent discriminator of previous arrhythmic events than QTc. In one case with electrical storm, EMW was dynamic and very negative prior to TdP, but increased significantly after clinical stabilization. Our data confirm that inherited repolarization prolongation and instability are crucial factors for TdP, but they also hint towards the importance of mechano-electric triggers, particularly in symptomatic LQTS patients at instances during their cardiac cycle when mechanical systole has ceased, but repolarization is still ongoing.³²² Diastolic spontaneous Ca^{2+} release from the sarcoplasmic reticulum and mechanical aftercontractions can be pivotal arrhythmogenic factors, particularly when myocardial Ca^{2+} load is enhanced, as shown experimentally.^{97, 112}

INTERACTION OF ELECTRICAL AND MECHANICAL SYSTOLE

Under normal conditions, myocardial membrane depolarization precedes and initiates contraction through Ca^{2+} -induced Ca^{2+} release from the SR, a process termed excitation-contraction coupling. Repolarization prolongation can increase cellular Ca^{2+} content by prolonging the inactivation phase of L-type Ca^{2+} current. Sympathetic stimulation, circulating catecholamines, and various positive-inotropic drugs enhance Ca^{2+} load. At the integrative level, preload and afterload are major determinants of myocardial inotropic state. To govern these mechanisms, electrical and mechanical activity are tightly linked. In healthy myocardium, mechanical relaxation terminates tens of milliseconds after repolarization.³⁰³ Likewise, we demonstrated a positive EMW value of 22 ± 19 ms in healthy controls, corresponding to a QT/QS₂ ratio of 0.94.^{307, 326} In clinical non-LQTS studies, the QT/QS₂ ratio was used to investigate electromechanical coupling at resting heart rate, during adrenergic stimulation,³⁰⁵ changes in autonomic tone,³⁰⁶ and in coronary artery disease.³⁰³ In patients with prior myocardial infarction, the presence of QT>QS₂ provided a risk indicator of mortality that was more potent than QTc.³⁰⁵

In this LQTS study consisting of probands and asymptomatic family members, we observed an average EMW of -43 ± 46 ms (QT/QS₂ ratio of 1.10), with symptomatic patients having more negative EMWs for a wide QTc range. We speculate that heterogeneous autonomic innervation³²⁷ and/or sympathetic hyperactivity could provoke EMW negativity by enhanced lusitropy in the presence of QT maladaptation, particularly in LQT1, LQT5, JLNS or other conditions when cAMP-dependent I_{Ks} cannot be adequately recruited to shorten

repolarization. This may also apply to other LQTS genotypes if I_{Ks} is intrinsically weak. In LQT3, increased late Na^+ current may contribute to electromechanical divergence via altered myocardial Na^+ and Ca^{2+} handling.¹¹⁰ Interestingly, a shorter QAOc was found to underlie the EMW in LQT3, being even shorter in symptomatic individuals (despite longer QTc). Any of these potential mechanisms requires further investigation.

Beta-blockade is more efficacious in preventing recurrence of major arrhythmic events in LQT1 than LQT2 or LQT3 patients. While beta-blockers lend their antiarrhythmic actions primarily by dampening myocardial responses to sympathetic stimuli, shortening of QTc has also been demonstrated, mainly through heart rate slowing with minimal effects on QT.¹⁶⁸ Based on our results in LQTS patients and controls, increased contraction duration and a less negative EMW may confer additional antiarrhythmic protection in LQTS, in line with experimental data.¹¹³

EMW NEGATIVITY AND PROARRHYTHMIC PROCLIVITY

Proarrhythmic aspects of EMW negativity have been evaluated in animal models of drug-induced LQTS.^{112, 113, 328} In anesthetized drug-induced LQT1 dogs, I_{Ks} blockade with HMR1556 or JNJ 303 markedly reduced EMW, but did not evoke TdP.^{112, 113} Additional beta-adrenergic provocation with isoproterenol, exacerbated EMW negativity (to -109 ms) and led to the emergence of LV aftercontractions within the window, and subsequent TdP onset.¹¹² Interventions (e.g., verapamil, esmolol, atenolol) that successfully prevented aftercontractions and/or rendered EMW less negative also prevented TdP.^{112, 113, 329} In anesthetized guinea-pigs, the administration of drugs with documented TdP liability (i.e., quinidine, haloperidol, terfenadine, moxifloxacin, ciprofloxacin, and dofetilide) produced TdP only after substantial EMW negativity (<-50 ms) and infusion of adrenaline.³²⁸ Negative-control compounds did not cause EMW negativity or arrhythmia, even though repolarization prolongation was observed. TdP was typically preceded by aftercontractions. These aftercontractions, and their relation to TdP, suggest mechano-electric influences during arrhythmogenesis.³²²

CLINICAL IMPLICATIONS

Along with other reports on the importance of mechanical abnormalities in LQTS,³³⁰ our data indicate that the assessment of electromechanical coupling has added value for arrhythmia-risk analysis. The EMW, an easy-to-obtain parameter, proved a better and independent discriminator than resting QTc in our large LQTS population. A cut-off value of <-62 ms predicted arrhythmic events with 72% accuracy. As such, it may be helpful to assess arrhythmia risk, guide antiarrhythmic maintenance therapy, and facilitate the timing of acute interventions in LQTS.

LIMITATIONS

The retrospective study design may have led to potential selection bias and confounding factors, among them possible under- and overestimation of arrhythmic events. Echocardiographic examinations were performed at various times without standardization



for diurnal sympathetic modulation of QT/QAoC and potential respiratory-cycle variation. This study did not allow for stratification according to beta-blocker therapy. A prospective cohort should confirm the association between EMW negativity and arrhythmic events, and address EMW dynamics over time.

CONCLUSIONS

There is mounting evidence of mechanical abnormalities in LQTS. Their quantitative analysis, besides QTc, has added value for arrhythmia-risk prediction. Using transthoracic echocardiography, we find that LQTS patients have a markedly negative EMW over a wide QTc range, which is most pronounced in those with documented arrhythmic events. In this study population, EMW proves superior to and independent from QTc in discriminating between a LQTS patient's historical arrhythmic events. Hence, we propose to consider this parameter in the clinical management of LQTS patients.

ACKNOWLEDGEMENTS

The authors thank Roel L.H.M.G. Spätjens, Cardiovascular Research Institute Maastricht, Maastricht University Medical Centre, The Netherlands for figure optimization, and Margareth Ribe, Oslo University Hospital, Rikshospitalet, Norway, for data collection.

FUNDING

This work was supported by the Foundation "Sint Annadal", Maastricht, The Netherlands (R.M.A.t.B.); a Vidi grant from the Netherlands Organization for Scientific Research, ZonMw 91710365 (P.G.A.V.), and funding by The Netherlands CardioVascular Research Initiative, CVON PREDICT (P.G.A.V.); the South-Eastern Norwegian health authorities (K.H.H.), Center for Cardiological Innovation (Norwegian Research Council) (T.E., K.H.H.), and Mayo Clinic Windland Smith Rice Comprehensive Sudden Cardiac Death Program (M.J.A.).

CONFLICT OF INTEREST

M.J.A. is a consultant for Boston Scientific, Medtronic, St. Jude Medical, and Transgenomic. Intellectual property resulted in license agreements (FAMILION-LQTS) in 2004 between Mayo Clinic Health Solutions and PGxHealth. All other authors have no conflict of interest.



EDITORIAL

VOX CLAMANTIS IN DESERTO.
WE SPOKE BUT NOBODY WAS LISTENING:
ECHOCARDIOGRAPHY CAN HELP RISK STRATIFICATION
OF THE LONG-QT SYNDROME.

Gaetano M. De Ferrari and Peter J. Schwartz

Eur Heart J 2015;36:148-150

Over 20 years ago we reported for the first time the presence of mechanical abnormalities in the contraction pattern of patients with the long QT syndrome, showing both the presence of rapid early contraction and of an extended “plateau” phase well visible at M-mode Doppler before rapid relaxation.²³⁴ These abnormalities were almost absent in controls and more prevalent among symptomatic than asymptomatic patients (77% versus 19%, RR 2.75) suggesting their potential value for diagnosis and risk stratification of LQTS patients. This report and our subsequent evidence that these abnormalities were abolished by calcium blockers²³⁷ and could be the mechanical counterparts of early afterdepolarizations, thus being markers of arrhythmic propensity, were received with skepticism and essentially ignored. Eventually, an abnormal contraction pattern was confirmed by others mostly using tissue Doppler imaging^{235, 236, 301} thus ending the era in which LQTS was considered a pure electrical disease.³³⁰

Once set in motion, the ball keeps rolling. In this issue of the Journal, ter Bekke *et al*³³¹ describe the presence of a negative “electromechanical window” in LQTS patients and report a strong association between a markedly negative value and arrhythmic events. One strength lies in the size of population, almost 250 genotype-positive LQTS patients and 74 controls, much larger than previous studies.^{234-237, 301} This allowed to conclusively demonstrate that the vast majority of LQTS patients do have abnormal echocardiographic features, with approximately 2/3 of LQTS patients showing EMW values >2SD below the values of controls, despite pharmacological treatment (found to reduce EMW negativity) in >40% of patients. This important study, carried out by 3 expert groups, shows that even in the era of intensive genotyping, echocardiography can provide valuable information, and within few minutes.

Importantly, the almost 100 patients with arrhythmic events allowed a reliable estimate of sensitivity and specificity of the echocardiographic indexes and the execution of multivariable analyses. Adding EMW to QTc resulted in a significant improvement in the identification of symptomatic patients; EMW but not QTc was an independent predictor of arrhythmic events. This finding is in agreement with the demonstration by Haugaa *et al*³⁰¹ that echocardiographic contraction duration identified symptomatic patients with better sensitivity and specificity compared to QTc (79% and 74% versus 70% and 50%, respectively), and with our original indication that echocardiography was superior to ECG.²³⁴

The time has come to start using echocardiographic indexes in addition to QTc in the risk stratification of patients with LQTS. It is unclear, however, which parameter performs best and in this regard neither the study by Haugaa *et al*³⁰¹ nor the present one are very helpful because they did not compare their index, EMW, with those previously described.²³⁴⁻²³⁷ The use of EMW was suggested as a risk marker for *Torsades des Pointes* in experimental studies^{113, 328} but its superiority to QTc has been questioned.³³²

The choice of the best mechanical index would be facilitated if we had a good understanding of the pathophysiology underlying the contraction and relaxation abnormalities present in LQTS patients. This is one weakness of the present manuscript, which suggests that LQTS patients may have enhanced lusitropy as a consequence of



heterogeneous sympathetic activation.³³¹ As a matter of fact, this is unlikely because LQTS patients actually show abnormally *impaired* rather than enhanced relaxation.

Ranolazine, a late I_{Na} blocker, shortened QTc by 4.5% from 578 ± 55 ms and by a significant 13% a previously prolonged isovolumic relaxation time of 125 ± 27 ms¹⁷³ in 12 patients with LQT3,¹⁷³ the LQTS subtype caused by enhanced late I_{Na} current.³²¹ A delay in LV relaxation was shown also in an animal model of LQT2.³³³ Post-systolic shortening and a significant biventricular diastolic dysfunction were found in LQT3 patients, suggesting that the diastolic dysfunction could be either secondary to systolic dysfunction, i.e. post-systolic shortening encroaching on diastole, or to deranged calcium homeostasis.³³⁴

Actually, the two mechanisms are not mutually exclusive. Our initial hypothesis that in patients with a “double peak” morphology the second shortening could have been the mechanical equivalent of an early after depolarization²³⁴ appeared to be confirmed by the subsequent demonstration that intravenous verapamil normalized the contraction pattern by abolishing both “plateau-like” and “double peak” morphologies.²³⁷ By focusing on the calcium transients linked to EADs in isolated cardiomyocytes we then showed that phase 2 EADs caused a marked secondary calcium rise (with accompanying contraction) by occurring at a time when $[Ca]_i$ is decreasing but not back to baseline³³⁵ (**Figure 3.6A**). Our combined studies supported the hypothesis of a mechanical counterpart of subthreshold EADs and, more broadly, our interpretation that the contraction/relaxation abnormality was a consequence of altered calcium handling.^{237, 335} A pivotal role for abnormal calcium handling was suggested also by Guns *et al*.³²⁸ who advocated the necessity of a negative EMW to allow the occurrence of TdP. Notably, they found after-contractions in the left ventricular pressure (LVP) signal. Indeed, the EADs cause both a significant QT interval prolongation and secondary pressure rises in LVP, which are however unable to delay aortic valve closure (**Figure 3.6B**). The ensuing QT prolongation with unmodified systolic time produces a negative EMW. Even in the absence of EADs, increased calcium influx because of prolonged action-potential duration may alter late contraction pattern and impair diastole, but this will likely be highly correlated with QT interval, thus not providing additional prognostic value. Notably, even in the absence of EADs an inhomogeneity in the end of contraction among different areas of the ventricle may exist (such as a transmural inhomogeneity, caused by markedly different APDs) causing the abnormal contraction pattern. Since the developed tension would be insufficient to maintain aortic valve opening, this phenomenon may explain the presence of myocardial contraction after aortic valve closure.

What often escapes clinical cardiologists is the fact that these non-homogeneous contractions and aftercontractions alter the geometry of the beating heart and activate the sensory endings of cardiac sympathetic mechanoreceptors³³⁶ thus eliciting an excitatory sympathetic reflex.³³⁷ This leads to the arrhythmogenic localized release of norepinephrine which further increases the heterogeneity of ventricular repolarization, already present in LQTS,^{338, 339} thus favoring reentry.³⁴⁰ This sequence of events also helps understanding the

antibrillatory efficacy of left cardiac sympathetic denervation for LQTS and other cardiovascular diseases associated with risk for sudden cardiac death.¹⁴⁹

In conclusion, the well-conceived report by ter Bekke *et al*³³¹ further demonstrates the critical role that echocardiography deserves in the clinical evaluation and management of LQTS patients and highlights how mechanical abnormalities can significantly contribute to risk stratification because, they appear linked to the mechanisms underlying TdP and can themselves trigger arrhythmogenic sympathetic activation. What remains to be defined, after proper comparison and prospective validation in an appropriately sized population, is which of the various echocardiographic parameters can represent the best marker of arrhythmic risk.

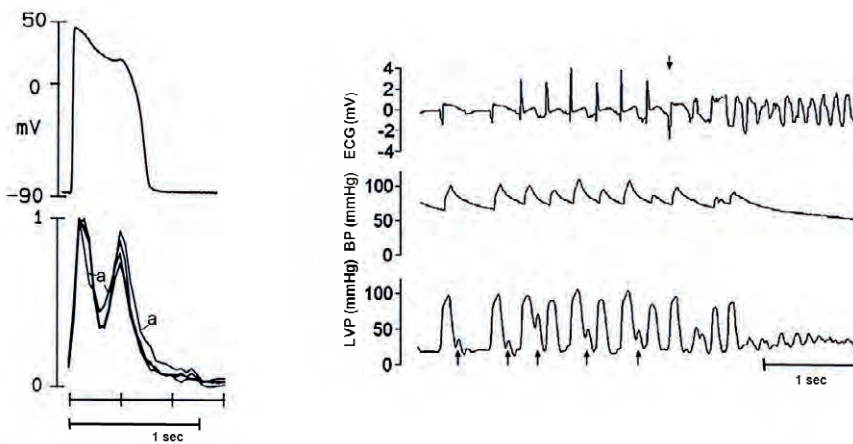


Figure 3.6 Left, Electrical signal and normalized calcium-fluorescence signal from isolated patch-clamped guinea-pig ventricular myocyte paced at 1 Hz. Marked [Ca]_i rise associated with EAD. Modified from De Ferrari GM, *et al. Circulation* 1995;91:2510-2515 [reproduced with permission].

Figure 3.6 Right, Example of TdP triggered by adrenaline+torsadogenic agents in closed chest guinea-pigs. Arrows indicate aftercontractions in LVP signal. Modified from Guns P-J, *et al. J. Pharmacol. Toxicol. Methods* 2012;66:125-134 [reproduced with permission].

ACKNOWLEDGEMENTS

The Authors are grateful to Pinuccia De Tomasi for her expert editorial support.





"Het hart klopt altijd van de liefde"



4

PROARRHYTHMIC PROCLIVITY OF LEFT-STELLATE GANGLION STIMULATION IN A CANINE MODEL OF DRUG-INDUCED LONG-QT SYNDROME TYPE 1

ABSTRACT**BACKGROUND**

Left-stellate ganglion stimulation (LSGS) can modify regional dispersion of ventricular refractoriness, promote triggered activity, and reduce the threshold for ventricular fibrillation. Sympathetic hyperactivity precipitates torsades de pointes and VF in susceptible patients with long-QT syndrome type 1.

OBJECTIVE

To investigate the effects of LSGS and right-stellate ganglion stimulation (RSGS) in anesthetized dogs with drug-induced LQT1 to unmask ventricular arrhythmogenic mechanisms.

METHODS

In nine mongrel dogs, the left and right stellate ganglia were exposed for electrical stimulation. ECG, left- and right-ventricular endocardial monophasic action potentials and intracavitary pressures were recorded simultaneously. The electromechanical window (Q to LVP at 90% relaxation minus QT) was calculated. LQT1 was mimicked by infusion of the KCNQ1 blocker HMR1556.

RESULTS

Under baseline conditions, LSGS and RSGS caused similar heart-rate acceleration and QT shortening. Positive inotropic and lusitropic effects were more pronounced under LSGS than RSGS. In-vivo I_{Ks} blockade prolonged QTc, triggered MAP-early afterdepolarizations and rendered the EMW negative, but ventricular tachyarrhythmias did not occur. Superimposed LSGS exaggerated EMW negativity and evoked TdP in 5/9 dogs within 30 s. Preceding extrasystoles originated mostly from the outflow-tracts region. TdP deteriorated into therapy-refractory VF in 4/5 animals. RSGS did not provoke TdP.

CONCLUSION

In this model of drug-induced LQT1, LSGS readily induced TdP and VF during repolarization prolongation and MAP-EAD generation, but only during marked LSGS-related EMW negativity and outflow-tract ventricular ectopy. Thus, mechano-electric coupling may be involved in the triggering of extrasystoles and/or exaggeration of regional dispersion of refractoriness.



INTRODUCTION

Stimulation of the left and right stellate ganglion produces generalized cardiovascular (i.e., heart-rate and blood-pressure rise) and localized myocardial effects. Marked differences in chronotropic, inotropic, lusitropic, and dromotropic effects among species, including humans, have been reported.^{142, 143} Electrophysiologically, LSGS mainly activates the left-ventricular inferior and lateral regions, whereas RSGS modulates predominantly the anterior sides of both ventricles.³⁴¹ Sympathetic hyperactivity and/or regionally dispersed sympathetic innervation impinge on ventricular electrophysiological properties,¹⁴³ potentially exaggerating dispersion of excitation and refractoriness. This facilitates triggered activity,⁹² shortens ventricular refractoriness,³⁴² and reduces the threshold for ventricular fibrillation.^{343, 344} There is also mounting evidence of significant parasympathetic postganglionic innervation of the ventricles in humans and canines.³⁴⁵ Vagal nerve stimulation operates mainly by antagonizing cardiac sympathetic activity. It reverses its action on the effective refractory period of canine LV myocardium via cholinergic-muscarinic pathways, increases the threshold for VF, and increases the variability of the dominant VF frequency.¹⁴⁵⁻¹⁴⁷ However, co-activation of both limbs of the autonomic nervous system can provoke various arrhythmias, including torsades de pointes.¹⁴⁸

Sympathetic-related ventricular tachyarrhythmias are a hallmark of the long-QT syndrome type 1, as arrhythmic events are mostly provoked during exercise and/or emotion (~90% of symptomatic LQT1 patients).¹⁵¹ The precise timing of such events in relation to the initiation, duration or cessation of the physical or mental stress is often not clear, but could provide crucial information about the arrhythmogenic contribution of sympathetic and vagal hyperactivity superimposed on loss-of-function of the slowly-activating delayed-rectifier potassium current (I_{Ks}).

Previous studies in canine LQTS models addressed the effects of unilateral or bilateral stellate ganglion stimulation during cesium-chloride-induced QT prolongation³⁴⁶ and *d*-sotalol-induced LQT2,³⁴⁷ but not LQT1. In anesthetized dogs with drug-induced LQT1, however, TdP was readily evoked by the beta-adrenergic agonist isoproterenol.¹¹² In those experiments, TdP was preceded by a reversed relationship between the duration of electrical and mechanical systole (i.e., electromechanical window negativity), and the occurrence of postsystolic aftercontractions. In LQTS patients, EMW negativity is a strong indicator of arrhythmic risk.³³¹

In the present investigation, we applied LSGS and RSGS to unmask ventricular arrhythmogenic mechanisms in the anesthetized canine model of drug-induced LQT1.¹¹² Electrical stimulation of the LSG and RSG was performed with sympathetic and vagal nerves left intact, during an anesthetic regime with minimal influence on beta-adrenergic responsiveness and baroreflex sensitivity, allowing near-to-normal autonomic reflexes during sympathetic stimulation. Simultaneous recordings of ECGs, monophasic action potentials and pressures from the left and right ventricle served to examine electromechanical coupling during LSGS and RSGS.

METHODS

Animal handling was in accordance with the Dutch Law on Animal Experimentation and the European Directive for the Protection of Vertebrate Animals used for experimental and other scientific purposes (European Union Directive 86/609/CEE). The Committee for Experiments on Animals of Maastricht University approved the experimental protocol (2008-116).

GENERAL

Nine adult mongrel dogs of either sex (body weight 32 ± 3 kg, Marshall BioResources) were used for this study. Food was withheld 12 hours before the experiment. General anesthesia was induced by a slow singular intravenous injection of remifentanyl ($0.1 \mu\text{g}/\text{kg}$), etomidate ($0.5\text{-}1.5 \text{ mg}/\text{kg}$), and succinylcholine ($1 \text{ mg}/\text{kg}$). A cuffed endotracheal tube was inserted and connected to a respirator with 30% oxygen in pressurized air to maintain normocapnia, PaCO_2 30-50 mm Hg. A thermal mattress was used to maintain body temperature and $1.25 \text{ mL}/\text{kg}/\text{h}$ 0.9% NaCl was administered to compensate for the perioperative fluid loss. Anticoagulation was achieved with $500 \text{ IU}/\text{kg}$ unfractionated heparin.

During the experiment, anesthesia was maintained by continuous infusion of etomidate ($1.0\text{-}3.0 \text{ mg}/\text{kg}/\text{h}$) and remifentanyl ($0.6\text{-}1.0 \mu\text{g}/\text{kg}/\text{min}$). This anesthetic regime was chosen because of minimal effects on beta-adrenergic responsiveness, baroreflex sensitivity, and basal hemodynamic parameters.^{112, 113, 348}

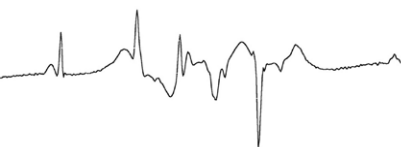
IN-VIVO EXPERIMENTAL DESIGN

In all experiments standard-lead ECGs were continuously registered. Additionally, MAP catheters (Hugo Sachs Elektronik, Harvard Bioscience, Inc.) were positioned in the LV and RV. Endocardial MAP signals were accepted on the basis of amplitude, morphology and stability. Two 7F pigtail tip-micromanometer catheters (Sentron, Cordis®) were advanced via arterial and venous (femoral or carotid) access into the LV and RV cavity for pressure recordings.

In all dogs, the left cardiac sympathetic chain was exposed beneath the parietal pleura by left thoracotomy between the first and second ribs, posteriorly. In three dogs, the contralateral stellate ganglion was also exposed and prepared for electrical stimulation. The vagal nerves were left intact, and sympathetic neural decentralization was not performed.

Custom-made bipolar electrodes were used for unilateral stellate stimulations. Pulses generated were 2-4 mA in amplitude, 2 ms in duration, 10-15 Hz in frequency, and were maintained for 33 ± 12 s. If both sympathetic stellate ganglia were to be stimulated in an experiment, the RSG was stimulated first. At least five minutes between successive stimulations were allowed for full recovery of the nerve, and hemodynamic and electrophysiological parameters. In three dogs, an isoproterenol bolus ($1.2\text{-}2.5 \mu\text{g}$) was given.

All modules (ECG registration, MAP signals, pressure recording, and pacer) were connected to the IdeeQ Data Acquisition Program (version 2.49.0 Maastricht Instruments



BV) for continuous and synchronous signal recording, electrical stimulation, and offline analysis.

Once a reproducible response to either stellate ganglion was established in at least two consecutive stimulations, HMR1556, an I_{Ks} blocker targeting KCNQ1,³⁴⁹ was administered intravenously at 25-50 $\mu\text{g}/\text{kg}/\text{min}$ (mean $46 \pm 10 \mu\text{g}/\text{kg}/\text{min}$) to mimic LQT1. HMR1556 was titrated to reach maximal I_{Ks} inhibition, as assessed by stable QT prolongation >25% from baseline,¹¹² before stellate ganglion stimulation was repeated. If TdP or VF was induced, electrical stimulation and HMR1556 infusion were discontinued immediately, followed by magnesium administration and external electrical cardioversion in attempts to restore sinus rhythm.

DATA ANALYSIS

Electrophysiological, hemodynamic and electromechanical parameters described below were analyzed during ten consecutive sinus-rhythm (or supraventricular) beats, momentarily before and at maximal SGS, both under baseline conditions and during I_{Ks} blockade.

Heart rate and QT interval were measured from an extremity lead (usually lead II) with a discernible T-wave ending and the longest QT interval. Heart-rate corrected QT (QTc) was calculated using van de Water's formula, $QTc = QT - 0.087(RR - 1000)$, which is superior to Bazett's in anesthetized dogs.³⁵⁰ $T_{\text{peak}} - T_{\text{end}}$ was calculated as a marker of spatial dispersion of ventricular repolarization.

LV and RV MAP durations were measured at 90% repolarization ($MAPD_{90}$). Beat-to-beat variability of repolarization was measured on LV and RV MAP recordings during 10 consecutive beats in the absence of ventricular ectopy. Short-term variability was calculated as: $STV = \sum(|MAPD_n - MAPD_{n-1}|) / (10 \cdot \sqrt{2})$. Long-term variability as: $LTV = \sum(|MAPD_n + MAPD_{n-1} - 2 \cdot MAPD_{\text{mean}}|) / (10 \cdot \sqrt{2})$.³⁵¹ Also, the occurrence of early afterdepolarizations (EADs) in MAPs, and EAD-preceding transient repolarization delays (i.e., when dV_{MAP}/dt turned less negative or zero) were noted.

Ventricular peak systolic and end-diastolic pressure, duration of ventricular contraction at 90% relaxation ($QLVP_{90}$), and the dP/dt_{max} , dP/dt_{min} were measured. The EMW was calculated by subtracting the QT interval from the $QLVP_{90}$. The pressure signals were carefully screened for (low-amplitude) aftercontractions.¹¹²

If ventricular tachyarrhythmia occurred, we located the origin of the triggering premature ventricular complex by analyzing the QRS morphology and the sequence of RV and LV MAP activation. The last supraventricular beat before TdP/VF was designated beat "0" with the preceding intervals being $I_{(-n)}$ (**Figure 4.1**). These RR intervals were measured to determine the pause dependency of arrhythmia initiation, defined as $I_{(-1)} \geq 150\% I_{(-2)}$.¹⁰⁶ QT, EMW, and $QLVP_{90}$ were compared between TdP-inducible and noninducible stimulations. Dogs were designated "resistant" if no TdP/VF could be induced during SGS.

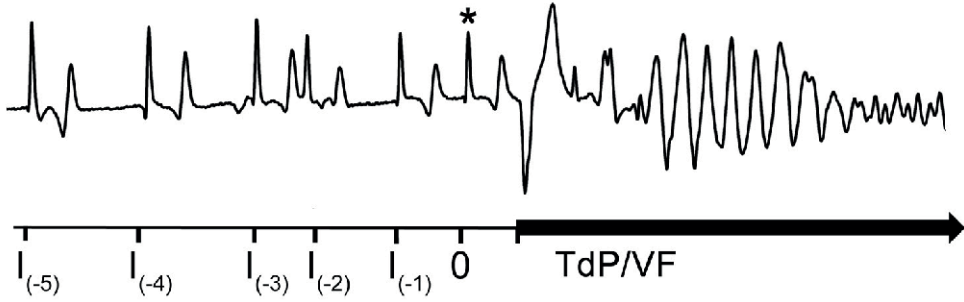


Figure 4.1 Method of ECG analysis. RR intervals are numbered in relation to the last supraventricular beat “0” prior to TdP/VF, with $I_{(-n)}$ referring to previous intervals.

STATISTICAL ANALYSIS

Data were measured in 10 consecutive beats, using the average for further statistical analysis. Pooled data were expressed as mean \pm standard deviation. Normality was assessed for each dataset using the Shapiro-Wilk test. Differences of parameters in paired data were assessed using the paired-samples *t*-test or the Wilcoxon signed rank test as appropriate. Intergroup comparison was performed using the student’s *t*-test or the Kruskal-Wallis test. A *P* value of <0.05 was considered statistically significant.

RESULTS

STELLATE GANGLION STIMULATION OF THE NORMAL CANINE HEART

Figure 4.2 depicts representative examples of the cardiac effects of LSGS and RSGS at baseline. During LSGS, heart rate increased by 79% and the QT interval shortened by 23%, effectively reducing QTc from 290 ± 24 to 253 ± 13 ms ($P=0.0003$; **Table 4.1**). LV and RV MAPD₉₀ analysis did not reveal augmented interventricular or temporal (i.e., beat-to-beat) dispersion of repolarization. In both ventricles, inotropy increased significantly: LV peak systolic pressure by 37% and RVP by 157%. LV dP/dt_{max} increased by 394%. LV dP/dt_{min} decreased by 110%, indicating increased lusitropy, and effectively leading QLVP₉₀ to shorten from 373 ± 65 to 214 ± 46 ms (-43%, $P=0.006$; **Table 4.1**). Changes in diastolic LVP did not reach statistical significance. LV EMW decreased from 95 ± 53 to 9 ± 42 ms ($P=0.009$). RV inotropy and lusitropy also increased significantly (**Table 4.1**).



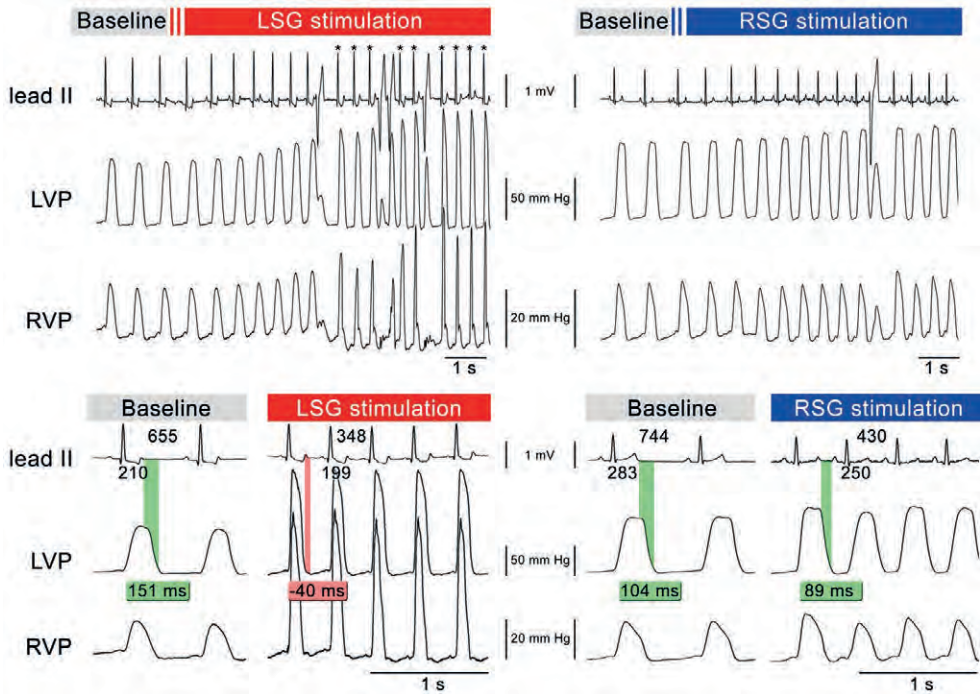


Figure 4.2 Representative examples of effects of LSGS and RSGS on ECG, LVP, and RVP characteristics. Upon LSGS, a junctional tachycardia appeared after 6 s (*) interspersed by ventricular extrasystoles. The EMW, being positive at baseline, turned negative during LSGS (-40 ms, red), but not during RSGS (89 ms, green). LSG indicates left stellate ganglion; RSG, right stellate ganglion; LVP, left-ventricular pressure; RVP, right-ventricular pressure.

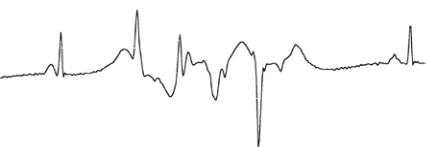
Table 4.1 Electrophysiological and hemodynamic effects of unilateral stellate ganglion stimulation at baseline

	Baseline	+ LSGS	<i>P</i> value	+ RSGS	<i>P</i> value
RR interval (ms)	667 ± 58	383 ± 79	<0.0001	341 ± 91	0.024
Heart rate (bpm)	91 ± 8	162 ± 32	<0.0001	188 ± 55	0.024
QT interval (ms)	261 ± 23	200 ± 18	<0.0001	198 ± 34	0.0004
QTc (ms)	290 ± 24	253 ± 13	0.0003	256 ± 27	0.002
Tp-Te (ms)	37 ± 13	36 ± 10	0.78	37 ± 7	0.21
Left ventricle					
MAPD ₉₀ (ms)	222 ± 25	175 ± 26	0.0001	176 ± 30	0.001
MAP-STV	4.8 ± 4.2	4.0 ± 2.9	0.24	1.8 ± 1.0	0.10
MAP-LTV	5.7 ± 3.3	5.1 ± 5.6	0.63	1.4 ± 0.5	0.03
LVP syst. (mm Hg)	94 ± 18	150 ± 23	<0.0001	137 ± 11	0.02
LVP diast. (mm Hg)	11 ± 4	9 ± 7	0.12	13 ± 11	0.008
dP/dt _{max} (mm Hg/s)	1750 ± 918	8649 ± 3583	0.0007	3665 ± 2295	0.048
dP/dt _{min} (mm Hg/s)	-2323 ± 1236	-4893 ± 2268	0.013	-3235 ± 1592	0.058
QLVP ₉₀ (ms)	373 ± 65	214 ± 46	0.006	245 ± 63	0.0008
EMW (ms)	95 ± 53	9 ± 42	0.009	47 ± 30	0.007
Right ventricle					
MAPD ₉₀ (ms)	211 ± 24	177 ± 27	0.02	168 ± 31	0.0009
RVP syst. (mm Hg)	23 ± 10	59 ± 13	0.0008	37 ± 18	0.09
RVP diast. (mm Hg)	4 ± 3	1 ± 3	0.002	4 ± 4	0.007
dP/dt _{max} (mm Hg/s)	597 ± 349	4005 ± 770	0.001	1435 ± 1200	0.04
dP/dt _{min} (mm Hg/s)	-323 ± 148	-1920 ± 1105	0.06	-889 ± 519	0.06

STV indicates short-term variability; LTV, long-term variability; MAPD₉₀, monophasic action potential duration at 90% repolarization; LVP, left-ventricular pressure; QLVP₉₀, time from QRS onset to 90% LV pressure normalization; EMW, electromechanical window.

LSGS readily evoked a junctional (or low-atrial) tachycardia, overriding the LSGS-induced accelerated sinus rhythm after 6 ± 3 s (asterisks in **Figure 4.2**). Occasionally, solitary RV/LV ectopic activity occurred during LSGS, but MAP-EADs, aftercontractions, or (non)sustained ventricular tachyarrhythmias (NSVT) were not observed. In approximately one third of LSG stimulations a short-lived paradoxical heart-rate slowing was observed, which could be counteracted by atropine.

We observed an immediate and protracted (87 ± 41 s) vagal rebound following LSGS (**Figure 4.3**), which was characterized by sinus bradycardia, ventricular ectopy, and episodes



of idioventricular rhythm. The post-LSGS systolic LVP remained elevated during this vagal episode, and returned to steady-state values parallel with the restoration of sinus rhythm. Vagal rebound was not observed after isoproterenol infusion, which may be explained by the absence of an inotropic response (113 ± 17 to 109 ± 12 mm Hg; $P=0.51$), despite heart-rate acceleration (+57%).

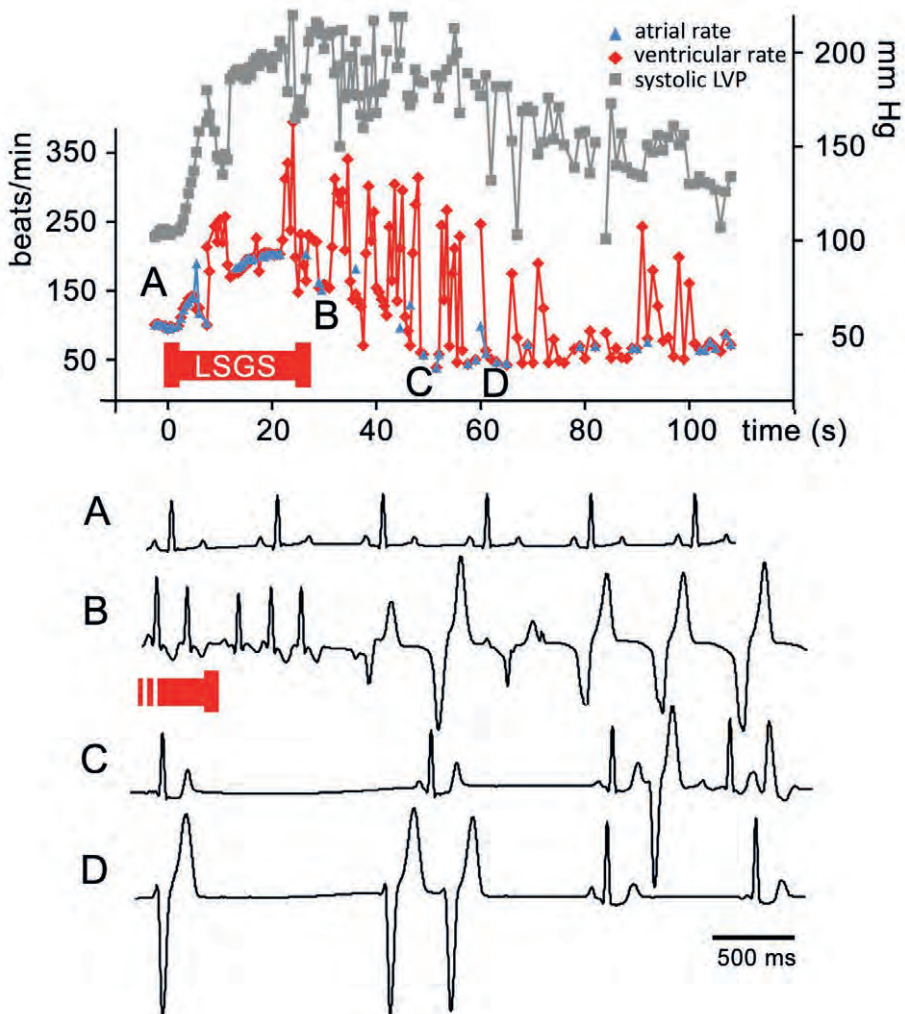
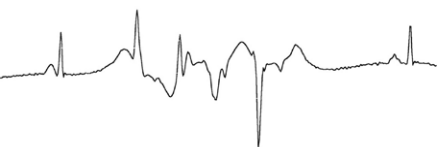


Figure 4.3 Vagal rebound post-LSGS at baseline. Upon termination of LSGS, and during a protracted positive inotropic response (upper panel), sinus and junctional bradycardia, ventricular extrasystoles and idioventricular rhythm occurred, indicating a vagal response by a baroreflex loop and/or sympathetic withdrawal. The lower ECG traces A, B, C, and D are ECG examples at different stages of the vagal rebound. LVP indicates left-ventricular pressure.

RSGS ($n=3$, **Figure 4.2**) caused comparable heart-rate accelerations (188 ± 55 bpm) as LSGS (in the absence of decentralization), without provoking supraventricular arrhythmias. Both QT and QTc intervals shortened significantly (by 29% and 18% respectively), but these were not different from the effects of LSGS. Endocardial MAPD₉₀ decreased similarly in both ventricles (**Table 4.1**). RSGS-evoked positive inotropy was less prominent than during LSGS. Similarly, we observed only limited QLVP₉₀ shortening upon RSGS, resulting in less EMW reduction (**Table 4.1**).

REPOLARIZATION INSTABILITY DURING I_{Ks} INHIBITION

Intravenous administration of HMR1556 prolonged QT and QTc to 373 ± 65 and 371 ± 61 ms, respectively (+21% and +20%; $P=0.002$ and $P=0.007$, **Table 4.2**). Heart rate decreased to 60 ± 11 bpm ($P=0.0003$). Preferential LV over RV MAPD₉₀ prolongation (335 ± 74 and 286 ± 50 ms; $P<0.0001$) resulted in augmented interventricular dispersion of repolarization. This was paralleled by a more pronounced LV temporal dispersion of repolarization with STV-MAPD₉₀ increasing by 129% and LTV-MAPD₉₀ by 173%. LV EADs emerged in four dogs at a wide range of cycle lengths; RV EADs in three (**Figure 4.4**). Upon I_{Ks} inhibition, the LV-peak systolic pressure and LV dp/dt_{max} increased to 114 ± 19 mm Hg (+23%; $P=0.01$) and 2373 ± 1159 mm Hg/s (+27%; $P=0.001$). Despite a significant prolongation of the electrical systole, QLVP₉₀ remained unaltered, providing an EMW negativity of -14 ± 69 ms ($P=0.001$). No sizeable aftercontractions or spontaneous ventricular arrhythmias were noted under these conditions.



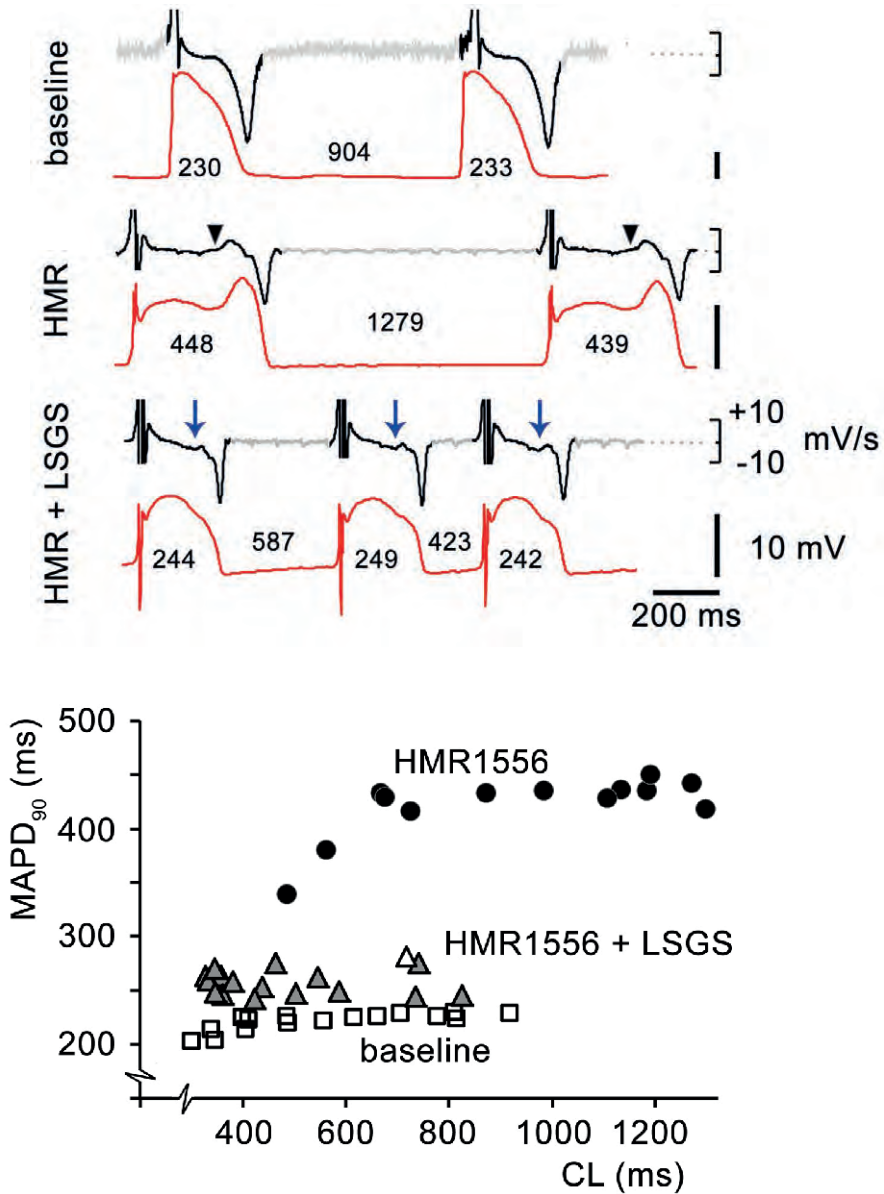


Figure 4.4 Top, LV MAPs and first derivative (dV/dt) of MAP signal. After HMR1556, EADs followed after an initial delay in repolarization (arrowheads). Upon concomitant LSGS at 10-15 Hz, frank EAD upstrokes were absent but a discernable delay in repolarization (arrows) remained present, contributing to MAPD₉₀ prolongation. **Bottom**, rate dependency of MAPD₉₀ at baseline (square), during HMR1556 (circle) and simultaneous LSGS (triangle). Black symbols: EAD present; gray symbols: initial delay in repolarization. LSGS indicates left-stellate ganglion stimulation; APD₉₀, action potential duration at 90% repolarization; CL, cycle length.

Table 4.2 Electrophysiological and hemodynamic effects of HMIR1556 and unilateral stellate ganglion stimulation


	Baseline	HMR	P value	+ LSGS	P value	+ RSGS	P value
RR interval (ms)	680 ± 116	1026 ± 168	0.0002	481 ± 184	<0.0001	407 ± 82	0.02
Heart rate (bpm)	91 ± 17	60 ± 11	0.0003	142 ± 48	<0.0001	152 ± 30	0.01
QT interval (ms)	280 ± 23	373 ± 65	0.002	260 ± 50	<0.0001	246 ± 37	0.005
QTc (ms)	308 ± 17	371 ± 61	0.007	306 ± 44	<0.0001	298 ± 34	0.003
Tp-Te (ms)	57 ± 27	92 ± 34	0.03	47 ± 16	<0.0001	44 ± 10	0.007
Left ventricle							
MAPD ₉₀ (ms)	238 ± 29	335 ± 74	0.001	225 ± 31	0.001	230 ± 58	0.14
MAP-STV	2.8 ± 1.6	6.4 ± 4.6	0.003	6.1 ± 3.9	0.08	8.9 ± 11.3	0.76
MAP-LTV	3.3 ± 1.5	9.0 ± 8.1	0.02	10.2 ± 10.0	0.42	7.3 ± 9.2	0.86
LVP syst. (mm Hg)	102 ± 24	114 ± 19	0.01	180 ± 22	<0.0001	150 ± 27	0.0003
LVP diast. (mm Hg)	12 ± 8	14 ± 8	0.003	5 ± 8	0.003	16 ± 14	0.35
dP/dt _{max} (mm Hg/s)	1734 ± 857	2373 ± 1159	0.001	9267 ± 3498	<0.0001	3556 ± 1615	0.02
dP/dt _{min} (mm Hg/s)	-3127 ± 2634	-4432 ± 3466	0.07	-8774 ± 7044	0.0004	-3025 ± 1063	0.04
QLVP ₉₀ (ms)	360 ± 31	355 ± 34	0.86	198 ± 77	0.0002	248 ± 45	0.002
EMW (ms)	79 ± 36	-14 ± 69	0.001	-61 ± 34	0.0004	11 ± 31	0.81
Right ventricle							
MAPD ₉₀ (ms)	213 ± 21	286 ± 50	0.008	209 ± 52	<0.0001	204 ± 33	0.03
RVP syst. (mm Hg)	25 ± 9	28 ± 8	0.03	64 ± 16	0.003	35 ± 4	0.0002
RVP diast. (mm Hg)	6 ± 4	8 ± 5	0.02	7 ± 5	0.05	6 ± 6	0.03
dP/dt _{max} (mm Hg/s)	610 ± 316	820 ± 641	0.13	4635 ± 1526	0.005	929 ± 309	0.03
dP/dt _{min} (mm Hg/s)	-266 ± 47	-329 ± 39	0.02	-3290 ± 4983	0.008	-483 ± 150	0.12

STV indicates short-term variability; LTV, long-term variability; MAPD₉₀, monophasic action potential duration at 90% repolarization; LVP, left-ventricular pressure; QLVP₉₀, time from QRS onset to 90% LV pressure normalization; EMW, electromechanical window.

PROARRHYTHMIC PROCLIVITY OF LSGS DURING DRUG-INDUCED LQT1

LSGS during I_{Ks} inhibition provoked TdP/VF in 5 of 9 dogs after 26 ± 6 s (Figure 4.5). Once TdP occurred, it rapidly degenerated into VF that was resistant to magnesium infusion and did not respond to immediate and repeated electrical cardioversion in all but one case. In that dog, after termination of VF, a protracted vagal period with intermittent episodes of nonsustained VT was observed. RSGS was never torsadogenic.

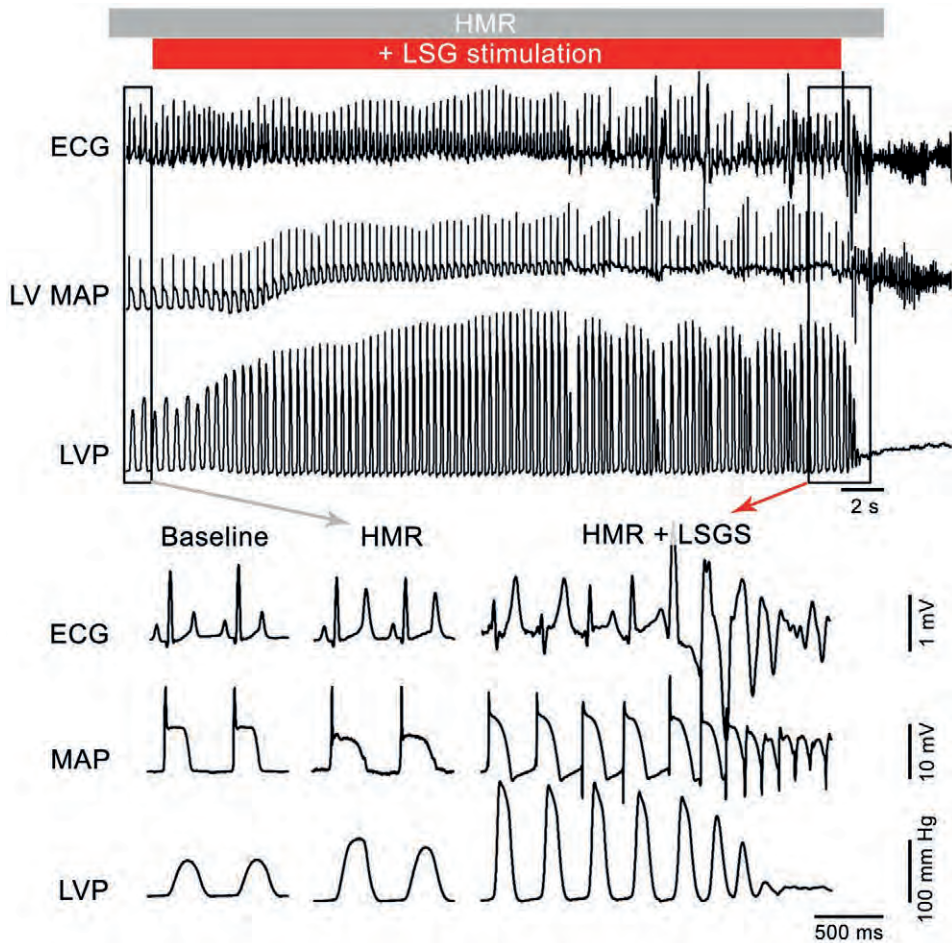


Figure 4.5 Induction of TdP, degenerating into VF, by LSGS in drug-induced LQT1. MAP indicates monophasic action potential; LVP, left-ventricular pressure; LSGS, left-stellate ganglion stimulation.

In the dogs with inducible TdP/VF, pre-LSGS QT was significantly more prolonged, and LV EMW more negative, than in resistant animals: 440 ± 67 versus 344 ± 56 ms ($P=0.007$) and -64 ± 87 versus 27 ± 40 ms ($P=0.04$), respectively (Figure 4.6). EMW negativity decreased significantly in the final beats preceding TdP/VF (reaching -94 ± 31 ms at $I_{(0)}$), compared with

the non-inducible group (-43 ± 25 ms; $P=0.002$, **Figure 4.6**). $QLVP_{90}$ did not differ between these groups. QT prolongation was more exaggerated (282 ± 53 ms; $P=0.02$) in the beats prior to TdP when compared to pre-NSVT (225 ± 21 ms) or solitary PVCs (229 ± 39 ms) in susceptible animals, and EMW was more negative -94 ± 31 ms prior to TdP/VF ($P=0.005$) versus -23 ± 37 ms (pre-NSVT), and -38 ± 37 ms (PVC).

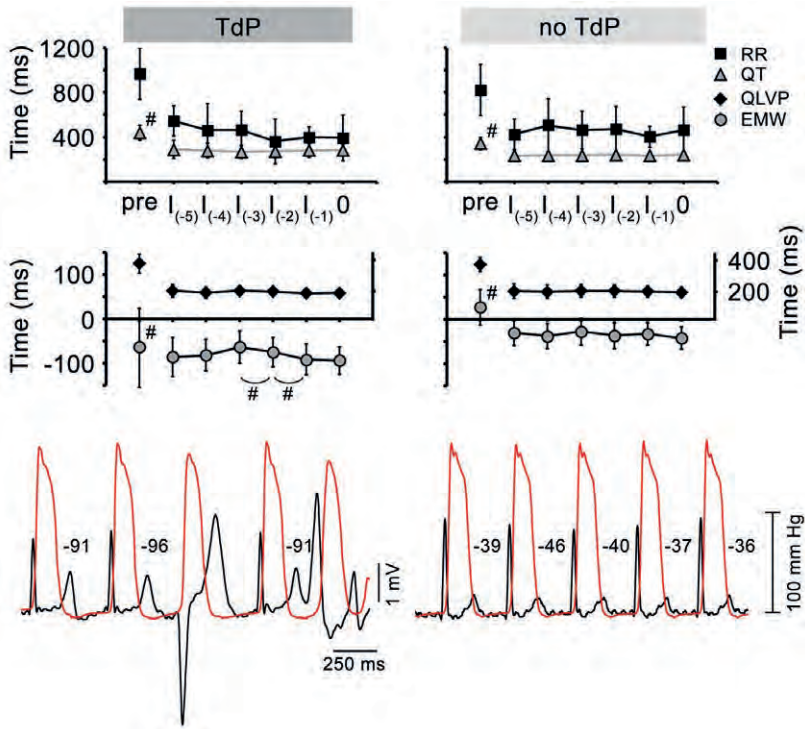


Figure 4.6 Top, beat-to-beat changes in RR interval, QT interval, $QLVP_{90}$, and EMW during HMR1556 and LSGS just prior to TdP (**left**) or at 26 s and maximal chronotropic response (no TdP; **right**). Pre-LSGS QT and EMW were significantly more pronounced in TdP-susceptible animals. # indicates $P<0.05$. **Below**, simultaneous recording of ECG lead II and LVP to illustrate EMW variations.

An initial delay in MAP repolarization was present throughout a broad range of RR cycle lengths during LSGS and I_{K_S} blockade, but EADs did not occur (**Figure 4.4**). Increased diastolic slopes suggesting delayed afterdepolarizations were also not observed. During this condition with fast-rate dependent electrical instability and mechano-electric heterogeneity, relatively short-coupled non-pause dependent PVCs occurred (**Figures 4.5-4.7**). Macroscopic aftercontractions preceded TdP in one dog. The TdP/VF-triggering PVCs typically had an intermediate QRS axis, large QRS amplitudes, and their earliest endocardial activation at the RV MAP signal (in 4/5 dogs, **Figure 4.7**), suggesting focal activation in the outflow tracts region. In one animal, TdP initiation emerged from the inferior LV. TdP onset



was non-pause dependent with $I_{(-1)}$ never exceeding $I_{(-2)}$. In some cases ventricular ectopy occurred prior to $I_{(-2)}$.

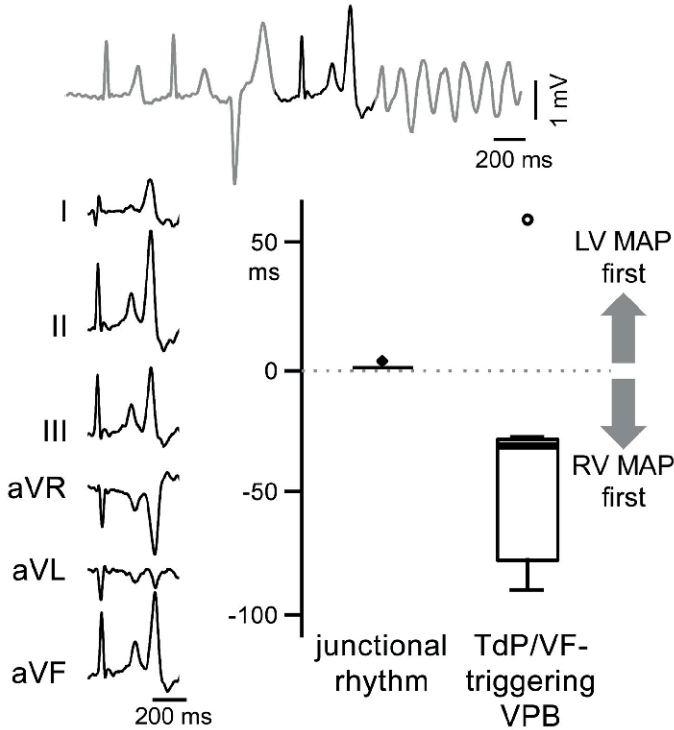


Figure 4.7 Outflow-tract origins of TdP/VF-triggering PVC. **Left**, 6-lead ECG recording showing an intermediate QRS axis with a relatively short duration. **Right**, box plot of interventricular activation delay of the junctional beats versus the TdP/VF-triggering extrasystoles demonstrating the earliest electrical activation in the RV in all but one case.

DISCUSSION

This is the first study to demonstrate the proarrhythmic consequences of LSGS in an in-vivo model of drug-induced LQT1¹¹² in which autonomic reflexes, neurocardiac transmission and cardiac electromechanical coupling are only mildly influenced by the applied anesthesia. In-vivo I_{Ks} blockade prolonged ventricular repolarization duration and augmented spatial and temporal repolarization dispersion, recapitulating LQT1 aspects. Only with concomitant LSGS did TdP occur. Arrhythmia initiation was always fast-rate (non-pause) dependent, with the majority of triggering beats originating in the outflow-tracts region. This is consistent with the site of TdP onset in the majority of LQTS patients.²⁷⁰

In most susceptible dogs with drug-induced LQT1 and LSGS, TdP rapidly deteriorated into defibrillation-resistant VF. In this undecentralized set-up, LSGS as well as RSGS caused

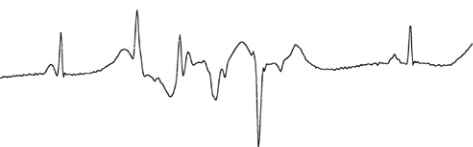
positive chronotropic effects, but inotropic and particularly lusitropic influences were more dominant by LSGS than by RSGS. Because of this, and in the face of repolarization prolongation by I_{Ks} blockade, LSGS exaggerated EMW disparity, mostly so in the seconds before TdP. RSGS was not torsadogenic under these conditions.

In a previous study in the same model, with isoproterenol as provocative agent, the combination of prolonged repolarization and shortened LVP favored the emergence of LV aftercontractions at instances with pending TdP.¹¹² In the present study, macroscopic aftercontractions were infrequently observed, but we speculate that the regional myocardial effects of LSGS could have produced low-amplitude aftercontractile events (below the radar of global intracavitary pressure) with similar arrhythmogenic significance during negative EMW. Pronounced EMW negativity related to TdP occurrence has also been observed by others during beta-adrenergic stimulation in experimental LQT1¹¹³ and by us in clinical studies on symptomatic patients with congenital LQTS.^{322, 331} Future studies could concentrate on examining mechano-electric triggers of arrhythmia in LQTS.

PROARRHYTHMIC PROCLIVITY OF LSGS DURING I_{Ks} INHIBITION

The present findings confirm the arrhythmogenic role of left-sided cardiac sympathetic hyperactivity in a clinically-relevant LQT1 model, like was demonstrated in other experimental preparations.³⁵² We found remarkable differences in the arrhythmogenic outcome between blood-borne beta-adrenergic and sympathetic stimulation in the anesthetized LQT1 model. In the former, the successful cardioversion of induced TdP allowed multiple provocations per dog,¹¹² whereas the sympathetically-induced TdP/VF were highly resistant to defibrillation attempts. Sympathetic hyperactivity, releasing norepinephrine locally at the myocardial nerve endings, accentuates heterogeneity in ventricular repolarization under these conditions, and favors reentrant excitation, whereas circulating catecholamines or infused isoproterenol act more uniformly.³⁴⁰ These differences are accompanied by a considerably larger positive inotropic (but similar chronotropic) response upon LSGS followed by a protracted vagal rebound in contrast to our observations with isoproterenol in the same model.¹¹² This vagal accentuation could be explained by the sudden sympathetic withdrawal and/or by baroreflex activation in response to the elevated arterial pressures. Assuming that a similar response occurs upon LSGS during drug-induced LQT1, and supported by the observation of a prominent vagal rebound in the rare case of successful cardioversion of VF, our results suggest that reflex vagal activation may have promoted the LQT1-related TdP to deteriorate into VF. Indeed, vagal nerve stimulation increases ventricular dispersion of repolarization and it has been demonstrated that this exacerbates in drug-induced LQT2.¹⁶⁰ Moreover, when applied during induced VF in pigs or sheep, vagal nerve stimulation increases the variability of the dominant VF frequency, potentially sustaining the arrhythmia.¹⁴⁷

The triggers for most life-threatening events for LQT1 patients are either physical (75%) or emotional stress (15%) while rest/sleep accounts for only 10%.¹⁵¹ One third of patients has events during swimming.¹⁵¹ These arrhythmias are effectively prevented in most LQT1



patients by beta-blockade³⁵³ or by left-cardiac sympathetic denervation.^{186, 353} On the other hand, strong vagal reflexes have been implicated in high-risk LQT1 patients,^{154, 155} and cold-water submersion and swimming, a genotype-specific trigger, provokes powerful co-stimulation of both sympathetic and parasympathetic limbs, at least in the first instances.³⁵⁴ Our experimental results do not allow firm conclusions on the contribution of vagal stimulation to ventricular proarrhythmia in LQTS, but they lend indirect support to the concept of “autonomic conflict”,¹⁴⁸ which indicates that a more convoluted vago-sympathetic interaction can facilitate ventricular tachyarrhythmia.

LIMITATIONS

The present study involved a relatively small number of animals, which was driven by ethical considerations. However, the differences in results obtained in paired analysis or group comparisons were so profound that they readily reached statistical significance.

The use of an anesthesia model always brings into question the cardiovascular and autonomic effects of anesthesia, especially when dealing with autonomic interventions. In the present study, we minimized potentially confounding effects^{113, 348} by the choice of anesthetics.

CONCLUSIONS

In this in-vivo canine model of drug-induced LQT1, LSGS readily induced TdP and VF in the presence of repolarization prolongation, MAP-EADs generation and exaggerated spatiotemporal dispersion of repolarization. Triggering PVCs most often emerged from the LV and RV outflow-tract regions. LSGS always rendered the EMW more negative prior to arrhythmia induction, which suggests that mechano-electric instability is somehow involved in the proarrhythmic proclivity. Our results offer novel mechanistic understanding of LQT1-related arrhythmogenesis and strengthen the rationale for left-cardiac sympathetic denervation in the prevention of life-threatening arrhythmias in several cardiac disorders, ranging from channelopathies¹⁴⁹ to structural heart diseases.^{149, 355}

ACKNOWLEDGEMENTS

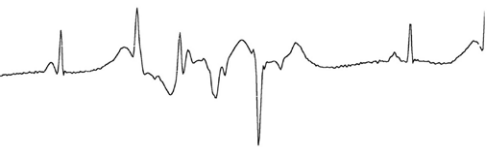
The authors wish to thank Roel L.H.M.G. Späjtens BSc, for excellent graphical support and Antonio Zaza, MD, for the fruitful discussions on neurocardiac physiology.

FUNDING

P.G.A.V. was supported by a Vidi grant from the Netherlands Organization for Scientific Research (ZonMw 91710365).



"Keep on ticking"



5

HERITABILITY IN A *SCN5A*-MUTATION FOUNDER POPULATION WITH FEMALE SUSCEPTIBILITY TO NON-NOCTURNAL VENTRICULAR TACHYARRHYTHMIA AND SUDDEN CARDIAC DEATH

Rachel M.A. ter Bekke, Aaron Isaacs, Andrei Barysenka, Marije B. Hoos, Jan D.H. Jongbloed,
Jan C.A. Hoorntje, Alfons S.M. Patelski, Apollonia T.J.M. Helderma-van den Enden,
Arthur van den Wijngaard, Monika Stoll, Paul G.A. Volders

Heart Rhythm 2017;14:1873-1881

ABSTRACT**BACKGROUND**

Heritable cardiac sodium-channel dysfunction is associated with various arrhythmia syndromes, some predisposing to ventricular fibrillation. Phenotypic diversity among carriers of identical-by-descent mutations is often remarkable, suggesting influences of genetic modifiers.

OBJECTIVE

We identified a unique *SCN5A*-mutation founder population with mixed clinical phenotypes and sudden cardiac death, and investigated the heritability of electromechanical traits besides the *SCN5A*-mutation effect.

METHODS

The 16-generation founder population segregating *SCN5A* c.4850_4852delTCT, p.(Phe1617del), was comprehensively phenotyped. Variance component analysis was used to evaluate the mutation's effects and assess heritability.

RESULTS

In 45 p.(Phe1617del) positives, the mutation associated strongly with QTc prolongation, 472 ± 60 versus 423 ± 35 ms in 26 mutation negatives ($P < 0.001$; OR for LQTS [95% C.I.] = 22.4 [4.5-224.2]; $P < 0.001$), and electromechanical window negativity, -29 ± 47 versus 34 ± 26 ms ($P < 0.001$). Overlapping phenotypes including conduction delay and Brugada syndrome were noted in 19. Polymorphic ventricular tachyarrhythmias occurred mostly at daytime, after arousal-evoked heart-rate acceleration and repolarization prolongation. Cox proportional hazards regression analysis revealed female gender as an independent risk factor for cardiac events (HR [95% C.I.] = 5.1 [1.6-16.3]; $P = 0.006$). p.(Phe1617del) was an important determinant of QTc_{baseline}, QTc_{max}, and EMW, explaining 18%, 28%, and 37% respectively of trait's variance. Significant heritability was observed for PQ interval ($P = 0.003$), after accounting for the p.(Phe1617del) effect.

CONCLUSION

This *SCN5A*-p.(Phe1617del) founder population with phenotypic divergence and overlap reveals LQTS-related and arousal-evoked ventricular tachyarrhythmias with a female preponderance. Variance component analysis indicates additional genetic variance for PQ interval hidden in the genome, besides a dominant p.(Phe1617del) effect on QTc and EMW.



INTRODUCTION

Sudden cardiac death accounts for a significant proportion of natural mortality in industrialized societies and imposes a sizable socioeconomic and psychosocial burden. VF is the main cause of SCD and occurs often in the setting of acute coronary events.^{9, 356} A prominent familial component contributing to the risk of SCD by ischemic VF has been recognized,^{8, 17, 18} but the underlying genetic mechanisms remain largely unclear.

The unraveling of genetic contributors to arrhythmia phenotypes is important for diagnostic purposes, risk stratification, elucidation of molecular pathways, and the identification of potential therapeutic targets. However, limited sample sizes of representative populations, heterogeneity of the arrhythmogenic substrate and the difficulty of obtaining phenotype information after cardiac arrest make this a challenging quest. Moreover, prominent phenotypic heterogeneity, including SCD susceptibility, has been observed among affected individuals sharing the same mutation.⁵⁷ This variability has been attributed to a low disease penetrance (25% in the long-QT syndrome⁵⁸ and 16% in Brugada syndrome),⁶³ differential expressivity, and non-genetic factors such as age,³⁵⁷ gender,⁶⁰ and the use of medication.⁵⁹ One study observed compound heterozygosity in ~8% of LQTS cases.⁶¹ Additionally, common variants in certain genes, such as *SCN5A*,⁸⁵ *SCN10A* and *HEY2*,⁸⁶ can contribute to disease penetrance in sick-sinus and Brugada syndrome, which indicates a complex genetic architecture. To investigate such complex genetic factors, family cohorts provide substantial benefits: they are robust to false-positive findings due to population substructure, they typically share a large proportion of environmental factors, and they may be enriched for rare variants that are difficult to study in the general population.

In this study, we investigated a large Dutch-German founder population with excess SCD over multiple generations, segregating an amino-acid deletion in *SCN5A* (c.4850_4852 delTCT, exon 28, p.(Phe1617del), rs749697698). Because cardiac differences between Phe1617del carriers appeared prominent, we used variance component analysis to first assess the effects imposed by the known *SCN5A* mutation and then calculate remaining heritabilities of various proarrhythmic phenotypes. Identifying new genetic risk factors can give profound insights into molecular mechanisms, assist in further diagnosis and yield novel information regarding the broader problem of SCD.

METHODS

All participants (≥18 years) gave written informed consent for clinical and genetic analyses. The Medical Research Ethics Committee of Maastricht University Medical Centre approved the study protocol. This study complies with the Declaration of Helsinki. It is registered under www.clinicaltrials.gov; NCT02014961.

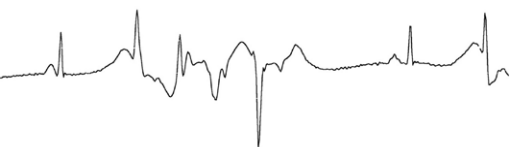
STUDY POPULATION

Between 2006 and 2015, seven probands presented independently at our Cardiogenetics Outpatient Clinic with QT prolongation, polymorphic ventricular tachycardia, prolonged-repolarization associated TdP, or SCD of a first-degree relative. After obtaining informed consent, genomic DNA was extracted from peripheral blood. Using Sanger sequencing the pathogenic *SCN5A* mutation c.4850_4852delTCT, p.(Phe1617del), rs749697698 was identified in all probands on a haplotype that also contained rs1805124 (*SCN5A* c.1673A>G, exon 12, p.(His558Arg)). One additional variant, rs1805128 in *KCNE1*, c.253G>A, exon 3, p.(Asp85Asn),⁷³ was found in two probands. Both had a prolonged QT interval, but no documented VT. The presence of this *KCNE1* variant in the pedigree is unlikely to affect our general results, as its transmission is independent of the *SCN5A*-founder haplotype. No pathogenic mutations were found in *ABCC9*, *AKAP9*, *ANK2*, *CACNA1C*, *CACNA2D1*, *CACNB2*, *CALM1*, *CASQ2*, *CAV3*, *DPP6* (only tested for 4 c.-340C>T), *GPD1L*, *HCN4*, *KCNE2*, *KCNE3*, *KCNH2*, *KCNJ2*, *KCNJ8*, *KCNJ8*, *KCNQ1*, *LMNA*, *RYR2*, *SCN1B*, *SCN3B*, *SCN5A*, *SNTA1*, *TNNT2*, and *TRDN*.

Relatedness of all Phe1617del probands was ascertained using regional genealogical archives, parish registers, and private databases, and common ancestry was confirmed. Haplotype sharing at 8 microsatellite markers spanning the *SCN5A* locus, 5 upstream (D3S1768, D3S1561, D3S1298, D3S3639, D3S1260) and 3 downstream (D3S1100, D3S2407, D3S3559) confirmed these genealogical relationships. Cascade screening revealed an autosomal dominant inheritance pattern.

PHENOTYPIC CHARACTERIZATION

Comprehensive phenotyping of Phe1617del-positive and mutation-negative family members was performed. Syncope, documented VT/VF, aborted cardiac arrest, and/or SCD were scored as cardiac events. Baseline 12-lead ECGs were digitally magnified and analyzed using on-screen calipers. First (≥ 18 years) and maximal documented PQ and QT intervals were determined. The longest QT interval in lead II or any precordial lead was measured for calculation of the heart-rate corrected QTc according to Bazett's formula. LQTS was diagnosed according to current guidelines.¹ Isorhythmic atrioventricular dissociation was noted as the wandering of sinus P waves in and out of their associated QRS complexes. Overlap was defined as the concomitant presence of two of the following traits: LQTS, Brugada syndrome, cardiac conduction disease (CCD) or isorhythmic atrioventricular dissociation. Echocardiography and cardiac magnetic imaging were used to determine the presence of structural abnormalities. The electromechanical window, defined as QaOC minus the concomitantly measured QT interval, was calculated during continuous-wave Doppler flow assessment of the aortic valve.³³¹ Ajmaline provocation testing (1 mg/kg in 10 minutes) was performed to unmask concealed Brugada syndrome. ICD readouts were analyzed for arrhythmia characteristics.



STATISTICAL AND VARIANCE COMPONENT ANALYSES

The normality of phenotype and residual distributions was assessed by the inspection of density plots and by the Shapiro-Wilk test. For continuous traits, mean differences between subgroups were tested using the Mann-Whitney U test. Odds ratios comparing the prevalence of dichotomous traits among subgroups were estimated using Fisher's exact test. Cox proportional hazards models were implemented to conduct survival analyses, and testing of the Schoenfeld residuals was performed. Analyses were conducted using the base R package (<https://www.R-project.org>) and the survival package (<https://CRAN.R-project.org/package=survival>).

To estimate the effects of the *SCN5A*-p.(Phe1617del) mutation, as well as trait heritabilities, a variance component approach, as implemented in the sequential oligogenic linkage analysis routines (SOLAR) software package, was used. Thus, we assessed the narrow-sense heritability estimate (h^2), referred to as "residual heritability", representing the percentage of variance of a quantitative phenotypic trait attributable to additional genetic factors. To satisfy distributional assumptions inherent to this method, phenotypes were regressed on age, sex, and height using linear regression models. The residuals from those models were transformed using the rank-based inverse normal transformation function in GenABEL and used as phenotypes for analysis in models including the *SCN5A* deletion.³⁵⁸ To correct for multiple comparisons, while accounting for the correlation between phenotypes, the effective number of independent traits was estimated. First, a Spearman's correlation matrix was constructed from all analyzed phenotypes in R. Then, matrix spectral decomposition was applied to these correlations using `matSpD` (<http://gump.qimr.edu.au/general/daleN/matSpD/>)³⁵⁹ to derive the number of effective tests ($n=12$); the nominal P value of 0.05 was divided by this number yielding a significance threshold of $P=0.004$. From the normalized residuals we computed the effect size (β , in standard deviations) attributed to the *SCN5A* mutation, the p.(H558R) polymorphism, and the familial component (h^2) by means of a kinship matrix, which was constructed utilizing the pedigree structure.

RESULTS

GENEALOGY, PEDIGREE STRUCTURE AND MORTALITY DATA

Figure 5.1 illustrates the 16-generation pedigree of the Phe1617del-positive family, which mainly resides in Limburg (The Netherlands) and North Rhine-Westphalia (Germany). Carriers living in Lund (Sweden) and Munich (Germany) had comparable DNA profiles, confirming relatedness but their lines of descent remained unclear. Genealogical research identified two ancestral couples that lived near the river Worm, at the south-eastern border of The Netherlands with Germany (hence our designation "Worm Study" to this research), in the 16th century.

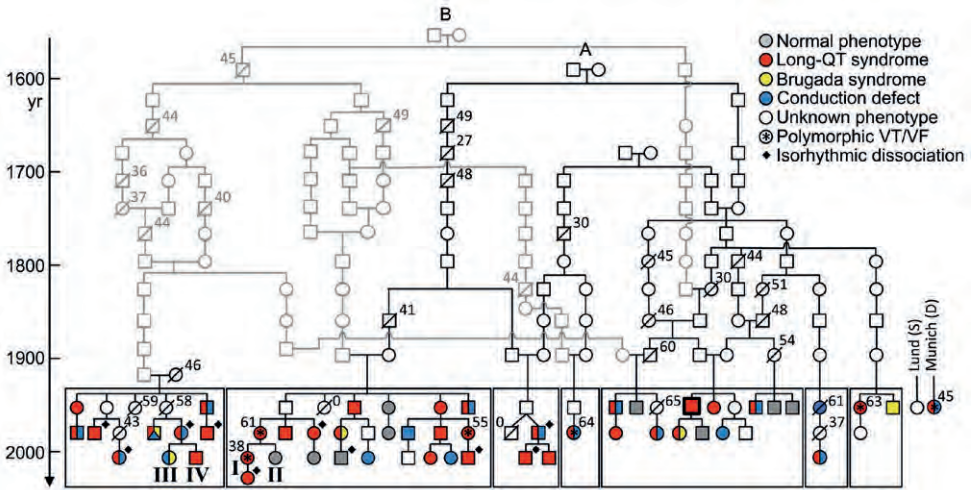
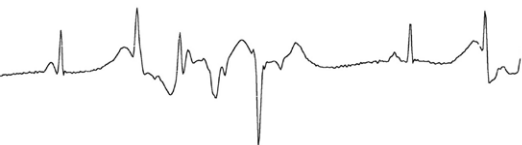


Figure 5.1 Pedigree of *SCN5A*-p.(Phe1617del)-mutation carriers for seven family groups. Black lines of descent for presumed founder couple A; grey lines for couple B. Deaths before 51 years of age are noted. Squares represent males (in bold: homozygous carrier), circles females. Only carriers are depicted. VT = ventricular tachycardia; VF = ventricular fibrillation.

Ancestral couple A connects five probands, and couple B four (**Figure 5.1**). Despite extensive efforts, a single founding couple connecting all probands has not yet been identified. In all likelihood, the *SCN5A* mutation emerged prior to 1600. **Figure 5.2** demonstrates the chronological migration of the mutation from its presumed first occurrence. At present, the total number of known family members exceeds 4,800.

The pedigree depicts interfamilial marriages within the third or fourth degree of consanguinity. A male proband born of consanguineous parents was found to be homozygous for *SCN5A*-p.(Phe1617del), **Figures 5.1** and **5.3**.



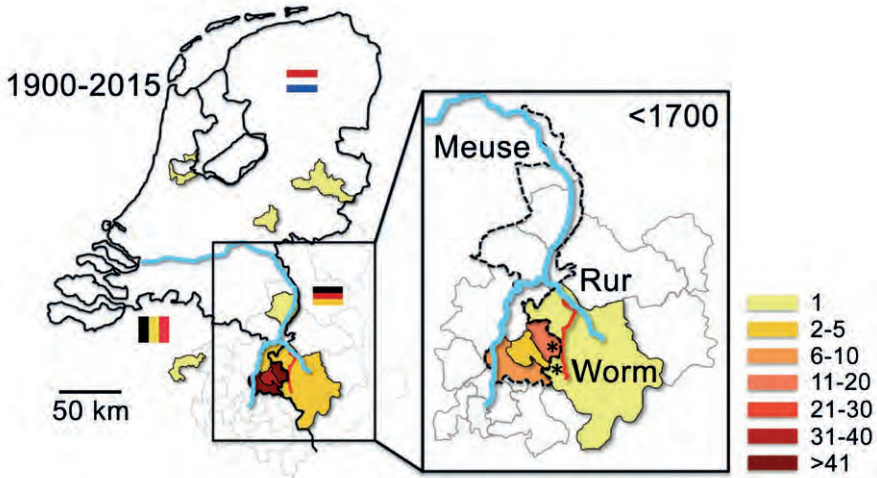


Figure 5.2 Geographic distribution and spread of *SCN5A*-p.(Phe1617del) in the Dutch-German-Belgian Euregion during the last 4 centuries. Asterisks mark the living areas of founder couples A and B.

PHENOTYPIC HETEROGENEITY AND OVERLAP

Clinical characteristics of the study population are presented in **Table 5.1**. Four main phenotypes were observed: LQTS, CCD, Brugada syndrome, and isorhythmic atrioventricular dissociation (**Figure 5.3**), with striking phenotypic heterogeneity among Phe1617del-positive patients, even between siblings (see I-IV in **Figure 5.1**).

As is illustrated by the color codes in **Figure 5.1**, LQTS was the prevailing phenotype, present throughout the pedigree. LQTS was diagnosed in 28 carriers and a strong association between Phe1617del and risk of LQTS was seen (OR [95% C.I.] = 22.4 [4.5-224.2]; $P < 0.001$). Prolonged repolarization, with a mean difference ($\Delta\mu$) of 48 ms ($P < 0.001$) compared to non-carriers, was present at a wide variety of heart rates (**Figure 5.4**).

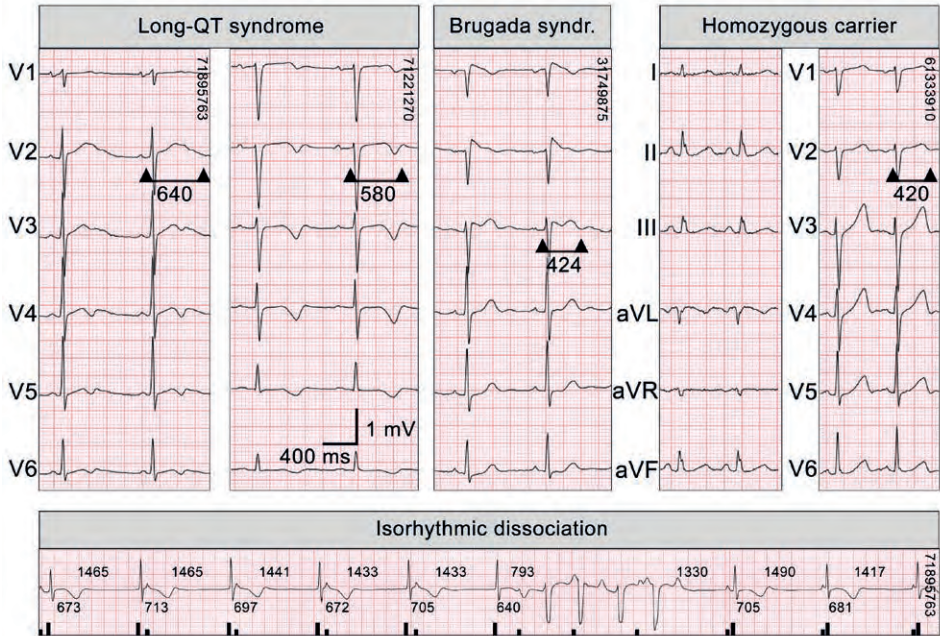


Figure 5.3 *SCN5A*-p.(Phe1617del)-related electrocardiographic phenotypes. During isorhythmic atrioventricular dissociation, long and short bars indicate QRS and P onset, respectively. Top numbers indicate RR intervals; bottom QT intervals.



Table 5.1 Clinical characteristics of the study population

	Worm study population			Phe1617del positives		
	mut. neg.	mut. pos.	<i>P</i> value	asympt.	sympt.	<i>P</i> value
Number, n	26	45		24	21	
Age, years	51 ± 18	49 ± 16	0.68	49 ± 17	50 ± 16	0.86
Female sex, n (%)	16 (62)	24 (53)	0.81	8 (33)	16 (76)	0.007
Height, cm	171 ± 13	174 ± 11	0.34	176 ± 9	170 ± 12	0.036
Weight, kg	73 ± 15	73 ± 13	0.71	75 ± 11	68 ± 15	0.048
Cardiac events, n (%)	5 (19)	21 (47)	0.022	0	21	
Beta-blocker, n (%)	8 (31)	13 (29)	0.78	5 (24)	8 (38)	0.18
<i>Cardiac phenotype</i>						
Normal, n (%)	15 (58)	8 (18)	0.003	6 (25)	2 (10)	0.43
LQTS, n (%)	2 (8)	28 (62)	<0.001	14 (58)	14 (67)	0.18
CCD, n (%)	10 (38)	15 (33)	1.00	8 (33)	7 (33)	0.75
Brugada syndr., n (%)	0 (0)	5 (11)	0.15	3 (13)	2 (10)	1.00
Isorhythm. diss., n (%)	0 (0)	9 (20)	0.010	5 (21)	4 (19)	1.00
Overlap, n (%)	1 (4)	19 (42)	<0.001	9 (38)	10 (48)	0.34
Unknown, n (%)		4 (9)			4 (19)	
<i>ECG</i>						
PQ, ms	164 ± 31	161 ± 25	0.80	166 ± 24	153 ± 24	0.076
PQ _{max} , ms	176 ± 37	186 ± 41	0.29	193 ± 48	177 ± 28	0.31
RR, ms	934 ± 150	910 ± 181	0.57	909 ± 192	912 ± 170	0.91
QRS, ms	100 ± 16	93 ± 14	0.12	92 ± 8	96 ± 19	0.94
QT, ms	408 ± 42	450 ± 74	0.008	424 ± 49	487 ± 88	0.03
QTc, ms	423 ± 35	472 ± 60	<0.001	448 ± 37	505 ± 71	0.006
QTc _{max} , ms	459 ± 46	523 ± 69	<0.001	499 ± 46	557 ± 83	0.043
<i>Echocardiography</i>						
LVEF, %	60 ± 6	62 ± 5	0.11	62 ± 5	61 ± 5	0.39
RVEDD, mm	34 ± 6	34 ± 4	0.71	33 ± 8	35 ± 4	0.60
QAoC, ms	420 ± 31	400 ± 32	0.029	399 ± 25	402 ± 42	0.68
RR, ms	957 ± 171	900 ± 123	0.14	897 ± 110	906 ± 146	0.84
QT, ms	386 ± 38	428 ± 54	0.001	410 ± 28	456 ± 72	0.037
EMW, ms	34 ± 26	-29 ± 47	<0.001	-11 ± 26	-56 ± 60	0.008

For continuous traits, mean differences were tested using the Mann-Whitney U test. Differences in prevalence of dichotomous traits were compared using Fisher's exact test. Four phenotypes were missing due to SCD. LQTS = long-QT syndrome; CCD = cardiac conduction disease; LVEF = left-ventricular ejection fraction; RVEDD = right-ventricular end-diastolic diameter; QAoC = time interval between onset QRS and aortic-valve closure; EMW = electromechanical window.

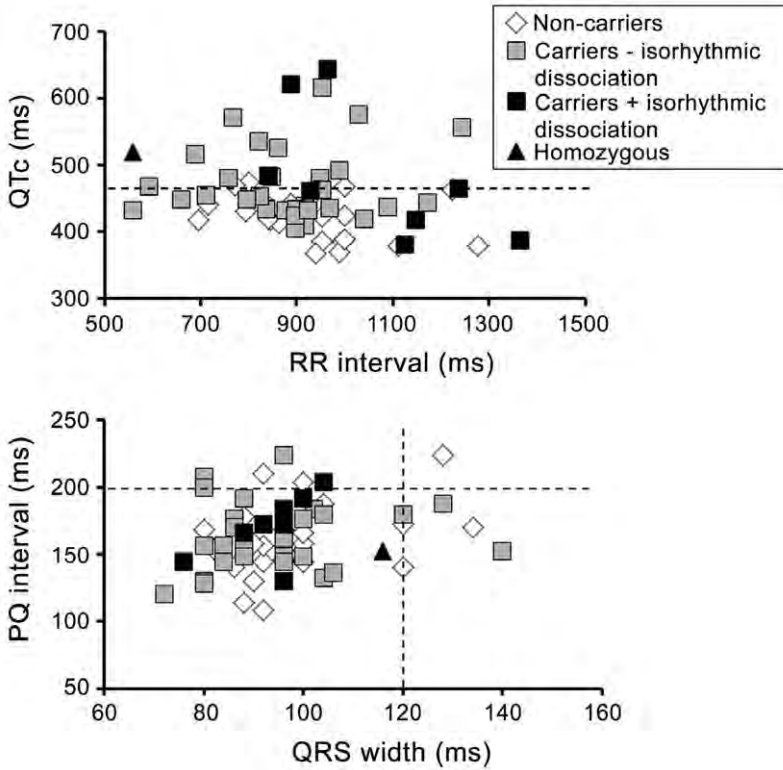


Figure 5.4 QTc/RR and PQ/QRS relationships of *SCN5A*-p.(Phe1617del) carries and non-carriers. Upper limits of normal values are indicated by the dotted lines.

Phe1617del positives with previous cardiac events exhibited a significantly longer QTc and were more often female compared to event-free carriers (QTc 505 ± 71 versus 448 ± 37 ms, $P=0.006$; female gender 76 versus 33%, $P=0.007$). On echocardiography, QAOcs were significantly shorter ($\Delta\mu=20$ ms, $P=0.028$) despite (simultaneously measured) longer QT intervals, causing more pronounced EMW negativity in mutation positives (**Table 5.1**; $\Delta\mu=-63$ ms). Symptomatic cases had more negative EMWs compared to asymptomatic individuals, -56 ± 60 versus -11 ± 26 ms, $P=0.008$.³³¹ *SCN5A*-p.(Phe1617del) carriers frequently exhibited broad-based T-wave inversion or bifid T waves (**Figure 5.3**), unlike “classic” LQT3 repolarization patterns. Interestingly, two Phe1617del-negative individuals also exhibited long QT intervals (**Figure 5.5** and **Figure 7.9**); mutations in known arrhythmia genes were excluded in them.



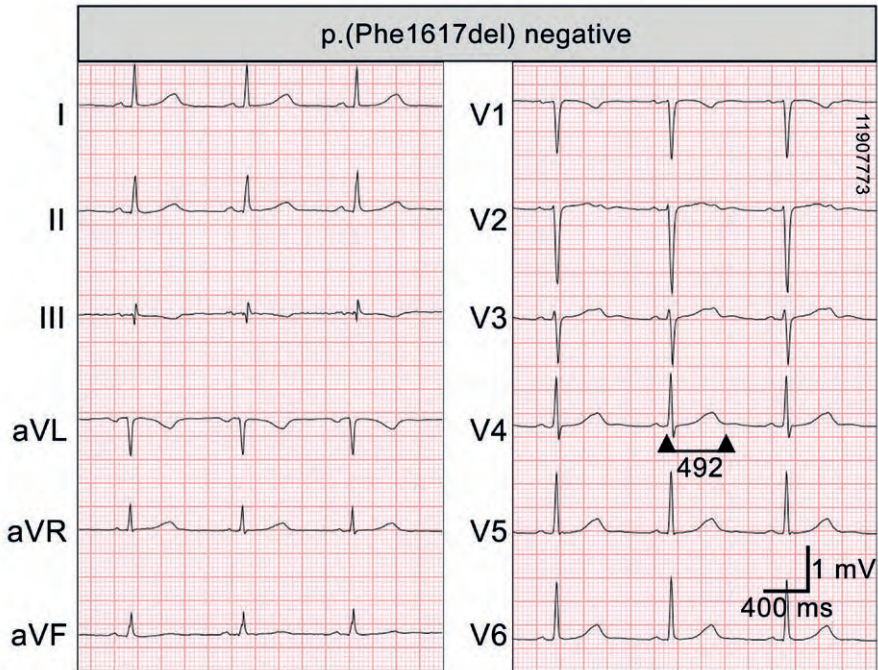


Figure 5.5 ECG of *SCN5A*-p.(Phe1617del)-negative individual with a long QT interval.

Whereas baseline PQ and QRS intervals generally remained within normal limits (**Figure 5.4**), transient atrioventricular conduction delay was observed in ten Phe1617del positives, second degree atrioventricular block in three, left-bundle branch block in three, and right-bundle branch block in one. A few mutation negatives demonstrated mild forms of CCD. Unique to the Phe1617del-positive cohort, spontaneous coved-type ST-segment elevation fitting with Brugada syndrome ($n=1$; **Figure 5.3**) and ajmaline-provoked type-1 Brugada-ECG pattern were observed ($n=4$; for example **Figure 5.6**).

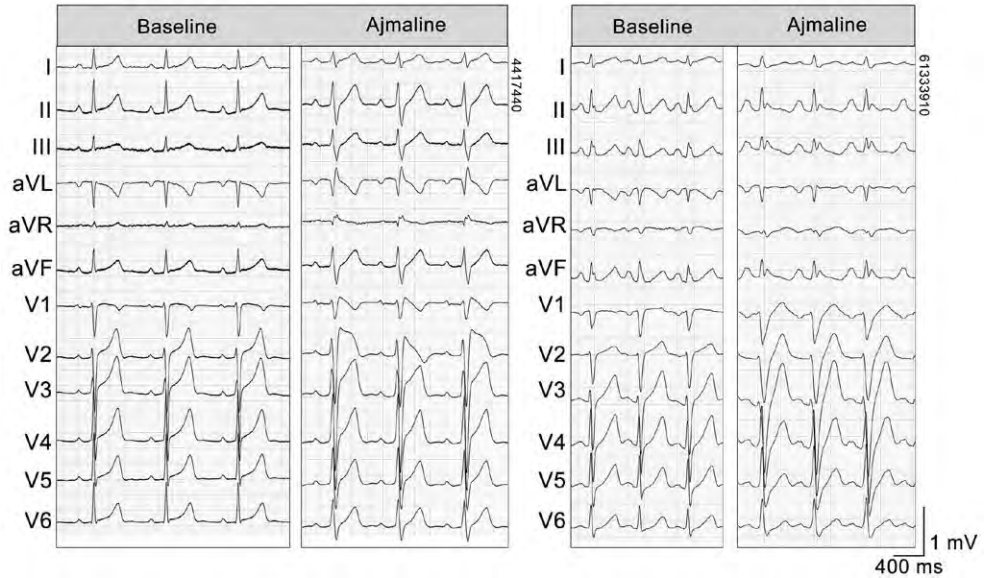
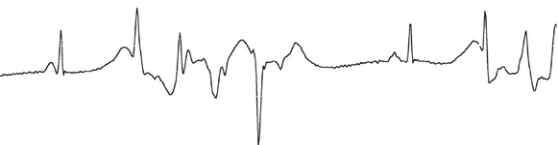


Figure 5.6 Ajmaline provocation testing. **Left**, *SCN5A*-p.(Phe1617del) heterozygous individual. **Right**, the p.(Phe1617del) homozygous patient.

A novel phenotype, isorhythmic atrioventricular dissociation, was present in 9/45 mutation carriers, but absent in non-carrying relatives (**Figures 5.3** and **5.7**; $P_{\text{Fisher's}}=0.010$). It occurred in three out of seven family subgroups mainly at night, between 9 PM and 10 AM, at a mean sinus/atrial rate of 41 ± 7 bpm. Besides episodic sinus and atrial bradycardia, no distinct atrial electropathology (such as atrial standstill or atrial fibrillation) was observed. *SCN5A*-related dilated cardiomyopathy was not seen.

The Venn diagram (**Figure 5.7**) demonstrates that most Phe1617del carriers, notably those with LQTS, exhibited overlap with other phenotypes, namely CCD, Brugada syndrome and/or isorhythmic atrioventricular dissociation ($n=19$). In eight Phe1617del-positive individuals we could not discern any cardiac abnormalities, despite thorough phenotyping, including ajmaline provocation testing.



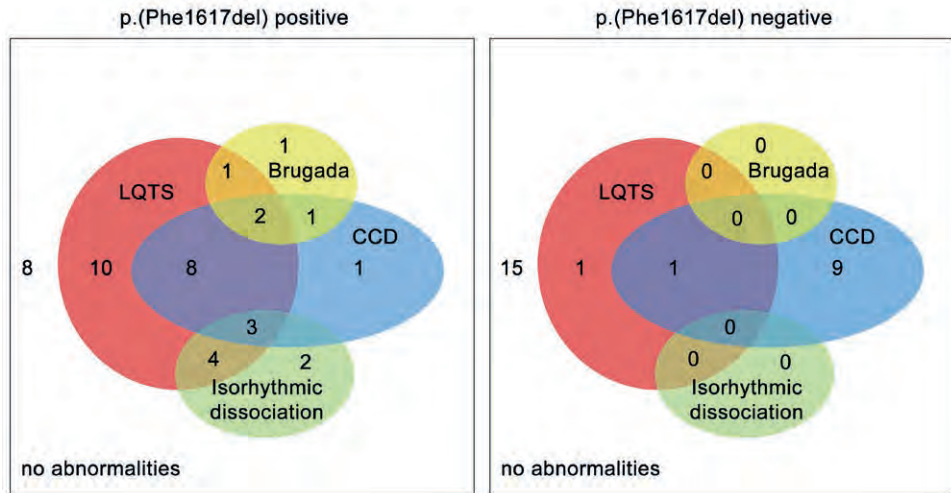


Figure 5.7 Venn diagram illustrating cardiac phenotypes and their overlap in the presence or absence of *SCN5A*-p.(Phe1617del). In both panels, some numbers are missing, because of incomplete cardiac recordings. LQTS = long-QT syndrome.

VENTRICULAR ARRHYTHMOGENESIS

In the last four decades, 47% of the Phe1617del positives experienced cardiac events (OR [95% C.I.] = 3.8 [1.1-15.1]; $P=0.022$), including syncope in nine, non-sustained VT in three, polymorphic VT/VF in six (**Figure 5.1**, asterisks), and SCD without arrhythmia documentation in three. Five ungenotyped first-degree relatives of Phe1617del positives died suddenly. The mean age at which SCD or VT/VF occurred first was 50 ± 10 years. ICD recordings of VT/VF in three patients, all females, are depicted in **Figure 5.8**.

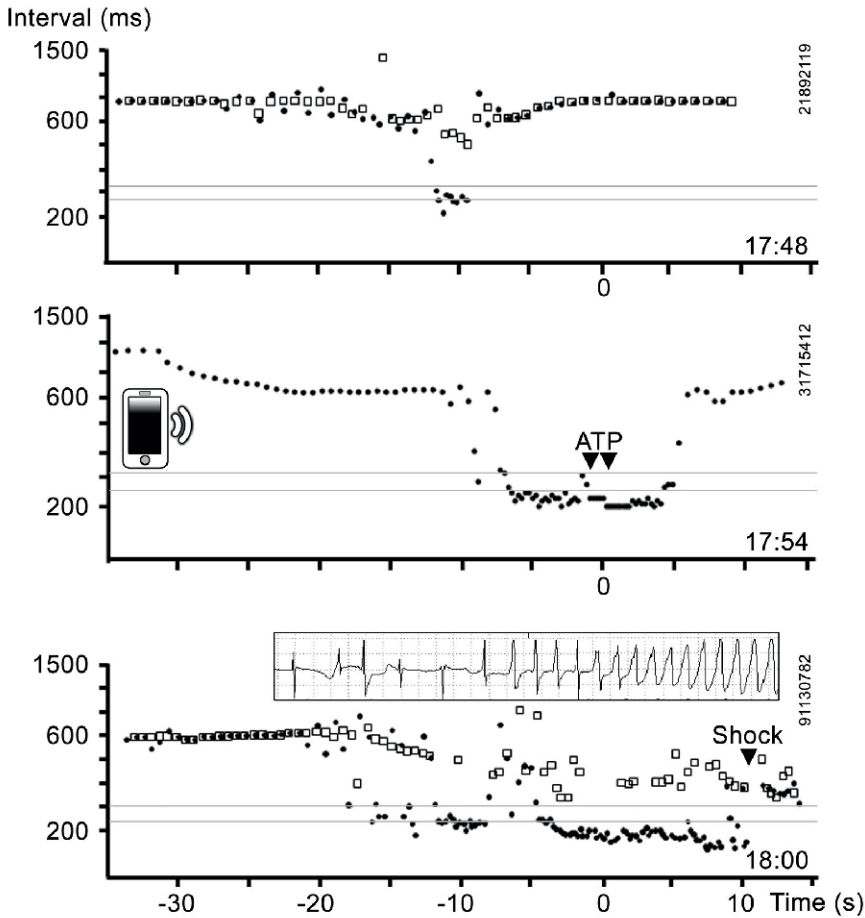
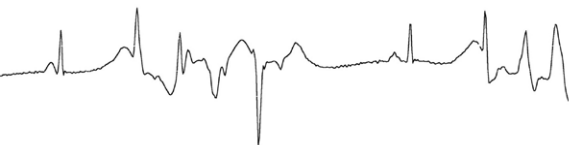


Figure 5.8 ICD recordings of polymorphic ventricular tachycardia in three females. **Top**, spontaneous recovery. **Middle**, cardioversion by antitachycardia pacing (ATP). **Bottom**, cardioversion by shock therapy. Time (h:min) indicates VT/VF occurrence. Squares = AA intervals; circles = VV intervals; VT = ventricular tachycardia; VF = ventricular fibrillation.

VT/VF episodes required internal/external cardioversion (lower panel), i.v. magnesium and isoproterenol,³²² antitachycardia pacing (middle), or recovered spontaneously (upper panel). Beta-Blocker treatment and high-rate atrial pacing did not prevent VT/VF in two patients. Ranolazine, however, reduced ventricular ectopy substantially. These life-threatening arrhythmias were found to occur only during daytime, between 9 AM and 9 PM, in line with the daytime occurrence of SCD in other confirmed or obligatory Phe1617del positives in this population. Proarrhythmic triggers included auditory stimuli (phone ringing; **Figure 5.8**), strong emotions, exercise (skiing), a period of excessive dieting (lower panel), and events in early postoperative and postpartum periods. VT occurred rarely during rest or



sleep. Often, sinus-rate acceleration with concomitant repolarization prolongation preceded premature ventricular complexes and polymorphic VT, as exemplified in **Figure 5.8**. TdP-like VT typically initiated after short-long-short RR intervals or could be non-pause-dependent.

We found a 15:1 female-to-male ratio of cardiac events ($P=0.007$) despite a similar mean QTc and EMW for both sexes (QTc: 470 ± 55 versus 474 ± 66 ms, $P=0.83$; EMW: -20 ± 43 and -36 ± 52 ms, $P=0.31$). **Figure 5.9** shows survival curves estimated using Cox proportional hazards models for event-free survival adjusted for gender, LQTS, EMW negativity (<-62 ms³³¹), and beta-blocker therapy. The survival curves are conditional based on the covariates. Hazard ratios indicated an independently increased risk for females (HR [95% C.I.]=5.1 [1.6-16.3]; $P=0.006$) and for individuals with substantial EMW negativity (HR [95% C.I.]=4.3 [1.2-15.6]; $P=0.024$). Testing of the Schoenfeld residuals demonstrated that the proportionality assumption held ($P=0.42$). EMW negativity enabled risk stratification in male ($P=0.004$), but not in female Phe1617del carriers ($P=0.15$).

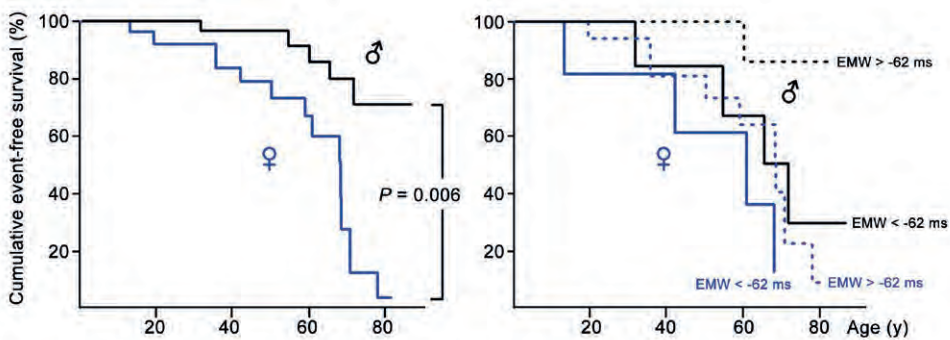


Figure 5.9 Cox proportional hazards curves for event-free survival adjusted for beta-blocker therapy, gender, EMW ($<$ or $>$ -62 ms), and LQTS; stratified by gender and EMW negativity. EMW = electromechanical window.

PHE1617DEL-RELATED EFFECTS AND RESIDUAL HERITABILITY

Analyses conducted in SOLAR, to properly account for the pedigree structure, recapitulated the strength of the associations between $p.(Phe1617del)$ and $QTc_{baseline}$, QTc_{max} , and EMW (**Table 5.2**). Effect sizes were large, on the order of magnitude of one standard deviation for $QTc_{baseline}$ (β (SE) = 0.91 (0.23)), QTc_{max} (1.11 (0.22)), and EMW (-1.26 (0.19)), explaining 18%, 28% and 37% of the trait's variance, respectively. These estimates corresponded well with the observed mean differences. Nominal associations were seen for QRS, QT, and QAOc.

Heritability estimates for baseline PQ interval (h^2 (SE) = 0.68 (0.25); $P=0.003$) showed that additive genetic effects accounted for a substantial proportion of PQ variation, independent of $p.(Phe1617del)$. Nominally significant heritabilities were observed for PQ_{max} (h^2 (SE) = 0.57 (0.27)), QT_{max} (0.43 (0.27)), and EMW (0.79 (0.29)).

Table 5.2 Residual heritabilities and effects of *SCN5A*-p.(Phe1617del)

	h^2 (SE)	<i>P</i> value	<i>SCN5A</i>	
			β (SE)	<i>P</i> value
ECG				
PQ	0.68 (0.25)	0.003	-0.01 (0.24)	0.98
PQ _{max}	0.57 (0.27)	0.010	0.47 (0.25)	0.056
RR	0.00 (NE)	0.50	-0.17 (0.27)	0.53
QRS	0.19 (0.23)	0.17	-0.52 (0.25)	0.040
QT	0.43 (0.27)	0.049	0.56 (0.24)	0.021
QTc	0.23 (0.37)	0.28	0.91 (0.23)	<0.001
QTc _{max}	0.35 (0.63)	0.36	1.11 (0.22)	<0.001
Echocardiography				
LVEF	0.59 (0.37)	0.19	0.28 (0.26)	0.27
RVEDD	0.08 (0.19)	0.31	0.09 (0.27)	0.75
QAoC	0.00 (NE)	0.50	-0.51 (0.25)	0.039
QT	0.55 (0.43)	0.10	0.94 (0.23)	<0.001
EMW	0.79 (0.29)	0.020	-1.26 (0.19)	<0.001

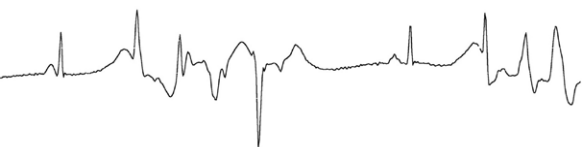
A variance component approach as implemented in SOLAR was used. β = effect size in standard deviations for *SCN5A*-p.(Phe1617del) carriership; h^2 = narrow-sense heritability; NE = not estimable; SE = standard error; other abbreviations as in Table 5.1.

The additional inclusion of *SCN5A*-p.(His558Arg), rs1805124, did not significantly alter the results and provided no evidence of an independent effect on any of the traits studied (all $P > 0.10$), with the possible exception of PQ_{max} ($P = 0.064$). Although the p.(His558Arg) polymorphism was in Hardy-Weinberg proportions in Phe1617del-negative family members ($P = 0.10$), there was a significant enrichment for the R allele in mutant carriers compared to the EUR samples from the 1000 Genomes Project Phase 3 (35 versus 22%; $P_{\text{Fisher's}} < 0.001$).

DISCUSSION

UNIQUE FOUNDER POPULATION

This *SCN5A*-p.(Phe1617del) founder population exhibited divergent and overlapping cardiac phenotypes, including LQTS, CCD, Brugada syndrome, and isorhythmic atrioventricular dissociation. Female carriers had a dominant susceptibility to ventricular arrhythmia and SCD, despite a similar QTc as males. Large p.(Phe1617del) effect sizes were found for QTc prolongation and EMW negativity. After accounting for the effects of the *SCN5A* deletion



mutation, significant heritability was identified for PQ interval, indicating the influence of additional genetic factor(s) on atrioventricular conduction.

PHENOTYPIC VARIABILITY IN CARDIAC SODIUM CHANNELOPATHIES

Since the first localization of the *SCN5A* locus to chromosome 3q21-24 and the description of the *SCN5A* mutation p.(KPQ1505-1507del) in 1995,⁴⁴ multiple pathogenic *SCN5A* mutations have been implicated in LQT3, Brugada syndrome, idiopathic VF, CCD, sinus-node dysfunction, atrial fibrillation, and dilated cardiomyopathy.³⁶⁰ In the present study, LQTS was the most prevalent phenotype of Phe1617del-positive individuals and possibly the result of an I_{Na} gain-of-function defect. Phenotypes reminiscent of I_{Na} loss-of-function, such as Brugada syndrome and CCD, were also present but less prominent. Previous patch-clamp experiments of Phe1617del-transfected HEK cells demonstrated a 7.0 mV-negative shift of the steady-state channel availability and impaired recovery from inactivation, contributing to a reduced peak I_{Na} density.³⁶¹ Those investigators found an increased late/peak I_{Na} ratio at positive command potentials, suggesting gain-of-function for part of the I_{Na} I-V curve. The presence of phenotypic divergence and phenotype-positive genotype-negative individuals alludes to the contribution of additional genetic variants. Furthermore, *SCN5A*-p.(Phe1617del) was identified in two individuals of different ethnicity (gnomAD database), who had LQTS and syncope without LQTS/Brugada syndrome characteristics. SOLAR analysis revealed a large effect of the mutation on repolarization prolongation, which is underscored by the segregation pattern. Combined, these results indicate that a definitive or monogenic causality cannot be assumed, and this has instigated subsequent studies into the area of complex genetics.

VARIANCE COMPONENT ANALYSIS AND HERITABILITY BEYOND *SCN5A*-p.(PHE1617DEL)

Although the presence of *SCN5A*-p.(Phe1617del) associated strongly with QTc, QAOc, and EMW, we did find evidence of other genetic influences on PQ interval, and possibly QT and EMW. PQ heritability (0.68) was higher than in a general population family-based study (0.40) in The Netherlands,²⁶ indicating strong genetic control in our pedigree. The *SCN5A* polymorphism p.(His558Arg) present in ~22% of EUR samples from the 1000 Genomes Project (<http://www.internationalgenome.org>), was significantly enriched in this population, 35%. Variance component analysis incorporating p.(His558Arg) provided no evidence of an independent effect on any of the traits investigated, although enrichment for the p.(Arg558) allele supported the notion of population isolate effects, particularly founder effects and genetic drift. Functional variants in other genes or regulatory elements on chromosome 3, such as *SCN10A*,³⁶² could also modulate regional *SCN5A* expression. Moreover, genetic modifiers on different chromosomes may be important. These aspects will be investigated in downstream high-density single nucleotide polymorphism genotyping and/or exome sequencing (**Figure 5.10**).

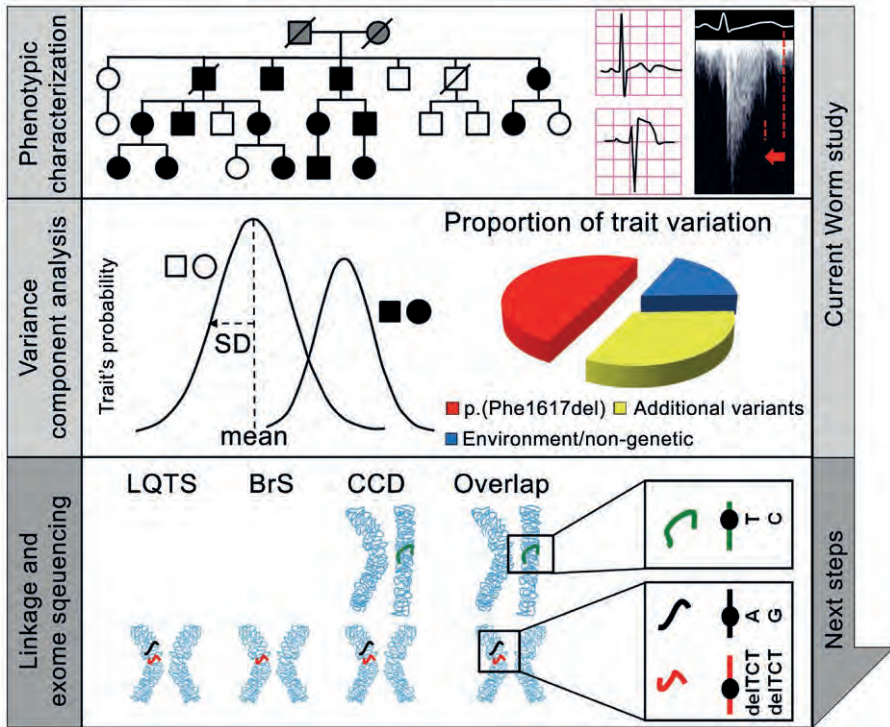
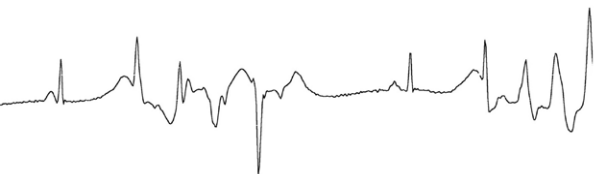


Figure 5.10 In-depth cardiac phenotyping coupled with variance component analysis explains electromechanical trait variation. The proportion of mutant and additional genetic variant (narrow-sense heritability)-imposed trait variation is estimated using SOLAR. As a perspective, subsequent studies will encompass linkage analysis and next-generation sequencing. Boxes/circles = males/females; open/filled = Phe1617del negatives/positives; BrS = Brugada syndrome; CCD = cardiac conduction disease; LQTS = long-QT syndrome; SD = standard deviation.

ARRHYTHMIA SUSCEPTIBILITY AND FEMALE PREPONDERANCE

Contrary to previously reported *SCN5A*-related arrhythmia features,³⁶⁰ we mainly observed stress-related, non-nocturnal VT/VF provoking cardiac arrest/SCD in our *SCN5A*-p.(Phe1617del) population. Stress- and arousal-evoked heart-rate acceleration and repolarization prolongation often preceded the life-threatening arrhythmias. These patterns suggest a proarrhythmic role for enhanced sympathetic activity to fuel electrical instability, which is uncommon for sodium channelopathies. Secondly, unlike reported sex-specific risk patterns,^{60, 363} we found that women with *SCN5A*-p.(Phe1617del) experienced major cardiac events more frequently than men. Fifty percent had (one or more) syncope or VT/VF/SCD before the age of 45. This female arrhythmia susceptibility may be evoked by altered myocardial ion-channel expression through the modulation by (non)gonadal hormones.³⁶⁴ Also, gene-gender interaction may play a role.



CONCLUSION

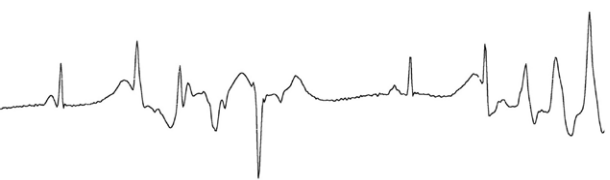
This unique *SCN5A*-p.(Phe1617del) founder population with phenotypic heterogeneity and overlap syndrome reveals a large impact of p.(Phe1617del) on QTc, QAoC, and EMW. SCD and polymorphic VT/VF occur predominantly in females, during daytime, and often after arousal-evoked heart-rate acceleration and repolarization prolongation. This suggests sympathetic arrhythmia triggering, unlike what is known for other sodium channelopathies. Substantial genetic variance for PQ (and possibly QT) after accounting for p.(Phe1617del) may contribute to the phenotypic diversity. Our approach of synergizing in-depth cardiac phenotyping with statistical genetics reveals crucial information on the electromechanical traits of this population and paves the way for linkage analysis and exome sequencing to pinpoint genetic variants associated with the arrhythmia syndrome.

FUNDING

This work was supported by The Netherlands CardioVascular Research Initiative [CVON PREDICT], Den Haag, The Netherlands [to J.J. and P.V.]; and the Health Foundation Limburg, Maastricht, The Netherlands [to R.t.B. and P.V.].

ACKNOWLEDGEMENTS

The authors wish to thank Dr Britt-Maria Beckmann, Ludwig Maximilians University Munich, Munich, Germany, and Drs Nina Larsson and Catarina Lundin, Division of Clinical Genetics, University and Regional Laboratories, Lund University, Lund, Sweden for providing valuable data. Pascal G.J.H. van Borren and Simone M.H. Schoonbroodt, Maastricht University Medical Centre, provided expert technical assistance.



EDITORIAL

FOUNDER POPULATIONS WITH CHANNELOPATHIES AND CHURCH
RECORDS REVEAL ALL SORTS OF INTERESTING SECRETS:
SOME ARE SCIENTIFICALLY RELEVANT

Peter J. Schwartz and Lia Crotti

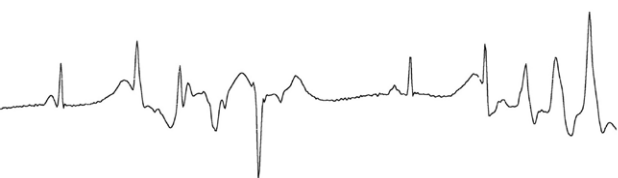
Heart Rhythm 2017;14:1882-1883

For those interested in channelopathies, and especially in the long QT syndrome, the simple and happy times of “ignorance bliss” are over. Things are getting more complex any day. If Thom James had been right, LQTS would be classified among infectious diseases. Genetics have changed everything, and one must admit, to try to understand what is going on has become a more stimulating and intellectually rewarding game, besides enabling a better and personalized management to patients.³²¹

A quick look backward sometimes helps put things in the proper context. We started with 3 genes, which, when mutated, would cause LQTS, but soon we found that if mutations on these same genes increased instead of reducing function, one would have *short* instead of *long* QT syndrome.²¹⁶ As to the cardiac sodium channel gene *SCN5A*, stormy weather started in the morning hours. First, it appeared that if the mutation instead of being a gain of function was a loss of function, then we would have had Brugada syndrome (BrS).⁶² It was just the beginning of trouble. We then learned that many variants on *SCN5A* were just either common or of uncertain significance (the dreadful variant of uncertain significance—a nightmare for anyone who must make a clinical decision based on their presence) and furthermore that mutations on *SCN5A* could associate with other diseases such as cardiac conduction disease (CCD), sick sinus syndrome, and others. Worst of all was the peace-shattering discovery made by Bezzina *et al.*³⁶⁵ that even the same *SCN5A* mutation could produce different cardiac disorders. Unfortunately, their finding did not remain isolated and we now face several *SCN5A* mutations having all divergent effects.³⁶⁶ Among them are 1759insD,³⁶⁵ G1406R,³⁶⁶ delK1500,³⁶⁶ E161K,³⁶⁶ E1784K.³⁶⁷ Indeed, the discovery of these so-called overlap syndromes has brought our confusion to the zenith.

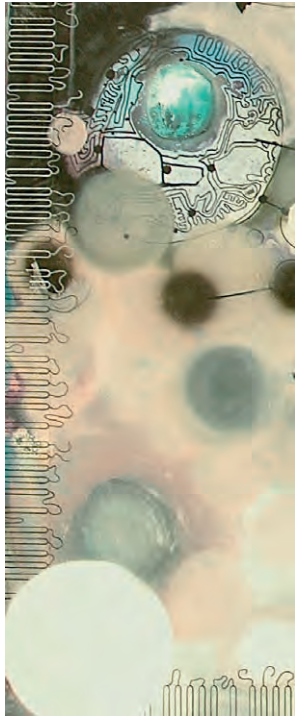
How can a single mutation on *SCN5A* produce either a gain-of-function phenotype (LQTS) or multiple phenotypes associated with a loss of function (BrS, CCD, and sick sinus syndrome)? In vitro functional studies suggested that this could be explained by the coexistence of a steady-state Na⁺ channel inactivation and a propensity to enhanced tonic block by class IC drugs.³⁶⁷ Studies in mice carrying the equivalent mutation of human *SCN5A*-1795insD proved that the presence of a single mutation is indeed sufficient to cause an overlap syndrome³⁶⁸ and that the genetic background plays a role.³⁶⁹ Indeed, if this mutation is inserted in 2 distinct mouse strains, the phenotype is different.³⁶⁹ Nonetheless, why a single patient develops one or another phenotype remains unclear.

In this issue of Heart Rhythm, ter Bekke *et al.*³⁷⁰ present a 16-generation family with a founder effect, in which the *SCN5A*-Phe1617del mutation is associated with overlapping cardiac phenotypes including LQTS, CCD, BrS, and isorhythmic atrioventricular dissociation. The authors should be congratulated on their painstaking search for the origin of this family. They identified 2 ancestral couples who lived in the 16th century in proximity to a small river, appropriately called Worm river, which runs between the Netherlands and Germany. Mostly through church records they identified a very large number of family members. The clinical manifestations in this family differ from those of most families with *SCN5A* mutations described previously. Indeed, polymorphic ventricular tachyarrhythmias occurred



mostly at daytime; proarrhythmic triggers included auditory stimuli, strong emotions, exercise, and postpartum periods; and female sex was an independent risk factor for cardiac events (hazard ratio 5.1; 95% confidence interval 1.6–16.3). Furthermore, T-wave morphology exhibited broad-based T-wave inversion or bifid T waves. Therefore, all LQTS-related clinical manifestations appear, without an explanation, more typical for a LQTS type 2 phenotype than for a LQTS type 3 phenotype.¹⁵¹ Equally puzzling are 11 subjects with a LQTS and/or a CCD phenotype but without the *SCN5A*-Phe1617del mutation. A second mutation in the family would have been an explanation, but was excluded because the authors screened all other known LQTS genes. Two possible but unlikely possibilities are that common screening tools are unable to detect large insertions and deletions, a rare cause of LQTS,³⁷¹ and that some intronic variants located outside the canonical donor and acceptor splice sites may not be immediately recognized as a cause of aberrant isoform expression and trafficking defect.^{372, 373} The atypical phenotypic features of this founder population match the variable expressivity already observed in other overlap families with *SCN5A* mutations, which probably reflects a combination of genetic, epigenetic, and environmental factors. Understanding the composition of this mysterious cocktail could help predict the individual risk associated with a given disease-causing mutation.

Ter Bekke, Volders, and their associates have an additional merit: to have provided 1 more piece of evidence for the gnostic value of founder populations. Founder populations are characterized by a single ancestor affected by the disease under study and by a large number of individuals and families, all related to the ancestor and carrying the same disease-causing mutation. They represent the ideal human model for the identification of “modifier genes”.³⁷⁴ And, indeed, the initial identification of genetic variants capable of modifying the risk of life-threatening arrhythmias⁸³ was made possible by the availability of a well-characterized LQTS South African founder population.^{375, 376} As well confirmed by ter Bekke’s study, the identification of founder populations requires a significant effort and the inborn gift of a special “hunting instinct”,¹⁶ but the rewards may be large.



*“Vaak moet er iets gebeuren om in te zien wat echt belangrijk is,
wacht niet tot het te laat is: begin nu met leven!”*



6

BEAUTY AND THE BEAT: A COMPLICATED CASE OF MULTIFOCAL ECTOPIC PURKINJE-RELATED PREMATURE CONTRACTIONS

CASE PRESENTATION

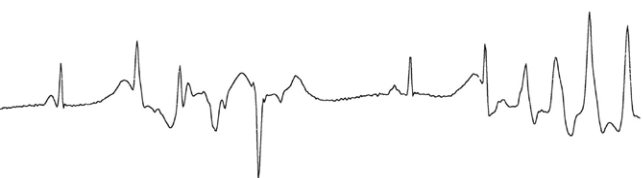
A 24-year-old female of Polish descent presented at the emergency department with exertional syncope that had occurred during housekeeping. Her unconsciousness struck without prior palpitations, chest discomfort or light-headedness. She regained full consciousness after several seconds, without confusion or amnesia. She had no tongue bite or incontinence. In the days before, no diarrhea, vomiting or febrile events had occurred. Her medical history was unremarkable. She did not take medication and denied the use of recreational drugs.

Exertional syncope without prodromi in young adults should raise the suspicion of ventricular arrhythmias with sympathetic susceptibility, such as in long-QT syndrome, catecholaminergic polymorphic ventricular tachycardia, arrhythmogenic (right-ventricular) cardiomyopathy, and Gallavardin's VT. Structural heart diseases that may be considered are obstructive hypertrophic cardiomyopathy, severe aortic valve stenosis, premature coronary artery stenosis or spasm, and coronary artery anomalies. Epileptic seizures can manifest without generalized convulsions, but often cause aura, tongue injury, and involuntary loss of bladder/bowel control. It is important to obtain a detailed family history on the occurrence of unexplained sudden (infant) death or cardiac arrest and other cardiac abnormalities, as this may allude to the presence of inherited arrhythmia syndromes.

The patient was a slender woman with a normal blood pressure. She smoked and was not active in sports. There was no hypercholesterolemia or diabetes mellitus. Over a period of months, she had experienced progressive fatigue with slight exertional dyspnea and sporadic light-headedness. Mother and a maternal aunt were known with frequent premature ventricular complexes of left-fascicular origin, a normal QTc, mild ventricular dilatation (mother) and impaired left-ventricular function (maternal aunt) since adolescence. Mother's twin sister and brother died postnatally after full-term gestation. The maternal grandmother died suddenly at age 33.

The family history of sudden death and ventricular arrhythmia may indicate an inherited arrhythmia syndrome or structural cardiomyopathy. The suspicion of premature coronary artery disease with ischemia is low, as her cardiovascular risk profile appears small. Coronary artery anomalies usually do not show familial clustering. Coronary spasm cannot yet be excluded.

Physical examination revealed a blood pressure of 120/70 mm Hg with an irregular heart rate of 114 beats per minute and a body temperature of 36.0°C (96.8°F). Breathing rate and oxygen saturation were normal. Body height was 180 cm and weight 68 kg. The ictus cordis was displaced laterally with a grade 2/6 blowing holosystolic murmur at the apex, and a third heart sound. Her jugular venous pressure was not elevated. Pulmonary and



abdominal investigations were normal. The extremities were warm with intact pulses and without ankle edema. Besides elevated NT-proBNP levels, 266 pmol/L, extensive laboratory testing revealed no abnormalities. The patient's 12-lead electrocardiogram showed sinus rhythm with frequent multiform PVCs and non-sustained VTs, with swift intrinsicoid deflections (Figure 6.1) and left- or right-bundle branch block-like morphologies. Ventricular ectopy increased upon emotional distress and excitement, and reached a daily burden of 25,000 (~17%). PQ and QT intervals were normal. The QRS amplitudes and inferolateral T-wave abnormalities fulfilled the criteria of LV hypertrophy: $S V1 + R V5/V6 \geq 35$ mm (Sokolow-Lyon), and $R V5/V6 \geq 30$ mm with typical ST-T wave changes (Romhilt-Estes).

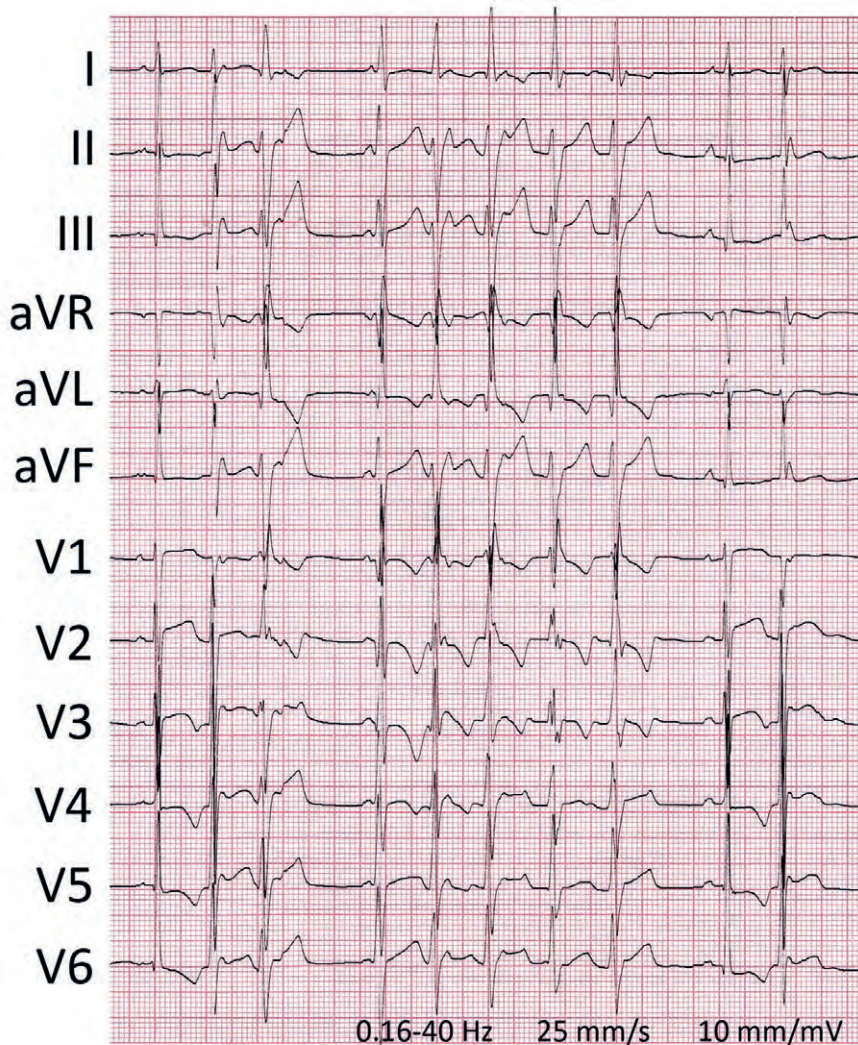
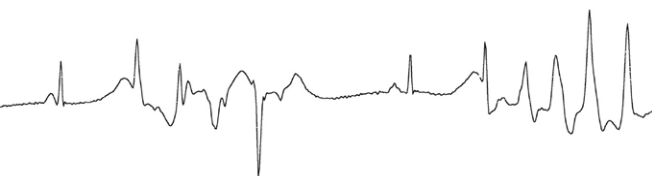


Figure 6.1 12-Lead electrocardiogram on admission showing ventricular ectopy and non-sustained ventricular tachycardia.

Patient's physical and electrocardiographic findings suggest a sympathetically-driven primary electrical disorder or a proarrhythmic structural cardiomyopathy with signs of LV hypertrophy and reduced systolic function. Catecholaminergic polymorphic VT may be considered, but this is typically associated with preserved cardiac contractility. The morphology of the dominant PVCs is reminiscent of left-fascicular and/or Purkinje-related foci, which is not typical for arrhythmogenic (right ventricular) cardiomyopathy or Gallavardin's VT. A normal QT duration does not rule out long-QT syndrome, but this is an



unlikely cause of the abundant ventricular ectopy observed. For subsequent diagnostic evaluation an echocardiogram would be appropriate.

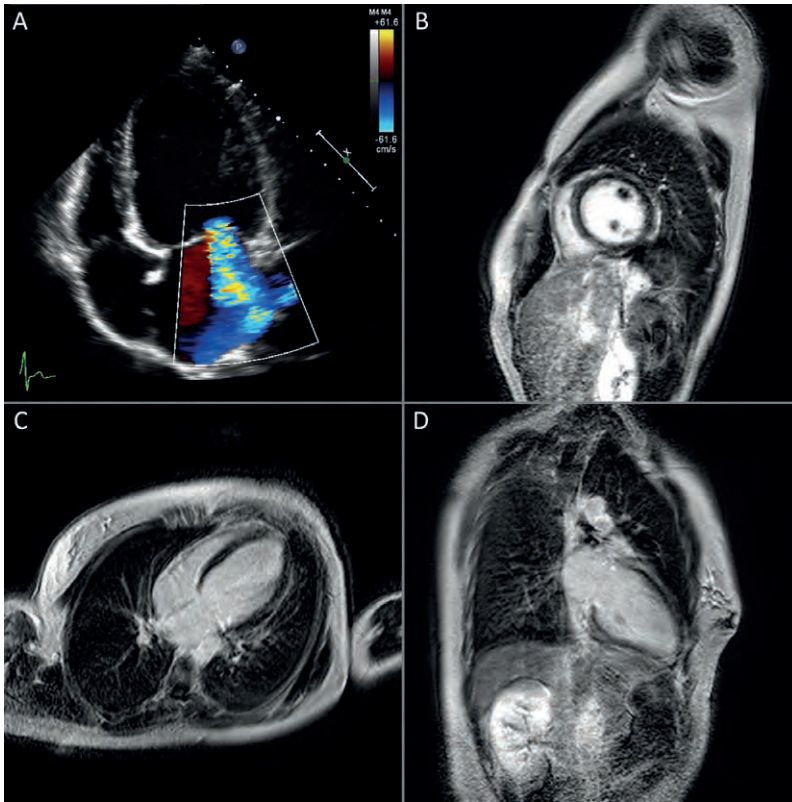


Figure 6.2 Dilated left-ventricular cardiomyopathy and mitral regurgitation on echocardiogram (A), without apparent myocardial fibrosis (delayed-enhancement magnetic resonance imaging) on short-axis (B), 4-chamber (C) and 2-chamber views (D).

On echocardiography, the LV was dilated (end-diastolic diameter 64 mm, end-systolic diameter 56 mm) and its ejection fraction (LVEF) reduced, 23%. A secondary grade B mitral regurgitation was found (Figure 6.2). No signs of active myocarditis, significant fibrosis, storage or infiltrative diseases were observed with cardiac magnetic resonance imaging and in right-ventricular septal endomyocardial biopsies. Coronary angiography was normal without aberrant coronary artery originations. Additional laboratory testing, including viral serology, autoimmune markers, thyroid function, iron status, corticosteroids, soluble IL-2 receptor, and urinary metanefrine concentrations remained unremarkable. During invasive electrophysiological study, intracardiac conduction times were normal, and no VT could be induced by programmed electrical stimulation.

Spontaneous PVCs were often preceded by high-frequency potentials in the ventricle, suggesting ectopic sites in the fascicular-Purkinje system. No ablation was attempted owing to the multifocality of the PVCs.

The combination of multifocal fascicular-Purkinje-related ectopy, nonsustained VT, and dilated cardiomyopathy without identifiable structural substrate suggests irregulopathy as the cause of heart failure. Along with the autosomal dominant pattern of arrhythmic disease in the family, these features imply a genetic origin, warranting molecular-genetic analysis.

With informed consent of the patient, genomic DNA was extracted and screened for gene mutations associated with inherited arrhythmia and/or cardiomyopathy. Meanwhile, several antiarrhythmic drugs proved inefficacious: metoprolol, carvedilol, labetalol, and lidocaine. Amiodarone administration successfully suppressed all ectopic activity, albeit at the expense of substantial QT prolongation (~730 ms; Figure 6.3A). Alas, recurrent episodes of torsades de pointes ((N-desethyl)amiodarone plasma level (0.4) 1.0 mg/L; Figure 6.3B) emerged after 9 days requiring immediate discontinuation of the drug; this normalized the QT interval within a week. Ventricular ectopy recurred and an ICD was inserted. Symptomatic hypotension and quinapril-induced angioedema hindered maintenance therapy with renin-angiotensin-aldosterone system blockers.

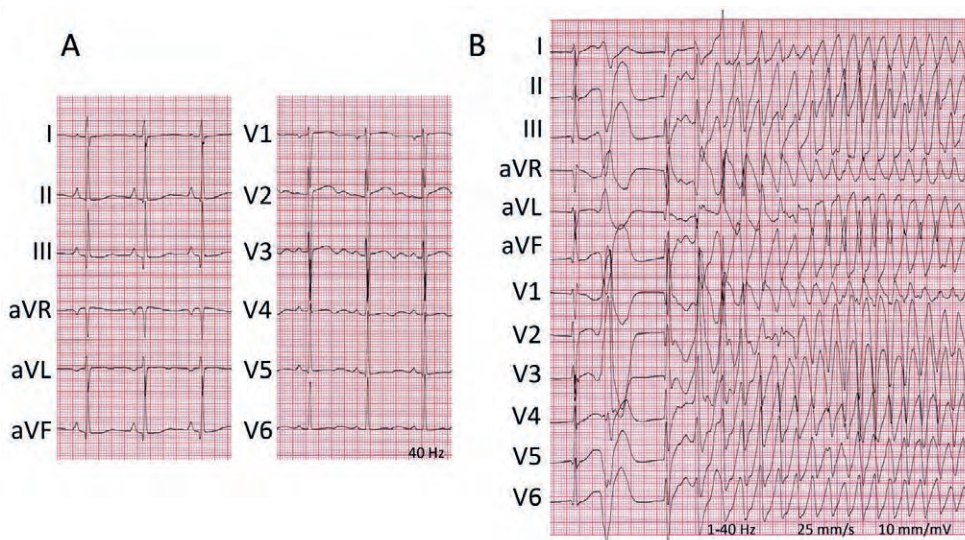
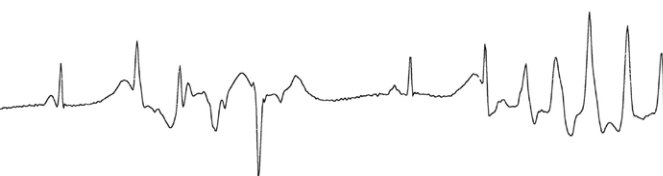


Figure 6.3 Electrocardiograms at 48 hours (A) and 9 days (B) after initiation of amiodarone showing repolarization prolongation and pause-dependent onset of torsades de pointes.



Amiodarone has class I, II, III, and IV antiarrhythmic properties according to the Vaughan-Williams classification and can be beneficially used in heart-failure patients. The incidence of amiodarone-induced proarrhythmia is low (0.7%), despite concomitant QT prolongation.³⁷⁷ Patient's TdP likely resulted from ventricular ectopics impacting on a substrate of amiodarone-exaggerated dispersion of repolarization in the setting of reduced repolarization reserve.

DNA analysis revealed allelic variation in the *SCN5A* gene (c.2482C>T, p.(Leu828Phe)), *KCNE1* gene (c.253G>A, p.(Asp85Asn)), and *DES* gene (c.638C>T, p.(Ala213Val)). In 36 other cardiomyopathy- and arrhythmia-associated genes variations were excluded. Patient's mother harbored the *SCN5A* and *DES* variant.

Although at this point the effects of the novel *SCN5A* variant on the sodium current are unclear, these features are reminiscent of a *SCN5A* channelopathy coined "multifocal ectopic Purkinje-related premature contractions (MEPPC)".¹³⁰ In the first report of MEPPC the *SCN5A* mutation p.(Arg222Gln) was described, which caused hyperexcitability of Purkinje fibers and was associated with cardiac dilatation. In our case, dilated cardiomyopathy could have been exaggerated by the rare polymorphism in *DES*. According to the MOGES classification the patient would be classified as $M_{D-PVC}O_{HGAD}E_{G-SCN5A}$ p.(Leu828Phe)+ DES p.(Ala213Val) $S_{(C-II)}$.³⁷⁸ Heart-failure induced electrical remodeling in combination with reduced potassium current by likely-pathogenic *KCNE1*-p.(Asp85Asn) led to a diminished repolarization reserve.⁷⁴ Amiodarone-induced proarrhythmia coincided with the time-dependent inhibition of the slowly-activating delayed rectifier potassium current.¹⁷⁷

The class-3 missense mutation *SCN5A*-p.(Leu828Phe) affected the highly-conserved leucine residue at domain II (S4-S5) of the cardiac sodium channel, juxtaposed to the voltage-sensing domain and was absent in the ExAC, gnomAD and ClinVar databases. We characterized *SCN5A*-p.(Leu828Phe) in transiently transfected Chinese hamster ovary cells (Figure 6.4). Heterozygous mutant I_{Na} showed similar amplitudes as wild-type I_{Na} , but with a significant leftward shift of the voltage dependence of activation. Because steady-state voltage-dependent inactivation remained unaltered, window I_{Na} increased, creating a broad voltage range of open-channel probability (between -80 and -50 mV), and a wide substrate for open and inactivated-state block by flecainide (10 μ mol/L), reflected by increased tonic and blunted use-dependent *SCN5A*-p.(Leu828Phe) I_{Na} inhibition.

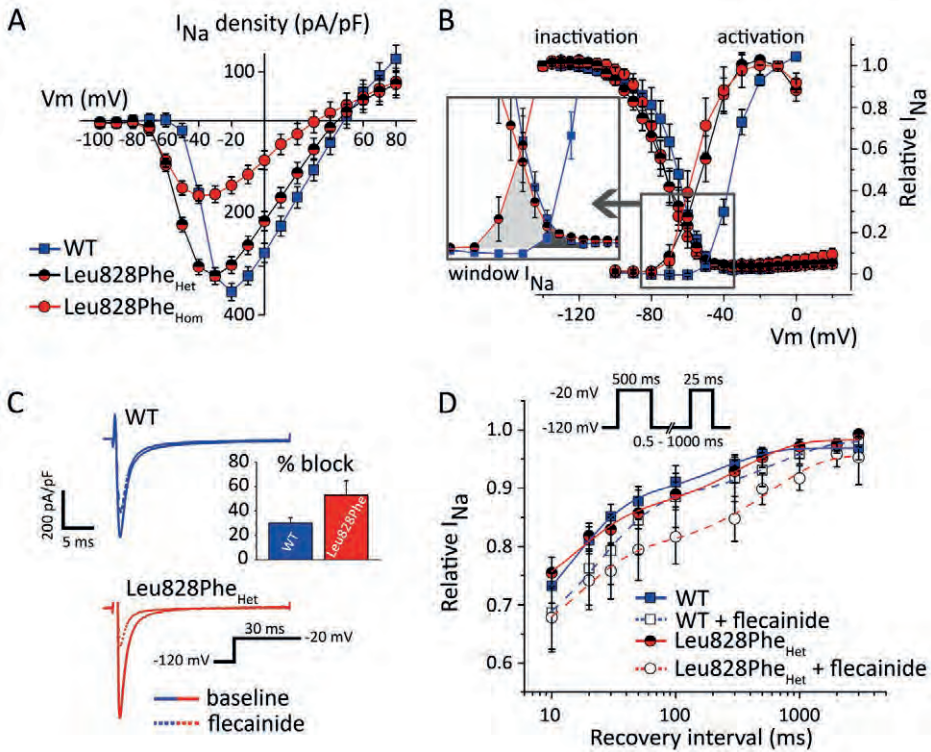


Figure 6.4 Functional characteristics of *SCN5A*-p.(Leu828Phe). (A) Current-voltage relationship normalized for cell capacitance in wild-type (WT), heterozygous (Het) and homozygous (Hom) mutant expression; beta subunits were not co-expressed. (B) Voltage-dependent steady-state (in)activation and enlarged window I_{Na} . (C) Tonic Leu828Phe_{Het} block at first test pulse (-20 mV). (D) Reduced Leu828Phe_{Het} current recovery from flecainide block.

The functional consequences of *SCN5A*-p.(Leu828Phe) resemble those of the p.(Arg222Gln) variant.¹³⁰ Flecainide's preferential block of p.(Leu828Phe)-mutant I_{Na} at short recovery intervals, and at clinically-relevant concentrations, suggests beneficial treatment of the patient with a class-I antiarrhythmic agent. Screening for adverse class-I side effects is advisable.

Short-acting sodium-channel inhibition with intravenous ajmaline (1 mg/kg in 10 minutes) almost completely suppressed PVCs without Brugada type-1 ECG abnormalities, QT prolongation, or other proarrhythmic characteristics. Oral maintenance therapy with flecainide (100 mg, twice daily) was successfully started thereafter. Vigilant monitoring of the patient revealed very low PVC counts and complete LV-function recovery within months. Now, nine years later, the patient is doing well and has not received ICD therapy. LVEF is 53%.



COMMENTARY

Our translational approach with combined clinical, genetic and cellular investigations identified the Achilles' heel of the disease of this patient, and it led to personalized therapy. Two important lessons were learned: 1) frequent multifocal fascicular-Purkinje-related PVCs with or without dilated cardiomyopathy should raise the suspicion of *SCN5A* channelopathy; 2) amiodarone-associated excessive QT prolongation and TdP should prompt genotyping of the patient.³⁷⁹

Sporadic PVCs are common in the general population, affecting about 39% of people (in 4% >100/day).³⁸⁰ They carry a favorable prognosis if occurring in the structurally normal heart. The risk of developing cardiomyopathy depends on the PVC burden ($\geq 16\text{--}24\%$)^{381, 382} and dyssynchronous myocardial activation, as is the case with wide PVC-QRS durations and/or epicardial foci,³⁸³ irrespective of a LV or right-ventricular origin. Multifocal PVCs originating in the conduction system often have narrow QRS widths and may be associated with familial sudden death (this study and¹³⁰).

MEPPC syndrome was first described in 2012 in three unrelated families segregating *SCN5A*-p.(Arg222Gln).¹³⁰ Patients can present with irregular palpitations with light-headedness, syncope attacks, or sudden death (21% of affected family members, at mean age of 32 years).¹³⁰ Symptoms of congestive cardiomyopathy can be present. The age at diagnosis varies from 24 weeks of gestation to 62 years (mean age 20 years) without gender predisposition.¹³⁰ Multifocal PVCs occur in isolation, doublets, or non-sustained VT. Contractile dysfunction can accompany this syndrome.^{130, 384, 385} Differential diagnoses to be considered are ischemic cardiomyopathy, viral myocarditis, digitalis intoxication, genetic cardiomyopathies such as laminopathy, and primary arrhythmia syndromes like catecholaminergic polymorphic VT, and short-coupled PVCs and TdP.¹²⁵

An erratic pattern of abundant junctional ectopics and PVCs with left- and right-bundle branch block-like morphologies but with sharp intrinsicoid deflections is characteristic and suggests an origin in the conduction system. Atrioventricular-node physiology and ventricular repolarization are unaffected. Although the echocardiographic features of LV dilatation and contractile dysfunction are non-specific, their co-occurrence with multilevel hyperexcitability should raise the suspicion of MEPPC syndrome. Typically, no signs of myocardial inflammation or fibrosis are found on cardiac magnetic resonance imaging.

DNA sequencing of the *SCN5A* gene hitherto identified two mutations associated with MEPPC: p.(Arg222Gln)¹³⁰ and p.(Arg225Pro).³⁸⁵ These mutations reside in homologous positions of the voltage-sensor region (S4 segment, domain I) of the cardiac sodium channel. Our novel mutation p.(Leu828Phe) also lies close to the S4 segment of *SCN5A* domain II. Common to all three *SCN5A* mutations is the leftward shift of voltage-dependent activation with resultant triggering of inward I_{Na} at more negative resting membrane potentials. This can facilitate PVCs in fascicular and Purkinje fibers in which I_{Na} channels are more abundantly expressed compared to ventricular myocytes, and as is predicted by *in-silico* analysis.¹³⁰

Sodium-channel blockade is the preferred therapy of this *SCN5A* disease to reduce the PVC burden. Besides flecainide, quinidine or amiodarone can be considered, but the latter can turn adverse in cases with an inherently reduced repolarization reserve. In our patient, the *KCNE1*-p.(Asp85Asn)⁷⁴ with known effect on repolarizing potassium currents I_{Ks} and I_{Kr} likely facilitated drug-induced repolarization prolongation and TdP.⁷³ Proarrhythmic side-effects of flecainide³⁸⁶ will be avoided by careful characterization (including class-I provocation testing) and on-treatment monitoring of the patient. Long-term outcome is beneficial if antiarrhythmic treatment suppresses the PVCs that cause the irregulopathy, thus enabling the recovery of LV function. Indeed, the recovery of dilated cardiomyopathy and reduced LVEF in our patients indicates an important pathogenic role of *SCN5A*-related irregulopathy. Besides, a disease-modifying effect of the DES variant in accompanying the *SCN5A* mutation cannot be excluded.³⁸⁷

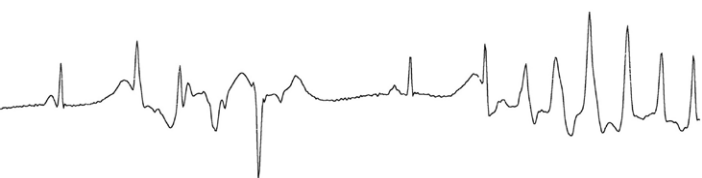
ACKNOWLEDGEMENTS

This work was supported by The Netherlands CardioVascular Research Initiative, CVON PREDICT (P.G.A.V.).





*“Wat duurt het toch lang
als je moet wachten.”*



7

LIFE-THREATENING VENTRICULAR ARRHYTHMIAS IN THE GENETICALLY-SUSCEPTIBLE HEART: TIME TO CHANGE CONCEPTS

CONTENTS

ARRHYTHMOGENIC MECHANO-ELECTRIC HETEROGENEITY	120
NEUROCARDIAC MODULATION AND VENTRICULAR ARRHYTHMOGENESIS	126
COMPLEX GENETIC ARCHITECTURE UNDERLYING SCD	129
TOWARDS PERSONALIZED ARRHYTHMIA MANAGEMENT	135
RELEVANCE FOR SCD IN GENERAL	138
CONCLUSIONS	138

Until recently, investigators focused mainly on purely electrical mechanisms to examine the arrhythmogenic consequences of cardiogenetic defects, with a prominent role for spatiotemporal dispersion of repolarization, afterdepolarizations, and reentrant excitation.¹¹¹ In this thesis, additional non-electrical parameters contributing to the onset of life-threatening ventricular tachyarrhythmias are put forward.

ARRHYTHMOGENIC MECHANO-ELECTRIC HETEROGENEITY

In the intact heart, there is a tight link between electrical and mechanical functions to ensure electrical stability and adequate contractile performance. Under normal conditions, cardiac excitation-contraction coupling is followed by myocardial relaxation, which terminates within tens of milliseconds after the completion of repolarization. In other words, the ventricular electrical systole (represented by the QT interval on the ECG) terminates before the completion of contractile relaxation (invasive correlate: QLVP_{end}; noninvasive: QAoC or QS₂), thus creating a positive electromechanical window (in ms; **Figure 7.1**). In normal subjects, we found an EMW of $+22 \pm 19$ ms (QAoC minus QT).³³¹

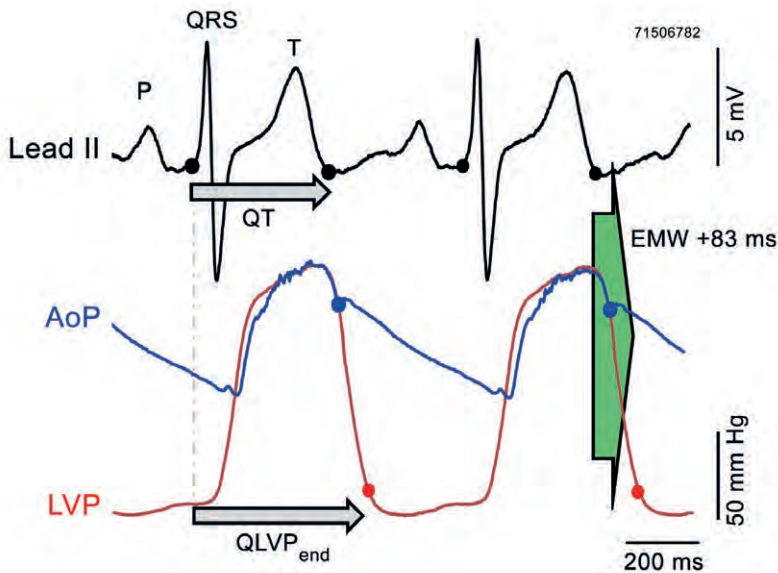
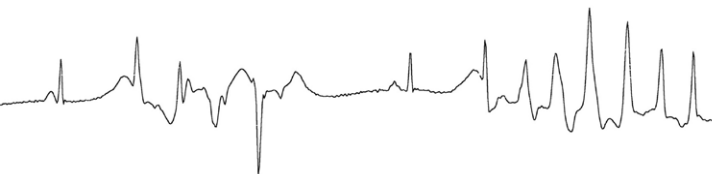


Figure 7.1 Invasive measurement of the EMW in a normal subject undergoing diagnostic electrophysiological testing for symptomatic multiform PVCs. Here, the time difference between QT and QLVP₉₀ creates a positive EMW of 83 ms. Of note, noninvasive measurement of the EMW using the QAoC would give a less positive result.

In the case of genetic syndromes with pathologic ventricular repolarization prolongation (i.e., the long-QT syndromes), QT exceeds QAoC, which renders the EMW negative (**Chapters 2, 3 and 4** of this thesis, and refs^{322, 331, 370}). An obvious question would be: does



EMW negativity itself contribute to electrical instability?³³² In order to find an answer, it is important to remember that the heart is not only an electrically-driven mechanical pump, but also an organ that can transform mechanical stimuli into electrical signals (i.e., mechano-electric feedback), with the general aim of maintaining beat-to-beat electromechanical homeostasis. In healthy hearts with normal electromechanical coupling, the majority of diastole is occupied by the passive and active filling of the ventricles, whilst maintaining low pressures (**Figure 7.2, left panel**). Electrically, this phase is paralleled by a large part of phase 4 of the ventricular AP and (on the ECG) the isoelectric segment between the T wave and the subsequent QRS complex, including the P wave. Electrical depolarization (Q/R onset on ECG) initiates ventricular contraction after a short electromechanical delay. Initially, contraction is isovolumetric until the increasing intraventricular pressure opens the semilunar valves. The QRS complex ends halfway this isovolumetric contraction phase, and the ST segment (paralleling phase 1-2 of the AP) ensues. The ventricular ejection and part of the isovolumetric relaxation are paralleled by the T wave (or phase 3 of the AP).

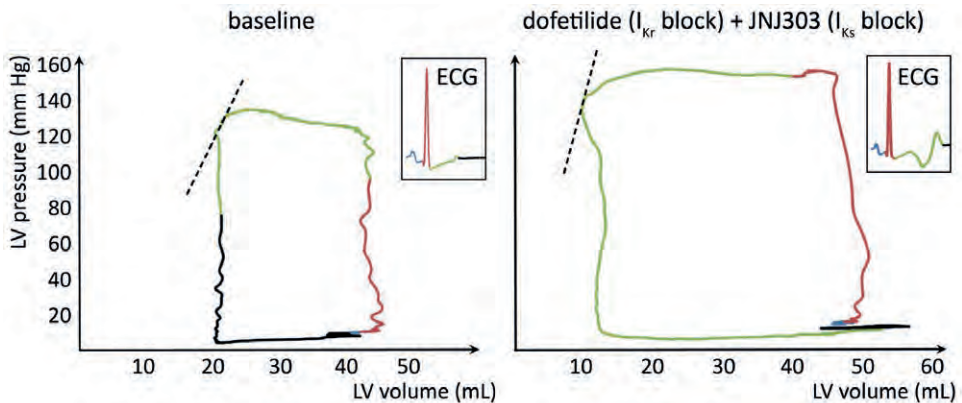


Figure 7.2 Electro-pressure-volume loops at baseline (**left**, EMW noninvasive +15 ms, invasive + 62 ms) and after I_{Kr} and I_{Ks} block with dofetilide and JNJ303, respectively (**right**, EMW noninvasive -221 ms, invasive -159 ms). Dotted line: end-systolic pressure volume relationships indicating increased inotropy during repolarization prolongation. [Courtesy of H. van der Linde, Janssen Research & Development, a division of Janssen Pharmaceutica NV, Beerse, Belgium].

Owing to electromechanical alterations in drug-induced LQTS, the ventricular myocardium senses substantial volume loading during the prolonged and dispersed ventricular repolarization phase (**Figure 7.2, right panel** green line). Ventricular volume is a major determinant of myofiber stress (σ_f) and strain (ϵ_f),³⁸⁸ more than LVP (see formulas next page), and thus it imposes significant mechanical impact during this vulnerable cardiac phase.

$$e_f = \ln\left(\frac{l}{l_{ref}}\right) = \frac{1}{3} \ln\left(\frac{\frac{1}{3}V_W + V_{LV}}{\frac{1}{3}V_{W,ref} + V_{LV,ref}}\right)$$

$$\sigma_f = LVP \left(1 + 3 \frac{V_{LV}}{V_{Wall}}\right)$$

Cardiac mechano-electrical coupling is coordinated by specialized cation-selective and nonselective stretch-activated ion channels, but it also involves ion channels with either voltage or ligand sensitivity, including Na⁺ channels,²⁸⁵ K⁺ channels,³⁸⁹ the ATP-sensitive K⁺ channel,³⁹⁰ I_f channels,³⁹¹ large-conductance Ca²⁺-sensing K⁺ (BK) channels and L-type Ca²⁺ channels. Crucial is the timing of the mechanical impulse with respect to the trailing edge of repolarization,³⁹² since SAC_{NS} accelerate repolarization in myocytes at membrane potentials >-10 mV and depolarize cells that have already reached a more negative membrane potential (**Figure 2.1** and ²⁹¹). Steep ventricular repolarization gradients that can be present in LQTS hearts³³⁹ may thus increase the vulnerability to arrhythmia by locally dispersed responses to mechanical influences. Related to this, in the canine model of chronic complete atrioventricular block and acquired QT prolongation, beat-to-beat variability in ventricular preload associated with beat-to-beat repolarization instability, which was abolished by streptomycin, a nonselective inhibitor of SAC_{NS}.³⁹³ In another canine model, that of drug-induced long-QT1 syndrome, incremental LV adrenergic-dependent aftercontractions emerged in a negative EMW and always just prior to TdP.^{112, 113} These aftercontractions, manifesting as humps in the nadir of concomitant T waves, preceded the onset of late MAP EADs and occurred even in the absence of EADs. Pharmacological intervention with esmolol or verapamil did not completely eliminate the EADs, but did abolish the aftercontractions and life-threatening TdP.¹¹² The effect of SAC inhibition on the potential mechano-electric link during the negative EMW under these conditions has not yet been investigated.

Clinical confirmation of mechano-electric feedback and LQT-associated proarrhythmia is sparse. Using tissue-Doppler imaging we captured myocardial contractions preceding ectopy and TdP in a *SCN5A*-p.(Phe1617del) patient with electrical storm, which suggests that instantaneous mechano-electric instability is linked to arrhythmogenesis, at least in LQT3 (**Chapters 2** and **3**). Shimizu *et al* performed epinephrine challenges in genotyped LQT1 patients and readily evoked adrenergic MAP EADs and large-sized U waves³¹⁰ reminiscent of the electrical footprint of postsystolic aftercontractions in the canine LQTS model.¹¹² Alas, no intraventricular pressure recordings were available to confirm the possible presence of underlying aftercontractions.³¹⁰ Proarrhythmic aftercontractions (by beta-adrenergic receptor stimulation) were recorded in a patient with syncope and abnormal repolarization, just prior to ventricular ectopy and nonsustained VT (**Figure 7.3**).¹¹⁴ Verapamil and esmolol suppressed both the mechanical events and subsequent arrhythmias.



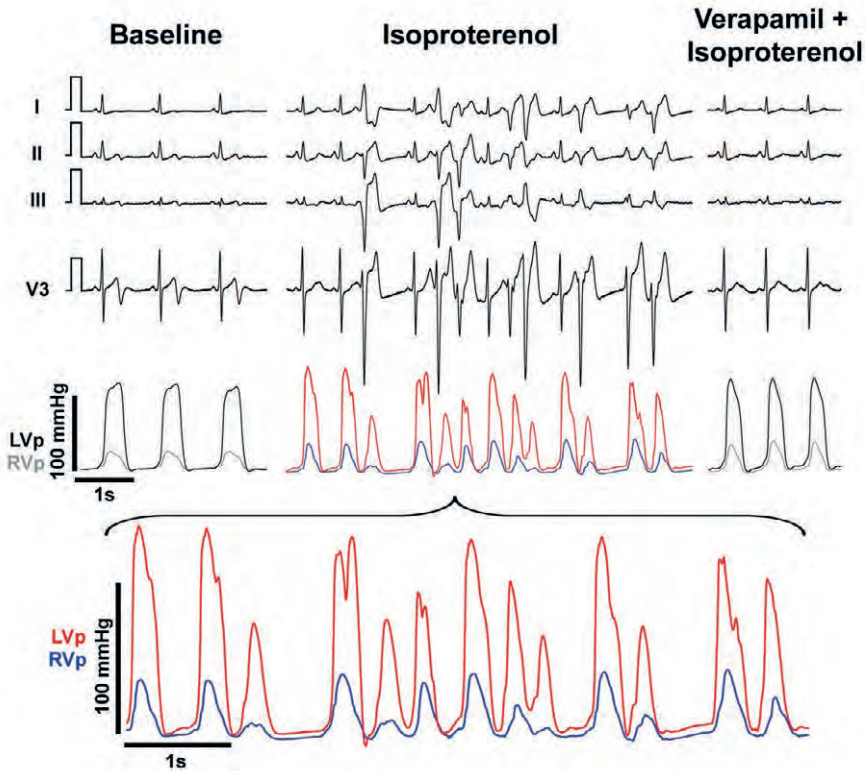


Figure 7.3 Aftercontractions in a LQTS patient provoked by beta-adrenergic stimulation. Esmolol and verapamil suppressed these aftercontractions and ventricular arrhythmias. [From “Cardiac Mechano-Electric Coupling and Arrhythmias”, reproduced with permission from Oxford University Press].¹¹⁴

In 1991, Vincent and colleagues investigated the electromechanical interrelation during instances of congenital repolarization prolongation in an ungenotyped Romano-Ward family.³⁰⁷ They found increased QT/QS₂ ratios indicative of EMW negativity in affected family members. In the present PhD thesis (**Chapters 2 and 3**), I focused on the EMW behavior in a large population of (mostly) LQT1, LQT2, and LQT3 patients in relation to cardiac events. Patients with prolonged repolarization demonstrated mean negative EMWs of -43 ± 46 ms, and EMW values were even more negative in symptomatic patients than event-free subjects (-67 ± 42 vs. -27 ± 41 ms; $P < 0.0001$). Importantly, ROC analysis and multivariate logistic regression analysis revealed that EMW was a better discriminator of arrhythmic risk than the conventionally used QT/QTc (odds ratio for 10-ms EMW decrease of 1.25 (95% CI, 1.11–1.40; $P = 0.001$)). Using this easy-to-obtain parameter on top of QTc resulted in a net reclassification index of 13%. The optimal cut-off value of < -62 ms predicted arrhythmic events with 72% accuracy. As such, the EMW is a useful parameter to

assess arrhythmia risk, and it can potentially guide antiarrhythmic maintenance therapy in the LQT syndrome.

EMW negativity was similar in the three genotypes. In symptomatic patients with inherited I_{Ks} and I_{Kr} defects QT prolongation occurred in the setting of unchanged QAOcs, whereas LQT3 patients displayed shorter mechanical systoles during concomitant QT prolongation. This *SCN5A*-specific pattern suggests that the persistent sodium current can interfere with the cardiac contractile properties, potentially through altered cellular Ca^{2+} cycling.¹¹⁰ As expected, most negative EMWs were observed in compound heterozygosity and in autosomal recessive JLNS patients.

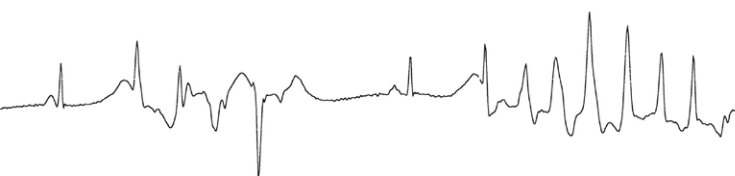
Anton Jervell and Fred Lange-Nielsen, when first describing the familial long-QT syndrome with concomitant congenital deaf-mutism in 1957,³⁹⁴ probably without realizing, were the first to illustrate EMW negativity in a 9-year-old symptomatic JLNS boy after quinidine provocation (**Figure 7.4**).



Figure 7.4 Profound EMW negativity during quinidine challenge in a symptomatic JLNS patient recorded three weeks prior to his sudden demise [adapted from Jervell *et al*³⁹⁴ with permission from the American Heart Journal].

Simultaneous recording of the QT (620 ms) and QS_2 (350 ms) intervals unmasked an extremely negative EMW of -270 ms that could have been augmented by the potassium-channel blocking properties of quinidine. The young boy died suddenly 20 days later.

At the opposite end of the spectrum one can wonder about the electromechanical consequences of short-QT syndrome.³⁹⁵ SQTs patients exhibit EMW *positivity* primarily due to a shortened QT in the presence of an unchanged mechanical systolic duration.³⁹⁵ Investigators have reported systolic impairment as assessed by a reduced global longitudinal strain and myocardial performance index, next to increased mechanical dispersion.³⁹⁶ Whether there is a role for mechano-electric feedback in arrhythmogenesis in the SQTs is a largely uncharted area of research, although in-silico modeling of *SQT1-KCNH2*



p.(Asp588Lys) hinted on a modulation of repolarization by the incorporation of I_{SAC} in the model.³⁹⁷

The results of this PhD thesis, together with other reports on aberrant cardiac mechanics in LQTS,^{236, 301, 302, 330, 335} thus refute the notion that LQTS is a 'purely electrical disease' and therefore, it is time to claim that LQTS is a disease with *electromechanical* and *mechanoelectric* consequences.^{330, 398}

FUTURE PERSPECTIVES

Future experiments could be directed to elucidate the link between EMW negativity, aftercontractions and arrhythmias in the LQTS. To co-locate electromechanical events in the myocardium, deformable non-contact multielectrode endocardial mapping (avoiding catheter-induced ectopy) could be combined with high-resolution epicardial mapping and high-resolution mechanical tracking in drug-induced LQTS. In this regard, the non-contact ultrasound basket catheter (Acutus Medical, Carlsbad, CA, USA) is an interesting tool as it encompasses high-resolution dipole density mapping and ultrasound techniques that could detect local myocardial deformation. Alternatively, mechanical deformations could be imaged by (3D) speckle-tracking echocardiography or by MRI techniques like phase-contrast imaging. Also, non-invasive ECG-imaging could potentially be adapted to reconstruct local epicardial repolarization times, and to yield gradients together with mechanical mapping. In such experimental set-up, during drug-induced QT prolongation, interventions that alter mechanical impact can be implemented: 1) mechanical stimuli timed exactly during a negative EMW and 2) non-selective (streptomycine) or selective pharmacological SAC inhibition (using the peptide GsMTx4, isolated from the venom of the tarantula *Grammostola spatulata*) during provocative conditions culminating in aftercontractions and ventricular ectopy/tachycardia. To this aim, the availability of large-animal models with preserved hemodynamic responses and autonomic reflexes is crucial.

Clinically, similar multimodality imaging techniques as just described could be applied to assess genotype-specific electromechanical heterogeneities at baseline and during smart provocations under controlled conditions. In specific VF cases, these non-invasive (epicardial-focused) investigations could be complemented with endocardial electrophysiological mapping to uncover transmural dispersion of activation/repolarization, and potentially guide acute pharmacological intervention or trigger ablation.

Besides, cardiac mechanoelectric feedback fueling electrical instability and arrhythmias has been sparsely addressed in other cardiac diseases. Stretch-induced depolarizations in the pulmonary veins or the atrium can evoke premature atrial activation in susceptible patients.²⁸⁶ In a human electrophysiology-force myocyte model of hypertrophic cardiomyopathy, myofilament protein mechanics affected EAD formation.³⁹⁹ Collectively, these results underscore the importance of assessing malignant mechanotransduction in cardiac arrhythmogenesis in the clinical and experimental electrophysiology laboratory.

NEUROCARDIAC MODULATION AND VENTRICULAR ARRHYTHMOGENESIS

The autonomic nervous system is comprised of sympathetic and parasympathetic limbs and, classically, is thought to exert its cardiac control via a yin-and-yang reciprocal interaction, although co-activation occurs during many reflexes.⁴⁰⁰ The two autonomic components, individually, but also in conjunction, have been implicated in ventricular arrhythmogenesis.

Generally, an enhanced parasympathetic tone exerts antiarrhythmic and antifibrillatory effects on the heart.^{401, 402} The vagal nerves operate mainly by antagonizing cardiac sympathetic actions, but also modulate the myocardium directly by prolonging the effective refractory period¹⁴⁶ and by increasing the variability of the dominant VF frequency.¹⁴⁷ In Brugada syndrome, LQT3, and early repolarization syndrome, arrhythmic events occur predominantly in periods of rest or sleep, i.e., in conditions with an anticipated high vagal tone. Cholinergic stimulation incited ventricular tachycardia in an experimental LQT3 model,¹⁵⁹ but hitherto no direct recordings of vagal nerve activity are available in the conditions upstream to ventricular tachyarrhythmias.^{140, 151, 403} However, since intermittent strong sympathetic surges are present during REM sleep⁴⁰⁴ and an elevated sympathetic tone is often present in high-risk Brugada patients,⁴⁰⁵ a more complex vago-sympathetic proarrhythmic propensity is to be suspected.

Sympathetic hyperactivity is associated with increased susceptibility to ventricular tachyarrhythmias and SCD in acquired and inherited cardiac diseases.⁹ The circadian occurrence of SCD at times of anticipated high sympathetic tone (peak between 7 and 11 AM) underscores this relation.⁴⁰⁶ LQT1 is considered exemplary for sympathetic-related ventricular tachyarrhythmias,^{151, 318} but also CPVT-related arrhythmias depend heavily on increased sympathetic cardiac stimulation.^{407, 408} Here, ventricular tachyarrhythmias during exercise are common, which is at variance with the LQT syndrome, in which they are less frequent despite pre- and postexercise QT malaccommodation.⁴⁰⁹ Mechanistically, sympathoexcitation impinges on ventricular electrophysiological properties by exaggerating dispersion of excitation and refractoriness,¹⁴³ facilitating triggered activity,⁹² and reducing the threshold for VF.⁴¹⁰ While there is some degree of overlap in sympathetic efferent postganglionic neurons arising from the major cardiac ganglionated plexus, there is significant laterality in the input from either stellate ganglion to the heart. Stimulation of postganglionic neurons by the LSG imposes more pronounced dispersion of repolarization mainly in the anterior⁴¹¹ and posterolateral regions.⁴¹² The proarrhythmic input of the LSG was further demonstrated by increased discharge activity of the left-sided ganglionated plexus prior to the onset of VT in a canine model of scar-related SCD.³⁴⁴ In other models, MAP DADs,⁴¹³ triggered activity,⁴¹³ and large-sized LV MAP EADs^{414, 346} were elicited by enhanced left-sided sympathetic stimulation. The electromechanical and arrhythmogenic effects of enhanced left-sided ganglionated plexus activity in an in-vivo drug-induced LQT1 model have been described in this thesis (**Chapter 4**). Anesthetized dogs were infused with the I_{Ks} blocker HMR1556 and underwent unilateral sympathetic stimulation. LSG, not RSG, stimulation readily induced TdP, precipitating intractable VF. This irreversible nature of



sympathetic LQT1-VF arrhythmogenesis may be the experimental correlate of LQT1 patients dying at their (first) arrhythmic event. In the setting of I_{Ks} -block-induced QT prolongation and MAP EAD generation, TdP occurred only upon LSGS-exaggerated EMW negativity and after about 26 seconds of stimulation, suggesting the necessity of local norepinephrine accumulation.⁴¹⁵

The association of a negative EMW with the induction of TdP suggests a role for mechano-electric coupling in the triggering of extrasystoles. During *global* beta-adrenergic receptor stimulation with i.v. isoproterenol such role appeared likely given the incremental aftercontractions that almost always preceded TdP.¹¹² These aftercontractions emerged in the negative EMW and before the upstroke of concomitant EADs. During regional sympathetic stimulation from the LSG, macroscopic aftercontractions appeared largely absent, but we consider it likely that small Ca^{2+} -mediated mechanical events, not picked up by the intracavitary pressure catheter, did occur. The physiological heterogeneous distribution of sympathetic nerve endings in the LV myocardium, with dispersed norepinephrine release upon LSG stimulation, could have diluted the concerted organization of sizable aftercontractions, along with the increased regional dispersion of repolarization under these conditions.⁴¹²

TdP-initiating ventricular extrasystoles emerged predominantly from the RV and LV outflow-tracts region, in accordance with clinical observations.²⁷⁰ Several factors determine this susceptibility of this region: 1) a generally shorter APD and effective refractory period,⁴¹⁶ 2) a higher I_{to} density in the RV epicardium,¹³⁶ 3) a lower $Nav1.5$ expression in the RV outflow-tract subepicardium,⁴¹⁷ 4) the presence of slowly-conducting, nodal-like RV outflow-tract tissue with I_{CaL} -dependent AP upstrokes,⁴¹⁸ 5) rich sympathetic innervation (ventromedial cardiac nerve),⁴¹⁹ 6) thin-walled anatomy with reduced electrotonic capacity,²⁷⁰ and thereby, hypothetically, an increased sensitivity to stretch and strain.^{322, 420}

It has been increasingly recognized that simultaneous hyperactivity of both limbs of the autonomic nervous system can turn arrhythmogenic particularly in the susceptible heart.^{153, 400} Cold-water submersion is a classical trigger of autonomic co-stimulation eliciting a simultaneous cold shock (sympathetic trigger) and a diving response (parasympathetic trigger).³⁵⁴ Cold-water swimming is a genotype-specific trigger of potentially lethal arrhythmia in LQT1,^{152, 421} but also in CPVT.⁴²² Approximately 30% of victims of swimming-related drowning harbor a *KCNQ1* or *RYR2* mutation.⁴²³ Additionally, some reports hint towards the proarrhythmic potential of high vagal tone/reflexes in LQT1 patients.^{154, 155} In our in-vivo anesthetized canine LQT1 model with preserved autonomic nervous system reflexes, I speculate that co-activation of the sympathetic and parasympathetic branches contributed to the observed VF in our in-vivo anesthetized canine LQT1 model. The present experimental results do not allow firm conclusions regarding this aspect. In other LQT2¹⁶⁰ and LQT3¹⁵⁹ whole-heart models, vagal stimulation led to augmented dispersion of repolarization and the induction of VT. Some clinical data have suggested high parasympathetic activity even during or immediately after VF-induced blood pressure fall.⁴²⁴

Figure 7.5 illustrates examples of suspected vagal-mediated sinus bradycardia and atrioventricular block in two LQT patients after the spontaneous termination of TdP/VF.

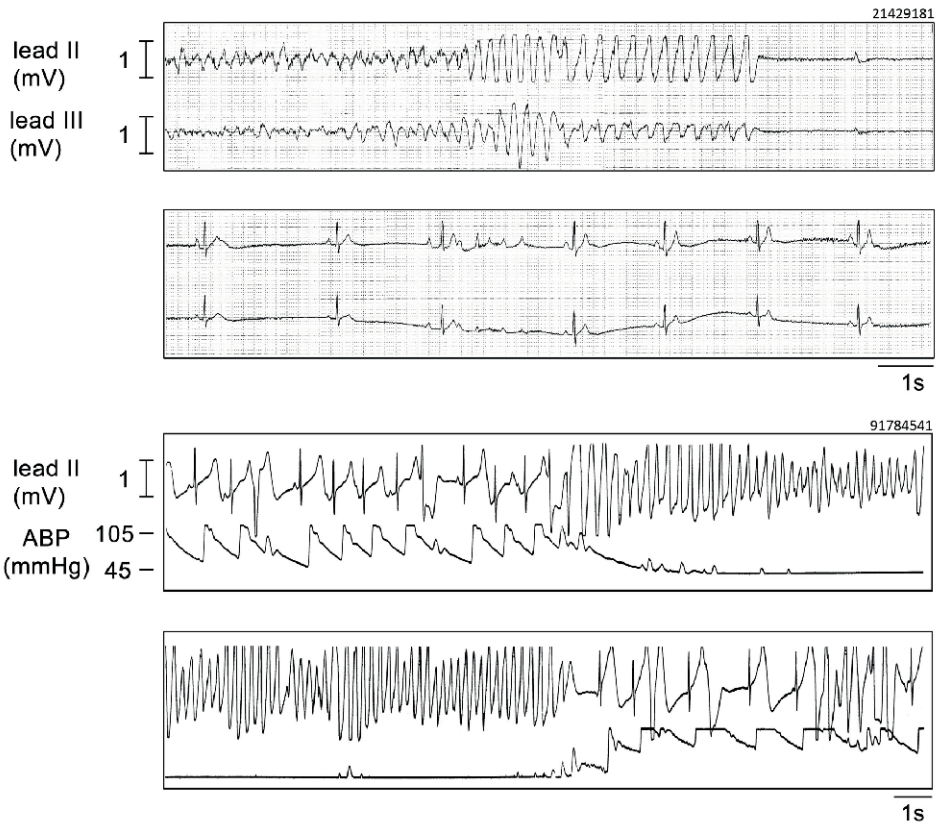
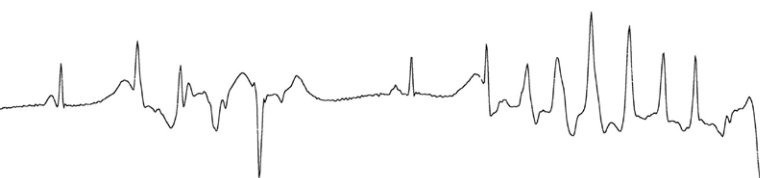


Figure 7.5 Suspected vagal hyperactivity in a patient with genetically elusive LQT syndrome (**upper panel**) and a LQT1 patient (**lower panel**) with sinus bradycardia and atrioventricular block after spontaneous termination of TdP/VF.

In summary, left-sided sympatho-excitation during LQT1(-mimicking) conditions imposes electromechanical instabilities, that may facilitate reentrant excitation and provoke TdP/VF. The convoluted vago-sympathetic synergy conspiring to this arrhythmogenesis, while highly intriguing, is still poorly understood. Our findings underscore the importance of interventions aimed at dampening the effects of sympathocardiac stimulation, like beta-blocking therapy^{1, 168} and LCSD.^{184, 185, 425} One small retrospective pilot study demonstrated increased (i.e., less negative) EMWs upon LCSD in LQT1 and LQT2, mainly by reducing the QT interval.⁴²⁶



FUTURE PERSPECTIVES

Future studies could focus on the proarrhythmic contribution of parasympathetic stimulation on top of augmented sympathetic cardiac outflow in LQT syndrome. To this aim, vagal activity could be recorded during sympatho-excitation in an in-vivo canine LQT1 model like ours. At the cellular level, one could investigate the downstream effects of simultaneous stimulation of muscarinic and adrenergic receptors on ion currents targets like I_{CaL} and I_{Ks} . For cholinergic stimulation, carbachol or the selective muscarinic inhibitor AFDX116 can be used. Ultimately, the impact of autonomic modulation on APD, beat-to-beat variability of repolarization, EMW and ventricular arrhythmogenesis could be investigated. In corollary to these experimental set-ups in LQT1-mimicking conditions, the vagosympathetic triggering of *SCN5A*-related arrhythmias warrants further investigation.

The contemporary diagnostic work-up of patients with inherited or acquired susceptibility to ventricular tachyarrhythmia should encompass an evaluation of the autonomic nervous system. Cardiac innervation maps using ^{123}I -meta-iodobenzylguanidine scans can be incorporated besides standard high-density electro-anatomic maps to uncover neurocardiac substrates, if present, and potentially alter invasive and noninvasive treatment strategy.⁴²⁷

COMPLEX GENETIC ARCHITECTURE UNDERLYING SCD

The field of genetics, in particular the exploration of genetic determinants that increase the risk of SCD, is rapidly evolving and is increasingly incorporated in clinical-decision making. Starting from the 1990s when the primary focus was on high-effect size mutations with monogenic inheritance patterns, we have entered the era of complex genetics in which there is mounting understanding of the role of allelic variants with different effect sizes to explain missing heritability and disease expression. These emerging complexities will be illustrated in the next sections using *SCN5A* channelopathies as example.

SCN5A-RELATED DISEASES: A TEMPLATE OF COMPLEXITY

Allelic variants in the *SCN5A* gene encoding the $Na_v1.5$ have been associated with a plethora of arrhythmia syndromes (**Figure 7.6**). Initially, *SCN5A* mutations were recognized for LQT3⁴⁴ and Brugada syndrome.^{428, 429} Later other disease entities like cardiac conduction disease,^{429, 430} sick-sinus node syndrome,⁴³¹ atrial fibrillation,⁴³² atrial standstill,⁴³³ dilated cardiomyopathy,³⁸⁴ and, more recently, multifocal Purkinje-related ectopy¹³⁰ were added to the list. Extensive experimental electrophysiological characterization has revealed that $Na_v1.5$ not only provides for AP upstrokes and conduction, but (when mutated) can also be involved in repolarization instability and structural cardiac abnormalities, depending on the variant-imposed functional consequences. $Na_v1.5$ gain-of-function effects, like impaired channel inactivation with late I_{Na} or increased window I_{Na} can prolong ventricular repolarization resulting in LQT3 or can facilitate multifocal Purkinje-related ectopy, respectively.

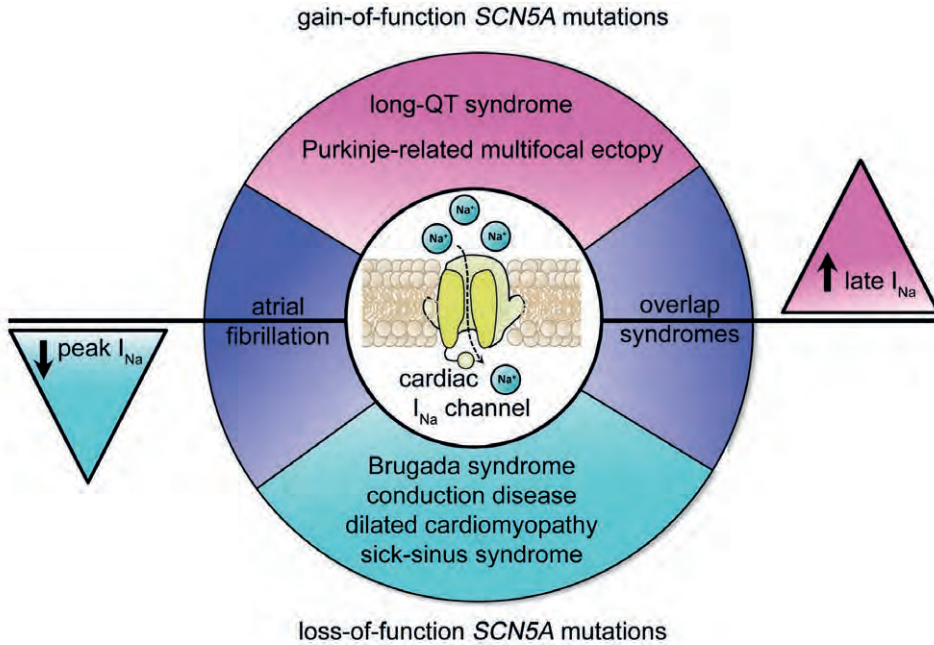


Figure 7.6 Clinical phenotypes according to functional effect of *SCN5A* mutation. [Modified from⁴³⁴ with permission].

On the other hand, electropathological mechanisms underlying Brugada syndrome can comprise of reduced peak I_{Na} due to a hyperpolarizing shift of the voltage dependence of steady-state channel inactivation or decreased expression of I_{Na} channels in the membrane (loss of function). In overlap syndromes, mutation-induced loss- and gain-of-function I_{Na} features co-exist.

The heterogeneous phenotypic expression of *SCN5A* mutations is intriguing and complex. In order to gain further insights into the genetic inheritance patterns and functional abnormalities, it is crucial to consider $Na_v1.5$'s modulators of expression, its binding partners and cellular regulators (**Figure 7.7**). $Na_v1.5$ operates through a macromolecular signaling complex by interactions with its auxiliary beta-subunits, several proteins and other ion channels that modulate channel trafficking, expression, localization, and gating,⁴³⁵ and it is the target of extensive post-translational modifications.^{436, 437}



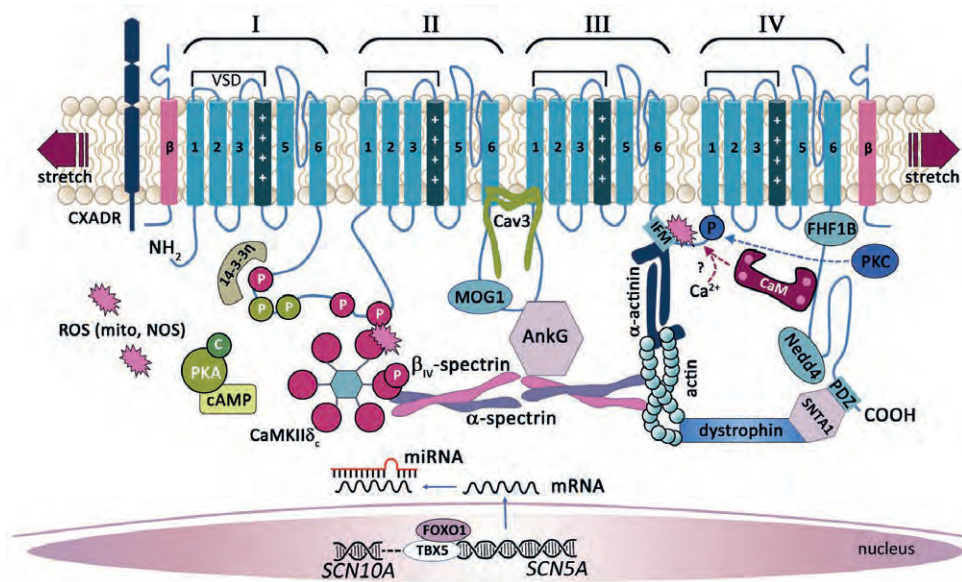


Figure 7.7 Transcriptional, translational and posttranslational modulators of the $\text{Na}_v1.5$ macromolecular channel and signaling complex. AnkG indicates ankyrin-G; CaM, calmoduline; CaMKII δ_c , calcium calmoduline kinase II, cAMP, cyclic adenosine monophosphatase; Cav3, caveolin-3; CXADR, coxsackievirus and adenovirus receptor; FHF1B, fibroblast growth factor homologous factor 1; FOXO1, forkhead box protein O1; IFM, Ile-Phe-Met; mRNA, messenger RNA; miRNA, microRNA; mito, mitochondria; MOG1, multicopy suppressor of Gsp1; Nedd4, neural precursor cell expressed developmentally downregulated protein 4; NOS, nitrous oxide systems; PDZ, postsynaptic density protein/Drosophila disk large tumor suppressor/zonula occludens-1; PKA, protein kinase A; PKC, protein kinase C; ROS, reactive oxygen species; SNTA1, alpha-1-syntrophin; TBX5, T-box transcription factor 5; VSD, voltage-sensing domain. [Modified from⁴³⁶ with permission].

Mechanical stress, regulatory kinases (PKA, protein kinase C), oxidative stress, Ca^{2+} , calmoduline, and CaMKII are important post-translational regulators of $\text{Na}_v1.5$ that can confer functional effects on I_{Na} .^{285, 436} Of interest is the CaMKII-dependent modulation of $\text{Na}_v1.5$ as it imposes both a gain of late I_{Na} and a negative shift of the steady-state inactivation, enhanced accumulation of intermediate/slow inactivation and slowed recovery from inactivation.⁴³⁶ As such, CaMKII may increase the risk of VT and SCD in the setting of heart failure or ischemia-reperfusion, representing an acquired form of $\text{Na}_v1.5$ dysfunction. Another channel-interacting protein is the coxsackie-and-adenovirus receptor that co-localizes with $\text{Na}_v1.5$ at the intercalated disks, modifies its current amplitude, and predisposes to ischemia-related arrhythmias.³⁷ Furthermore, some authors claim that a second gating pore can be formed besides the physiological alpha pore by mutations to neutrally charged amino acids in the voltage-sensing domain.^{438, 439}

Variation in the juxtaposed *SCN10A* gene on chromosome 3 can regulate the expression of *SCN5A* in cardiac tissue.³⁶² Also, transcription factors like Forkhead box O 1 (FOXO1) and nuclear factor- κ B (NF- κ B) can reduce *SCN5A* transcription. T-box transcription factor 5

(TBX5) plays an essential role in the normal expression of $\text{Na}_v1.5$ in the ventricular conduction system.⁴⁴⁰ Other important regulators of *SCN5A* transcription are miRNAs (e.g., 125a/b, 195, 378)^{441, 442} that can either restrict transcription or induce mRNA degradation.

Collectively, these different $\text{Na}_v1.5$ modulators with their potential common gene variants (or “genetic modifiers”) can complicate genotype-phenotype interpretation, which may explain the low disease penetrance of *SCN5A* channelopathies with a variable expressivity.⁶³ In this context, it does not come as a surprise that *SCN5A* mutations are diagnosed in only 20-25% of Brugada patients, despite the autosomal dominant pattern of transmission of the syndrome.³⁶⁰ The complexity increases further if one realizes that family members of *SCN5A*-mutation indexes with Brugada syndrome may have spontaneous or drug-induced type-1 Brugada ECGs while not carrying the familial *SCN5A* mutation.⁶⁴ This hints to an oligogenic mode of inheritance¹⁵ with an important role for genetic background in the pathogenesis of Brugada syndrome.

Large founder populations sharing an identical-by-descent gene mutation but with variable disease expression are gold mines for the elucidation of genetic modifiers that are difficult to uncover in a genetically-diverse population with a common phenotype.^{15, 16} We built on the availability of a *SCN5A*-p.(Phe1617del) founder population (this PhD thesis, **Chapter 5**) with an increased susceptibility to SCD and variable cardiac phenotypes, including LQTS, Brugada syndrome, cardiac conduction disease, and isorhythmic atrioventricular dissociation with overlapping features. Besides the strong association between *SCN5A*-p.(Phe1617del) and LQTS, large mutation effect sizes on QTc (explaining 18-28% of QTc variability), mechanical systole, and EMW were present. Somewhat unexpectedly, no persistent or late I_{Na} was present during whole-cell patch-clamp recordings in transiently transfected Chinese hamster ovary (CHO) cells, in experiments thus far.⁴⁴³ Mutant I_{Na} density for *SCN5A*-p.(Phe1617del)_{homo} was reduced, which indicates loss-of-function I_{Na} effects. This is partly in contrast with observations by Chen *et al*³⁶¹ who found an increased voltage-dependent late/peak I_{Na} ratio at positive command potentials in p.(Phe1617del)-transfected tsA201 cells. Other known LQT-related gene variants did not segregate in this pedigree. The modifier gene *SCN5A*-p.(His558Arg), always on the same allele as the deletion (cis), appeared to partially rescue the mutant I_{Na} without increasing late I_{Na} .⁸⁵

Conditions leading to cellular Ca^{2+} overload (sympathetic stimulation, tachycardia, short-long-short RR cycles, i.e., conditions facilitating arrhythmia in vivo) could modulate $\text{Na}_v1.5$ via Ca^{2+} , CaM, or CaMKII, and PKA and impair I_{Na} fast inactivation, effectively shifting I_{Na} availability to negative potentials.⁴³⁶ Alternatively, *SCN10A*-driven genomic expression of *SCN5A* could be dysregulated, and we cannot rule out that more distant genes and/or variants impact on the expression of $\text{Na}_v1.5$. Some *SCN5A* mutations render a different sensitivity of $\text{Na}_v1.5$ to I_{Na} -channel blockers (**Chapter 6** and ref⁴⁴⁴). And, although speculative at this point, $\text{Na}_v1.5$'s mechanosensitivity may be subject to genetic modulation.



Next, our variance component analysis (**Chapter 5**) alludes to missing heritabilities for PQ interval on the ECG, and possibly for the QT interval and EMW, after accounting for the effects of *SCN5A*-p.(Phe1617del). The enrichment of p.(Arg558) strengthened the concept of founder effects and genetic drift, but did not exert an independent effect on the identified phenotypes (thus far). These genetic complexities are substantiated by the presence of LQTS and even TdP in p.(Phe1617del)-*negative* family members (**Figure 7.8**). Further refinement of the genetic and molecular underpinnings of altered I_{Na} benefits also patients with other *SCN5A*-gene mutations, and even patients with acquired cardiac diseases with a propensity to arrhythmias.

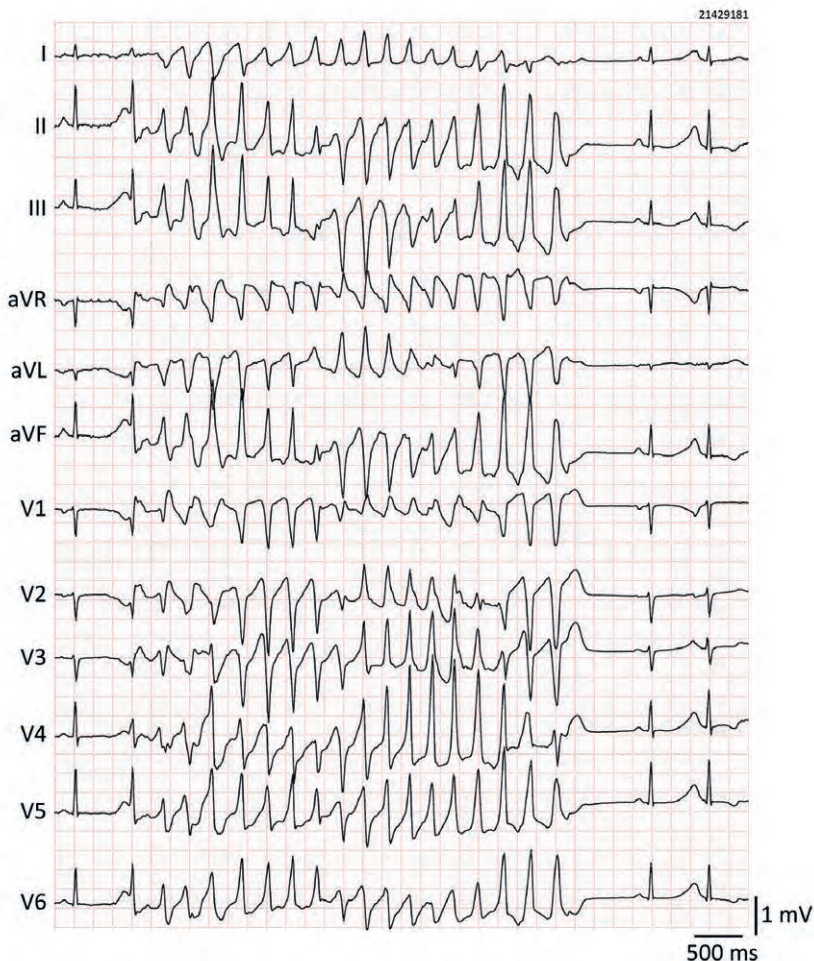


Figure 7.8 LQTS and the induction of TdP in a p.(Phe1617del)-negative Worm study patient. No mutations were found in 24 arrhythmia-associated genes.

Careful analysis of arrhythmia mechanisms in the presence of the *SCN5A*-p.(Phe1617del) mutation brought forward unique (non-*SCN5A* typical) aspects with arousal-related, non-nocturnal VT/VF and striking female preponderance (**Chapter 5**).^{60, 151, 360, 363, 365, 445} Sinus-rate acceleration, QT prolongation and EMW negativity foreshadowed the instigation of polymorphic VT. In one case, tissue-Doppler-imaging correlates of postsystolic aftercontractions were present just prior to TdP. In contrast to other *SCN5A* channelopathies, this indicates that sympathetic surges fuel the arrhythmias in these patients. Triggered by these clinical observations, future patch-clamp experiments and in-silico investigations will encompass PKA- and Ca^{2+} -mediated regulation of the mutant sodium.¹⁵⁹ Furthermore, the unexpected propensity of LQT3 females to VT occurred in the absence of baseline QTc/EMW gender differences.⁴⁴⁶ Previous cellular data point to increased transmural differences in I_{CaL} (increased epicardial I_{CaL} conductance) and ~20% lower I_{Kr} density in female cardiomyocytes that exaggerated dispersion of repolarization.^{447, 448} This transmural I_{CaL} gradient was attenuated by castration of female rabbits. In the future, altered ion-channel expression due to modulatory effects of (non)gonadal hormones or gene-gender interactions could be addressed.

FUTURE PERSPECTIVES

In the Worm study, preliminary non-parametric linkage analysis for the arrhythmia trait allocated a large proportion of the genetic risk to a specific locus on chromosome 3, containing the three juxtaposed *SCN5A*, *SCN10A*, and *SCN11A* genes encoding different Na_v channels. The overall phenotypic complexity of the study population triggered us to investigate this chromosome-3 locus. Furthermore, the genome of the Worm population will be compared to the genome of the Dutch and Limburg population through collaborations with the GoNL Project consortium.⁴⁴⁹ Genetic association studies with linkage analysis of quantitative traits will be performed to identify remote allelic variants that contribute to the diverse phenotypic tableau and the susceptibility to SCD. We strive to validate and replicate our genetic findings in other populations with a well-defined risk of SCD, such as the Arrhythmia Genetics in The Netherlands Study (AGNES).³⁶ The ultimate goal will be to identify genetic modifiers relevant for the prediction of SCD in the general population (**Figure 7.9**).

In the near future, understanding of the genetic determinants of VT/VF and translational mechanistic understanding will increase considerably, necessitating the use of disease expression systems that allow simultaneous multivariable assessment in models with preserved hemodynamic and autonomic reflexes. To account for oligogenic disease expression and/or genetic background, we will generate patient-specific induced pluripotent stem-cells (iPSC)-derived cardiomyocytes (CMs). By using iPSC-CMs, complex genotype-phenotype relationships can be investigated and gene-editing techniques like CRISPR/Cas9⁴⁵⁰ can be employed to correct for the mutation or insert the mutation in a specific genetic background. Sophisticated multiscale computational modeling incorporating



autonomic modulation and mechano-electric feedback mechanisms will provide additional new insights.

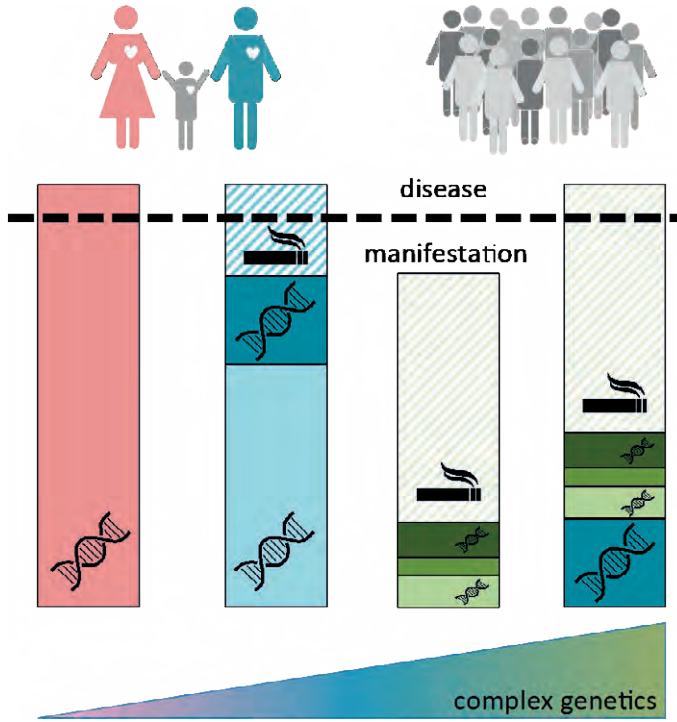


Figure 7.9 Genotype-phenotype investigations in family-based cohorts will ascertain common variants with modest impact on disease manifestation alone, but with large influence during instances of additional stress. This way, gene discovery in a highly selected family can forward risk stratification and treatment of millions of patients.

TOWARDS PERSONALIZED ARRHYTHMIA MANAGEMENT

The accumulating knowledge on mechanisms of arrhythmia, partly surpassing the conventional electrophysiological arena, in combination with the unraveling of the individual genetic make-up increasingly provides the physician the tools for tailored arrhythmia treatment per genotype-phenotype combination. Such personalized arrhythmia management requires a dedicated translational arrhythmia team should be composed, consisting of clinical/translational/cellular electrophysiologists, molecular and clinical geneticists, cardiac-imaging and heart-failure specialists with expertise on mechanisms of arrhythmia in the setting of electrophysiological and hemodynamic instability, and with state-of-the-art knowledge on antiarrhythmic drug actions, biophysical properties of ion

channels and their mutations, neurocardiac modulation, and in-silico modeling (**Figure 7.10**).

For complex VT/VF cases, once the arrhythmic trigger and substrate have been identified, a personalized antiarrhythmic management consisting of appropriate preventive, pharmacological, and/or invasive measures is designed. Preventive measures could encompass individualized lifestyle modifications, watchful waiting via periodic cardiac risk stratification but also arrhythmia-risk gene profiling.^{451, 452} In low-medium risk patients not suitable for prophylactic ICD implantation a wearable VF alarm with GPS locator would be beneficial.⁴⁵³ Unfortunately, such a device is not available yet. The choice of antiarrhythmic drug agent depends heavily on the arrhythmia mechanism(s) and the patient characteristics e.g., pre-existing conduction delay, LV dysfunction, or LV hypertrophy. Interestingly, ranolazine²⁸⁵ and bepridil⁴⁵⁴ possess mechano-inhibitory, besides conventional, antiarrhythmic drug actions. Secondary prevention of SCD often involves the implantation of an ICD, but this does not interfere with the mechanism of arrhythmia. If VTs recur despite antiarrhythmic drug therapy and ICD interventions follow, catheter-based radiofrequency ablation is indicated. As an adjuvant invasive strategy, there is increased interest for the modulation of the autonomic nervous system. Temporal or permanent block of the stellate ganglia suppresses malignant ventricular arrhythmias in LQTS, CPVT, and electrical storm.^{1, 184-187, 455} Renal denervation, another neuromodulatory therapy, reduced VT burden in small studies.⁴⁵⁶⁻⁴⁵⁸

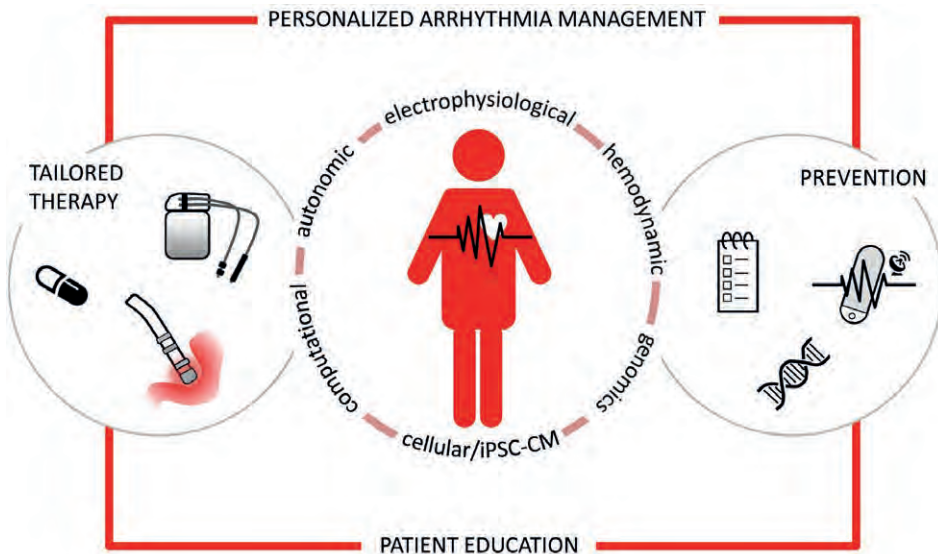
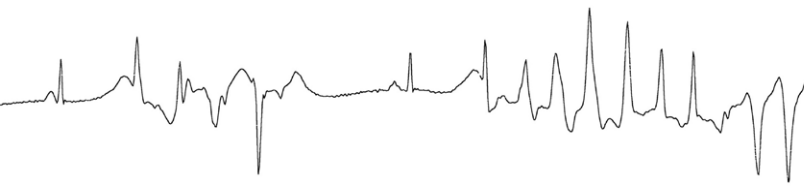


Figure 7.10 Schematic representation of personalized arrhythmia management



In the midst of all this convoluted scientific knowledge we tend to overlook the most important radar: the patient and his/her reconciliation. Shared-decision making is the crux of patient-centered healthcare, improving quality, safety and patient satisfaction.⁴⁵⁹ The treating physician needs to avoid jargon to seek a patient's participation, understanding, and collaboration. Communication skills of healthcare providers should be optimized with emphasis on choices, patient autonomy, and beneficence. Art-based or visual communication can add to this in a non-conventional way (**Chapter 8**).

In Maastricht, we are adopting such integrative approach towards individual arrhythmia management. As an example, it was only through multidisciplinary teamwork that we successfully treated the patient with multifocal ectopic Purkinje-related contractions (**Chapter 6**). Patch-clamp experiments demonstrating flecainide-sensitive increased window I_{Na} current guided the successful administration of this sodium-channel blocker in the *SCN5A*-p.(Leu828Phe) patient. The Worm study is another example of integrative personalized arrhythmia management; consenting patients undergo a very thorough electrophysiological, cardiac-structural and genetic work-up. In the near future, the generation of patient-specific iPSC-CMs expressing patient's unique genetic context will enhance individualized understanding and therapy. To ascertain shared-decision making, we have organized Worm Information Days, published news articles, and developed an online Worm study platform.

Finally, the HeArt project (**Figure 7.11**), a project on the synergy of art and science (and inspired by the Worm study), will provide an interactive playground to stimulate scientific physician-patient communication an exposition at the outpatient clinic of Maastricht University Medical Center+ (**Chapter 8**).



Figure 7.11 Logo of the HeArt project.

FUTURE PERSPECTIVES

Personalized arrhythmia management as depicted in **Figure 7.10** should become standard for all arrhythmia patients seeking topreferral treatment at the MUMC+. With the arrival of the consumer society, better-informed patients (dr. Google, health apps) and increased pressure by Regulatory Authorities, we need to adapt and improve our communication and collaborative skills.⁴⁵⁹ This also applies to the participation in multidisciplinary, national and

international collaborations. Ideally, these shared-decision making skills should be taught during the medical training. At the Maastricht University, the program “Does Art Make You a Better Doctor” focuses on improving observational skills. We are currently exploring the possibilities to use art-based interventions to improve physician-patient/study subject contact and to stimulate creativity in PhD students (**Chapter 8**).

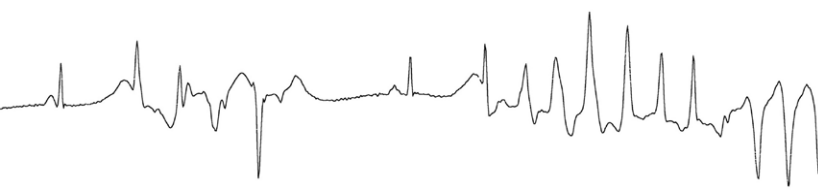
RELEVANCE FOR SCD IN GENERAL

The aforementioned multidisciplinary management of ventricular arrhythmogenesis requires an individualized systems approach, much beyond the electrophysiological-oriented examination alone. The incorporation of extra-electrophysiological parameters improved arrhythmia-risk prediction in LQTS and enhanced understanding of sympathetic-related electromechanical instability (this thesis). Deep phenotyping and genotyping of a *SCN5A* founder population underscored that complex oligogenic phenotype-genotype relations underlie disease expression.

Similarly, integrative approaches will also apply to VT/VF in the setting of acquired structural heart disease. Mechanoelectric feedback fueling electrical instability is anticipated in patients with mitral valve prolapse and cardiac arrhythmias or in cardiomyopathy patients with overload-induced arrhythmias. Divergent electromechanical relations likely underlie (non)-ischemic cardiomyopathy, short-QT syndrome, Brugada syndrome, and acquired repolarization prolongation, including postmyocardial infarction QT prolongation. Postinfarction inhomogeneities in myocardial sympathetic innervation are deemed arrhythmogenic and can be targeted by catheter-based VT ablation.⁴²⁷ Finally, continued unraveling of the genetic risk factors for SCD will improve risk stratification and guide personalized arrhythmia management also in patients with scar-related VT/VF. Taken together, our integrative approaches, provide a road map for future antiarrhythmic management in patients with genetic susceptibility to SCD and VT/VF owing to structural heart diseases.

CONCLUSIONS

In this chapter, I elaborated on the contribution of mechano-electric instability besides primary electrical mechanisms of ventricular arrhythmogenesis in the genetically-predisposed heart. Prolonged-repolarization-associated EMW negativity creates a substrate for life-threatening arrhythmias and commands immediate vigilance. EMW negativity, however, is a vehicle but not the *sine qua non* for arrhythmic deterioration. Superimposed triggers like sympathetic hyperactivity, dynamic cycle-length variations, and/or mechano-electric impulses are required to exaggerate spatiotemporal dispersion of repolarization and promote myocardial Ca^{2+} (over) loading. This potentiates regenerative SR Ca^{2+} release that can feedback on $[\text{Ca}^{2+}]_{\text{cyt}}$ -activated inward membrane currents but also on mechanosensitive elements via contractile events. The high lethality of enhanced left-sided



sympathetic activity, compared to adrenergic stimulation, during drug-induced LQT1 is explained by the heterogeneous electrophysiological response to sympathetic LV stimulation besides increased inotropic responses and electromechanical deviation.

Cardiologists, electrophysiologists and geneticists involved in VT/VF patient care are confronted with mounting mechanistic and genetic complexity. Even classical monogenic disease entities appear to have oligogenic or polygenic determinants of disease expressivity and SCD risk. Meticulous cardiac phenotyping is of key importance to unravel distinct genotype-phenotype relationships. In this way, novel disease entities, like *SCN5A*-associated MEPPC syndrome and isorhythmic dissociation, but also atypical arrhythmia-provoking triggers are identified. Isolated family cohorts facilitate the discovery of clinically relevant modifier genes that could also modulate disease expressivity in unrelated populations with comparable (severe) phenotypes. With the increased availability of next-generation DNA sequencing techniques, advanced bioinformatics, publicly accessible genealogy archives, and thorough cardiac clinical and cellular phenotyping, the electrophysiological field is maturing and personalized arrhythmia management is within reach. An ethical debate on the delicate balance between privacy laws and preventive medicine is ineluctable.

To conclude, my research, based on translational and integrative approaches, has provided novel insights in ventricular arrhythmogenesis in the genetically-susceptible heart, facilitated personalized arrhythmia management, and provided a useful itinerary for the management of arrhythmias owing to cardiac structural abnormalities.



"Kunst synoniem voor troost!"



8

HEART PROJECT

Rachel M.A. ter Bekke, Claudia A.A. Volders

Accepted for publication in Tijdschrift voor Gezondheidswetenschappen, 2018

NVVC "Kunst uit het hart" art exhibition, Amsterdam, 2013
Hart en Vaatcentrum outpatient clinic art exhibition, Maastricht, 2018
Minderbroedersberg art exhibition, Maastricht, 2018

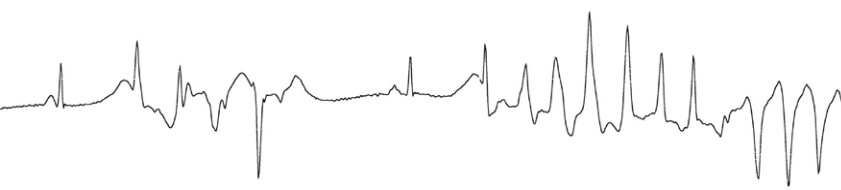
THE HEART PROJECT

The scientific endeavors to unravel arrhythmogenic mechanisms in the genetically-susceptible heart, described in **Chapters 1-7**, were paralleled by artistic enterprises, designated as the “HeArt project”. In the HeArt project, years of collaboration led to unconventional approaches to elevate scientific understanding and presentation by artistic input, and by using HeArt-derived imaging to improve patient-doctor communication. Synergy between the scientist (Rachel ter Bekke) and the artist (Claudia Volders; www.claudiovolders.nl) was reached. Conversely, the excitement of scientific breakthroughs and cutting-edge technology often sparked artistic inspiration.

The HeArt project encompassed a variety of art-based interventions aimed at detaching the researcher out of her scientific comfort zone to stimulate creativity. Multiple art-and-science brainstorm sessions (**Figure 8.1** and **8.2**) provoked out-of-the-box thinking, leading the scientist to evaluate her work from a different perspective. Original paintings, created for these sessions by the artist, served to trigger alternative reflections on scientific achievements and views on next developments (**Figure 8.2**). Outdoor expeditions were undertaken to get exposed to the historical and sociocultural contexts of research projects (**Figure 8.3**). Finally, the scientist’s artistic inclination was enhanced by joined painting studies (**Figure 8.1** and **8.7**) that reiterated insights into visuals. Such artistic assignments stimulated the feeling of humbly following in the footsteps of the greatest artistic scientist ever, Leonardo da Vinci. An impression of the different aspects of the HeArt project can be appreciated at <http://www.youtube.com/watch?v=iLEkIH28vIA>.

As one concrete example of the HeArt project, we explored the birthplaces, living areas and memorial grounds of designated founders and relatives of the Worm pedigree (**Chapter 5** of this PhD thesis), hypothesizing that physical visits would trigger new ideas for the scientific and artistic progress of the Worm Study. An old door post with inscriptions commemorating the death of a presumed *SCN5A*-p.(delPhe1617) carrier (**Figure 8.3**) was found, symbolizing a gateway to the past where relevant pieces of the Worm puzzle came together.

Regarding the Worm ancestors and their regions of living, there were marked differences between Waubach (the Netherlands, birthplaces of ancestral couple A) and Bank (Unterherschaft Heiden, Kreis Aachen, Germany, birthplaces of ancestral couple B; **Figure 5.1**); the latter being a hamlet in the midst of farmlands, and the former at a busy intersection of the important Roman main trade road called Via Belgica (**Figure 8.4**). The Via Belgica connected Boulogne-sur-Mer, France (Latin: Gesoriacum) with Cologne, Germany (Colonia Agrippina), and was crucial for the local and regional economy, the military defenses and governance (www.viabelgica.nl). We hypothesized that population, and thus also migration of the *SCN5A* mutation, occurred predominantly along these historical routes, namely in the East-West direction. Genealogical research confirmed these migration patterns (**Figure 8.4**). This led to the concentration of extramural medical communications and societal alerts to this Maastricht-Aachen-Liège Euregio. Personal encounters with



German inhabitants of the Bank area (Kreis Aachen) highlighted the psychosocial impact of increased susceptibility to cardiac arrest to a population unfamiliar with the origins of their problem. This enforced us to identify the genetic contributors to VF across the border, and to seek collaborations with heart researchers at the Uniklinik RWTH Aachen.

Under the motto *“To Innovate One Has To Embrace History”*, I investigated the history of medicine with the aim of rediscovering the *“ikigai”* (Japanese for *“reason of existence”*) of a doctor. In ancient cultures the *“healing arts”* comprised of tending and caring for the sick, besides applying primitive interventions. In the last centuries, medicine has evolved into an evidence-based and cost-effectiveness-driven medical science. Often, this came along with blunted emotional sensitivity to the patient’s needs, and (sometimes very) limited time for patient-doctor contacts. However, a hospital is more than a laboratory, and medicine is not an exact science. Because of this and because of the mounting complexities of medical science, health-care professionals are increasingly faced with challenges of adequate communication with their patients. Knowledge transfer from the physician to the patient and vice versa requires excellent communication skills, empathic abilities and expertise. It exceeds, by far, a simple *“Dr. Google consultation”*, and a patient is not simply a diagnosis. Sophisticated capacities such as the art of empathy, humanity, communication, observational skills, creativity, and outside-the-box thinking benefit knowledge transfer and patient-centered care with shared decision making. True communication comes often through a person’s eyes, as they show unfiltered emotion and state-of-mind. **Figure 8.6** shows a close-up of eye contact between a patient and the physician, exemplary of the value of non-verbal communication.

Experiments using abstract pieces of art, and artistic brainstorming, can enhance the physician’s self-awareness and explorative mind. They identify strengths and weaknesses, elements that are crucial for an expert communication, especially with patients at risk for sudden cardiac arrest. Next to conventional physician-patient communication tools like online platforms (<https://hartenvaatcentrum.mumc.nl/de-worm-studie>), we use objects of art as supplementary vehicles to transfer complex medical information and stimulate interaction. As an example, we mention the finding of the female propensity towards sudden cardiac arrest described in **Chapter 5**, and in this context the use of artistic symbols like the *‘swnwt’* (hieroglyphic writing for the first known female physician, named Peseshet) including the half-spherical stepping stones (**Figure 8.7**). The *“ieb”*, the hieroglyphic symbol for heart, is also depicted. The handles of the *ieb* exemplify the arteries and veins to the organ. The water vase next to Virgin Mary during the Annunciation by Arthur Hacker (**Figure 8.7**) reminds of the *ieb* and stands for the feminine source.

We hypothesize that jointly experienced scientific achievements create larger support by the general community and willingness to participate in any next study. As such, the HeArt project was exhibited at the Netherlands Society of Cardiology (NVVC) *“Art from the Heart”* exposition in 2013, has recently been shown to the public at the Heart+Vascular Center at Maastricht University Medical Centre (a selection of quotes of anonymous patients are

portrayed at the title pages preceding each chapter of this thesis), and can now (2018) be seen and experience at the Main Building of Maastricht University at the Minderbroedersberg. Our exhibition will travel onward to the outpatient clinic of Zuyderland Medical Center in Heerlen, the Netherlands.

Finally, the cover of this thesis. This encompasses all elements investigated in the thesis project: the complexity of cardiac arrhythmias, genetics and holistic patient care with a feminine touch. **Figure 8.8** portrays different stages of the creation of the cover.

Our art-and-science xenogamy puts the scientist with her research activities in a broader societal context, much beyond the confined environment of the academia. We believe that the HeArt project can result in novel scientific perspectives, new research questions, pieces of arts, but also increased patient satisfaction and health.



TO THE HEART OF THE MATTER

As physicians we have the privilege and obligation to be the “*Saxum in Aquis Moventibus*” for patients and family members during vulnerable phases in their life. Patients place their hearts in our hands, when a fiduciary bond is created. The scientific quest to answer their stalling “why” after the unexpected loss of a relative requires many skills and empathic capabilities.

Negative consequences of poor communication can severely impact on the patient’s belief in medical services, patient-doctor relations, patient disease ownership, and reduced compliance. At a broader scope, scientific malcommunication can cause misunderstanding on genetics, gene therapy, in-vitro fertilization, organ donation, vaccination and broader topic like climate change/global warming. To solve this conundrum, patients, doctors, scientists and community-engagement organizations can benefit from art-based projects aimed at stimulating interpersonal communication, knowledge transfer, respect, empathy and creativity.





Figure 8.2 Interactive art-based coaching: the red square put on the painting (left and right panels) symbolizes the status of the current research activities by the scientist; the blue square indicates future endeavors.

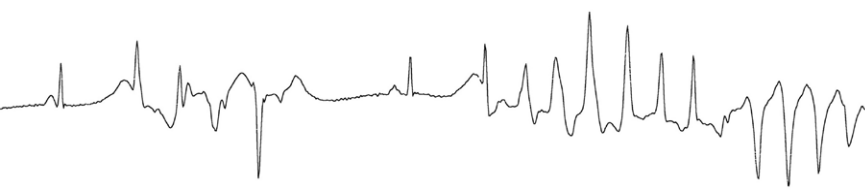




Figure 8.3 Wooden transom with inscriptions commemorating the death of Maria Anna Merckelbach (1764, October 9 at the age of 37 years), a presumed p.(Phe1617del)-carrier, in Hotel Brull, Mechelen, The Netherlands.



Figure 8.4 **Top left**, “Land without Borders” of Limburg, the Netherlands, in the 18th century, with the presumed course of the Roman trade road Via Belgica. **Top right**, East-West spreading of the Worm population (over generations) occurred mainly along the Via Belgica,. **Below left**, “Tree of Life”, oil painting by Claudia Volders, inspired on the Worm Study. **Below right**, Soil from ancestors’ farm in Waubach, the Netherlands.

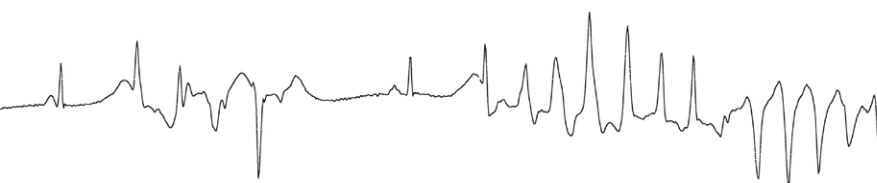
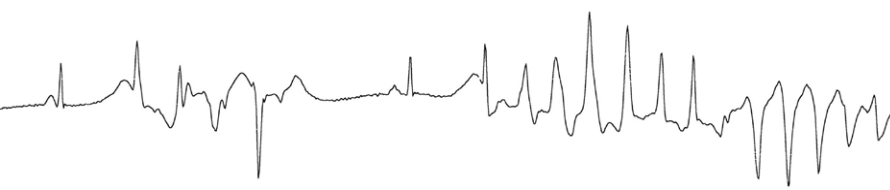




Figure 8.5 Art-based valorization and holistic HeArt paintings.



Figure 8.6 Eyes, the portals for empathic doctor-patient contact.



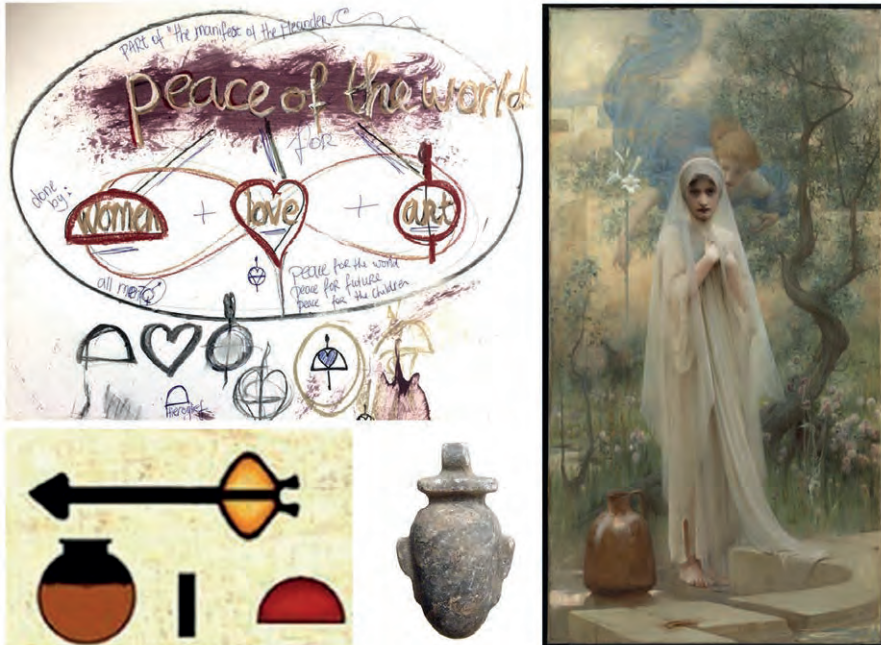


Figure 8.7 Upper left, “Manifest of the Meander”. Lower left, Hieroglyphic symbol for female physician or “swnwt”, the half-spherical stepping stone, and heart or “ieb”, lower middle. Right, “The Annunciation” (1892) by Arthur Hacker with a water vase symbolizing the female fertility (Tate Britain, London, United Kingdom).

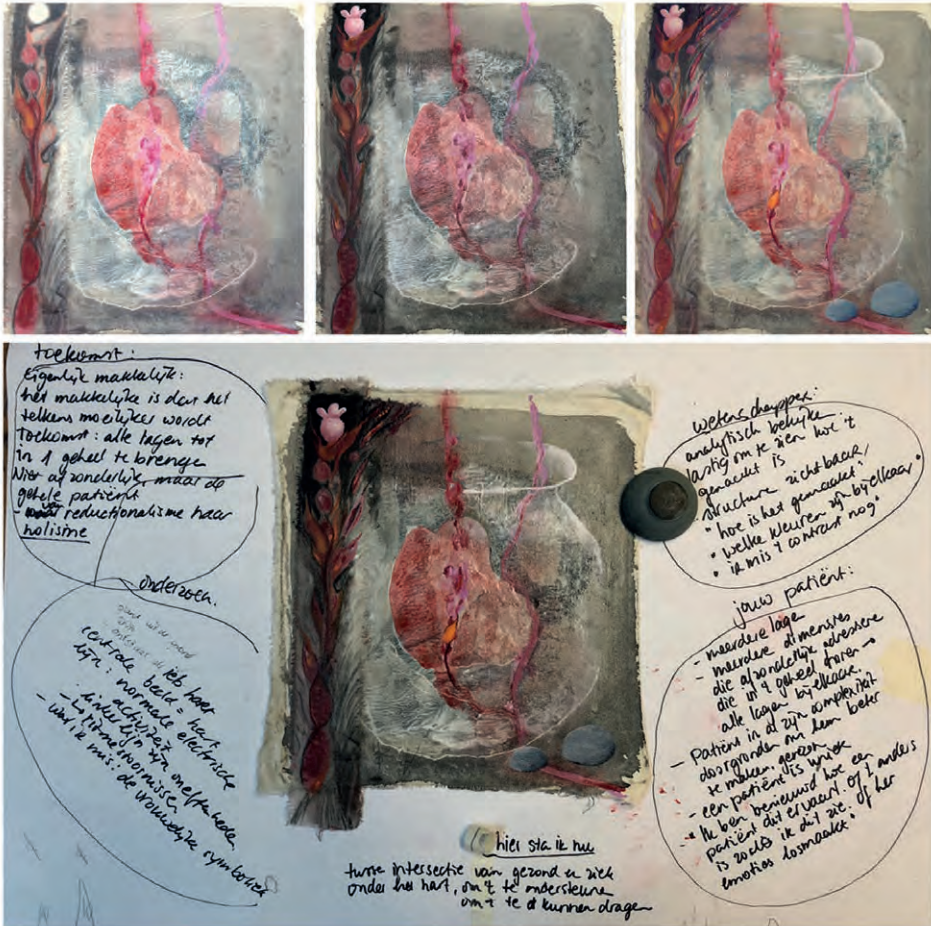


Figure 8.8 Top, Thesis cover in different stages of development. Below, Different scientific and personal perspectives on cover painting serve as tools for inspiration.



SUMMARY/SAMENVATTING

SUMMARY

In the healthy heart, coordinated contraction is triggered by electrical impulses that initiate in the sinus node and travel to the atria and ventricles, timely and with synchronous coordination. Perturbations of ventricular electrical activity can lead to life-threatening arrhythmias and, if not treated appropriately, to sudden cardiac death. Such malignant arrhythmias can occur in the presence of a structural or functional arrhythmogenic substrate. Concomitant brisk autonomic-tone variations may facilitate arrhythmogenesis. Besides these and other classical proarrhythmic ingredients, it is increasingly recognized that electromechanical uncoupling and mechano-electric feedback contribute to proarrhythmic instability. The mechanisms and management of ventricular arrhythmias in the genetically-susceptible heart are the main topics of the present PhD thesis.

After a general introduction of the main topic “sudden cardiac arrest” in **Chapter 1**, **Chapter 2** recapitulates important aspects of ventricular arrhythmogenesis, and it provides unique data demonstrating the presence of electromechanical disparity just prior to the onset of TdP in a patient with congenital LQTS.

Within an international consortium, we examined the relation between altered electromechanical coupling and arrhythmia susceptibility in a large cohort of LQTS patients. The results are described in **Chapter 3**. We show, for the first time, that the EMW is a robust arrhythmia risk indicator in these patients, irrespective of their genotype, and superior to QTc. The EMW was found constant during consecutive measurements in the same individual at clinically-stable conditions, but could turn very negative during instances of ventricular ectopy and prior to TdP. In **Chapter 4**, we report novel data collected in a clinically-relevant canine model of drug-induced LQT1. In this model, LSGS has a high arrhythmic propensity, causing TdP and ventricular fibrillation during profound EMW negativity. We surmise that LSGS-induced positive lusitropy during QT prolongation cause this electromechanical disparity, and speculate that co-activation of the sympathetic and vagal nervous system occurs during LSGS (under undecentralized conditions), with both autonomic limbs contributing to arrhythmogenesis.

In **Chapter 5**, our results of the Worm Study are described. By investigating a large founder population with the *SCN5A* mutation p.(Phe1617del), we identified novel *SCN5A*-related phenotypes and arrhythmia patterns in this inherited sudden-cardiac-death syndrome. Heritability estimates provide a road map to downstream genetic analyses, aimed at identifying genetic modifiers genes that influence disease expression.

The “multifocal ectopic Purkinje-related premature contractions syndrome” that is described in **Chapter 6** underscores the multifaceted phenotypic appearance of cardiac sodium-channel mutations. This syndrome can lead to heart failure. In the case of the young woman described, the additional presence of a *KCNE1* variant also contributed to drug-induced TdP during treatment with amiodarone. By personalized translational arrhythmia management, this patient was successfully treated with flecainide, suppressing ectopy and restoring a poor LV ejection fraction.



Chapter 7 puts the insights obtained in this PhD project in broader perspective. Avenues for future scientific directions are projected. I propose that forthcoming investigations of the prevention of sudden cardiac arrest should encompass the multimodality integration of electrics, mechanics, autonomics, and complex genetics.

Chapter 8 describes the synergy between an artist and a scientist. This unconventional collaboration has elevated scientific processes to a new level, making it also more accessible to the general public.

SAMENVATTING

In het gezonde hart wordt de contractie voorafgegaan door tijdige en gesynchroniseerde elektrische impulsen die vanuit de sinusknop naar de atria en ventrikels worden doorgegeven. Verstoringen van deze elektrische impulsen in de ventrikels kunnen aanleiding geven tot levensbedreigende kamerritmestoornissen en, indien niet adequaat behandeld, tot een acute hartstilstand. Dergelijke gevaarlijke ritmestoornissen kunnen ontstaan door een structureel of functioneel substraat in het kamermyo-card. Gelijktijdige en plotse variaties in de autonome tonus kunnen aritmogene ontaarding voeden. Naast deze klassieke, proaritmische ingrediënten wordt in toenemende mate duidelijk dat elektromechanische koppeling en mechano-elektrische feedback bijdragen aan de proaritmische instabiliteit van het hart. Verschillende genetische factoren kunnen onderliggend zijn aan deze functionele heterogeniteiten. De mechanismen en behandeling van kamerritmestoornissen in het genetisch-gevoelige hart zijn de hoofdonderwerpen van dit proefschrift.

Na een algemene introductie over “plotse hartstilstand” in **Hoofdstuk 1**, worden bovenstaande aspecten in **Hoofdstuk 2** samengevat, en hun individuele bijdragen aan het ontstaan van kamerritmestoornissen in detail bediscussieerd. Tevens bevat dit hoofdstuk unieke data over de elektromechanische dispersie in het hart vlak voor het optreden van TdP in een patiënt met congenitaal LQTS.

Binnen een internationaal consortium onderzochten wij de relatie tussen veranderde elektromechanische koppeling en aritmie-gevoeligheid in een grote populatie van LQTS patiënten. De resultaten worden beschreven in **Hoofdstuk 3**. Wij vonden dat het zogenaamde “elektromechanische venster” (EMW) een robuuste aritmie-risicomarker is voor LQTS patiënten, onafhankelijk van hun genotype, en dat de EMW superieur is ten opzichte van de QTc. Verder toonde de EMW constante waarden tijdens opeenvolgende metingen bij een stabiele patiënt, maar deze kon fors negatief worden tijdens momenten van ventriculaire ectopie en vlak voor TdP. In **Hoofdstuk 4** beschrijven wij onze onderzoeksbevindingen in een klinisch-relevant hondenmodel van het lange-QT1 syndroom. In dit model had linker stellatum-ganglion-stimulatie (LSGS) een hoge aritmische potentie, waarbij TdP en ventrikelfibrilleren werden uitgelokt op momenten dat de EMW fors negatief was. Wij postuleren dat LSGS-geïnduceerde positieve lusitropie tijdens QT-verlenging deze elektromechanische dispersie veroorzaakt, en dat co-activatie van het

sympathische en vagale zenuwstelsel optreedt tijdens LSGS (onder niet-gedecentraliseerde omstandigheden), waarbij beide componenten van het autonome zenuwstelsel bijdragen aan de aritmogenese.

In **Hoofdstuk 5** staan onze resultaten over de Worm-Studie beschreven. We onderzochten een grote founderpopulatie met de *SCN5A* mutatie p.(Phe1617del) en vonden nieuwe *SCN5A*-gerelateerde fenotypes en aritmiepatronen in dit syndroom dat predisponeert voor plotse hartstilstand. Heritabiliteitsschattingen worden gebruikt als richtingaanduiders voor verdere genetische analyse met het doel om aanvullende genen te identificeren die de ziekte-expressie en susceptibiliteit voor plotse hartstilstand beïnvloeden.

Het “multifocale ectopische Purkinje-gerelateerde contractie syndroom” wordt beschreven in **Hoofdstuk 6**. Dit is een andere aandoening die door *SCN5A*-mutaties kan worden veroorzaakt, en tot hartfalen kan leiden. De beschreven casus betreft een jonge patiënte met dit syndroom door een nieuwe *SCN5A*-mutatie, die bovendien amiodarone-geïnduceerde TdP ontwikkelde tijdens beoogde antiaritmische behandeling van haar excessieve ventriculaire ectopie. Additioneel dragerschap van een *KCNE1*-variant lag aan de basis van de TdP-gevoeligheid. Gepersonaliseerd translationeel aritmie-onderzoek leidde tot succesvolle behandeling met flecainide bij deze patiënte, en tot onderdrukking van de ectopie en herstel van het hartfalen.

In **Hoofdstuk 7** worden de resultaten van dit proefschrift in breder perspectief geplaatst. Richtingen voor toekomstige wetenschappelijke onderzoeken worden aangegeven. Daarbij is het naar mijn mening van groot belang dat nieuwe studies naar de preventie van plotse hartstilstand zich richten op de integratie van elektrische, mechanische, autonome en complex-genetische modaliteiten.

Hoofdstuk 8 beschrijft de synergie tussen een kunstenaar en een wetenschapper. Een dergelijk niet-alledaags verbond tilt het wetenschappelijke proces naar een hoger niveau. Daardoor het ook toegankelijker wordt voor het algemene publiek.



VALORIZATION

The insights obtained in this thesis are highly suitable for valorization and will be described in three parts: EMW, Worm study, HeArt project.

SOCIO-ECONOMIC RELEVANCE

Sudden cardiac death claims almost a million deaths annually in Western Europe and the United States. It accounts for one fifth of all natural deaths and up to 50% of all cardiovascular deaths.^{2, 3} In the Netherlands, out-of-hospital SCD occurs with a yearly incidence of approximately 1 per 1,000 individuals,⁵ with ~15 fatal cases per week in Limburg.⁶ The most common cause of SCD is ventricular fibrillation secondary to acute coronary ischemia. Inherited primary electrical arrhythmia syndromes account for 5-10% of VF cases and occur often, but not exclusively, in the young.¹⁰ In <5% of VF cases no cardiac structural or electrical abnormalities can be ascertained. It remains a challenge to adequately address the risk of apparently healthy, but genetically-susceptible, subjects for developing such life-threatening ventricular arrhythmias. It goes without saying that SCD imposes a substantial socio-economic burden, next to the devastating psychosocial impact on survivors of SCA and affected family members.

ELECTROMECHANICAL WINDOW

First, risk stratification in patients with the long-QT syndrome traditionally relies on the determination of the QTc, besides assessing the occurrence of previous syncopal or arrhythmic events. It is well-known that the ubiquitously applied Bazett's formula to correct QT for the heart rate is less reliable at the higher or lower ends of cardiac cycle lengths. As is discussed in this PhD thesis, the noninvasive evaluation of the relation between the duration of the electrical and mechanical systole, notably the electromechanical window, is an easy-to-obtain parameter that improves risk stratification beyond QTc in patients with inherited repolarization defects. The EMW is not significantly affected by heart-rate variations.¹¹³ Improved risk assessment will (re)classify LQTS patients in either low or high risk categories, leading to reduced overtreatment of medium-to-low-risk subjects, for example by reducing prophylactic pharmacological or interventional treatment, but it may also justify a more aggressive approach in EMW-based high-risk patients. In the former, subjects may be reassured, need less intensive follow-up and will not be subjected to unnecessary therapies, whereas in the latter intensified follow-up will result in psychological reassurance and, ideally, reduced mortality. In both circumstances, socio-economic and psychosocial benefit is evident. Clinicians or technicians can easily perform EMW measurements during a standard echocardiogram at relatively low cost.



WORM STUDY

Secondly, through genealogical investigation the Worm study has identified a large familial population at increased risk of SCD in South Limburg and North Rhine-Westphalia. The total number of related individuals approaches 10,000. The striking phenotypic heterogeneity within mutation carriers and the genotype-negative phenotype-positive family members indicate the effect of modifier genes besides the familial *SCN5A* deletion, which has triggered in-depth genetic analyses. These genetic modifiers may have a nontrivial allelic frequency in the “general population”, and may add to the risk of SCD in non-related patients, for instance in the setting of acquired heart disease. As such, the potential outreach of our family-based results can be large. Future genetic risk profiling could identify patients with an increased arrhythmic risk, advocating more stringent cardiovascular risk management and lifestyle amendments. Furthermore, by cardiogenetic scrutiny we uncovered p.(Phe1617del)-specific arrhythmia patterns reminiscent of LQT1-/LQT2-like behavior with sympathetic (often auditory) triggering. This has led to mutation-specific patient counseling and therapy, aiming to reduce sympathetic triggering. The p.(Phe1617del)-related female proarrhythmic proclivity was surprising, but it primed increased clinical vigilance towards mutation-carrying women by initiating preventive antiarrhythmic measures at an earlier age.

HEART PROJECT

Thirdly, we describe the synergism between art and science. Besides personal satisfaction for the artist or scientist, this venture may serve as an inspiring example for future academic entrepreneurs, clinicians, and patients. We are faced with an increasingly shallow patient-doctor relationship, as the current trend of health-care organizations is to constrain patient-doctor time slots, for financial reasons. Despite the availability of sophisticated communication tools, doctors often fail to be good conversationalists. High-standard patient care anno 2020 mandates careful communication with a clear definition of the patient’s expectations, knowledge sharing, advising on test results and treatment options, and shared-decision making. Art can facilitate this communicative process by stimulating empathy, insight, creativity and shift in motivation.

TARGET GROUPS

These three major valorization topics target different populations. Enhanced risk prediction using the EMW is relevant for patients with inherited or acquired repolarization prolongation worldwide, and this non-invasive tool is cheap and easy to measure. Genealogical and cardiogenetic profiling of the Worm population affects subjects in the larger Euregio. Moreover, we anticipate that the discovery of modifier genes could be of great importance for the general population, to screen out patients at risk for severe arrhythmias. The HeArt project targets academic entrepreneurs, clinicians, PhD candidates, residents, scientists, artists, and patients.

ACTIVITIES, PRODUCTS AND INNOVATION

The mechanical part of determining the EMW is usually performed by continuous-wave Doppler imaging of the aortic-valve outflow. Attempts have been made to develop hand-held devices that assess electromechanical coupling using phonocardiography. This will allow bedside risk evaluation and guidance of therapy. Future incorporation of phonocardiography (or techniques alike) into ICDs could enable diurnal EMW monitoring, alerting physicians to treat patients in case of a significant drop.

The Worm project has a strong impact on the (eu)regional cardiac and psychosocial health. In anticipation, we have informed the local community through articles in local news media (de Limburger, Nummer 1, Gezond Idee, Observant), a Belgian (Belang van Limburg) and a German newspaper (die Aachener Zeitung). Furthermore, we have developed a website for interested individuals who wish to receive additional information on the (cardiac) consequences of this *SCN5A* founder mutation, and the Worm study in general (www.hartenvaatcentrum.mumc.nl/de-worm-studie). Specific questions related to the Worm study can be asked directly by telephone or by mail at wormstudie@mumc.nl. In April 2015, we organized the first Worm Information Day for family members, where patients were informed about the latest scientific progress, but also were given a platform to meet distant family members and to share experiences. Finally, we currently face a situation of knowing thousands of names of relatives within the large Worm pedigree, but are unable to reach out to individuals because of privacy laws. This raises ethical challenges. To solve these matters, we will contact Dutch and German ethical and legal experts.

We plan to offer art-based interventions (preferably in a randomized fashion) to current PhD candidates at the Cardiology department, aiming to increase creativity, stimulate out-of-the-box thinking and facilitate communication. Output variables like creativity, out-of-the-box thinking and communication skills will be measured, for instance by using the Torrance Tests of Creative Thinking, which assesses fluency, flexibility, originality, and elaboration. Originality can be graded using the taxonomy of creative design (<http://www.senseandsensation.com/2012/03/assessing-creativity.html>). Finally, in my personal HeArt project, I have been involved in creating art objects that will be exhibited at the Heart+Vascular Center outpatient clinic from March 2018. In this innovative and unprecedented way, patients waiting for the consultation with their cardiovascular specialist will learn about the values of combining art and science, in this case through the HeArt project, and about the scientific findings of the Worm study. Also, they can actively participate in the creation of patient-scientist mindmaps displayed on hospital tables, in order to stimulate patient-scientist communication and get feedback (**Figure A**). This feedback will serve as a tool to improve patient-centered health care. This exhibition will travel fourth to the Main Building of Maastricht University at the Minderbroedersberg, and onward to Zuyderland Medical Centre later in 2018, aiming to reach as many patients and family members in the region as possible. Finally, we plan to further expand this art-based patient communication to other Dutch and European medical facilities.



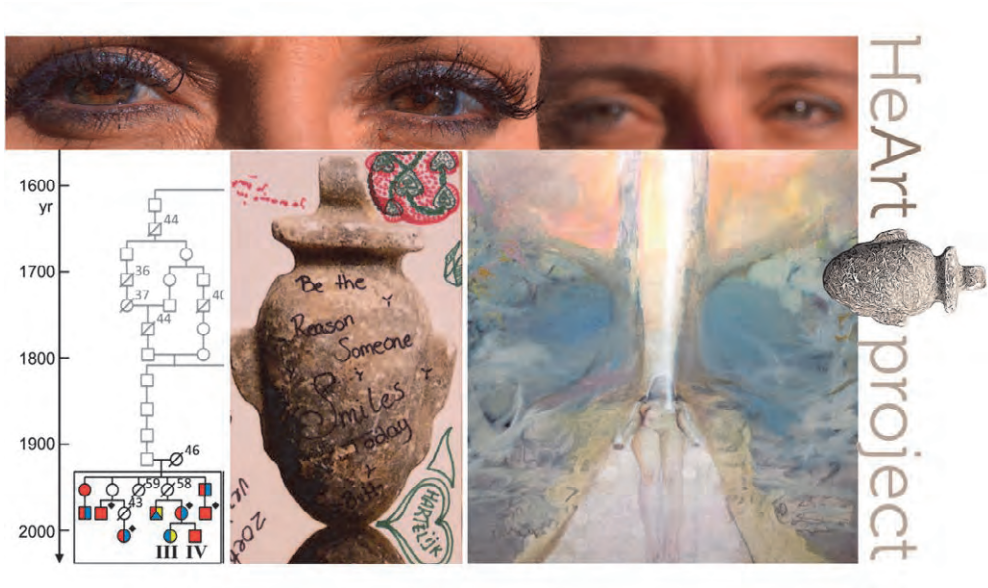


Figure A. Complex scientific information, artistic objects and patient's response to stimulate patient-doctor interaction, opening eyes in both of them.



REFERENCES

1. Priori SG, Blomström-Lundqvist C, Mazzanti A, et al. 2015 ESC Guidelines for the management of patients with ventricular arrhythmias and the prevention of sudden cardiac death: The task force for the management of patients with ventricular arrhythmias and the prevention of sudden cardiac death of the European Society of Cardiology (ESC) endorsed by: Association for European Paediatric and Congenital Cardiology (AEPC). *Eur Heart J* 2015;36:2793-2867.
2. Gillum RF. Geographic variation in sudden coronary death. *Am Heart J* 1990;119:380-389.
3. Myerburg RJ, Interian A, Simmons J, Castellanos A. Sudden cardiac death. Cardiac electrophysiology: From cell to bedside: Philadelphia: WB; 2004:720-731.
4. de Vreede-Swagemakers JJ, Gorgels AP, Dubois-Arbouw WI, van Ree JW, Daemen MJ, Houben LG, Wellens HJ. Out-of-hospital cardiac arrest in the 1990s: a population-based study in the Maastricht area on incidence, characteristics and survival. *J Am Coll Cardiol* 1997;30:1500-1505.
5. Zijlstra JA, Radstok A, Pijls R, et al. Reanimatie in Nederland 2016. Reanimatie in Nederland, 2016. Den Haag: Hartstichting, 2016; 2016.
6. Pijls RW, Nelemans PJ, Rahel BM, Gorgels AP. A text message alert system for trained volunteers improves out-of-hospital cardiac arrest survival. *Resuscitation* 2016;105:182-187.
7. Callans DJ. Out-of-hospital cardiac arrest-the solution is shocking. *N Engl J Med* 2004;351:632-634.
8. Jouven X, Desnos M, Guerot C, Ducimetière P. Predicting sudden death in the population: the Paris Prospective Study I. *Circulation* 1999;99:1978-1983.
9. Wellens HJ, Schwartz PJ, Lindemans FW, et al. Risk stratification for sudden cardiac death: current status and challenges for the future. *Eur Heart J* 2014;35:1642-1651.
10. Priori SG, Aliot E, Blomstrom-Lundqvist C, et al. Task force on sudden cardiac death, European society of cardiology. *Europace* 2002;4:3-18.
11. Friedlander Y, Siscovick DS, Weinmann S, Austin MA, Psaty BM, Lemaitre RN, Arbogast P, Raghunathan TE, Cobb LA. Family history as a risk factor for primary cardiac arrest. *Circulation* 1998;97:155-160.
12. Mizusawa Y, Wilde AA. Brugada syndrome. *Circ Arrhythm Electrophysiol* 2012;5:606-616.
13. Consortium CAD, Deloukas P, Kanoni S, et al. Large-scale association analysis identifies new risk loci for coronary artery disease. *Nat Genet* 2013;45:25-33.
14. Manolio TA, Collins FS, Cox NJ, et al. Finding the missing heritability of complex diseases. *Nature* 2009;461:747-753.
15. Marsman RF, Tan HL, Bezzina CR. Genetics of sudden cardiac death caused by ventricular arrhythmias. *Nat Rev Cardiol* 2014;11:96-111.
16. Schwartz PJ. Sudden cardiac death, founder populations, and mushrooms: what is the link with gold mines and modifier genes? *Heart Rhythm* 2011;8:548-550.
17. Dekker LR, Bezzina CR, Henriques JP, et al. Familial sudden death is an important risk factor for primary ventricular fibrillation: a case-control study in acute myocardial infarction patients. *Circulation* 2006;114:1140-1145.
18. Kaikkonen KS, Kortelainen ML, Linna E, Huikuri HV. Family history and the risk of sudden cardiac death as a manifestation of an acute coronary event. *Circulation* 2006;114:1462-1467.



19. Schwartz PJ, Wolf S. QT interval prolongation as predictor of sudden death in patients with myocardial infarction. *Circulation* 1978;57:1074-1077.
20. Dekker JM, Crow RS, Hannan PJ, Schouten EG, Folsom AR, Study A. Heart rate-corrected QT interval prolongation predicts risk of coronary heart disease in black and white middle-aged men and women: the ARIC study. *J Am Coll Cardiol* 2004;43:565-571.
21. Russell MW, Law I, Sholinsky P, Fabsitz RR. Heritability of ECG measurements in adult male twins. *J Electrocardiol* 1998;30 Suppl:64-68.
22. Carter N, Snieder H, Jeffery S, Saumarez R, Varma C, Antoniadou L, Spector TD. QT interval in twins. *J Hum Hypertens* 2000;14:389-390.
23. Hong Y, Rautaharju PM, Hopkins PN, Arnett DK, Djousse L, Pankow JS, Sholinsky P, Rao DC, Province MA. Familial aggregation of QT-interval variability in a general population: results from the NHLBI Family Heart Study. *Clin Genet* 2001;59:171-177.
24. Newton-Cheh C, Larson MG, Corey DC, Benjamin EJ, Herbert AG, Levy D, D'Agostino RB, O'Donnell CJ. QT interval is a heritable quantitative trait with evidence of linkage to chromosome 3 in a genome-wide linkage analysis: the Framingham heart study. *Heart Rhythm* 2005;2:277-284.
25. Dalageorgou C, Ge D, Jamshidi Y, Nolte IM, Riese H, Savelieva I, Carter ND, Spector TD, Snieder H. Heritability of QT interval: how much is explained by genes for resting heart rate? *J Cardiovasc Electrophysiol* 2008;19:386-391.
26. Silva CT, Kors JA, Amin N, Dehghan A, Witteman JC, Willemssen R, Oostra BA, van Duijn CM, Isaacs A. Heritabilities, proportions of heritabilities explained by GWAS findings, and implications of cross-phenotype effects on PR interval. *Hum Genet* 2015;134:1211-1219.
27. Arking DE, Pfeufer A, Post W, et al. A common genetic variant in the *NOS1* regulator *NOS1AP* modulates cardiac repolarization. *Nat Genet* 2006;38:644-651.
28. Arking DE, Pulit SL, Crotti L, et al. Genetic association study of QT interval highlights role for calcium signaling pathways in myocardial repolarization. *Nat Genet* 2014;46:826-836.
29. Kao WH, Arking DE, Post W, et al. Genetic variations in nitric oxide synthase 1 adaptor protein are associated with sudden cardiac death in US white community-based populations. *Circulation* 2009;119:940-951.
30. Eijgelsheim M, Newton-Cheh C, Aarnoudse AL, van Noord C, Witteman JC, Hofman A, Uitterlinden AG, Stricker BH. Genetic variation in *NOS1AP* is associated with sudden cardiac death: evidence from the Rotterdam Study. *Hum Mol Genet* 2009;18:4213-4218.
31. Crotti L, Lundquist AL, Insolia R, Pedrazzini M, Ferrandi C, De Ferrari GM, Vicentini A, Yang P, Roden DM, George AL, Jr., Schwartz PJ. *KCNH2-K897T* is a genetic modifier of latent congenital long-QT syndrome. *Circulation* 2005;112:1251-1258.
32. Crotti L, Hu D, Barajas-Martinez H, et al. Torsades de pointes following acute myocardial infarction: evidence for a deadly link with a common genetic variant. *Heart Rhythm* 2012;9:1104-1112.
33. Splawski I, Timothy KW, Tateyama M, Clancy CE, Malhotra A, Beggs AH, Cappuccio FP, Sagnella GA, Kass RS, Keating MT. Variant of *SCN5A* sodium channel implicated in risk of cardiac arrhythmia. *Science* 2002;297:1333-1336.

34. Albert CM, Nam EG, Rimm EB, Jin HW, Hajjar RJ, Hunter DJ, MacRae CA, Ellinor PT. Cardiac sodium channel gene variants and sudden cardiac death in women. *Circulation* 2008;117:16-23.
35. Arking DE, Juntila MJ, Goyette P, et al. Identification of a sudden cardiac death susceptibility locus at 2q24.2 through genome-wide association in European ancestry individuals. *PLoS Genet* 2011;7:e1002158.
36. Bezzina CR, Pazoki R, Bardai A, et al. Genome-wide association study identifies a susceptibility locus at 21q21 for ventricular fibrillation in acute myocardial infarction. *Nat Genet* 2010;42:688-691.
37. Marsman RF, Bezzina CR, Freiberg F, et al. Coxsackie and adenovirus receptor is a modifier of cardiac conduction and arrhythmia vulnerability in the setting of myocardial ischemia. *J Am Coll Cardiol* 2014;63:549-559.
38. Bugert P, Elmas E, Stach K, Weiss C, Kalsch T, Dobrev D, Borggrefe M. No evidence for an association between the rs2824292 variant at chromosome 21q21 and ventricular fibrillation during acute myocardial infarction in a German population. *Clin Chem Lab Med* 2011;49:1237-1239.
39. Jabbari R, Risgaard B, Fosbøl EL, et al. Factors associated with and outcomes after ventricular fibrillation before and during primary angioplasty in patients with ST-segment elevation myocardial infarction. *Am J Cardiol* 2015;116:678-685.
40. Jabbari R, Glinge C, Jabbari J, et al. A common variant in *SCN5A* and the risk of ventricular fibrillation caused by first ST-segment elevation myocardial infarction. *PLoS One* 2017;12:e0170193.
41. Keating M, Atkinson D, Dunn C, Timothy K, Vincent GM, Leppert M. Linkage of a cardiac arrhythmia, the long QT syndrome, and the Harvey *ras-1* gene. *Science* 1991;252:704-706.
42. Wang Q, Curran ME, Splawski I, et al. Positional cloning of a novel potassium channel gene: *KVLQT1* mutations cause cardiac arrhythmias. *Nat Genet* 1996;12:17-23.
43. Curran ME, Splawski I, Timothy KW, Vincent GM, Green ED, Keating MT. A molecular basis for cardiac arrhythmia: *HERG* mutations cause long QT syndrome. *Cell* 1995;80:795-803.
44. Wang Q, Shen J, Splawski I, Atkinson D, Li Z, Robinson JL, Moss AJ, Towbin JA, Keating MT. *SCN5A* mutations associated with an inherited cardiac arrhythmia, long QT syndrome. *Cell* 1995;80:805-811.
45. Yang Y, Yang Y, Liang B, et al. Identification of a Kir3.4 mutation in congenital long QT syndrome. *Am J Hum Genet* 2010;86:872-880.
46. Splawski I, Tristani-Firouzi M, Lehmann MH, Sanguinetti MC, Keating MT. Mutations in the *hminK* gene cause long QT syndrome and suppress I_{Ks} function. *Nat Genet* 1997;17:338-340.
47. Abbott GW, Sesti F, Splawski I, Buck ME, Lehmann MH, Timothy KW, Keating MT, Goldstein SA. MiRP1 forms I_{Kr} potassium channels with *HERG* and is associated with cardiac arrhythmia. *Cell* 1999;97:175-187.
48. Chen L, Marquardt ML, Tester DJ, Sampson KJ, Ackerman MJ, Kass RS. Mutation of an A-kinase-anchoring protein causes long-QT syndrome. *Proc Natl Acad Sci U S A* 2007;104:20990-20995.
49. Vatta M, Ackerman MJ, Ye B, Makielski JC, Ughanze EE, Taylor EW, Tester DJ, Balijepalli RC, Foell JD, Li Z, Kamp TJ, Towbin JA. Mutant caveolin-3 induces



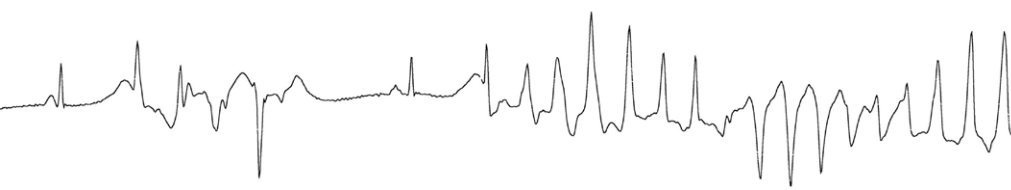
- persistent late sodium current and is associated with long-QT syndrome. *Circulation* 2006;114:2104-2112.
50. Medeiros-Domingo A, Kaku T, Tester DJ, Iturralde-Torres P, Itty A, Ye B, Valdivia C, Ueda K, Canizales-Quinteros S, Tusié-Luna MT, Makielski JC, Ackerman MJ. *SCN4B*-encoded sodium channel $\beta 4$ subunit in congenital long-QT syndrome. *Circulation* 2007;116:134-142.
 51. Ueda K, Valdivia C, Medeiros-Domingo A, Tester DJ, Vatta M, Farrugia G, Ackerman MJ, Makielski JC. Syntrophin mutation associated with long QT syndrome through activation of the nNOS-*SCN5A* macromolecular complex. *Proc Natl Acad Sci U S A* 2008;105:9355-9360.
 52. Crotti L, Johnson CN, Graf E, et al. Calmodulin mutations associated with recurrent cardiac arrest in infants. *Circulation* 2013;127:1009-1017.
 53. Mohler PJ, Schott JJ, Gramolini AO, et al. Ankyrin-B mutation causes type 4 long-QT cardiac arrhythmia and sudden cardiac death. *Nature* 2003;421:634-639.
 54. Schott JJ, Charpentier F, Peltier S, Foley P, Drouin E, Bouhour JB, Donnelly P, Vergnaud G, Bachner L, Moisan JP, Le Marec H, Pascal O. Mapping of a gene for long QT syndrome to chromosome 4q25-27. *Am J Hum Genet* 1995;57:1114-1122.
 55. Plaster NM, Tawil R, Tristani-Firouzi M, et al. Mutations in *Kir2.1* cause the developmental and episodic electrical phenotypes of Andersen's syndrome. *Cell* 2001;105:511-519.
 56. Splawski I, Timothy KW, Sharpe LM, et al. *Cav1.2* calcium channel dysfunction causes a multisystem disorder including arrhythmia and autism. *Cell* 2004;119:19-31.
 57. Vincent GM, Timothy KW, Leppert M, Keating M. The spectrum of symptoms and QT intervals in carriers of the gene for the long-QT syndrome. *N Engl J Med* 1992;327:846-852.
 58. Priori SG, Napolitano C, Schwartz PJ. Low penetrance in the long-QT syndrome: clinical impact. *Circulation* 1999;99:529-533.
 59. Napolitano C, Schwartz PJ, Brown AM, Ronchetti E, Bianchi L, Pinnavaia A, Acquaro G, Priori SG. Evidence for a cardiac ion channel mutation underlying drug-induced QT prolongation and life-threatening arrhythmias. *J Cardiovasc Electrophysiol* 2000;11:691-696.
 60. Priori SG, Schwartz PJ, Napolitano C, Bloise R, Ronchetti E, Grillo M, Vicentini A, Spazzolini C, Nastoli J, Bottelli G, Folli R, Cappelletti D. Risk stratification in the long-QT syndrome. *N Engl J Med* 2003;348:1866-1874.
 61. Westenskow P, Splawski I, Timothy KW, Keating MT, Sanguinetti MC. Compound mutations: a common cause of severe long-QT syndrome. *Circulation* 2004;109:1834-1841.
 62. Chen Q, Kirsch GE, Zhang D, et al. Genetic basis and molecular mechanism for idiopathic ventricular fibrillation. *Nature* 1998;392:293-296.
 63. Priori SG, Napolitano C, Gasparini M, et al. Clinical and genetic heterogeneity of right bundle branch block and ST-segment elevation syndrome: A prospective evaluation of 52 families. *Circulation* 2000;102:2509-2515.
 64. Probst V, Wilde AA, Barc J, et al. *SCN5A* mutations and the role of genetic background in the pathophysiology of Brugada syndrome. *Circ Cardiovasc Genet* 2009;2:552-557.

65. Visser M, van der Heijden JF, Doevendans PA, Loh P, Wilde AA, Hassink RJ. Idiopathic ventricular fibrillation: the struggle for definition, diagnosis, and follow-up. *Circ Arrhythm Electrophysiol* 2016;9:1-11.
66. Viskin S, Belhassen B. Idiopathic ventricular fibrillation. *Am Heart J* 1990;120:661-671.
67. Marsman RF, Barc J, Beekman L, Alders M, Dooijes D, van den Wijngaard A, Ratbi I, Sefiani A, Bhuiyan ZA, Wilde AA, Bezzina CR. A mutation in *CALM1* encoding calmodulin in familial idiopathic ventricular fibrillation in childhood and adolescence. *J Am Coll Cardiol* 2014;63:259-266.
68. Cheung JW, Meli AC, Xie W, et al. Short-coupled polymorphic ventricular tachycardia at rest linked to a novel ryanodine receptor (RyR2) mutation: leaky RyR2 channels under non-stress conditions. *Int J Cardiol* 2015;180:228-236.
69. Paulussen AD, Gilissen RA, Armstrong M, Doevendans PA, Verhasselt P, Smeets HJ, Schulze-Bahr E, Haverkamp W, Breithardt G, Cohen N, Aerssens J. Genetic variations of *KCNQ1*, *KCNH2*, *SCN5A*, *KCNE1*, and *KCNE2* in drug-induced long QT syndrome patients. *J Mol Med* 2004;82:182-188.
70. Lehtonen A, Fodstad H, Laitinen-Forsblom P, Toivonen L, Kontula K, Swan H. Further evidence of inherited long QT syndrome gene mutations in antiarrhythmic drug-associated torsades de pointes. *Heart Rhythm* 2007;4:603-607.
71. Itoh H, Sakaguchi T, Ding WG, et al. Latent genetic backgrounds and molecular pathogenesis in drug-induced long-QT syndrome. *Circ Arrhythm Electrophysiol* 2009;2:511-523.
72. Ramirez AH, Shaffer CM, Delaney JT, Sexton DP, Levy SE, Rieder MJ, Nickerson DA, George AL, Jr., Roden DM. Novel rare variants in congenital cardiac arrhythmia genes are frequent in drug-induced torsades de pointes. *Pharmacogenomics J* 2013;13:325-329.
73. Kääh S, Crawford DC, Sinner MF, et al. A large candidate gene survey identifies the *KCNE1* D85N polymorphism as a possible modulator of drug-induced torsades de pointes. *Circ Cardiovasc Genet* 2012;5:91-99.
74. Nishio Y, Makiyama T, Itoh H, et al. D85N, a *KCNE1* polymorphism, is a disease-causing gene variant in long QT syndrome. *J Am Coll Cardiol* 2009;54:812-819.
75. van Noord C, Aarnoudse AJ, Eijgelsheim M, Sturkenboom MC, Straus SM, Hofman A, Kors JA, Newton-Cheh C, Witteman JC, Stricker BH. Calcium channel blockers, *NOS1AP*, and heart-rate-corrected QT prolongation. *Pharmacogenet Genomics* 2009;19:260-266.
76. Jamshidi Y, Nolte IM, Dalageorgou C, et al. Common variation in the *NOS1AP* gene is associated with drug-induced QT prolongation and ventricular arrhythmia. *J Am Coll Cardiol* 2012;60:841-850.
77. Behr ER, Ritchie MD, Tanaka T, et al. Genome wide analysis of drug-induced torsades de pointes: lack of common variants with large effect sizes. *PLoS One* 2013;8:e78511.
78. Earle N, Yeo Han D, Pilbrow A, Crawford J, Smith W, Shelling AN, Cameron V, Love DR, Skinner JR. Single nucleotide polymorphisms in arrhythmia genes modify the risk of cardiac events and sudden death in long QT syndrome. *Heart Rhythm* 2014;11:76-82.
79. Kapplinger JD, Erickson A, Asuri S, Tester DJ, McIntosh S, Kerr CR, Morrison J, Tang A, Sanatani S, Arbour L, Ackerman MJ. *KCNQ1* p.L353L affects splicing and modifies the



- phenotype in a founder population with long QT syndrome type 1. *J Med Genet* 2017;54:390-398.
80. Amin AS, Giudicessi JR, Tijssen AJ, et al. Variants in the 3' untranslated region of the *KCNQ1*-encoded Kv7.1 potassium channel modify disease severity in patients with type 1 long QT syndrome in an allele-specific manner. *Eur Heart J* 2012;33:714-723.
 81. Duchatelet S, Crotti L, Peat RA, et al. Identification of a *KCNQ1* polymorphism acting as a protective modifier against arrhythmic risk in long-QT syndrome. *Circ Cardiovasc Genet* 2013;6:354-361.
 82. Lahtinen AM, Marjamaa A, Swan H, Kontula K. *KCNE1* D85N polymorphism--a sex-specific modifier in type 1 long QT syndrome? *BMC Med Genet* 2011;12:11.
 83. Crotti L, Monti MC, Insolia R, Peljto A, Goosen A, Brink PA, Greenberg DA, Schwartz PJ, George AL, Jr. *NOS1AP* is a genetic modifier of the long-QT syndrome. *Circulation* 2009;120:1657-1663.
 84. Schwartz PJ, Vanoli E, Crotti L, et al. Neural control of heart rate is an arrhythmia risk modifier in long QT syndrome. *J Am Coll Cardiol* 2008;51:920-929.
 85. Gui J, Wang T, Trump D, Zimmer T, Lei M. Mutation-specific effects of polymorphism H558R in *SCN5A*-related sick sinus syndrome. *J Cardiovasc Electrophysiol* 2010;21:564-573.
 86. Bezzina CR, Barc J, Mizusawa Y, et al. Common variants at *SCN5A-SCN10A* and *HEY2* are associated with Brugada syndrome, a rare disease with high risk of sudden cardiac death. *Nat Genet* 2013;45:1044-1049.
 87. Crotti L, Lahtinen AM, Spazzolini C, et al. Genetic modifiers for the long-QT syndrome: how important is the role of variants in the 3' untranslated region of *KCNQ1*? *Circ Cardiovasc Genet* 2016;9:330-339.
 88. Morad M, Trautwein W. The effect of the duration of the action potential on contraction in the mammalian heart muscle. *Pflugers Arch* 1968;299:66-82.
 89. Wood EH, Heppner RL, Weidmann S. Inotropic effects of electric currents. I. Positive and negative effects of constant electric currents or current pulses applied during cardiac action potentials. II. Hypotheses: calcium movements, excitation-contraction coupling and inotropic effects. *Circ Res* 1969;24:409-445.
 90. Tande PM, Refsum H. Class III antiarrhythmic action linked with positive inotropy: effects of the *d*- and *l*-isomer of sotalol on isolated rat atria at threshold and suprathreshold stimulation. *Pharmacol Toxicol* 1988;62:272-277.
 91. Carlsson L, Abrahamsson C, Almgren O, Lundberg C, Duker G. Prolonged action potential duration and positive inotropy induced by the novel class III antiarrhythmic agent H 234/09 (Almokalant) in isolated human ventricular muscle. *J Cardiovasc Pharmacol* 1991;18:882-887.
 92. Volders PG, Vos MA, Szabo B, Sipido KR, de Groot SH, Gorgels AP, Wellens HJ, Lazzara R. Progress in the understanding of cardiac early afterdepolarizations and torsades de pointes: time to revise current concepts. *Cardiovasc Res* 2000;46:376-392.
 93. Wickenden AD, Kaprielian R, Kassiri Z, Tsoporis JN, Tsushima R, Fishman GI, Backx PH. The role of action potential prolongation and altered intracellular calcium handling in the pathogenesis of heart failure. *Cardiovasc Res* 1998;37:312-323.
 94. Nēmec J, Kim JJ, Gabris B, Salama G. Calcium oscillations and T-wave lability precede ventricular arrhythmias in acquired long QT type 2. *Heart Rhythm* 2010;7:1686-1694.

95. Priori SG, Chen SR. Inherited dysfunction of sarcoplasmic reticulum Ca^{2+} handling and arrhythmogenesis. *Circ Res* 2011;108:871-883.
96. Zygmunt AC, Goodrow RJ, Weigel CM. I_{NaCa} and $I_{\text{Cl(Ca)}}$ contribute to isoproterenol-induced delayed after depolarizations in midmyocardial cells. *Am J Physiol* 1998;275:H1979-H1992.
97. Johnson DM, Heijman J, Bode EF, Greensmith DJ, van der Linde H, Abi-Gerges N, Eisner DA, Trafford AW, Volders PG. Diastolic spontaneous calcium release from the sarcoplasmic reticulum increases beat-to-beat variability of repolarization in canine ventricular myocytes after β -adrenergic stimulation. *Circ Res* 2013;112:246-256.
98. Volders PG, Kulcsár A, Vos MA, Sipido KR, Wellens HJ, Lazzara R, Szabo B. Similarities between early and delayed afterdepolarizations induced by isoproterenol in canine ventricular myocytes. *Cardiovasc Res* 1997;34:348-359.
99. Antzelevitch C, Sicouri S, Litovsky SH, Lukas A, Krishnan SC, Di Diego JM, Gintant GA, Liu DW. Heterogeneity within the ventricular wall. Electrophysiology and pharmacology of epicardial, endocardial, and M cells. *Circ Res* 1991;69:1427-1449.
100. Szentadrassy N, Banyasz T, Biro T, Szabo G, Toth BI, Magyar J, Lazar J, Varró A, Kovacs L, Nanasi PP. Apico-basal inhomogeneity in distribution of ion channels in canine and human ventricular myocardium. *Cardiovasc Res* 2005;65:851-860.
101. Laurita KR, Katra R, Wible B, Wan X, Koo MH. Transmural heterogeneity of calcium handling in canine. *Circ Res* 2003;92:668-675.
102. Katra RP, Laurita KR. Cellular mechanism of calcium-mediated triggered activity in the heart. *Circ Res* 2005;96:535-542.
103. Xiong W, Tian Y, DiSilvestre D, Tomaselli GF. Transmural heterogeneity of Na^+ - Ca^{2+} exchange: evidence for differential expression in normal and failing hearts. *Circ Res* 2005;97:207-209.
104. Flaim SN, Giles WR, McCulloch AD. Contributions of sustained I_{Na} and I_{Kv43} to transmural heterogeneity of early repolarization and arrhythmogenesis in canine left ventricular myocytes. *Am J Physiol Heart Circ Physiol* 2006;291:H2617-2629.
105. Soltysinska E, Olesen SP, Christ T, Wettwer E, Varró A, Grunnet M, Jespersen T. Transmural expression of ion channels and transporters in human nondiseased and end-stage failing hearts. *Pflugers Arch* 2009;459:11-23.
106. Tan HL, Bardai A, Shimizu W, Moss AJ, Schulze-Bahr E, Noda T, Wilde AA. Genotype-specific onset of arrhythmias in congenital long-QT syndrome: possible therapy implications. *Circulation* 2006;114:2096-2103.
107. Viswanathan PC, Rudy Y. Pause induced early afterdepolarizations in the long QT syndrome: a simulation study. *Cardiovasc Res* 1999;42:530-542.
108. Nuyens D, Stengl M, Dugarmaa S, et al. Abrupt rate accelerations or premature beats cause life-threatening arrhythmias in mice with long-QT3 syndrome. *Nat Med* 2001;7:1021-1027.
109. Fredj S, Lindegger N, Sampson KJ, Carmeliet P, Kass RS. Altered Na^+ channels promote pause-induced spontaneous diastolic activity in long QT syndrome type 3 myocytes. *Circ Res* 2006;99:1225-1232.
110. Lindegger N, Hagen BM, Marks AR, Lederer WJ, Kass RS. Diastolic transient inward current in long QT syndrome type 3 is caused by Ca^{2+} overload and inhibited by ranolazine. *J Mol Cell Cardiol* 2009;47:326-334.



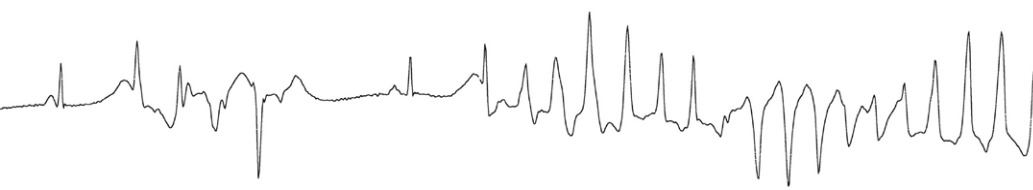
111. El-Sherif N, Caref EB, Yin H, Restivo M. The electrophysiological mechanism of ventricular arrhythmias in the long QT syndrome. Tridimensional mapping of activation and recovery patterns. *Circ Res* 1996;79:474-492.
112. Gallacher DJ, Van de Water A, van der Linde H, Hermans AN, Lu HR, Towart R, Volders PG. In vivo mechanisms precipitating torsades de pointes in a canine model of drug-induced long-QT1 syndrome. *Cardiovasc Res* 2007;76:247-256.
113. van der Linde HJ, Van Deuren B, Somers Y, Loenders B, Towart R, Gallacher DJ. The electro-mechanical window: a risk marker for torsade de pointes in a canine model of drug induced arrhythmias. *Br J Pharmacol* 2010;161:1444-1454.
114. Moers AME, Volders PGA. Mechanical heterogeneity and aftercontractions as trigger for torsades de pointes. In: Kohl P, Franz MR, Sachs F, eds. *Cardiac Mechano-Electric Coupling and Arrhythmias*. Oxford University Press; 2011:345-351.
115. Link MS. Commotio cordis: ventricular fibrillation triggered by chest impact-induced abnormalities in repolarization. *Circ Arrhythm Electrophysiol* 2012;5:425-432.
116. Janse MJ, Coronel R, Wilms-Schopman FJ, de Groot JR. Mechanical effects on arrhythmogenesis: from pipette to patient. *Prog Biophys Mol Biol* 2003;82:187-195.
117. Eckardt L, Kirchhof P, Breithardt G, Haverkamp W. Load-induced changes in repolarization: evidence from experimental and clinical data. *Basic Res Cardiol* 2001;96:369-380.
118. Dun W, Boyden PA. The Purkinje cell; 2008 style. *J Mol Cell Cardiol* 2008;45:617-624.
119. Sampson KJ, Iyer V, Marks AR, Kass RS. A computational model of Purkinje fibre single cell electrophysiology: implications for the long QT syndrome. *J Physiol* 2010;588:2643-2655.
120. Xiao L, Koopmann TT, Ördög B, et al. Unique cardiac Purkinje fiber transient outward current beta-subunit composition: a potential molecular link to idiopathic ventricular fibrillation. *Circ Res* 2013;112:1310-1322.
121. Nattel S, Quantz MA. Pharmacological response of quinidine induced early afterdepolarisations in canine cardiac Purkinje fibres: insights into underlying ionic mechanisms. *Cardiovasc Res* 1988;22:808-817.
122. Maruyama M, Joung B, Tang L, Shinohara T, On YK, Han S, Choi EK, Kim DH, Shen MJ, Weiss JN, Lin SF, Chen PS. Diastolic intracellular calcium-membrane voltage coupling gain and postshock arrhythmias: role of purkinje fibers and triggered activity. *Circ Res* 2010;106:399-408.
123. Boyden PA, Pu J, Pinto J, Keurs HE. Ca²⁺ transients and Ca²⁺ waves in Purkinje cells : role in action potential initiation. *Circ Res* 2000;86:448-455.
124. Scheinman MM. Role of the His-Purkinje system in the genesis of cardiac arrhythmia. *Heart Rhythm* 2009;6:1050-1058.
125. Leenhardt A, Glaser E, Burguera M, Nürnberg M, Maison-Blanche P, Coumel P. Short-coupled variant of torsade de pointes: a new electrocardiographic entity in the spectrum of idiopathic ventricular tachyarrhythmias. *Circulation* 1994;89:206-215.
126. Haïssaguerre M, Shoda M, Jaïs P, et al. Mapping and ablation of idiopathic ventricular fibrillation. *Circulation* 2002;106:962-967.
127. Alders M, Koopmann TT, Christiaans I, et al. Haplotype-sharing analysis implicates chromosome 7q36 harboring *DPP6* in familial idiopathic ventricular fibrillation. *Am J Hum Genet* 2009;84:468-476.

128. Postema PG, Christiaans I, Hofman N, Alders M, Koopmann TT, Bezzina CR, Loh P, Zeppenfeld K, Volders PG, Wilde AA. Founder mutations in the Netherlands: familial idiopathic ventricular fibrillation and *DPP6*. *Neth Heart J* 2011;19:290-296.
129. Haïssaguerre M, Extramiana F, Hocini M, et al. Mapping and ablation of ventricular fibrillation associated with long-QT and Brugada syndromes. *Circulation* 2003;108:925-928.
130. Laurent G, Saal S, Amarouch MY, et al. Multifocal ectopic Purkinje-related premature contractions: a new *SCN5A*-related cardiac channelopathy. *J Am Coll Cardiol* 2012;60:144-156.
131. Wilde AA, Postema PG, Di Diego JM, Viskin S, Morita H, Fish JM, Antzelevitch C. The pathophysiological mechanism underlying Brugada syndrome: depolarization versus repolarization. *J Mol Cell Cardiol* 2010;49:543-553.
132. Bébarová M, O'Hara T, Geelen JL, Jongbloed RJ, Timmermans C, Arens YH, Rodriguez LM, Rudy Y, Volders PG. Subepicardial phase 0 block and discontinuous transmural conduction underlie right precordial ST-segment elevation by a *SCN5A* loss-of-function mutation. *Am J Physiol Heart Circ Physiol* 2008;295:H48-H58.
133. Coronel R, Casini S, Koopmann TT, et al. Right ventricular fibrosis and conduction delay in a patient with clinical signs of Brugada syndrome: a combined electrophysiological, genetic, histopathologic, and computational study. *Circulation* 2005;112:2769-2777.
134. Frustaci A, Priori SG, Pieroni M, Chimenti C, Napolitano C, Rivolta I, Sanna T, Bellocci F, Russo MA. Cardiac histological substrate in patients with clinical phenotype of Brugada syndrome. *Circulation* 2005;112:3680-3687.
135. Hoogendijk MG, Potse M, Linnenbank AC, et al. Mechanism of right precordial ST-segment elevation in structural heart disease: excitation failure by current-to-load mismatch. *Heart Rhythm* 2010;7:238-248.
136. Di Diego JM, Sun ZQ, Antzelevitch C. I_{to} and action potential notch are smaller in left vs. right canine ventricular epicardium. *Am J Physiol* 1996;271:H548-H561.
137. Fish JM, Antzelevitch C. Role of sodium and calcium channel block in unmasking the Brugada syndrome. *Heart Rhythm* 2004;1:210-217.
138. Kurita T, Shimizu W, Inagaki M, Suyama K, Taguchi A, Satomi K, Aihara N, Kamakura S, Kobayashi J, Kosakai Y. The electrophysiologic mechanism of ST-segment elevation in Brugada syndrome. *J Am Coll Cardiol* 2002;40:330-334.
139. Matsuo K, Kurita T, Inagaki M, Kakishita M, Aihara N, Shimizu W, Taguchi A, Suyama K, Kamakura S, Shimomura K. The circadian pattern of the development of ventricular fibrillation in patients with Brugada syndrome. *Eur Heart J* 1999;20:465-470.
140. Kasanuki H, Ohnishi S, Ohtuka M, Matsuda N, Nirei T, Isogai R, Shoda M, Toyoshima Y, Hosoda S. Idiopathic ventricular fibrillation induced with vagal activity in patients without obvious heart disease. *Circulation* 1997;95:2277-2285.
141. Miyazaki T, Mitamura H, Miyoshi S, Soejima K, Aizawa Y, Ogawa S. Autonomic and antiarrhythmic drug modulation of ST segment elevation in patients with Brugada syndrome. *J Am Coll Cardiol* 1996;27:1061-1070.
142. Ardell JL, Andresen MC, Armour JA, Billman GE, Chen PS, Foreman RD, Herring N, O'Leary DS, Sabbah HN, Schultz HD, Sunagawa K, Zucker IH. Translational



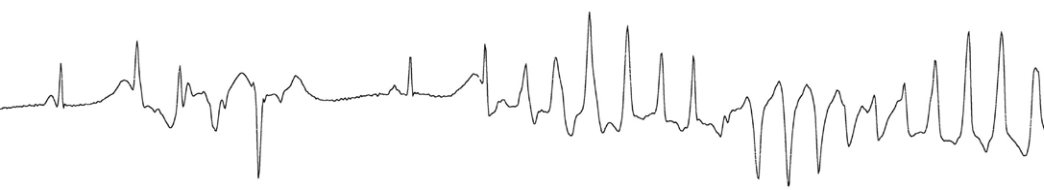
- neurocardiology: preclinical models and cardioneural integrative aspects. *J Physiol* 2016;594:3877-3909.
143. Opthof T, Misier AR, Coronel R, Vermeulen JT, Verberne HJ, Frank RG, Moulijn AC, van Capelle FJ, Janse MJ. Dispersion of refractoriness in canine ventricular myocardium. Effects of sympathetic stimulation. *Circ Res* 1991;68:1204-1215.
 144. Ng GA, Brack KE, Patel VH, Coote JH. Autonomic modulation of electrical restitution, alternans and ventricular fibrillation initiation in the isolated heart. *Cardiovasc Res* 2007;73:750-760.
 145. Brack KE, Patel VH, Mantravardi R, Coote JH, Ng GA. Direct evidence of nitric oxide release from neuronal nitric oxide synthase activation in the left ventricle as a result of cervical vagus nerve stimulation. *J Physiol* 2009;587:3045-3054.
 146. Martins JB, Zipes DP. Effects of sympathetic and vagal nerves on recovery properties of the endocardium and epicardium of the canine left ventricle. *Circ Res* 1980;46:100-110.
 147. Naggar I, Nakase K, Lazar J, Saliccioli L, Selesnick I, Stewart M. Vagal control of cardiac electrical activity and wall motion during ventricular fibrillation in large animals. *Auton Neurosci* 2014;183:12-22.
 148. Winter J, Tipton M, Shattock MJ. Autonomic conflict exacerbates long QT associated ventricular arrhythmia. *J Mol Cell Cardiol* 2018;116:145-154.
 149. Schwartz PJ. Cardiac sympathetic denervation to prevent life-threatening arrhythmias. *Nat Rev Cardiol* 2014;11:346-353.
 150. Shivkumar K, Ajjola OA, Anand I, et al. Clinical neurocardiology defining the value of neuroscience-based cardiovascular therapeutics. *J Physiol* 2016;594:3911-3954.
 151. Schwartz PJ, Priori SG, Spazzolini C, et al. Genotype-phenotype correlation in the long-QT syndrome: gene-specific triggers for life-threatening arrhythmias. *Circulation* 2001;103:89-95.
 152. Ackerman MJ, Tester DJ, Porter CJ. Swimming, a gene-specific arrhythmogenic trigger for inherited long QT syndrome. *Mayo Clin Proc* 1999;74:1088-1094.
 153. Paton JF, Boscan P, Pickering AE, Nalivaiko E. The yin and yang of cardiac autonomic control: vago-sympathetic interactions revisited. *Brain Res Rev* 2005;49:555-565.
 154. Crotti L, Spazzolini C, Porretta AP, et al. Vagal reflexes following an exercise stress test: a simple clinical tool for gene-specific risk stratification in the long QT syndrome. *J Am Coll Cardiol* 2012;60:2515-2524.
 155. Porta A, Girardengo G, Bari V, George AL, Jr., Brink PA, Goosen A, Crotti L, Schwartz PJ. Autonomic control of heart rate and QT interval variability influences arrhythmic risk in long QT syndrome type 1. *J Am Coll Cardiol* 2015;65:367-374.
 156. Schwartz PJ, Priori SG, Locati EH, Napolitano C, Cantu F, Towbin JA, Keating MT, Hammoude H, Brown AM, Chen LS, Colatsky TJ. Long QT syndrome patients with mutations of the *SCN5A* and *HERG* genes have differential responses to Na⁺ channel blockade and to increases in heart rate. Implications for gene-specific therapy. *Circulation* 1995;92:3381-3386.
 157. Priori SG, Napolitano C, Cantu F, Brown AM, Schwartz PJ. Differential response to Na⁺ channel blockade, β -adrenergic stimulation, and rapid pacing in a cellular model mimicking the *SCN5A* and *HERG* defects present in the long-QT syndrome. *Circ Res* 1996;78:1009-1015.

158. Postema PG, Van den Berg M, Van Tintelen JP, Van den Heuvel F, Grundeken M, Hofman N, Van der Roest WP, Nannenberg EA, Krapels IP, Bezzina CR, Wilde A. Founder mutations in the Netherlands: *SCN5A* 1795insD, the first described arrhythmia overlap syndrome and one of the largest and best characterised families worldwide. *Neth Heart J* 2009;17:422-428.
159. Fabritz L, Damke D, Emmerich M, et al. Autonomic modulation and antiarrhythmic therapy in a model of long QT syndrome type 3. *Cardiovasc Res* 2010;87:60-72.
160. Winter J, Lee AW, Niederer S, Shattock MJ. Vagal modulation of dispersion of repolarisation in the rabbit heart. *J Mol Cell Cardiol* 2015;85:89-101.
161. Zhou Q, Xiao J, Jiang D, et al. Carvedilol and its new analogs suppress arrhythmogenic store overload-induced Ca^{2+} release. *Nat Med* 2011;17:1003-1009.
162. Bankston JR, Kass RS. Molecular determinants of local anesthetic action of beta-blocking drugs: Implications for therapeutic management of long QT syndrome variant 3. *J Mol Cell Cardiol* 2010;48:246-253.
163. Abu-Zeitone A, Peterson DR, Polonsky B, McNitt S, Moss AJ. Efficacy of different beta-blockers in the treatment of long QT syndrome. *J Am Coll Cardiol* 2014;64:1352-1358.
164. Chockalingam P, Crotti L, Girardengo G, et al. Not all beta-blockers are equal in the management of long QT syndrome types 1 and 2: higher recurrence of events under metoprolol. *J Am Coll Cardiol* 2012;60:2092-2099.
165. Priori SG, Napolitano C, Schwartz PJ, Grillo M, Bloise R, Ronchetti E, Moncalvo C, Tulipani C, Veia A, Bottelli G, Nastoli J. Association of long QT syndrome loci and cardiac events among patients treated with β -blockers. *JAMA* 2004;292:1341-1344.
166. Villain E, Denjoy I, Lupoglazoff JM, Guicheney P, Hainque B, Lucet V, Bonnet D. Low incidence of cardiac events with beta-blocking therapy in children with long QT syndrome. *Eur Heart J* 2004;25:1405-1411.
167. Vincent GM, Schwartz PJ, Denjoy I, et al. High efficacy of beta-blockers in long-QT syndrome type 1: contribution of noncompliance and QT-prolonging drugs to the occurrence of beta-blocker treatment "failures". *Circulation* 2009;119:215-221.
168. Moss AJ, Zareba W, Hall WJ, et al. Effectiveness and limitations of β -blocker therapy in congenital long-QT syndrome. *Circulation* 2000;101:616-623.
169. Shimizu W, Antzelevitch C. Differential effects of beta-adrenergic agonists and antagonists in LQT1, LQT2 and LQT3 models of the long QT syndrome. *J Am Coll Cardiol* 2000;35:778-786.
170. Wilde AA, Moss AJ, Kaufman ES, et al. Clinical aspects of type 3 long-QT syndrome: an international multicenter study. *Circulation* 2016;134:872-882.
171. Antzelevitch C, Belardinelli L, Zygmunt AC, Burashnikov A, Di Diego JM, Fish JM, Cordeiro JM, Thomas G. Electrophysiological effects of ranolazine, a novel antianginal agent with antiarrhythmic properties. *Circulation* 2004;110:904-910.
172. Belardinelli L, Liu G, Smith-Maxwell C, et al. A novel, potent, and selective inhibitor of cardiac late sodium current suppresses experimental arrhythmias. *J Pharmacol Exp Ther* 2013;344:23-32.
173. Moss AJ, Zareba W, Schwarz KQ, Rosero S, McNitt S, Robinson JL. Ranolazine shortens repolarization in patients with sustained inward sodium current due to type-3 long QT syndrome. *J Cardiovasc Electrophysiol* 2008;19:1289-1293.



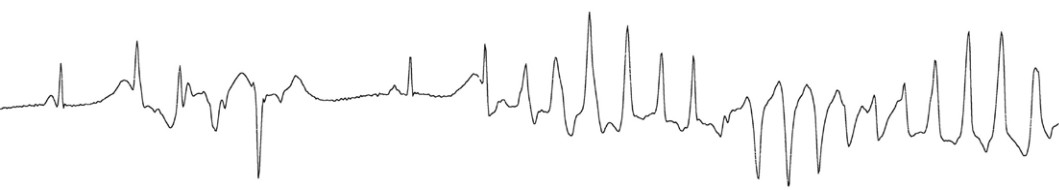
174. Chorin E, Hu D, Antzelevitch C, Hochstadt A, Belardinelli L, Zeltser D, Barajas-Martinez H, Rozovski U, Rosso R, Adler A, Benhorin J, Viskin S. Ranolazine for congenital long-QT syndrome type III: experimental and long-term clinical data. *Circ Arrhythm Electrophysiol* 2016;9:1-9.
175. van den Berg MP, van den Heuvel F, van Tintelen JP, Volders PG, van Gelder IC. Successful treatment of a patient with symptomatic long QT syndrome type 3 using ranolazine combined with a beta-blocker. *Int J Cardiol* 2014;171:90-92.
176. Moss AJ, Windle JR, Hall WJ, Zareba W, Robinson JL, McNitt S, Severski P, Rosero S, Daubert JP, Qi M, Cieciorcka M, Manalan AS. Safety and efficacy of flecainide in subjects with long QT-3 syndrome (deltaKPQ mutation): a randomized, double-blind, placebo-controlled clinical trial. *Ann Noninvasive Electrocardiol* 2005;10:59-66.
177. Kamiya K, Nishiyama A, Yasui K, Hojo M, Sanguinetti MC, Kodama I. Short- and long-term effects of amiodarone on the two components of cardiac delayed rectifier K⁺ current. *Circulation* 2001;103:1317-1324.
178. Papp JG, Németh M, Krassóí II, Mester L, Hála O, Varró A. Differential electrophysiologic effects of chronically administered amiodarone on canine purkinje fibers versus ventricular muscle. *J Cardiovasc Pharmacol Ther* 1996;1:287-296.
179. Sicouri S, Moro S, Litovsky S, Elizari MV, Antzelevitch C. Chronic amiodarone reduces transmural dispersion of repolarization in the canine heart. *J Cardiovasc Electrophysiol* 1997;8:1269-1279.
180. Haïssaguerre M, Shah DC, Jais P, et al. Role of Purkinje conducting system in triggering of idiopathic ventricular fibrillation. *Lancet* 2002;359:677-678.
181. Noda T, Shimizu W, Taguchi A, Aiba T, Satomi K, Suyama K, Kurita T, Aihara N, Kamakura S. Malignant entity of idiopathic ventricular fibrillation and polymorphic ventricular tachycardia initiated by premature extrasystoles originating from the right ventricular outflow tract. *J Am Coll Cardiol* 2005;46:1288-1294.
182. Jonnesco T. Traitement chirurgical de l'angine de poitrine par la résection du sympathique cervico-thoracique. *Presse Med* 1921;20:193-194.
183. Zipes DP, Festoff B, Schaal SF, Cox C, Sealy WC, Wallace AG. Treatment of ventricular arrhythmia by permanent atrial pacemaker and cardiac sympathectomy. *Ann Intern Med* 1968;68:591-597.
184. Moss AJ, McDonald J. Unilateral cervicothoracic sympathetic ganglionectomy for the treatment of long QT interval syndrome. *N Engl J Med* 1971;285:903-914.
185. Schwartz PJ, Locati EH, Moss AJ, Crampton RS, Trazzi R, Ruberti U. Left cardiac sympathetic denervation in the therapy of congenital long QT syndrome. A worldwide report. *Circulation* 1991;84:503-511.
186. Schwartz PJ, Priori SG, Cerrone M, et al. Left cardiac sympathetic denervation in the management of high-risk patients affected by the long-QT syndrome. *Circulation* 2004;109:1826-1833.
187. Collura CA, Johnson JN, Moir C, Ackerman MJ. Left cardiac sympathetic denervation for the treatment of long QT syndrome and catecholaminergic polymorphic ventricular tachycardia using video-assisted thoracic surgery. *Heart Rhythm* 2009;6:752-759.
188. Vaseghi M, Barwad P, Malavassi Corrales FJ, Tandri H, Mathuria N, Shah R, Sorg JM, Gima J, Mandal K, Saenz Morales LC, Lokhandwala Y, Shivkumar K. Cardiac

- sympathetic denervation for refractory ventricular arrhythmias. *J Am Coll Cardiol* 2017;69:3070-3080.
189. Duggal P, Vesely MR, Wattanasirichaigoon D, Villafane J, Kaushik V, Beggs AH. Mutation of the gene for *IsK* associated with both Jervell and Lange-Nielsen and Romano-Ward forms of long-QT syndrome. *Circulation* 1998;97:142-146.
 190. Splawski I, Shen J, Timothy KW, Lehmann MH, Priori S, Robinson JL, Moss AJ, Schwartz PJ, Towbin JA, Vincent GM, Keating MT. Spectrum of mutations in long-QT syndrome genes. *KVLQT1*, *HERG*, *SCN5A*, *KCNE1*, and *KCNE2*. *Circulation* 2000;102:1178-1185.
 191. Schulze-Bahr E, Wang Q, Wedekind H, et al. *KCNE1* mutations cause Jervell and Lange-Nielsen syndrome. *Nat Genet* 1997;17:267-268.
 192. London B, Michalec M, Mehdi H, et al. Mutation in glycerol-3-phosphate dehydrogenase 1 like gene (*GPD1-L*) decreases cardiac Na^+ current and causes inherited arrhythmias. *Circulation* 2007;116:2260-2268.
 193. Antzelevitch C, Pollevick GD, Cordeiro JM, et al. Loss-of-function mutations in the cardiac calcium channel underlie a new clinical entity characterized by ST-segment elevation, short QT intervals, and sudden cardiac death. *Circulation* 2007;115:442-449.
 194. Cordeiro JM, Marieb M, Pfeiffer R, Calloe K, Burashnikov E, Antzelevitch C. Accelerated inactivation of the L-type calcium current due to a mutation in *CACNB2b* underlies Brugada syndrome. *J Mol Cell Cardiol* 2009;46:695-703.
 195. Watanabe H, Koopmann TT, Le Scouarnec S, et al. Sodium channel $\beta 1$ subunit mutations associated with Brugada syndrome and cardiac conduction disease in humans. *J Clin Invest* 2008;118:2260-2268.
 196. Delpón E, Cordeiro JM, Núñez L, et al. Functional effects of *KCNE3* mutation and its role in the development of Brugada syndrome. *Circ Arrhythm Electrophysiol* 2008;1:209-218.
 197. Hu D, Barajas-Martinez H, Burashnikov E, Springer M, Wu Y, Varró A, Pfeiffer R, Koopmann TT, Cordeiro JM, Guerchicoff A, Pollevick GD, Antzelevitch C. A mutation in the $\beta 3$ subunit of the cardiac sodium channel associated with Brugada ECG phenotype. *Circ Cardiovasc Genet* 2009;2:270-278.
 198. Itoh H, Sakaguchi T, Ashihara T, et al. A novel *KCNH2* mutation as a modifier for short QT interval. *Int J Cardiol* 2009;137:83-85.
 199. Medeiros-Domingo A, Tan BH, Crotti L, et al. Gain-of-function mutation S422L in the *KCNJ8*-encoded cardiac K_{ATP} channel Kir6.1 as a pathogenic substrate for J-wave syndromes. *Heart Rhythm* 2010;7:1466-1471.
 200. Burashnikov E, Pfeiffer R, Barajas-Martinez H, et al. Mutations in the cardiac L-type calcium channel associated with inherited J-wave syndromes and sudden cardiac death. *Heart Rhythm* 2010;7:1872-1882.
 201. Kattynarath D, Maugren S, Neyroud N, et al. *MOG1*: a new susceptibility gene for Brugada syndrome. *Circ Cardiovasc Genet* 2011;4:261-268.
 202. Ohno S, Zankov DP, Ding WG, et al. *KCNE5* (*KCNE1L*) variants are novel modulators of Brugada syndrome and idiopathic ventricular fibrillation. *Circ Arrhythm Electrophysiol* 2011;4:352-361.
 203. Giudicessi JR, Ye D, Tester DJ, Crotti L, Mugione A, Nesterenko VV, Albertson RM, Antzelevitch C, Schwartz PJ, Ackerman MJ. Transient outward current (I_{to}) gain-of-



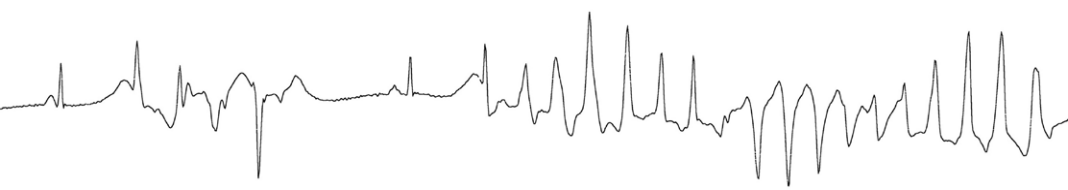
- function mutations in the *KCND3*-encoded K_v4.3 potassium channel and Brugada syndrome. *Heart Rhythm* 2011;8:1024-1032.
204. Crotti L, Marcou CA, Tester DJ, Castelletti S, Giudicessi JR, Torchio M, Medeiros-Domingo A, Simone S, Will ML, Dagradi F, Schwartz PJ, Ackerman MJ. Spectrum and prevalence of mutations involving BrS1- through BrS12-susceptibility genes in a cohort of unrelated patients referred for Brugada syndrome genetic testing: implications for genetic testing. *J Am Coll Cardiol* 2012;60:1410-1418.
 205. Ishikawa T, Sato A, Marcou CA, et al. A novel disease gene for Brugada syndrome: sarcolemmal membrane-associated protein gene mutations impair intracellular trafficking of hNav1.5. *Circ Arrhythm Electrophysiol* 2012;5:1098-1107.
 206. Liu H, Chatel S, Simard C, et al. Molecular genetics and functional anomalies in a series of 248 Brugada cases with 11 mutations in the TRPM4 channel. *PLoS One* 2013;8:e54131.
 207. Riuró H, Beltran-Alvarez P, Tarradas A, et al. A missense mutation in the sodium channel β 2 subunit reveals *SCN2B* as a new candidate gene for Brugada syndrome. *Hum Mutat* 2013;34:961-966.
 208. Hu D, Barajas-Martinez H, Terzic A, et al. *ABCC9* is a novel Brugada and early repolarization syndrome susceptibility gene. *Int J Cardiol* 2014;171:431-442.
 209. Hu D, Barajas-Martínez H, Pfeiffer R, et al. Mutations in *SCN10A* are responsible for a large fraction of cases of Brugada syndrome. *J Am Coll Cardiol* 2014;64:66-79.
 210. Cerrone M, Lin X, Zhang M, et al. Missense mutations in plakophilin-2 cause sodium current deficit and associate with a Brugada syndrome phenotype. *Circulation* 2014;129:1092-1103.
 211. Boczek NJ, Ye D, Johnson EK, et al. Characterization of *SEMA3A*-encoded semaphorin as a naturally occurring Kv4.3 protein inhibitor and its contribution to Brugada syndrome. *Circ Res* 2014;115:460-469.
 212. Koizumi A, Sasano T, Kimura W, et al. Genetic defects in a His-Purkinje system transcription factor, *IRX3*, cause lethal cardiac arrhythmias. *Eur Heart J* 2016;37:1469-1475.
 213. Visser M, Dooijes D, van der Smagt JJ, van der Heijden JF, Doevendans PA, Loh P, Asselbergs FW, Hassink RJ. Next-generation sequencing of a large gene panel in patients initially diagnosed with idiopathic ventricular fibrillation. *Heart Rhythm* 2017;14:1035-1040.
 214. Cluitmans MJM, Heijman J, ter Bekke RMA, Peeters RLM, Westra RL, Crijns HJGM, Volders PGA. Integration of noninvasive imaging of repolarization with cellular modeling in a clinical case. PhD Thesis, Maastricht University, 2016.
 215. Valdivia CR, Medeiros-Domingo A, Ye B, Shen WK, Algiers TJ, Ackerman MJ, Makielski JC. Loss-of-function mutation of the *SCN3B*-encoded sodium channel β 3 subunit associated with a case of idiopathic ventricular fibrillation. *Cardiovasc Res* 2010;86:392-400.
 216. Brugada R, Hong K, Dumaine R, et al. Sudden death associated with short-QT syndrome linked to mutations in *HERG*. *Circulation* 2004;109:30-35.
 217. Bellocq C, van Ginneken AC, Bezzina CR, Alders M, Escande D, Mannens MM, Baró I, Wilde AA. Mutation in the *KCNQ1* gene leading to the short QT-interval syndrome. *Circulation* 2004;109:2394-2397.

218. Priori SG, Pandit SV, Rivolta I, et al. A novel form of short QT syndrome (SQT3) is caused by a mutation in the *KCNJ2* gene. *Circ Res* 2005;96:800-807.
219. Templin C, Ghadri JR, Rougier JS, et al. Identification of a novel loss-of-function calcium channel gene mutation in short QT syndrome (SQT56). *Eur Heart J* 2011;32:1077-1088.
220. Thorsen K, Dam VS, Kjær-Sørensen K, et al. Loss-of-activity-mutation in the cardiac chloride-bicarbonate exchanger AE3 causes short QT syndrome. *Nat Commun* 2017;8:1696.
221. Haïssaguerre M, Chatel S, Sacher F, et al. Ventricular fibrillation with prominent early repolarization associated with a rare variant of *KCNJ8/KATP* channel. *J Cardiovasc Electrophysiol* 2009;20:93-98.
222. Watanabe H, Nogami A, Ohkubo K, et al. Electrocardiographic characteristics and *SCN5A* mutations in idiopathic ventricular fibrillation associated with early repolarization. *Circ Arrhythm Electrophysiol* 2011;4:874-881.
223. Priori SG, Napolitano C, Tiso N, Memmi M, Vignati G, Bloise R, Sorrentino V, Danieli GA. Mutations in the cardiac ryanodine receptor gene (*hRyR2*) underlie catecholaminergic polymorphic ventricular tachycardia. *Circulation* 2001;103:196-200.
224. Lahat H, Pras E, Olender T, Avidan N, Ben-Asher E, Man O, Levy-Nissenbaum E, Khoury A, Lorber A, Goldman B, Lancet D, Eldar M. A missense mutation in a highly conserved region of *CASQ2* is associated with autosomal recessive catecholamine-induced polymorphic ventricular tachycardia in Bedouin families from Israel. *Am J Hum Genet* 2001;69:1378-1384.
225. Mohler PJ, Splawski I, Napolitano C, Bottelli G, Sharpe L, Timothy K, Priori SG, Keating MT, Bennett V. A cardiac arrhythmia syndrome caused by loss of ankyrin-B function. *Proc Natl Acad Sci U S A* 2004;101:9137-9142.
226. Bhuiyan ZA, Hamdan MA, Shamsi ET, Postma AV, Mannens MM, Wilde AA, Al-Gazali L. A novel early onset lethal form of catecholaminergic polymorphic ventricular tachycardia maps to chromosome 7p14-p22. *J Cardiovasc Electrophysiol* 2007;18:1060-1066.
227. Vega AL, Tester DJ, Ackerman MJ, Makielski JC. Protein kinase A-dependent biophysical phenotype for V227F-*KCNJ2* mutation in catecholaminergic polymorphic ventricular tachycardia. *Circ Arrhythm Electrophysiol* 2009;2:540-547.
228. Nyegaard M, Overgaard MT, Søndergaard MT, et al. Mutations in calmodulin cause ventricular tachycardia and sudden cardiac death. *Am J Hum Genet* 2012;91:703-712.
229. Roux-Buisson N, Cacheux M, Fourest-Lieuvin A, et al. Absence of triadin, a protein of the calcium release complex, is responsible for cardiac arrhythmia with sudden death in human. *Hum Mol Genet* 2012;21:2759-2767.
230. Jimenez-Jaimez J, Palomino Doza J, Ortega A, Macias-Ruiz R, Perin F, Rodriguez-Vazquez del Rey MM, Ortiz-Genga M, Monserrat L, Barriales-Villa R, Blanca E, Alvarez M, Tercedor L. Calmodulin 2 mutation N98S is associated with unexplained cardiac arrest in infants due to low clinical penetrance electrical disorders. *PLoS One* 2016;11:e0153851.
231. Gomez-Hurtado N, Boczek NJ, Kryshtal DO, Johnson CN, Sun J, Nitu FR, Cornea RL, Chazin WJ, Calvert ML, Tester DJ, Ackerman MJ, Knollmann BC. Novel CPVT-



- associated calmodulin mutation in *CALM3* (CALM3-A103V) activates arrhythmogenic Ca waves and sparks. *Circ Arrhythm Electrophysiol* 2016;9:1-10.
232. Antzelevitch C. Role of spatial dispersion of repolarization in inherited and acquired sudden cardiac death syndromes. *Am J Physiol Heart Circ Physiol* 2007;293:H2024-H2038.
 233. Brutsaert DL. Nonuniformity: a physiologic modulator of contraction and relaxation of the normal heart. *J Am Coll Cardiol* 1987;9:341-348.
 234. Nador F, Beria G, De Ferrari GM, Stramba-Badiale M, Locati EH, Lotto A, Schwartz PJ. Unsuspected echocardiographic abnormality in the long QT syndrome. Diagnostic, prognostic, and pathogenetic implications. *Circulation* 1991;84:1530-1542.
 235. Nakayama K, Yamanari H, Otsuka F, Fukushima K, Saito H, Fujimoto Y, Emori T, Matsubara H, Uchida S, Ohe T. Dispersion of regional wall motion abnormality in patients with long QT syndrome. *Heart* 1998;80:245-250.
 236. Savoye C, Klug D, Denjoy I, Ennezat PV, Le Tourneau T, Guicheney P, Kacet S. Tissue Doppler echocardiography in patients with long QT syndrome. *Eur J Echocardiogr* 2003;4:209-213.
 237. De Ferrari GM, Nador F, Beria G, Sala S, Lotto A, Schwartz PJ. Effect of calcium channel block on the wall motion abnormality of the idiopathic Long QT syndrome. *Circulation* 1994;89:2126-2132.
 238. Haugaa KH, Smedsrud MK, Steen T, Kongsgaard E, Loennechen JP, Skjaerpe T, Voigt JU, Willems R, Smith G, Smiseth OA, Amlie JP, Edvardsen T. Mechanical dispersion assessed by myocardial strain in patients after myocardial infarction for risk prediction of ventricular arrhythmia. *J Am Coll Card Cardiovasc Imaging* 2010;3:247-256.
 239. duBell WH, Houser SR. Voltage and beat dependence of Ca²⁺ transient in feline ventricular myocytes. *Am J Physiol* 1989;257:H746-H759.
 240. Cannell MB, Berlin JR, Lederer WJ. Effect of membrane potential changes on the calcium transient in single rat cardiac muscle cells. *Science* 1987;238:1419-1423.
 241. Sato D, Bers DM. How does stochastic ryanodine receptor-mediated Ca leak fail to initiate a Ca spark? *Biophys J* 2011;101:2370-2379.
 242. Venetucci LA, Trafford AW, O'Neill SC, Eisner DA. The sarcoplasmic reticulum and arrhythmogenic calcium release. *Cardiovasc Res* 2008;77:285-292.
 243. Fabiato A, Fabiato F. Contractions induced by a calcium-triggered release of calcium from the sarcoplasmic reticulum of single skinned cardiac cells. *J Physiol* 1975;249:469-495.
 244. Fabiato A. Two kinds of calcium-induced release of calcium from the sarcoplasmic reticulum of skinned cardiac cells. *Adv Exp Med Biol* 1992;311:245-262.
 245. Lakatta EG. Functional implications of spontaneous sarcoplasmic reticulum Ca²⁺ release in the heart. *Cardiovasc Res* 1992;26:193-214.
 246. Heijman J, Volders PG, Westra RL, Rudy Y. Local control of beta-adrenergic stimulation: Effects on ventricular myocyte electrophysiology and Ca²⁺-transient. *J Mol Cell Cardiol* 2011;50:863-871.
 247. Kashimura T, Briston SJ, Trafford AW, Napolitano C, Priori SG, Eisner DA, Venetucci LA. In the RyR2(R4496C) mouse model of CPVT, beta-adrenergic stimulation induces Ca waves by increasing SR Ca content and not by decreasing the threshold for Ca waves. *Circ Res* 2010;107:1483-1489.

248. Stern MD, Capogrossi MC, Lakatta EG. Spontaneous calcium release from the sarcoplasmic reticulum in myocardial cells: mechanisms and consequences. *Cell Calcium* 1988;9:247-256.
249. Bouchard RA, Clark RB, Giles WR. Effects of action potential duration on excitation-contraction coupling in rat ventricular myocytes. Action potential voltage-clamp measurements. *Circ Res* 1995;76:790-801.
250. Burashnikov A, Antzelevitch C. Acceleration-induced action potential prolongation and early afterdepolarizations. *J Cardiovasc Electrophysiol* 1998;9:934-948.
251. Milberg P, Pott C, Fink M, Frommeyer G, Matsuda T, Baba A, Osada N, Breithardt G, Noble D, Eckardt L. Inhibition of the $\text{Na}^+/\text{Ca}^{2+}$ exchanger suppresses torsades de pointes in an intact heart model of long QT syndrome-2 and long QT syndrome-3. *Heart Rhythm* 2008;5:1444-1452.
252. Yong SL, Ni Y, Zhang T, Tester DJ, Ackerman MJ, Wang QK. Characterization of the cardiac sodium channel *SCN5A* mutation, N1325S, in single murine ventricular myocytes. *Biochem Biophys Res Comm* 2007;352:378-383.
253. Berlin JR, Cannell MB, Lederer WJ. Cellular origins of the transient inward current in cardiac myocytes. role of fluctuations and waves of elevated intracellular calcium. *Circ Res* 1989;65:115-126.
254. Ehara T, Noma A, Ono K. Calcium-activated non-selective cation channel in ventricular cells isolated from adult guinea-pig hearts. *J Physiol* 1988;403:117-133.
255. Guinamard R, Demion M, Chatelier A, Bois P. Calcium-activated nonselective cation channels in mammalian cardiomyocytes. *Trends Cardiovasc Med* 2006;16:245-250.
256. January CT, Riddle JM, Salata JJ. A model for early afterdepolarizations: induction with the Ca^{2+} channel agonist Bay K 8644. *Circ Res* 1988;62:563-571.
257. Yamada KA, Corr PB. Effects of beta-adrenergic receptor activation on intracellular calcium and membrane potential in adult cardiac myocytes. *J Cardiovasc Electrophysiol* 1992;3:209-224.
258. Priori SG, Corr PB. Mechanisms underlying early and delayed afterdepolarizations induced by catecholamines. *Am J Physiol* 1990;258:H1796-H1805.
259. Johnson DM, Heijman J, Pollard CE, Valentin JP, Crijns HJ, Abi-Gerges N, Volders PG. I_{Ks} restricts excessive beat-to-beat variability of repolarization during beta-adrenergic receptor stimulation. *J Mol Cell Cardiol* 2010;48:122-130.
260. Spencer CI, Sham JS. Effects of $\text{Na}^+/\text{Ca}^{2+}$ exchange induced by SR Ca^{2+} release on action potentials and afterdepolarizations in guinea pig ventricular myocytes. *Am J Physiol Heart Circ Physiol* 2003;285:H2552-H2562.
261. Zhao Z, Wen H, Fefelova N, Allen C, Baba A, Matsuda T, Xie LH. Revisiting the ionic mechanisms of early afterdepolarizations in cardiomyocytes: predominant by Ca waves or Ca currents? *Am J Physiol Heart Circ Physiol* 2012;302:H1636-H1644.
262. Antoons G, Volders PG, Stankovicova T, Bito V, Stengl M, Vos MA, Sipido KR. Window Ca^{2+} current and its modulation by Ca^{2+} release in hypertrophied cardiac myocytes from dogs with chronic atrioventricular block. *J Physiol* 2007;579:147-160.
263. Launay P, Fleig A, Perraud AL, Scharenberg AM, Penner R, Kinet JP. TRPM4 is a Ca^{2+} -activated nonselective cation channel mediating cell membrane depolarization. *Cell* 2002;109:397-407.



264. Hofmann T, Chubanov V, Gudermann T, Montell C. TRPM5 is a voltage-modulated and Ca²⁺-activated monovalent selective cation channel. *Curr Biol* 2003;13:1153-1158.
265. Guinamard R, Bois P. Involvement of transient receptor potential proteins in cardiac hypertrophy. *Biochim Biophys Acta* 2007;1772:885-894.
266. Nélaton A. Elements de pathologie chirurgicale 1876. Located at: Librairie Germer Bateliere et Co, Paris.
267. Calkins H, Maughan WL, Weisman HF, Sugiura S, Sagawa K, Levine JH. Effect of acute volume load on refractoriness and arrhythmia development in isolated, chronically infarcted canine hearts. *Circulation* 1989;79:687-697.
268. Hansen DE, Craig CS, Hondeghem LM. Stretch-induced arrhythmias in the isolated canine ventricle. Evidence for the importance of mechano-electrical feedback. *Circulation* 1990;81:1094-1105.
269. Seo K, Inagaki M, Nishimura S, Hidaka I, Sugimachi M, Hisada T, Sugiura S. Structural heterogeneity in the ventricular wall plays a significant role in the initiation of stretch-induced arrhythmias in perfused rabbit right ventricular tissues and whole heart preparations. *Circ Res* 2010;106:176-184.
270. Birati EY, Belhassen B, Bardai A, Wilde AA, Viskin S. The site of origin of torsade de pointes. *Heart* 2011;97:1650-1654.
271. Ravens U. Mechano-electric feedback and arrhythmias. *Prog Biophys Mol Biol* 2003;82:255-266.
272. Wang Y, Joyner RW, Wagner MB, Cheng J, Lai D, Crawford BH. Stretch-activated channel activation promotes early afterdepolarizations in rat ventricular myocytes under oxidative stress. *Am J Physiol Heart Circ Physiol* 2009;296:H1227-H1235.
273. Franz MR, Burkhoff D, Yue DT, Sagawa K. Mechanically induced action potential changes and arrhythmia in isolated and in situ canine hearts. *Cardiovasc Res* 1989;23:213-223.
274. Ward ML, Williams IA, Chu Y, Cooper PJ, Ju YK, Allen DG. Stretch-activated channels in the heart: contributions to length-dependence and to cardiomyopathy. *Prog Biophys Mol Biol* 2008;97:232-249.
275. Chen RL, Penny DJ, Greve G, Lab MJ. Stretch-induced regional mechano-electric dispersion and arrhythmia in the right ventricle of anesthetized lambs. *Am J Physiol Heart Circ Physiol* 2004;286:H1008-H1014.
276. Zeng T, Bett GC, Sachs F. Stretch-activated whole cell currents in adult rat cardiac myocytes. *Am J Physiol Heart Circ Physiol* 2000;278:H548-H557.
277. Iribe G, Ward CW, Camelliti P, Bollensdorff C, Mason F, Burton RA, Garny A, Morphew MK, Hoenger A, Lederer WJ, Kohl P. Axial stretch of rat single ventricular cardiomyocytes causes an acute and transient increase in Ca²⁺ spark rate. *Circ Res* 2009;104:787-795.
278. Guharay F, Sachs F. Stretch-activated single ion channel currents in tissue-cultured embryonic chick skeletal muscle. *J Physiol* 1984;352:685-701.
279. Maroto R, Raso A, Wood TG, Kurosky A, Martinac B, Hamill OP. TRPC1 forms the stretch-activated cation channel in vertebrate cells. *Nat Cell Biol* 2005;7:179-185.
280. Dyachenko V, Husse B, Rueckschloss U, Isenberg G. Mechanical deformation of ventricular myocytes modulates both TRPC6 and Kir2.3 channels. *Cell Calcium* 2009;45:38-54.

281. Langton PD. Calcium channel currents recorded from isolated myocytes of rat basilar artery are stretch sensitive. *J Physiol* 1993;471:1-11.
282. Groh WJ, Gibson KJ, Maylie JG. Hypotonic-induced stretch counteracts the efficacy of the class III antiarrhythmic agent E-4031 in guinea pig myocytes. *Cardiovasc Res* 1996;31:237-245.
283. Morris CE, Juranka PF. Nav channel mechanosensitivity: activation and inactivation accelerate reversibly with stretch. *Biophys J* 2007;93:822-833.
284. Cingolani HE, Perez NG, Pieske B, von Lewinski D, Camilion de Hurtado MC. Stretch-elicited Na^+/H^+ exchanger activation: the autocrine/paracrine loop and its mechanical counterpart. *Cardiovascular Research* 2003;57:953-960.
285. Beyder A, Strege PR, Reyes S, Bernard CE, Terzic A, Makielski J, Ackerman MJ, Farrugia G. Ranolazine decreases mechanosensitivity of the voltage-gated sodium ion channel $\text{Na}_v1.5$: a novel mechanism of drug action. *Circulation* 2012;125:2698-2706.
286. Otway R, Vandenberg JI, Guo G, et al. Stretch-sensitive *KCNQ1* mutation A link between genetic and environmental factors in the pathogenesis of atrial fibrillation? *J Am Coll Cardiol* 2007;49:578-586.
287. Bode F, Sachs F, Franz MR. Tarantula peptide inhibits atrial fibrillation. *Nature* 2001;409:35-36.
288. Craelius W, Chen V, el-Sherif N. Stretch activated ion channels in ventricular myocytes. *Biosci Rep* 1988;8:407-414.
289. Zabel M, Koller BS, Sachs F, Franz MR. Stretch-induced voltage changes in the isolated beating heart: importance of the timing of stretch and implications for stretch-activated ion channels. *Cardiovasc Res* 1996;32:120-130.
290. Hu H, Sachs F. Mechanically activated currents in chick heart cells. *J Membr Biol* 1996;154:205-216.
291. Kohl P, Bollensdorff C, Garny A. Effects of mechanosensitive ion channels on ventricular electrophysiology: experimental and theoretical models. *Exp Physiol* 2006;91:307-321.
292. Taggart P, Sutton P, Opthof T, Coronel R, Kallis P. Electrotonic cancellation of transmural electrical gradients in the left ventricle in man. *Prog Biophys Mol Biol* 2003;82:243-254.
293. Zygmunt AC, Goodrow RJ, Antzelevitch C. I_{NaCa} contributes to electrical heterogeneity within the canine ventricle. *Am J Physiol Heart Circ Physiol* 2000;278:H1671-H1678.
294. Gaborit N, Le Bouter S, Szuts V, Varró A, Escande D, Nattel S, Demolombe S. Regional and tissue specific transcript signatures of ion channel genes in the non-diseased human heart. *J Physiol* 2007;582:675-693.
295. Wan X, Laurita KR, Pruvot EJ, Rosenbaum DS. Molecular correlates of repolarization alternans in cardiac myocytes. *J Mol Cell Cardiol* 2005;39:419-428.
296. Liu DW, Antzelevitch C. Characteristics of the delayed rectifier current (I_{Kr} and I_{Ks}) in canine ventricular epicardial, midmyocardial, and endocardial myocytes. A weaker I_{Ks} contributes to the longer action potential of the M cell. *Circ Res* 1995;76:351-365.
297. Cheng J, Kamiya K, Liu W, Tsuji Y, Toyama J, Kodama I. Heterogeneous distribution of the two components of delayed rectifier K^+ current: a potential mechanism of the proarrhythmic effects of methanesulfonanilide class III agents. *Cardiovasc Res* 1999;43:135-147.



298. Volders PG, Sipido KR, Carmeliet E, Spatjens RL, Wellens HJ, Vos MA. Repolarizing K^+ currents I_{TO1} and I_{Ks} are larger in right than left canine ventricular midmyocardium. *Circulation* 1999;99:206-210.
299. Brahmajothi MV, Morales MJ, Reimer KA, Strauss HC. Regional localization of ERG, the channel protein responsible for the rapid component of the delayed rectifier, K^+ current in the ferret heart. *Circ Res* 1997;81:128-135.
300. Komiya N, Tanaka K, Doi Y, Fukae S, Nakao K, Isomoto S, Seto S, Yano K. A patient with LQTS in whom verapamil administration and permanent pacemaker implantation were useful for preventing torsade de pointes. *Pacing Clin Electrophysiol* 2004;27:123-124.
301. Haugaa KH, Edvardsen T, Leren TP, Gran JM, Smiseth OA, Amlie JP. Left ventricular mechanical dispersion by tissue Doppler imaging: a novel approach for identifying high-risk individuals with long QT syndrome. *Eur Heart J* 2009;30:330-337.
302. Haugaa KH, Amlie JP, Berge KE, Leren TP, Smiseth OA, Edvardsen T. Transmural differences in myocardial contraction in long-QT syndrome: mechanical consequences of ion channel dysfunction. *Circulation* 2010;122:1355-1363.
303. Boudoulas H, Sohn YH, O'Neill W, Brown R, Weissler AM. The QT greater than QS_2 syndrome: a new mortality risk indicator in coronary artery disease. *Am J Cardiol* 1982;50:1229-1235.
304. Chambers JB, Ward DE. The QT and QS_2 intervals in patients with mitral leaflet prolapse. *Am Heart J* 1987;114:355-361.
305. Boudoulas H, Geleris P, Lewis RP, Leier CV. Effect of increased adrenergic activity on the relationship between electrical and mechanical systole. *Circulation* 1981;64:28-33.
306. De Caprio L, Ferro G, Cuomo S, Volpe M, Artiaco D, De Luca N, Ricciardelli B. QT/ QS_2 ratio as an index of autonomic tone changes. *Am J Cardiol* 1984;53:818-822.
307. Vincent GM, Jaiswal D, Timothy KW. Effects of exercise on heart rate, QT, QTc and QT/ QS_2 in the Romano-Ward inherited long QT syndrome. *Am J Cardiol* 1991;68:498-503.
308. ter Bekke RMA, Haugaa KH, van den Wijngaard A, Edvardsen T, Volders PGA. Electro-mechanical window: arrhythmogenic marker in genotyped long-QT syndrome. *Heart rhythm* 2012;9:S86.
309. Volders PG, Stengl M, van Opstal JM, Gerlach U, Spatjens RL, Beekman JD, Sipido KR, Vos MA. Probing the contribution of I_{Ks} to canine ventricular repolarization: key role for β -adrenergic receptor stimulation. *Circulation* 2003;107:2753-2760.
310. Shimizu W, Kurita T, Matsuo K, Suyama K, Aihara N, Kamakura S, Towbin JA, Shimomura K. Improvement of repolarization abnormalities by a K^+ channel opener in the LQT1 form of congenital long-QT syndrome. *Circulation* 1998;97:1581-1588.
311. Shimizu W, Ohe T, Kurita T, Kawade M, Arakaki Y, Aihara N, Kamakura S, Kamiya T, Shimomura K. Effects of verapamil and propranolol on early afterdepolarizations and ventricular arrhythmias induced by epinephrine in congenital long QT syndrome. *J Am Coll Cardiol* 1995;26:1299-1309.
312. Shimizu W, Ohe T, Kurita T, Takaki H, Aihara N, Kamakura S, Matsuhisa M, Shimomura K. Early afterdepolarizations induced by isoproterenol in patients with congenital long QT syndrome. *Circulation* 1991;84:1915-1923.

313. Wellens HJ, Vermeulen A, Durrer D. Ventricular fibrillation occurring on arousal from sleep by auditory stimuli. *Circulation* 1972;46:661-665.
314. Wilde AA, Jongbloed RJ, Doevendans PA, Duren DR, Hauer RN, van Langen IM, van Tintelen JP, Smeets HJ, Meyer H, Geelen JL. Auditory stimuli as a trigger for arrhythmic events differentiate HERG-related (LQTS2) patients from KVLQT1-related patients (LQTS1). *J Am Coll Cardiol* 1999;33:327-332.
315. Liu GX, Choi BR, Ziv O, Li W, de Lange E, Qu Z, Koren G. Differential conditions for early after-depolarizations and triggered activity in cardiomyocytes derived from transgenic LQT1 and LQT2 rabbits. *J Physiol* 2012;590:1171-1180.
316. Kozhevnikov DO, Yamamoto K, Robotis D, Restivo M, El-Sherif N. Electrophysiological mechanism of enhanced susceptibility of hypertrophied heart to acquired torsade de pointes arrhythmias: tridimensional mapping of activation and recovery patterns. *Circulation* 2002;105:1128-1134.
317. Brugada P, Wellens HJ. Early afterdepolarizations: role in conduction block, "prolonged repolarization-dependent reexcitation," and tachyarrhythmias in the human heart. *Pacing Clin Electrophysiol* 1985;8:889-896.
318. Zipes DP. The long QT interval syndrome. A Rosetta stone for sympathetic related ventricular tachyarrhythmias. *Circulation* 1991;84:1414-1419.
319. Hales PW, Schneider JE, Burton RA, Wright BJ, Bollensdorff C, Kohl P. Histological structure of the living isolated rat heart in two contraction states assessed by diffusion tensor MRI. *Prog Biophys Mol Biol* 2012;110:319-330.
320. Blazeski A, Zhu R, Hunter DW, Weinberg SH, Zambidis ET, Tung L. Cardiomyocytes derived from human induced pluripotent stem cells as models for normal and diseased cardiac electrophysiology and contractility. *Prog Biophys Mol Biol* 2012;110:166-177.
321. Schwartz PJ, Ackerman MJ, George AL, Jr, Wilde AA. Impact of genetics on the clinical management of channelopathies. *J Am Coll Card* 2013;62:169-180.
322. ter Bekke RM, Volders PG. Arrhythmogenic mechano-electric heterogeneity in the long-QT syndrome. *Prog Biophys Mol Biol* 2012;110:347-358.
323. Schwartz PJ, Crotti L. QTc behavior during exercise and genetic testing for the long-QT syndrome. *Circulation* 2011;124:2181-2184.
324. Lei M, Cooper PJ, Camelliti P, Kohl P. Role of the 293b-sensitive, slowly activating delayed rectifier potassium current, iKs, in pacemaker activity of rabbit isolated sinoatrial node cells. *Cardiovasc Res* 2002;53:68-79.
325. Aase SA, Torp H, Støylen A. Aortic valve closure: relation to tissue velocities by Doppler and speckle tracking in normal subjects. *Eur J Echocardiogr* 2008;9:555-559.
326. Boudoulas H, Geleris P, Lewis RP, Rittgers SE. Linear relationship between electrical systole, mechanical systole, and heart rate. *Chest* 1981;80:613-617.
327. Kies P, Paul M, Gerss J, Stegger L, Mönning G, Schober O, Wichter T, Schäfers M, Schulze-Bahr E. Impaired cardiac sympathetic innervation in symptomatic patients with long QT syndrome. *Eur J Nucl Med Mol Imaging* 2011;38:1899-1907.
328. Guns PJ, Johnson DM, Weltens E, Lissens J. Negative electro-mechanical windows are required for drug-induced Torsades de Pointes in the anesthetized guinea pig. *J Pharmacol Toxicol Methods* 2012;66:125-134.
329. Johnson DM, Heijman J, Bode EF, Greensmith DJ, van der Linde H, Abi-Gerges N, Eisner DA, Trafford AW, Volders PG. Diastolic spontaneous calcium release from the



- sarcoplasmic reticulum increases beat-to-beat variability of repolarization in canine ventricular myocytes after beta-adrenergic stimulation. *Circ Res* 2013;112:246-256.
330. De Ferrari GM, Schwartz PJ. Long QT syndrome, a purely electrical disease? Not anymore. *Eur Heart J* 2009;30:253-255.
 331. ter Bekke RM, Haugaa KH, van den Wijngaard A, Bos JM, Ackerman MJ, Edvardsen T, Volders PG. Electromechanical window negativity in genotyped long-QT syndrome patients: relation to arrhythmia risk. *Eur Heart J* 2015;36:179-186.
 332. Stams TR, Bourgonje VJ, Beekman HD, Schoenmakers M, van der Nagel R, Oosterhoff P, van Opstal JM, Vos MA. The electromechanical window is no better than QT prolongation to assess risk of Torsade de Pointes in the complete atrioventricular block model in dogs. *Br J Pharmacol* 2014;171:714-722.
 333. Belardinelli L, Dhalla A, Shryock J. Abnormal left ventricular relaxation in patients with long QT syndrome. *Eur Heart J* 2009;30:2813-2814.
 334. Hummel YM, Wilde AA, Voors AA, Bugatti S, Hillege HL, van den Berg MP. Ventricular dysfunction in a family with long QT syndrome type 3. *Europace* 2013;15:1516-1521.
 335. De Ferrari GM, Viola MC, D'Amato E, Antolini R, Forti S. Distinct patterns of calcium transients during early and delayed afterdepolarizations induced by isoproterenol in ventricular myocytes. *Circulation* 1995;91:2510-2515.
 336. Malliani A, Recordati G, Schwartz PJ. Nervous activity of afferent cardiac sympathetic fibres with atrial and ventricular endings. *J Physiol* 1973;229:457-469.
 337. Schwartz PJ, Pagani M, Lombardi F, Malliani A, Brown AM. A cardiocardiac sympathovagal reflex in the cat. *Circ Res* 1973;32:215-220.
 338. De Ambroggi L, Bertoni T, Locati E, Stramba-Badiale M, Schwartz PJ. Mapping of body surface potentials in patients with the idiopathic long QT syndrome. *Circulation* 1986;74:1334-1445.
 339. Vijayakumar R, Silva JNA, Desouza KA, Abraham RL, Strom M, Sacher F, Van Hare GF, Haïssaguerre M, Roden DM, Rudy Y. Electrophysiologic substrate in congenital long QT syndrome: noninvasive mapping with electrocardiographic imaging (ECGI). *Circulation* 2014;130:1936-1943.
 340. Han J, Moe GK. Nonuniform recovery of excitability in ventricular muscle. *Circ Res* 1964;14:44-60.
 341. Yanowitz F, Preston JB, Abildskov JA. Functional distribution of right and left stellate innervation to the ventricles. Production of neurogenic electrocardiographic changes by unilateral alteration of sympathetic tone. *Circ Res* 1966;18:416-428.
 342. Schwartz PJ, Verrier RL, Lown B. Effect of stellectomy and vagotomy on ventricular refractoriness in dogs. *Circ Res* 1977;40:536-540.
 343. Schwartz PJ, Snebold NG, Brown AM. Effects of unilateral cardiac sympathetic denervation on the ventricular fibrillation threshold. *Am J Cardiol* 1976;37:1034-1040.
 344. Zhou S, Jung BC, Tan AY, Trang VQ, Gholmieh G, Han SW, Lin SF, Fishbein MC, Chen PS, Chen LS. Spontaneous stellate ganglion nerve activity and ventricular arrhythmia in a canine model of sudden death. *Heart Rhythm* 2008;5:131-139.
 345. Pauza DH, Skripka V, Pauziene N. Morphology of the intrinsic cardiac nervous system in the dog: a whole-mount study employing histochemical staining with acetylcholinesterase. *Cells Tissues Organs* 2002;172:297-320.

346. Ben-David J, Zipes DP. Differential response to right and left ansae subclaviae stimulation of early afterdepolarizations and ventricular tachycardia induced by cesium in dogs. *Circulation* 1988;78:1241-1250.
347. Vanoli E, Priori SG, Nakagawa H, Hirao K, Napolitano C, Diehl L, Lazzara R, Schwartz PJ. Sympathetic activation, ventricular repolarization and I_{kr} blockade: implications for the antifibrillatory efficacy of potassium channel blocking agents. *J Am Coll Cardiol* 1995;25:1609-1614.
348. Van Deuren B, Van Ammel K, Somers Y, Cools F, Straetemans R, van der Linde HJ, Gallacher DJ. The fentanyl/etomidate-anaesthetised beagle (FEAB) dog: a versatile in vivo model in cardiovascular safety research. *J Pharmacol Toxicol Methods* 2009;60:11-23.
349. Lerche C, Seebohm G, Wagner CI, Scherer CR, Dehmelt L, Abitbol I, Gerlach U, Brendel J, Attali B, Busch AE. Molecular impact of MinK on the enantiospecific block of I_{Ks} by chromanols. *Br J Pharmacol* 2000;131:1503-1506.
350. Van de Water A, Verheyen J, Xhonneux R, Reneman RS. An improved method to correct the QT interval of the electrocardiogram for changes in heart rate. *J Pharmacol Methods* 1989;22:207-217.
351. Thomsen MB, Verduyn SC, Stengl M, Beekman JD, de Pater G, van Opstal J, Volders PG, Vos MA. Increased short-term variability of repolarization predicts *d*-sotalol-induced torsades de pointes in dogs. *Circulation* 2004;110:2453-2459.
352. Schwartz PJ. The role of the sympathetic nervous system in the long QT syndrome: the long road from pathophysiology to therapy. *Cardiac Electrophysiology Clinics* 2012;4:75-85.
353. Schwartz PJ, Ackerman MJ. The long QT syndrome: a transatlantic clinical approach to diagnosis and therapy. *Eur Heart J* 2013;34:3109-3116.
354. Shattock MJ, Tipton MJ. 'Autonomic conflict': a different way to die during cold water immersion? *J Physiol* 2012;590:3219-3230.
355. Schwartz PJ, De Ferrari GM, Pugliese L. Cardiac sympathetic denervation 100 years later: Jonnesco would have never believed it. *Int J Cardiol* 2017;237:25-28.
356. Myerburg RJ, Junttila MJ. Sudden cardiac death caused by coronary heart disease. *Circulation* 2012;125:1043-1052.
357. Makita N, Sumitomo N, Watanabe I, Tsutsui H. Novel *SCN5A* mutation (Q55X) associated with age-dependent expression of Brugada syndrome presenting as neurally mediated syncope. *Heart Rhythm* 2007;4:516-519.
358. Aulchenko YS, Ripke S, Isaacs A, van Duijn CM. GenABEL: an R library for genome-wide association analysis. *Bioinformatics* 2007;23:1294-1296.
359. Nyholt DR. A simple correction for multiple testing for single-nucleotide polymorphisms in linkage disequilibrium with each other. *Am J Hum Genet* 2004;74:765-769.
360. Wilde AA, Brugada R. Phenotypical manifestations of mutations in the genes encoding subunits of the cardiac sodium channel. *Circ Res* 2011;108:884-897.
361. Chen T, Inoue M, Sheets MF. Reduced voltage dependence of inactivation in the *SCN5A* sodium channel mutation delF1617. *Am J Physiol Heart Circ Physiol* 2005;288:H2666-H2676.



362. van den Boogaard M, Smemo S, Burnicka-Turek O, et al. A common genetic variant within *SCN10A* modulates cardiac *SCN5A* expression. *J Clin Invest* 2014;124:1844-1852.
363. Benito B, Sarkozy A, Mont L, Henkens S, Berruezo A, Tamborero D, Arzamendi D, Berne P, Brugada R, Brugada P, Brugada J. Gender differences in clinical manifestations of Brugada syndrome. *J Am Coll Cardiol* 2008;52:1567-1573.
364. Furukawa T, Kurokawa J. Regulation of cardiac ion channels via non-genomic action of sex steroid hormones: implication for the gender difference in cardiac arrhythmias. *Pharmacol Ther* 2007;115:106-115.
365. Bezzina C, Veldkamp MW, van Den Berg MP, Postma AV, Rook MB, Viersma JW, van Langen IM, Tan-Sindhunata G, Bink-Boelkens MT, van Der Hout AH, Mannens MM, Wilde AA. A single Na⁺ channel mutation causing both long-QT and Brugada syndromes. *Circ Res* 1999;85:1206-1213.
366. Remme CA, Wilde AA, Bezzina CR. Cardiac sodium channel overlap syndromes: different faces of *SCN5A* mutations. *Trends Cardiovasc Med* 2008;18:78-87.
367. Makita N, Behr E, Shimizu W, et al. The E1784K mutation in *SCN5A* is associated with mixed clinical phenotype of type 3 long QT syndrome. *J Clin Invest* 2008;118:2219-2229.
368. Remme CA, Verkerk AO, Nuyens D, et al. Overlap syndrome of cardiac sodium channel disease in mice carrying the equivalent mutation of human *SCN5A*-1795insD. *Circulation* 2006;114:2584-2594.
369. Remme CA, Scicluna BP, Verkerk AO, et al. Genetically determined differences in sodium current characteristics modulate conduction disease severity in mice with cardiac sodium channelopathy. *Circ Res* 2009;104:1283-1292.
370. Ter Bekke RMA, Isaacs A, Barysenka A, Hoos MB, Jongbloed JDH, Hoorntje JCA, Patelski ASM, Helderman-van den Enden A, van den Wijngaard A, Stoll M, Volders PGA. Heritability in a *SCN5A*-mutation founder population with increased female susceptibility to non-nocturnal ventricular tachyarrhythmia and sudden cardiac death. *Heart Rhythm* 2017;14:1873-1881.
371. Eddy CA, MacCormick JM, Chung SK, Crawford JR, Love DR, Rees MI, Skinner JR, Shelling AN. Identification of large gene deletions and duplications in *KCNQ1* and *KCNH2* in patients with long QT syndrome. *Heart Rhythm* 2008;5:1275-1281.
372. Crotti L, Lewandowska MA, Schwartz PJ, Insolia R, Pedrazzini M, Bussani E, Dagradi F, George AL, Jr., Pagani F. A *KCNH2* branch point mutation causing aberrant splicing contributes to an explanation of genotype-negative long QT syndrome. *Heart Rhythm* 2009;6:212-218.
373. Mura M, Mehta A, Ramachandra CJ, Zappatore R, Pisano F, Ciuffreda MC, Barbaccia V, Crotti L, Schwartz PJ, Shim W, Gneccchi M. The *KCNH2*-IVS9-28A/G mutation causes aberrant isoform expression and hERG trafficking defect in cardiomyocytes derived from patients affected by long QT syndrome type 2. *Int J Cardiol* 2017;240:367-371.
374. Brink PA, Schwartz PJ. Of founder populations, long QT syndrome, and destiny. *Heart Rhythm* 2009;6:S25-S33.
375. Brink PA, Crotti L, Corfield V, et al. Phenotypic variability and unusual clinical severity of congenital long-QT syndrome in a founder population. *Circulation* 2005;112:2602-2610.

376. Crotti L, Spazzolini C, Schwartz PJ, et al. The common long-QT syndrome mutation *KCNQ1/A341V* causes unusually severe clinical manifestations in patients with different ethnic backgrounds: toward a mutation-specific risk stratification. *Circulation* 2007;116:2366-2375.
377. Hohnloser SH, Klingenhoben T, Singh BN. Amiodarone-associated proarrhythmic effects. A review with special reference to torsade de pointes tachycardia. *Ann Intern Med* 1994;121:529-535.
378. Arbustini E, Narula N, Tavazzi L, Serio A, Grasso M, Favalli V, Bellazzi R, Tajik JA, Bonow RO, Fuster V, Narula J. The MOGE(S) classification of cardiomyopathy for clinicians. *J Am Coll Cardiol* 2014;64:304-318.
379. Behr ER, Roden D. Drug-induced arrhythmia: pharmacogenomic prescribing? *Eur Heart J* 2013;34:89-95.
380. Kostis JB, McCrone K, Moreyra AE, Gotzoyannis S, Aglitz NM, Natarajan N, Kuo PT. Premature ventricular complexes in the absence of identifiable heart disease. *Circulation* 1981;63:1351-1356.
381. Baman TS, Lange DC, Ilg KJ, et al. Relationship between burden of premature ventricular complexes and left ventricular function. *Heart Rhythm* 2010;7:865-869.
382. Hasdemir C, Ulucan C, Yavuzgil O, Yuksel A, Kartal Y, Simsek E, Musayev O, Kayikcioglu M, Payzin S, Kultursay H, Aydin M, Can LH. Tachycardia-induced cardiomyopathy in patients with idiopathic ventricular arrhythmias: the incidence, clinical and electrophysiologic characteristics, and the predictors. *J Cardiovasc Electrophysiol* 2011;22:663-668.
383. Yokokawa M, Kim HM, Good E, et al. Impact of QRS duration of frequent premature ventricular complexes on the development of cardiomyopathy. *Heart Rhythm* 2012;9:1460-1464.
384. McNair WP, Ku L, Taylor MR, Fain PR, Dao D, Wolfel E, Mestroni L. *SCN5A* mutation associated with dilated cardiomyopathy, conduction disorder, and arrhythmia. *Circulation* 2004;110:2163-2167.
385. Beckermann TM, McLeod K, Murday V, Potet F, George AL, Jr. Novel *SCN5A* mutation in amiodarone-responsive multifocal ventricular ectopy-associated cardiomyopathy. *Heart Rhythm* 2014;11:1446-1453.
386. Echt DS, Liebson PR, Mitchell LB, Peters RW, Obias-Manno D, Barker AH, Arensberg D, Baker A, Friedman L, Greene HL, et al. Mortality and morbidity in patients receiving encainide, flecainide, or placebo. The Cardiac Arrhythmia Suppression Trial. *N Engl J Med* 1991;324:781-788.
387. Goudeau B, Rodrigues-Lima F, Fischer D, et al. Variable pathogenic potentials of mutations located in the desmin alpha-helical domain. *Hum Mutat* 2006;27:906-913.
388. Donker DW, Volders PG, Arts T, Bekkers BC, Hofstra L, Spätjens RL, Beekman JD, Borgers M, Crijns HJ, Vos MA. End-diastolic myofiber stress and ejection strain increase with ventricular volume overload--Serial in-vivo analyses in dogs with complete atrioventricular block. *Basic Res Cardiol* 2005;100:372-382.
389. Schmidt D, del Mármol J, MacKinnon R. Mechanistic basis for low threshold mechanosensitivity in voltage-dependent K^+ channels. *Proc Natl Acad Sci U S A* 2012;109:10352-10357.
390. Van Wagoner DR. Mechanosensitive gating of atrial ATP-sensitive potassium channels. *Circ Res* 1993;72:973-983.



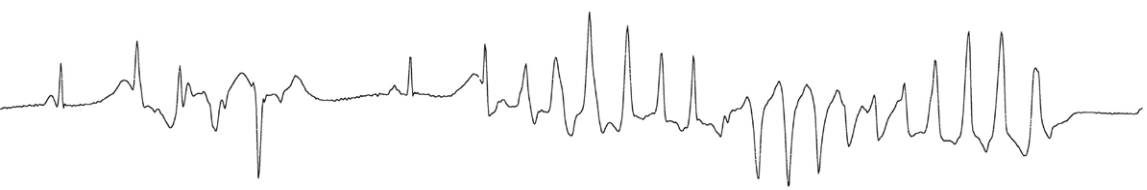
391. Morris CE, Laitko U. The mechanosensitivity of voltage-gated channels may contribute to cardiac mechano-electric feedback. In: Kohl P, Sachs F, Franz M, eds. Cardiac mechano-electric feedback and arrhythmias: from pipette to patient. Philadelphia: Elsevier; 2005:33-41.
392. Quinn TA, Jin H, Lee P, Kohl P. Mechanically induced ectopy via stretch-activated cation-nonspecific channels is caused by local tissue deformation and results in ventricular fibrillation if triggered on the repolarization wave edge (commotio cordis). *Circ Arrhythm Electrophysiol* 2017;10:e004777.
393. Stams TR, Oosterhoff P, Heijdel A, Dunnink A, Beekman JD, van der Nagel R, van Rijen HV, van der Heyden MA, Vos MA. Beat-to-beat variability in preload unmasks latent risk of torsade de pointes in anesthetized chronic atrioventricular block dogs. *Circ J* 2016;80:1336-1345.
394. Jervell A, Lange-Nielsen F. Congenital deaf-mutism, functional heart disease with prolongation of the Q-T interval and sudden death. *Am Heart J* 1957;54:59-68.
395. Schimpf R, Antzelevitch C, Haghi D, Giustetto C, Pizzuti A, Gaita F, Veltmann C, Wolpert C, Borggrefe M. Electromechanical coupling in patients with the short QT syndrome: further insights into the mechano-electrical hypothesis of the U wave. *Heart Rhythm* 2008;5:241-245.
396. Frea S, Giustetto C, Capriolo M, Scrocco C, Fornengo C, Benedetto S, Bianchi F, Pidello S, Morello M, Gaita F. New echocardiographic insights in short QT syndrome: More than a channelopathy? *Heart Rhythm* 2015;12:2096-2105.
397. Adeniran I, Hancox JC, Zhang H. In silico investigation of the short QT syndrome, using human ventricle models incorporating electromechanical coupling. *Front Physiol* 2013;4:166.
398. De Ferrari GM, Schwartz PJ. Vox clamantis in deserto. We spoke but nobody was listening: echocardiography can help risk stratification of the long-QT syndrome. *Eur Heart J* 2015;36:148-150.
399. Zile MA, Trayanova NA. Myofilament protein dynamics modulate EAD formation in human hypertrophic cardiomyopathy. *Prog Biophys Mol Biol* 2017;130:418-428.
400. Paton JF, Nalivaiko E, Boscan P, Pickering AE. Reflexly evoked coactivation of cardiac vagal and sympathetic motor outflows: observations and functional implications. *Clin Exp Pharmacol Physiol* 2006;33:1245-1250.
401. Lown B, Verrier RL. Neural activity and ventricular fibrillation. *N Engl J Med* 1976;294:1165-1170.
402. Vanoli E, De Ferrari GM, Stramba-Badiale M, Hull SS, Jr., Foreman RD, Schwartz PJ. Vagal stimulation and prevention of sudden death in conscious dogs with a healed myocardial infarction. *Circ Res* 1991;68:1471-1481.
403. van den Berg MP, Haaksma J, Veeger NJ, Wilde AA. Diurnal variation of ventricular repolarization in a large family with LQT3-Brugada syndrome characterized by nocturnal sudden death. *Heart Rhythm* 2006;3:290-295.
404. Somers VK, Dyken ME, Mark AL, Abboud FM. Sympathetic-nerve activity during sleep in normal subjects. *N Engl J Med* 1993;328:303-307.
405. Kumagai N, Ogawa M, Zhang B, Koyoshi R, Morii J, Yasuda T, Matsumoto N, Matsuo K, Saku K. Paradoxical nocturnal elevation of sympathetic tone and spontaneous ventricular fibrillation in Brugada syndrome. *J Cardiol* 2016;67:229-235.

406. Muller JE, Ludmer PL, Willich SN, Tofler GH, Aylmer G, Klangos I, Stone PH. Circadian variation in the frequency of sudden cardiac death. *Circulation* 1987;75:131-138.
407. Leenhardt A, Lucet V, Denjoy I, Grau F, Ngoc DD, Coumel P. Catecholaminergic polymorphic ventricular tachycardia in children. A 7-year follow-up of 21 patients. *Circulation* 1995;91:1512-1519.
408. Priori SG, Napolitano C, Memmi M, et al. Clinical and molecular characterization of patients with catecholaminergic polymorphic ventricular tachycardia. *Circulation* 2002;106:69-74.
409. Horner JM, Ackerman MJ. Ventricular ectopy during treadmill exercise stress testing in the evaluation of long QT syndrome. *Heart Rhythm* 2008;5:1690-1694.
410. Schwartz PJ, Billman GE, Stone HL. Autonomic mechanisms in ventricular fibrillation induced by myocardial ischemia during exercise in dogs with healed myocardial infarction. An experimental preparation for sudden cardiac death. *Circulation* 1984;69:790-800.
411. Vaseghi M, Zhou W, Shi J, Ajjola OA, Hadaya J, Shivkumar K, Mahajan A. Sympathetic innervation of the anterior left ventricular wall by the right and left stellate ganglia. *Heart Rhythm* 2012;9:1303-1309.
412. Yagishita D, Chui RW, Yamakawa K, Rajendran PS, Ajjola OA, Nakamura K, So EL, Mahajan A, Shivkumar K, Vaseghi M. Sympathetic nerve stimulation, not circulating norepinephrine, modulates T-peak to T-end interval by increasing global dispersion of repolarization. *Circ Arrhythm Electrophysiol* 2015;8:174-185.
413. Priori SG, Mantica M, Schwartz PJ. Delayed afterdepolarizations elicited in vivo by left stellate ganglion stimulation. *Circulation* 1988;78:178-185.
414. Hanich RF, Levine JH, Spear JF, Moore EN. Autonomic modulation of ventricular arrhythmia in cesium chloride-induced long QT syndrome. *Circulation* 1988;77:1149-1161.
415. Nadeau R, Lamontagne D, Cardinal R, de Champlain J, Armour JA. Coronary sinus norepinephrine concentrations during ventricular tachycardia induced by left stellate ganglion stimulation in dogs. *Can J Physiol Pharmacol* 1988;66:419-421.
416. Franz MR, Bargheer K, Rafflenbeul W, Haverich A, Lichtlen PR. Monophasic action potential mapping in human subjects with normal electrocardiograms: direct evidence for the genesis of the T wave. *Circulation* 1987;75:379-386.
417. Boukens BJ, Sylva M, de Gier-de Vries C, Remme CA, Bezzina CR, Christoffels VM, Coronel R. Reduced sodium channel function unmasks residual embryonic slow conduction in the adult right ventricular outflow tract. *Circ Res* 2013;113:137-141.
418. de Jong F, Opthof T, Wilde AA, Janse MJ, Charles R, Lamers WH, Moorman AF. Persisting zones of slow impulse conduction in developing chicken hearts. *Circ Res* 1992;71:240-250.
419. Randall WC, Armour JA, Geis WP, Lippincott DB. Regional cardiac distribution of the sympathetic nerves. *Fed Proc* 1972;31:1199-1208.
420. Haemers P, Sutherland G, Cikes M, Jakus N, Holemans P, Sipido KR, Willems R, Claus P. Further insights into blood pressure induced premature beats: Transient depolarizations are associated with fast myocardial deformation upon pressure decline. *Heart Rhythm* 2015;12:2305-2315.
421. Batra AS, Silka MJ. Mechanism of sudden cardiac arrest while swimming in a child with the prolonged QT syndrome. *J Pediatr* 2002;141:283-284.



422. Choi G, Kopplin LJ, Tester DJ, Will ML, Haglund CM, Ackerman MJ. Spectrum and frequency of cardiac channel defects in swimming-triggered arrhythmia syndromes. *Circulation* 2004;110:2119-2124.
423. Tester DJ, Medeiros-Domingo A, Will ML, Ackerman MJ. Unexplained drownings and the cardiac channelopathies: a molecular autopsy series. *Mayo Clin Proc* 2011;86:941-947.
424. Wall TS, Wasmund SL, Freedman RA, Akoum NW, Page RL, Hamdan MH. "Vasovagal" response during ventricular fibrillation: incidence and implications. *Pacing Clin Electrophysiol* 2015;38:376-382.
425. Wilde AA, Bhuiyan ZA, Crotti L, Facchini M, De Ferrari GM, Paul T, Ferrandi C, Koolbergen DR, Odero A, Schwartz PJ. Left cardiac sympathetic denervation for catecholaminergic polymorphic ventricular tachycardia. *N Engl J Med* 2008;358:2024-2029.
426. Schneider AE, Bos JM, Ackerman MJ. Effect of left cardiac sympathetic denervation on the electromechanical window in patients with either type 1 or type 2 long QT syndrome: a pilot study. *Congenit Heart Dis* 2016;11:437-443.
427. Klein T, Abdulghani M, Smith M, et al. Three-dimensional ¹²³I-meta-iodobenzylguanidine cardiac innervation maps to assess substrate and successful ablation sites for ventricular tachycardia: feasibility study for a novel paradigm of innervation imaging. *Circ Arrhythm Electrophysiol* 2015;8:583-591.
428. Rook MB, Bezzina Alshinawi C, Groenewegen WA, van Gelder IC, van Ginneken AC, Jongsma HJ, Mannens MM, Wilde AA. Human *SCN5A* gene mutations alter cardiac sodium channel kinetics and are associated with the Brugada syndrome. *Cardiovasc Res* 1999;44:507-517.
429. Probst V, Kyndt F, Potet F, Trochu JN, Mialet G, Demolombe S, Schott JJ, Baró I, Escande D, Le Marec H. Haploinsufficiency in combination with aging causes *SCN5A*-linked hereditary Lenègre disease. *J Am Coll Cardiol* 2003;41:643-652.
430. Schott JJ, Alshinawi C, Kyndt F, Probst V, Hoorntje TM, Hulsbeek M, Wilde AA, Escande D, Mannens MM, Le Marec H. Cardiac conduction defects associate with mutations in *SCN5A*. *Nat Genet* 1999;23:20-21.
431. Benson DW, Wang DW, Dymont M, Knilans TK, Fish FA, Strieper MJ, Rhodes TH, George AL, Jr. Congenital sick sinus syndrome caused by recessive mutations in the cardiac sodium channel gene (*SCN5A*). *J Clin Invest* 2003;112:1019-1028.
432. Olson TM, Michels VV, Ballew JD, Reyna SP, Karst ML, Herron KJ, Horton SC, Rodeheffer RJ, Anderson JL. Sodium channel mutations and susceptibility to heart failure and atrial fibrillation. *JAMA* 2005;293:447-454.
433. van Opstal JM, Volders PG, Crijns HJ. Provocation of silence. *Europace* 2009;11:385-387.
434. Liu M, Yang KC, Dudley SC, Jr. Cardiac sodium channel mutations: why so many phenotypes? *Nat Rev Cardiol* 2014;11:607-615.
435. Abriel H. Cardiac sodium channel Na_v1.5 and interacting proteins: physiology and pathophysiology. *J Mol Cell Cardiol* 2010;48:2-11.
436. Herren AW, Bers DM, Grandi E. Post-translational modifications of the cardiac Na channel: contribution of CaMKII-dependent phosphorylation to acquired arrhythmias. *Am J Physiol Heart Circ Physiol* 2013;305:H431-H445.

437. Daimi H, Lozano-Velasco E, Haj Khelil A, Chibani JB, Barana A, Amoros I, Gonzalez de la Fuente M, Caballero R, Aranega A, Franco D. Regulation of *SCN5A* by microRNAs: miR-219 modulates *SCN5A* transcript expression and the effects of flecainide intoxication in mice. *Heart Rhythm* 2015;12:1333-1342.
438. Gosselin-Badaroudine P, Keller DI, Huang H, Pouliot V, Chatelier A, Osswald S, Brink M, Chahine M. A proton leak current through the cardiac sodium channel is linked to mixed arrhythmia and the dilated cardiomyopathy phenotype. *PLoS One* 2012;7:e38331.
439. Moreau A, Gosselin-Badaroudine P, Boutjdir M, Chahine M. Mutations in the voltage sensors of domains I and II of $Na_v1.5$ that are associated with arrhythmias and dilated cardiomyopathy generate gating pore currents. *Front Pharmacol* 2015;6:301.
440. Arnolds DE, Liu F, Fahrenbach JP, Kim GH, Schillinger KJ, Smemo S, McNally EM, Nobrega MA, Patel VV, Moskowitz IP. *TBX5* drives *Scn5a* expression to regulate cardiac conduction system function. *J Clin Invest* 2012;122:2509-2518.
441. Yang B, Lu Y, Wang Z. Control of cardiac excitability by microRNAs. *Cardiovasc Res* 2008;79:571-580.
442. Luo X, Zhang H, Xiao J, Wang Z. Regulation of human cardiac ion channel genes by microRNAs: theoretical perspective and pathophysiological implications. *Cell Physiol Biochem* 2010;25:571-586.
443. Altrocci C, Spätjens RLHMG, Sutanto H, ter Bekke RMA, Seyen S, Heijman J, Moreno C, Volders PGA. I_{Na} loss-of-function by compound variants in *SCN5A* from a large founder population with excess sudden cardiac death. *Biophys J* 2018;114:635a.
444. Barajas-Martinez HM, Hu D, Cordeiro JM, Wu Y, Kovacs RJ, Meltser H, Kui H, Elena B, Brugada R, Antzelevitch C, Dumaine R. Lidocaine-induced Brugada syndrome phenotype linked to a novel double mutation in the cardiac sodium channel. *Circ Res* 2008;103:396-404.
445. van den Berg MP, Wilde AA, Viersma TJW, Brouwer J, Haaksma J, van der Hout AH, Stolte-Dijkstra I, Bezzina TCR, van Langen IM, Beaufort-Krol GC, Cornel JH, Crijns HJ. Possible bradycardic mode of death and successful pacemaker treatment in a large family with features of long QT syndrome type 3 and Brugada syndrome. *J Cardiovasc Electrophysiol* 2001;12:630-636.
446. Makkar RR, Fromm BS, Steinman RT, Meissner MD, Lehmann MH. Female gender as a risk factor for torsades de pointes associated with cardiovascular drugs. *JAMA* 1993;270:2590-2597.
447. Pham TV, Robinson RB, Danilo P, Jr., Rosen MR. Effects of gonadal steroids on gender-related differences in transmural dispersion of L-type calcium current. *Cardiovasc Res* 2002;53:752-762.
448. Pham TV, Rosen MR. Sex, hormones, and repolarization. *Cardiovasc Res* 2002;53:740-751.
449. Genome of the Netherlands C. Whole-genome sequence variation, population structure and demographic history of the Dutch population. *Nat Genet* 2014;46:818-825.
450. Ledford H. CRISPR, the disruptor. *Nature* 2015;522:20-24.
451. Yang P, Kanki H, Drolet B, et al. Allelic variants in long-QT disease genes in patients with drug-associated torsades de pointes. *Circulation* 2002;105:1943-1948.



452. Niemeijer MN, van den Berg ME, Eijgelsheim M, Rijnbeek PR, Stricker BH. Pharmacogenetics of drug-induced QT interval prolongation: an update. *Drug Saf* 2015;38:855-867.
453. Wellens HJ, Lindemans FW, Houben RP, Gorgels AP, Volders PGA, Ter Bekke RMA, Crijns HJ. Improving survival after out-of-hospital cardiac arrest requires new tools. *Eur Heart J* 2016;37:1499-1503.
454. Jin H, Iribe G, Naruse K. Effects of bepridil on stretch-activated BK_{Ca} channels and stretch-induced extrasystoles in isolated chick hearts. *Physiol Res* 2017;66:459-465.
455. Vaseghi M, Gima J, Kanaan C, Ajijola OA, Marmureanu A, Mahajan A, Shivkumar K. Cardiac sympathetic denervation in patients with refractory ventricular arrhythmias or electrical storm: intermediate and long-term follow-up. *Heart Rhythm* 2014;11:360-366.
456. Bradfield JS, Vaseghi M, Shivkumar K. Renal denervation for refractory ventricular arrhythmias. *Trends Cardiovasc Med* 2014;24:206-213.
457. Remo BF, Preminger M, Bradfield J, Mittal S, Boyle N, Gupta A, Shivkumar K, Steinberg JS, Dickfeld T. Safety and efficacy of renal denervation as a novel treatment of ventricular tachycardia storm in patients with cardiomyopathy. *Heart Rhythm* 2014;11:541-546.
458. Evranos B, Canpolat U, Kocyigit D, Coteli C, Yorgun H, Aytemir K. Role of adjuvant renal sympathetic denervation in the treatment of ventricular arrhythmias. *Am J Cardiol* 2016;118:1207-1210.
459. Godolphin W. Shared decision-making. *Healthc Q* 2009;12:e186-190.



GENEALOGICAL SOURCES

Genealogist A.S.M. Patelski constructed detailed ancestors charts of all genotyped *SCN5A*-p.(Phe1617del) indexes, aiming to identify the designated Worm study founder couple by the identification of common ancestors. Per family group 63-778 ancestors were identified. Subsequently, Patelski generated descendant charts to complete the pedigree as much as possible.

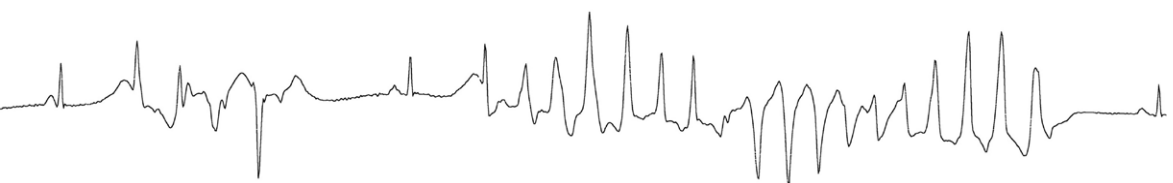
All genealogical data are edited and stored in the freely available program Aldfaer (www.aldfaer.net, version 6.2). Patelski's private file is not accessible to the general public and contains amply 10.000 Worm study related-person cards. A person cards encloses the index' name, date and place of birth, date of death including the similar information of their parents and offspring. The majority of the descendants are legitimate with few documented natural descents that have been acknowledged by the biological father. The data file mostly contains genealogical information on deceased persons. For the living individuals we relied on information provided by the index or their family members. When available, official documentation like a marriage license served to verify the verbally obtained genealogical information. Below, one can appreciate the consulted genealogical sources of the Netherlands, Belgium and Germany including consulted archival institutions, websites, and books. All documented relationships and lineages of descent have been confirmed from original sources and can be verified. In case of the slightest uncertainty, the presumed relationship was discarded.

CONSULTED SOURCES

THE NETHERLANDS

Period from ± 1550 to ± 1800

- Baptismal, marriage, and burial registers of Roman Catholic parishes, Protestant churches and other documents from parishes or community archives.
- Judicial archives of aldermen, farmsteads and jurisdictional files from Limburg Centre of Regional History (RHCL) in Maastricht and Rijckheyt in Heerlen.
- Archives of the Landen van Overmaas (RHCL, 01.075 LvO).
- Archives of the feudatory of the bishop of Köln (Keurkeulse Mankamer) in Heerlen (RHCL, 01.075 LvO).
- Archives of the feudatory of Dahlem (RHCL, 01.075 LvO).
- Archives of the feudatory of 's-Hertogenrade (RHCL, 01.075 LvO).
- Archives of the feudatory of Valkenburg (RHCL, 01.075 LvO).
- Archives of the "Vrije Rijksheerlijkheid" Eijs (Eys) (RHCL, 01.195).
- Archives of the "Vrije Rijksheerlijkheid" Wittem (RHCL, 01.194).
- Archives of the "Rijksheerlijkheid" Wijlre (RHCL, 01.192).
- Notarial and surveyor archives in the province Limburg, also beyond 1800 (RHCL).
- Monastery archives of Hoog-Cruts (RHCL, 14.D057), Sint-Gerlach (RHCL, 14.D003), abbey of Kloosterrade (Rolduc) (RHCL, 14.D004).



- Archive of the first Roman Catholic diocese of Roermond (RHCL, 14.A002A).
- French archive (RHCL, 03.01).

Period from ± 1795 to ± 1967

- Birth records and certificates (from ± 1795 to ± 1917), marriage records and certificates, including marital attachments (from ± 1795 to ± 1942) and death records and certificates (from ± 1795 to ± 1967) of the civil registry of the municipalities of Amby (± 1795 to 1970), Amstenrade, Bemelen, Berg en Terblijt, Bingelrade, Bocholtz, Borgharen (± 1795 to 1970), Bunde, Breust (± 1795 to 1828), Brunssum, Cadier (± 1795 to 1828), Cadier en Keer (from 1828), Eyselshoven, Gulpen, Itteren, (± 1795-1970), Jabeek, Heer, Heerlen, Hoensbroek, Horn, Houthem (± 1795 to 1940), Hulsberg, Kerkrade, Klimmen, Maastricht, Margraten, Meerssen, Merkelbeek, Mesch (± 1795 to 1942), Mheer, Nieuwenhagen, Noorbeek, Nuth, Oost (± 1795 to 1828), Oud-Valkenburg (± 1795 to 1940), Oud-Vroenhoven (± 1795 to 1919), Rimborg (± 1795 to 1817), Nederlands Rimborg (1817 to 1886), Roermond, Rijckholt (± 1795 to 1942), Schaesberg, Schin op Geul (± 1795 to 1940), Schinnen, Schinveld, Schimmert, Sint-Pieter (± 1795 to 1919), Simpelveld, Sittard, Slenaken, Strucht (± 1795 to 1878), Ubach over Worms, Ulestraten, Vaals, Vaesrade (± 1795 to 1821), Valkenburg (± 1795 to 1941), Valkenburg-Houthem (1941 to 1980), Venlo, Venray, Voerendaal, Wittem, Wijlre, Wijnandsrade.

Period from 1818 to 1920

- Archive Memories van Successie.

Period from 1850 to 1920

- Population registers of several municipalities.

Period from 1920 to 1940

- Family cards of relevant municipalities.

Period from 1940 to 1994

- Person cards of deceased individuals from the Central Bureau of Genealogy (CBG).

Period from 1995 to 2016

- Extracts from the municipal administration of the CBG (only from deceased individuals).

Family announcements from Limburg newspapers, like “Het Limburgsch Dagblad” (Heerlen), “Dagblad de Limburger” (Maastricht), and the “Limburger koerier” which can be consulted on www.delpher.nl.

Family announcements from archival institutions, online accessible.

Genealogical documents from archival institutions, local history associations, and private persons.

Interviews with indexes and their relatives.

BELGIUM

Period from ± 1550 to ± 1800

- Baptismal, marriage, and burial registers of Roman Catholic parishes, Protestant churches and other documents from parishes or community archives.
- Judicial archives of aldermen, farmsteads and jurisdictional files.

Period after ± 1800

- Records of the civil and registries of the municipalities of Grivegnée, Hombourg, Liège (Luik), Lixhe, Poucet, Vaux-sous-Chèvremont.

GERMANY

Period from ± 1500 to ± 1795

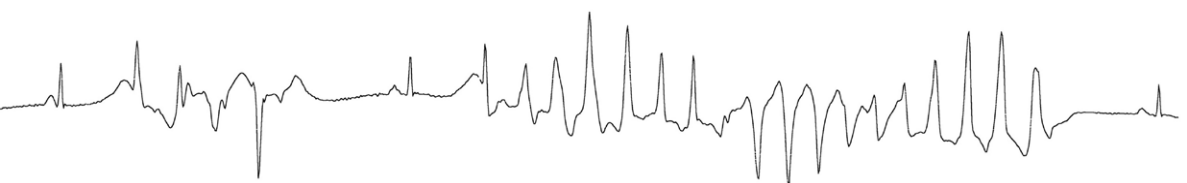
- Jülicher Gerichte, Amt Wilhelmstein (www.archiv.nrw.de).
- Archive Paffendorf (www.archiv.nrw.de).
- City archive Aachen, department of handwriting.
- Baptismal, marriage, and burial registers of Roman Catholic parishes, Protestant churches and other documents from parishes or community archives of Afden, Alsdorf, Bardenberg, Frelenberg, Herzogenrath, Marienberg, Merkstein, Übach, Weisweiler.

Period from ± 1670 to ± 1800

- Records of the civil and registries of the municipalities of Aachen, Bardenberg, Eschweiler, Gescher, Gladbeck, Kohlscheid, Herzogenrath, Merkstein, Preussisch Rimbürg (1817 to 1911), Stolberg.

CONSULTED ARCHIVAL INSTITUTIONS**THE NETHERLANDS**

- Limburg Centre of Regional History in Maastricht, www.rhcl.nl
- Social Historic Centre Limburg in Maastricht, www.shclimburg.nl
- Rijckheyt in Heerlen, www.rijckheyt.nl
- State archives of Limburg in Maastricht (situated in the RHCL).
- Community archive Maastricht (situated in the RHCL).
- Community archive Kerkrade, www.kerkrade.nl/de_stad_kerkrade/kerkrade_toen_en_nu/gemeentearchief
- Community archive Sittard-Geleen, www.sittard-geleen.nl/Bestuur/overig/Archief en www.dedomijnen.nl/collecties
- Community archive Roermond, www.roermond.nl/Gemeentearchief
- O.C.G.L. Landgraaf (local history association with euregional documents), www.heemkundelandgraaf.nl



BELGIUM

- State archives of Limburg in Hasselt, www.arch.be/index.php?1=nl&m=praktische-info&r=onze-leeszalen&d=hasselt
- Archives of État de Liège, www.arch.be/index.php?1=nl&m=praktische-info&r=onze-leeszalen&d=luik
- City archive in Tongeren, www.stadsarchieftongeren.be
- Algemeen Rijksarchief Brussel (ARA, “general state archive Brussel”), www.arch.be/index.php?1=nl&m=praktische-info&r=onze-leeszalen&d=ara

GERMANY

- City archive Aachen.
- www.aachen.de/de/kultur_freizeit/kultur/stadtarchiv/index.html
- Civil registry Nordrhein Westfalen, department Rheinland, Duisburg, www.archiv.nrw.de
- Community archive Gladbeck.

CONSULTED WEBSITES

www.rhcl.nl	Limburg Centre of Regional History.
www.wiewaswie.nl	portal website from Dutch civil registry containing general certificates.
www.zoekakten.nl	portal website from Dutch civil registry containing the original certificates of the civil registry and church records.
www.familysearch.com	website of Mormons with digitalized archives of the civil registry.
www.graftombe.nl	website containing descriptions and photos of graves.
www.cbg.nl	Central Bureau of Genealogy.
www.delpher.nl	
www.familienbuch-euregio.eu/	
nl.geneanet.org/fonds/individus/	

CONSULTED BOOKS

Citoyens en zielen in Kerkrade in 1796, by L. Augustus, H. Latten, L. Nijsten-Höfte, Kerkrade 1996, part 3 of the “Reeks Fontes Rodenses”.

Les actes du vicariat général de Liège au XVIIIe siècle. I Dispenses matrimoniales 1760-1769, item tome II 1770-1779, item tome III 1780-1794, by André Deblon, Liège 2001.

“De inwoners van Simpelveld en Bocholtz in 1694” by A.S.M. Patelski, in *Historische en heemkundige studies in en rond het Geuldal*, Jaarboek 1994, Valkenburg aan de Geul, 1994, p.55-72.

Das Handbuch des Bardenberger Notars Paul Sevenich. Erste vollständige Ausgabe mit Einleitung und Erläuterungen herausgegeben von Karl Schlebusch, Aachen, 2000.

Die Kölner Generalvikariatsprotokolle als Personengeschichtliche Quelle, Band I (in 2 Halbbänden), Aus der Zeit vor 1700 by Hermann Deitmer S.J., Köln 1970; *Item Band XII, Nichtkleriker in den Protokollen von 1786-1790*, Johannes Ströber and Hans-Joachim Otten, Köln, 2008.

Familienbuch der katholische Pfarrei Sankt Heinrich Horbach 1804-1899 by Käthe Wimmer, Köln, 2007.

Familienbuch Sankt Laurentius Laurensberg [Stadt Aachen] by Willi Dovern, 3 banden, Frankfurt am Main, 2000.

Das Pfarrarchiv St. Mariae Himmelfahrt Herzogenrath, by Louis Augustus, Grete Esser-Plum, Wolf D. Penning, Herzogenrath, 2008.

Inventaris archief Kasteel Haag, Inleiding, Regesten, Zegels, Register, by Rien van den Brand, Stefan Frankewitz, Venray, 2008. Publication nr 20 of the Stichting Historie Peel-Maas-Niersgebied.

Inventaris van de archieven en de handschriften der abdij Kloosterrade by J.A.K. Haas, Maastricht, 1986, part 36 of the inventories of the Rijksarchief Limburg.

Inventaris van de archieven van het klooster Hoog-Cruts te Noorbeek/Slenaken 1512-1798 (1803) by R.M. de la Haye, Maastricht, 1987, part 39 of the inventories of the Rijksarchief Limburg.

Inventaris van de archieven van de heerlijkheid en de schepenbank Wijlre 1464-1796 (1816) by R.M. de la Haye, Maastricht, 1993, part 49 of the inventories of the Rijksarchief Limburg.

Cunegondes ontvoering. Een geschiedenis van religieuze strijd in de tijd van de verlichting (Original title: Cunegonde's kidnapping. A story of religious conflict in the age of Enlightenment) by Benjamin J. Kaplan (translation by Roelof Posthuma), Amsterdam, 2014.

Die Rimburg. Geschichte der Burg, der ehemaligen Herrschaft bezw. freien Reichsherrschaft und der Gemeinde Rimburg by H. Hanssen, Aachen, 1912.



“Het Land van Rode: zijn naam, zijn territorium en zijn gebieders” by Lei Heijenrath, in *Facetten uit de geschiedenis van het Land van Rode*, Heerlen, 2017, part 11 of the Historische Reeks Parkstad, p.11-39.

“Van ‘s-Hertogenrade naar Limbourg sur Vesde: het tracé van de middeleeuwse Hertogsweg door Zuid-Limburg” by Lei Heijenrath, in *Facetten uit de geschiedenis van het Land van Rode*, Heerlen, 2017, part 11 of the Historische Reeks Parkstad, p.97-117.

“De Staten van het Oostenrijkse Land van Rode in de 18^e eeuw in vergadering bijeen” by Lei Heijenrath, in *Facetten uit de geschiedenis van het Land van Rode*, Heerlen, 2017, part 11 of the Historische Reeks Parkstad, p.160-212.

“Macht en onmacht in de processen tegen de bokkenrijders, Brussel en de justitie in de (Oostenrijkse) Landen van ‘s-Hertogenrade en Valkenburg” by Mathieu Huijnen, Hub van Wersch, in *Facetten uit de geschiedenis van het Land van Rode*, Heerlen, 2017, part 11 of the Historische Reeks Parkstad, p.40-95.

De abdij Kloosterrade – Rolduc (1104-1830), by Joep Offermans, Rotterdam, 2004.

“Zes eeuwen personae, pastoors, kapelaans en rectors in de H. Laurentiusparochie te Voerendaal” by A.S.M. Patelski, in *De goede herder, een geschiedenis van de parochie St. Laurentius te Voerendaal 1049-1999*, Heerlen, 1999, part 1 of the Historische Reeks Parkstad Limburg.

Licht op het zonneleen Gronsveld. Ontwikkeling en instellingen van het rijksonmiddellijke graafschap Gronsveld, elfde eeuw tot circa 1795, by Th.J. van Rensch, Maastricht, 2017.

Handboek voor de geschiedenis van Limburg, by P.J.H. Ubachs, Hilversum, 2000.

Eygelshoven gedurende acht eeuwen, 1131-1931. Gedenkboek uitgegeven door het gemeentebestuur bij de viering van het achthonderd jarig bestaan van Eygelshoven, by J.M. van de Venne, Eygelshoven, 1931.

Wissenschaftliche Genealogie, Eine Einführung in die wichtigsten Grundprobleme, by Otto Forst de Battaglia, Bern, 1948.

Limburgse voorouders. Handleiding voor genealogisch onderzoek in Limburg, by Régis de La Haye, Maastricht, 2005.

Herten in het Woud. Genealogie van de familie de La Haye, by Régis de La Haye, Jo Hoen, Geleen/Beek, 1996-2015, 15 parts.

“De familie Kicken uit Wijle in de 17e en 18e eeuw” by A.S.M. Patelski in *Historische en heemkundige studies in en rond het Geuldal, Jaarboek*, 1992, p.7-64.

“Merckelbach” in *Nederland's Patriciaat, Genealogieën van bekende geslachten*, 's-Gravenhage, 2014, p.201-224.

“Genealogie van de familie Merckelbach uit het Land van Herle in de 17^e en 18^e eeuw” by A.S.M. Patelski in *Zestig jaar vorsen in de geschiedenis van Parkstad Limburg*, Heerlen, 2005, p.182-284.

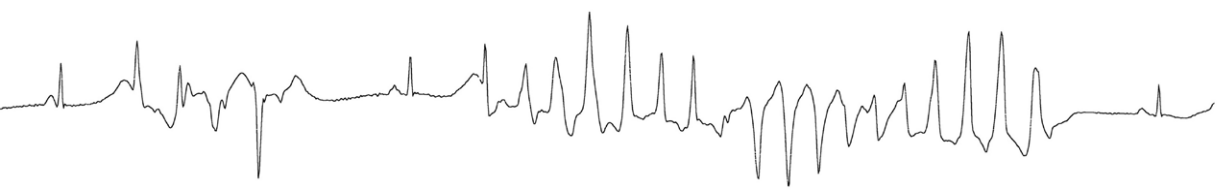
Limburgse verwantschappen. Bijzondere familierelaties gebaseerd op de kwartierstaat Van der Cruijs-Gilissen, by A.S.M. Patelski, Marie-Anne van der Cruijs, Gronsveld, Rotterdam, 2012.

“Limburgse nazaten van Karel de Grote”, by A.S.M. Patelski, in *Limburgs Tijdschrift voor Genealogie* 2014 (42):103-132.

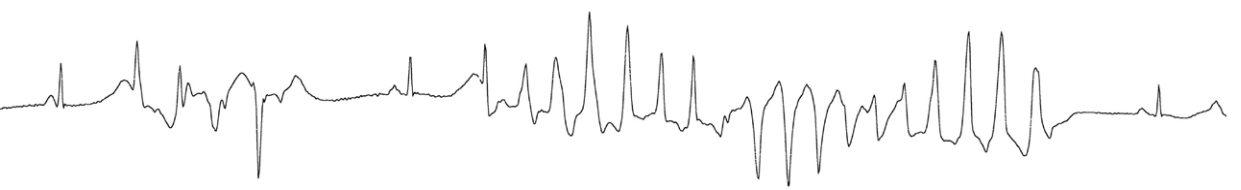


LIST OF ABBREVIATIONS

AED	Automated external defibrillator
APD	Action-potential duration
AUC	Area under the curve
BrS	Brugada syndrome
CaMKII	Ca ²⁺ /Calmodulin-kinase II
CCD	Cardiac conduction disease
CHO	Chinese hamster ovary
CM	Cardiomyocyte
CPVT	Catecholaminergic polymorphic ventricular tachycardia
DAD	Delayed afterdepolarization
EAD	Early afterdepolarization
ERS	Early-repolarization syndrome
EMW	Electromechanical window
FOXO1	Forkhead box O 1
I _{CaL}	L-type calcium current
I _{Cl(Ca)}	Ca ²⁺ -activated Cl ⁻ current
ICD	Implantable cardioverter defibrillator
I _{K1}	Inward rectifier potassium current
I _{Kr}	Rapidly-activating delayed-rectifier potassium current
I _{Ks}	Slowly-activating delayed-rectifier potassium current
I _{Na}	Voltage-dependent cardiac sodium current
I _{Na-Ca}	Sodium-calcium exchanger current
I _{Na,L}	Late component of I _{Na}
iPSC	Induced pluripotent stem cells
I _{ti}	Transient inward current
I _{to}	Transient outward current
JLNS	Jervell and Lange-Nielsen syndrome
LSGS	Left-stellate ganglion stimulation
LTV	Long-term variability
LV	Left ventricle
LVEF	Left-ventricular ejection fraction
LVP	Left-ventricular pressure
LQTS	Long-QT syndrome
LCSD	Left cardiac sympathetic denervation
MAP	Monophasic action potential
MEPPC	Multifocal ectopic Purkinje-related premature contractions
Na _v 1.5	Pore-forming alpha subunit of the cardiac sodium channel
NF-κB	Nuclear factor-κB
nNOS	Neural nitric oxide synthase
NRI	Net reclassification index
NSVT	Non-sustained VT
PKA	Protein-kinase A
PVC	Premature ventricular contraction
QAoC	Q-onset to aortic-valve closure
ROC	Receiver-operating characteristic
RSGS	Right-stellate ganglion stimulation



RV	Right ventricle
RVP	Right-ventricular pressure
RyR	Ryanodine receptor
SAC	Stretch-activated channel
SCD	Sudden cardiac death
SNP	Single nucleotide polymorphism
SR	Sarcoplasmic reticulum
SQTS	Short-QT syndrome
STV	Short-term variability
TBX5	T-box transcription factor 5
TdP	Torsades de pointes
TDI	Tissue-Doppler imaging
TRPM4	Transient receptor potential M4 channel
VF	Ventricular fibrillation
VT	Ventricular tachycardia
VUS	Variant of uncertain significance



ACKNOWLEDGEMENTS/DANKWOORD

Mijn allereerste dankbetuiging gaat uit naar **Paul Volders**: mijn copromotor, die tijdens mijn proefschrift 'promoveerde' tot promotor. Het is als de dag van gisteren dat ik jouw kamer binnenliep met de intentie mij te bekwamen in wetenschappelijk onderzoek. De innovatieve mix van elektromechanische mechanismen van kameraritmieën in het erfelijk belaste hart sprak mij direct aan; enerzijds vanwege de translationele aspecten, anderzijds triggerde dit onderwerp een passioneel gevoel van mysterie. Tegelijkertijd lag de wetenschappelijke lat van het Volders lab hoog. Paul, je beschikt over de uitzonderlijke gave om mensen op subtiele wijze te inspireren en te motiveren. Jouw parate kennis over uiteenlopende onderwerpen aangaande de Klinische Cardiologie/Elektrofysiologie, de Cellulaire Elektrofysiologie maar ook computermodellen is zeer indrukwekkend. Beter en sneller dan elke online Pubmed zoekopdracht! Menig manuscript werd naar een hoger niveau getild door jouw scherpzinnige gebruik van de Engelse taal en gevoel voor tekstbouw. Deze fijngevoeligheid ging, tot frustratie van velen, vaak gepaard met een niet te behoorlijke tijdsinvestering, maar, toegegeven, het eindresultaat was het wachten ruimschoots waard. Ik ben je zeer erkentelijk voor de visionaire rol die je vervulde tijdens mijn PhD- en carrièreplanning: *"The sky is the limit!"*. Je bent niet alleen een visionair maar ook een inspirator voor mij geweest. Ten slotte, denk ik graag terug aan de vele momenten, soms omlijst met een hapje en een drankje, waarop we vurig een veelvoud aan wetenschappelijke onderwerpen bediscussieerden die de basis vormden van de huidige manuscripten (**Figuur** PhD outline).

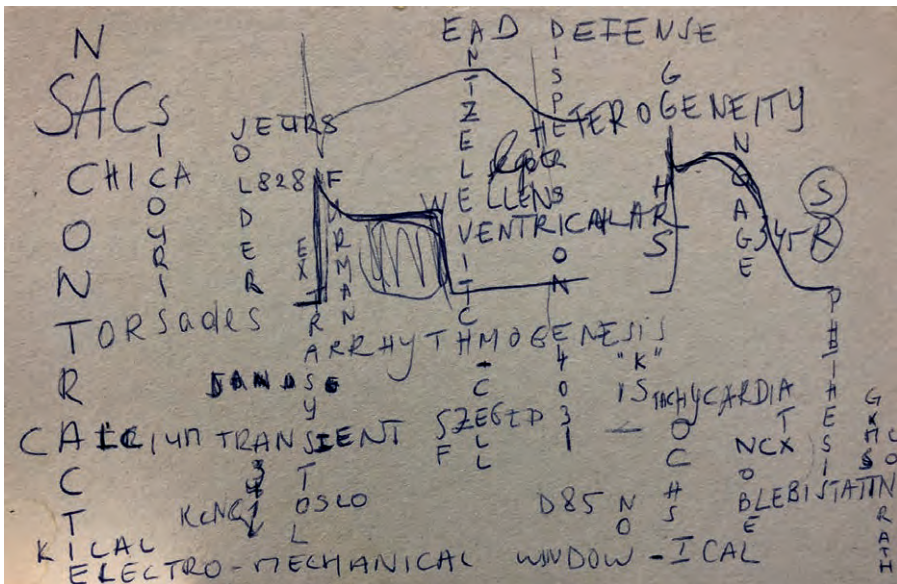
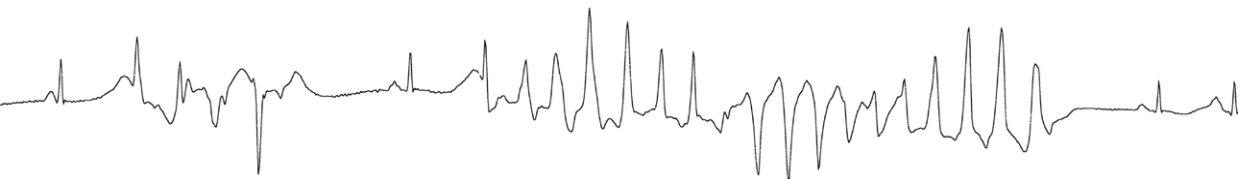


Figure PhD outline.



Natuurlijk ben ik veel dank verschuldigd aan het afdelingshoofd van de Cardiologie van het MUMC+, **Harry Crijns**, die in mij geloofde en mij onderzoekstijd toekende in tijden van hoge klinische werkdruk. Zeker ook ben ik **Hein Wellens**, de founding father van de Klinische Elektrofysiologie, zeer erkentelijk voor zijn voelbare steun, zijn visionaire inzichten en zijn mentorrol. Het is een enorme eer in zijn wetenschappelijke voetsporen te mogen treden door het onderwerp van kamerritmestoornissen/plotse hartsilstand verder uit te diepen. Einstein's uitspraak is van grote toepassing hier: "If I have seen further, it is by standing on the shoulders of Giants."

A special word of gratitude to all the highly esteemed members of the judgment committee: **Harry Crijns**, **Hein Wellens**, **Peter Schwartz**, **Connie Bezzina**, and **Frits Prinzen**. **Peter Schwartz**, thank you for the fruitful and stimulating discussions on the long-QT syndrome and the role of the autonomic nervous system in ventricular arrhythmogenesis. You are a genuine founding father of genetic cardiology. Your manuscripts are always a joy for the mind: a true language virtuoso! **Connie Bezzina**, I have profound respect for your revolutionary scientific contributions to the field of Cardiogenetics. Your work on topics like *SCN5A* and sudden arrhythmic death are the basis of many scientific endeavors that come to our table. Thank you for being such an inspiring female role model. The judgment committee would not be complete without **Frits Prinzen** with his impressive track record on electromechanics of the heart and cardiac pacing. I am very fortunate that such esteemed scientists have judged my scientific work.

Gedegen wetenschappelijk onderzoek is geen individuele maar een teamsport, waarbij door gemeenschappelijke inzet een hoger niveau kan worden bereikt. In ieder team is er een onmisbare centrale middenvelder of spelverdeler: een zeer warm dank-je-wel voor **Roel Spätjens**. Dé steun en toeverlaat van ieder patchclamp experiment: het lukte je zelfs om mij een natriumstroom te laten opnemen. Dé Eerste Hulp bij figuurreanimaties: van het opkuisen van 'vervuilde' ECG tracings tot de puntjes op de i bij figuuroopmaak en -verfraaiing. Dit alles is omlijst door vriendelijkheid, bescheidenheid en een flinke dosis humor. Diech bis de onmisbare liem vaan 't team! Maar evenzeer ben ik **Sandrine Seyen** een welgemeend dankwoord verschuldigd. Natuurlijk was jouw inzet bij de experimenten van onschatbare waarde, maar nog meer heb ik onze privégesprekken altijd gekoesterd.

Being part an international research team has been a stimulating and unforgettable experience. To all present and previous members of the Volders' lab, also known as the "work/vacation/vlaai" crew: **Cristina Altrocchi**, **Gudrun Antoons**, **Beatrice Badone**, **Mylène Champs**, **Michael Clerx**, **Matthijs Cluitmans**, **Miren David**, **Jordi Heijman**, **Daniel Johnson**, **Monique de Jong**, **Pieter Koopman**, **Enno de Lange**, **Gabriele Menini**, **Annerie Moers**, **Cristina Moreno**, **Bianca van Rees**, and **Job Stoks**. My deepest gratitude for sharing your ideas, thoughts, comments, vlaais, and funny-app remarks. It was an honor to have been part of this warm and respectful team.

A special thanks goes out to my paranymph, **Emilio Vanoli**, who was always happy and enthusiastic to join our experiments either by Moto Guzzi or plane. Your enthusiasm and

knowledge was infatuating to me. With warm feelings I remember our vivid discussions on many topics like the autonomic nervous system, electromechanics, risottos, pastas and Armani. “Rocky Bilbao”, thank you for being a friend.

Mijn andere paranimf, **Claudia Volders**, mijn artistieke evenknie, wat hebben we niet allemaal beleefd samen: van grafgraven tot het Pintje Project! Het is heerlijk voor een wetenschapper om te kunnen ontsnappen in de kunstwereld met haar onbegrensde mogelijkheden en tomeloze fantasie. Dank je dat je mijn ogen hebt geopend. Ik zie erg uit naar onze volgende uitdaging!

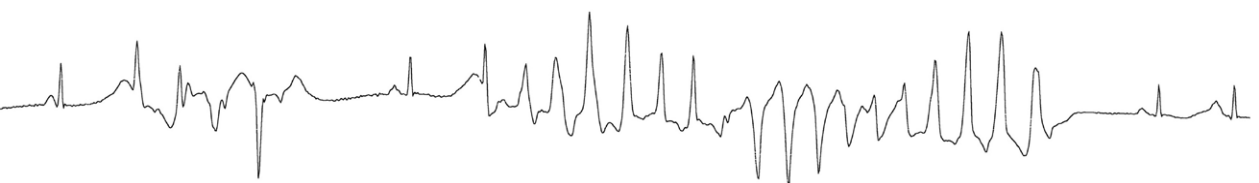
A heartfelt takk takk to my Norwegian collaborators and friends **Kristina Haugaa** and **Thor Edvardsen** for the fruitful collaborations and warm welcomes in Oslo. But also elsewhere at the globe I consistently enjoyed our get-togethers where work and leisure were always in the right balance, except when chardonnay was served. Johan Cruijff (European football player of the 20st century, 1947-2016) said once: “Als je ergens niet bent, ben je óf te vroeg óf te laat”, translated as “If you aren’t here, you either were too early or too late”. I look forward to extend our collaborations.

Het toegewijde Worm-onderzoeksteam verdient uiteraard een speciaal dankwoord: **Marije Hoos, Simone Schoonbroodt, Pascal van Borren, Tim Jacobs, Paula Helderman-van den Enden, Arthur van de Wijngaard, Vera Hovers, Funs Patelski, Aaron Isaacs, Andrei Barysenka, Anika Witten** en **Monika Stoll**. Zonder jullie inzet en passie was de Worm enkel een onbekend riviertje aan de grens tussen Nederland en Duitsland gebleven. **Funs**, jouw passie voor genealogie en geschiedenis werkt aanstekelijk: ik had nooit gedacht dat ik nog eens foto’s van grafzerken zou maken! Furthermore, I am very grateful for the collaboration with **Aaron Isaacs, Andrei Barysenka, Anika Witten** and **Monika Stoll**. You have the power to make hardcore statistics and genetics understandable to a cardiologist. Ook wil ik de andere collega’s van de Klinische Genetica bedanken voor onze vruchtbare en stimulerende samenwerking: **Ingrid Krapels, Els Vanhoutte, Lieve Claes, Bianca van den Bosch** en **Aimée Paulussen**. Natuurlijk wil ik ook alle **Worm-Studie-patiënten** bedanken voor het in mij gestelde vertrouwen.

Special thanks to the *Preclinical Development & Safety* team at *Janssen Pharmaceutica NV* in Beerse, in particular **David Gallacher, Henk van der Linde, Deborah Dhuyvetter** and **Bruno Van Deuren**, for high-level discussions on TdP induction and EMW characteristics. **Henk**, thank you for your warm support in Szeged during my first battle with the premier-league players. BMW cars will remain EMW cars. Een Mooi Weekend: EMW!

Antonio Zaza, I appreciate the stimulating discussions on cellular mechanisms of arrhythmias that we had, including the cardiac impact of autonomic-tone variations. Thank you for being an inspiring teacher (besides professional slide acrobat and best traditional “Dutch Milk Maid” look-a-like)!

Michael Ackerman, thank you for our highly appreciated collaboration. Looking forward to extend these activities.



A high level of excellence, which is achieved through intense national collaborations, characterizes the Dutch Cardiogenetic community. The Worm Study has benefitted substantially from such collaboration within the CVON-PREDICT consortium. **Arthur Wilde, Connie Bezzina, Toon van Veen, Hanno Tan, Marc Vos, Paul Volders, Maarten van de Berg, Jan Jongbloed, and Peter van Tintelen**, thank you all for your support, valuable discussions and contributions.

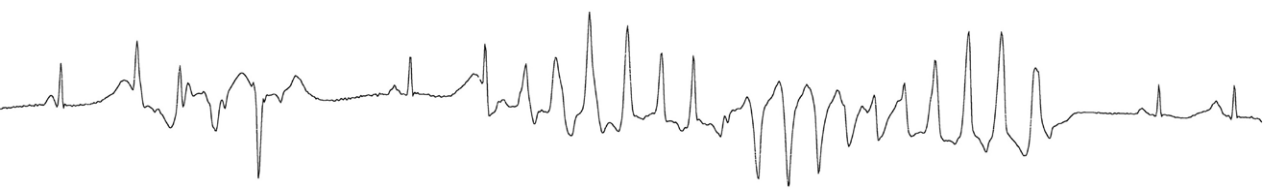
Natuurlijk ook een warm dankwoord voor mijn collega's van de Divisie Elektrofysiologie **Justin Luermans, Laurent Pison, Carl Timmermans, Randy Manusama, Kevin Vernooy, Trang Dinh** en **Ton Gorgels**. Onze samenwerking stimuleert mij iedere dag om te streven naar excellentie. Bedankt voor jullie steun in de afgelopen jaren. Ook wil ik mijn dank uitspreken aan alle EFO/PM technici en laboranten **Alexander Laurensen, John Nakken, Ruud Duysings, Luuk Debie, Niky Claessens, Michel Janssen, Marjolein Dijcks, Dorien Leenders, Irma Bartholomeus, Sylvia Janssen, Thieu Verstappen, Xavier Smits, Marloes Smits** en **Mariska Frohn-Merken**, maar ook alle andere zeer gewaardeerde collega's van de omloopverpleegkundigen tot **Willy Rempelberg** en **Netty Claessens**. Bedankt voor jullie steun en humor tijdens deze periode. Met een lach en een traan werd menige procedure succesvol gedaan. Ik ben trots op ons team!

Ik ben ook dank verschuldigd aan mijn overige collega's binnen de afdeling Cardiologie. In het bijzonder mijn kamergenoten **Trang Dinh** en **Petra Kuijpers. Petra**, hartelijk dank voor je waardevolle tips and trics om een PhD tot een goed einde te brengen.

Uiteraard mag een groot dank-je-wel naar de Health Foundation Limburg niet ontbreken metname **Ellen van de Ven, Sanne Voorzee, Cecile Giesen, Babette Frank** en **Maggie Kooman**. Dankzij hun tomeloze inzet tijdens tal van evenementen waaronder het jaarlijkse "Loop met je Dokter" werd een groot maatschappelijk draagvlak gecreëerd voor wetenschappelijk onderzoek naar hart- en vaatziekten. Daarnaast maakte de financiële steun die daaruit voortvloeide de Worm-Studie mogelijk. Ook wil ik graag alle **vrijwilligers** die **Loop met je Dokter** tot een groot succes maakten, uit het diepst van mijn hart bedanken! Jullie gedrevenheid is een dagelijkse inspiratiebron.

De allerbelangrijkste steun die ik heb mogen ontvangen zonder dewelke dit proefschrift nimmer voltooid zou zijn kwam van mijn ouders **Frans ter Bekke** en **Marga ter Bekke-Bosmans** en mijn kinderen **Jade, Myrthe** en **Inez**. Menige zomer- en kerstvakantie werd overheersd door onmogelijke deadlines waardoor de Macbook vaker voor de openhaard werd geopend dan de kerstsok die er hing. Jullie onvoorwaardelijke en liefdevolle steun ontroert mij nog iedere dag. Voor alle chica's is 'Lopen met je Doc(h)ter(s)' een vast familie-uitje geworden... **Myrthe**, jij testte de proefpersonen-informatiefolder als een heuze wetenschapper en was altijd een uitstekende hulp bij de Worm-informatiedagen! Daarnaast leerden jullie mama dat dit niet een boekje is maar een BOEK. Ook wil ik **Merle, Julian** en **Samuel** bedanken voor hun steun, liefde en betrokkenheid. **Esther** en **Brent Vermeulen-ter Bekke** en de **jongens** jullie liefdevolle en nietaflatende steun (als een Zwitsers precisieklokje), zij het op de achtergrond, heb ik immer nabij gevoeld. **Georges Laheij** dank voor

jouw gastvrijheid: jouw deur stond altijd open ook al waren we vaak met velen. Ten slotte ben ik dankbaar voor de geweldige steun van mijn onmisbare 'hulpouders': **Marga ter Bekke-Bosmans, Liny Volders-Willems, Lies** en **John Freeth-Bosmans, Annette Bosmans** en **Maria Patelski-Heunen**. De combinatie van carrière, promotie en (stief)moederschap met 6 kinderen zou nooit zijn gelukt zonder jullie tomeloze inzet om de kinderen op te vangen: dank uit de grond van mijn hart.



CURRICULUM VITAE

Rachel ter Bekke was born on November 5, 1976 in Nijmegen, the Netherlands.

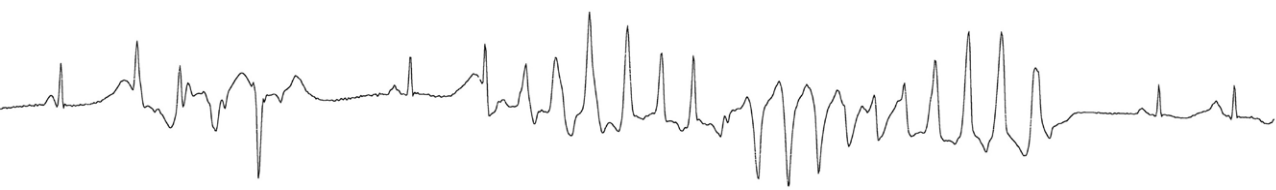
After attending the gymnasium, she moved to Antwerp to study Medicine. It was within this comprehensive but highly-competitive educational program that her scientific basis was formed. Especially the wonders of Physiology, inspiringly explained by prof. dr. Dirk Brutsaert, sparked her interest. Besides her hunger for knowing the deeper reasons of “why”, she enjoyed the acute patient care/interaction and technological challenges that were inherent to Cardiology.



After obtaining her bachelor degree, she obtained the master degree in Medicine (cum laude) in 2002. Although she was appointed as a resident at the Cardiology department at the University of Antwerp, she returned to the Netherlands to apply for a Cardiology residency, which she obtained at the academic hospital Maastricht (currently MUMC+) under the guidance of prof. dr. H.J.G.M. Crijns. During this residency, she found her niche at the clinical experimental cardiac electrophysiology and genetic cardiology, treating cardiogenetic patients and performing invasive cardiac electrophysiologic studies and ablations. In 2011 (her last year as resident), she embarked on this PhD journey, next to her “daytime-job” as clinical invasive electrophysiologist/ cardiologist that resulted in obtaining her PhD degree in 2018.

During her PhD research trajectory, Rachel combined clinical, experimental and collaborative skills to motivate patient populations and international colleagues to join forces with the aim to unravel mechanisms behind inherited arrhythmia syndromes in general, but in long-QT syndrome in particular. She established various international collaborations, spent working visits at the University of Oslo (Norway), the Heart Center in Leipzig (Germany) co-organized the 38th meeting of the European Working Group of Cardiac Cellular Electrophysiology in Maastricht, was a member of the organizing committee of Women in Electrophysiology of the European Heart Rhythm Association and received several awards.

Rachel has found her Walhalla at an old marlstone farmstead in the ‘Heerlijkheid Terblijt’ where she lives with her partner, three beautiful chicas (Jade, Myrthe, and Inez) and her three beloved plus-children (Merle, Samuel, and Julian), not to forget domesticated chickens and not-for-experimental-use guinea pigs. Recently, Vin joined the family. She enjoys running in the hills of Limburg accompanied by biking children, Italian red wine and all sorts of good food.



AWARDS AND CERTIFICATIONS

European Heart Rhythm Association (EHRA) certification exam in cardiac pacing and ICD implantation: ECDS level 2.

EHRA certification exam in clinical electrophysiology: ECES level 2.

Seymour Furman Fund Travel Scholarship, Heart Rhythm Society, 2011, San Francisco, California, United States.

Winner of Case College Session: “Amiodarone-induced torsades de pointes: importance of genotyping the patient”, Europace, 2011, Madrid, Spain.

Travel grant of ESC Working Group on Cardiac Cellular Electrophysiology: “Torsadogenic proclivity in a canine model of drug-induced long-QT1 syndrome: left- versus right-stellate ganglion stimulation”. 37th Meeting of the European Working Group of Cardiac Cellular Electrophysiology, 2013, Athens, Greece.

HRS Young Investigator Award (finalist): “Residual heritability of electromechanical traits in a unique *SCN5A* founder mutation with non-nocturnal ventricular tachyarrhythmia and sudden cardiac death”, Heart Rhythm Society, 2016, San Francisco, California, United States.

Awardee PREDICT Young Talent Program 2018

PUBLICATIONS

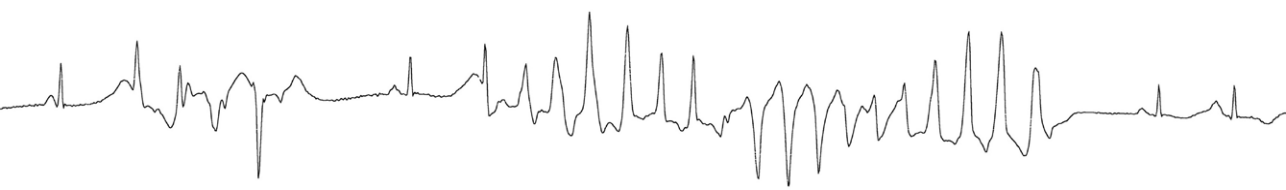
JOURNAL ARTICLES

1. M. Molenaar, C.C. Timmermans, M.F. Scholten, **R.M.A. ter Bekke**, T. Hesselink, J. Luermans, M. Brusse-Keizer, K. Kraaier, B. ten Haken, H.J.G.M. Crijns, J.M. van Opstal. Shorter cryoablation times result in similar acute pulmonary vein isolation but decrease the incidence of phrenic nerve palsy. Results of the 123 study. Submitted 2018.
2. A. Isaacs, A. Barysenka, **R.M.A. ter Bekke**, A.T.J.M. Helderma-van den Enden, J.D.H. Jongbloed, A. van den Wijngaard, P.G.A. Volders, M. Stoll. Standing genetic variation affects phenotypic heterogeneity in a *SCN5A*-mutation founder population. Submitted 2018.
3. **R.M.A. ter Bekke**, A. Isaacs, A. Barysenka, M.B. Hoos, J.D.H. Jongbloed, J.C.A. Hoorntje, A.S.M. Patelski, A.T.J.M. Helderma-van den Enden, A. van den Wijngaard, M. Stoll, P.G.A. Volders. Heritability in a *SCN5A*-mutation founder population with increased female susceptibility to non-nocturnal ventricular tachyarrhythmia and sudden cardiac death. *Heart rhythm* 2017;14:1873-1881.

4. L.G. Klæboe, T.F. Haland, I.S. Leren, **R.M.A. ter Bekke**, P.H. Brekke, H. Røsjø, T. Omland, L. Gullestad, S. Aakhus, K.H. Haugaa, T. Edvardsen. Prognostic value of left ventricular deformation parameters in patients with severe aortic stenosis: a pilot study of usefulness of strain echocardiography. *J Am Soc Echocardiogr* 2017;30:727-735.
5. H.J. Wellens, F.W. Lindemans, R.P. Houben, A.P. Gorgels, P.G.A. Volders, **R.M.A. ter Bekke**, H.J.G.M. Crijns. Improving survival after out-of-hospital cardiac arrest requires new tools. *Eur Heart J* 2016;37:1499-1503.
6. N. Kumar, M.M. Abbas, **R.M.A. ter Bekke**, C.M. de Jong, R. Choudhury, O. Bisht, S. Philippens, C. Timmermans. Maastricht experience with the second generation endoscopic laser balloon ablation system for the atrial fibrillation treatment. *Neth Heart J* 2015;23:383-378.
7. T.E. Verstraelen, **R.M.A. ter Bekke**, P.G.A. Volders, A.A. Masclee, J.W. Kruijmel. The role of *SCN5A*-encoded channelopathy in irritable bowel syndrome and other gastrointestinal disorders. *Neurogastroenterol Motil* 2015;27:906-913.
8. **R.M.A. ter Bekke**, K.H. Haugaa, A. van den Wijngaard, J.M. Bos, M.J. Ackerman, T. Edvardsen, P.G.A. Volders. Electromechanical window negativity in genotyped long-QT syndrome patients: relation to arrhythmia risk. *Eur Heart J* 2015;36:179-186.
9. R. Zusterzeel, **R.M.A. ter Bekke**, P.G.A. Volders, F.M. Leijten, A. van den Wijngaard, J. Serroyen, A.P. Gorgels. Right-ventricular enlargement in arrhythmogenic right-ventricular cardiomyopathy is associated with decreased QRS amplitudes and T-wave negativity. *Ann Noninvasive Electrocardiol* 2013;18:555-563.
10. **R.M.A. ter Bekke**, P.G.A. Volders. Arrhythmogenic mechano-electric heterogeneity in the long-QT syndrome. *Prog Biophys Mol Biol* 2012;110:347-358.
11. L.A. Van Garsse, **R.M.A. ter Bekke**, V.G. van Ommen. Percutaneous transcatheter valve-in-valve implantation in stenosed tricuspid valve bioprosthesis. *Circulation* 2011;123:e219-221.
12. **R.M.A. ter Bekke**, H.J.G.M. Crijns, A.A. Kroon, A.P. Gorgels. Pheochromocytoma-induced ventricular tachycardia and reversible cardiomyopathy. *Int J Cardiol* 2011;147:145-146.

ABSTRACTS

1. C. Altrocchi, R.L.H.M.G. Spätjens, H. Sutanto, **R.M.A. ter Bekke**, S. Seyen, J. Heijman, C. Moreno, P.G.A. Volders. I_{Na} loss-of-function by compound variants in *SCN5A* from a large founder population with excess sudden cardiac death. *Biophysical J* 2018;114:635a.
2. **R.M.A. ter Bekke**, A. Isaacs, A.T.J.M. Helderma-van den Enden, A. van den Wijngaard, M. Stoll, P.G.A. Volders. Residual heritability of electromechanical traits in a unique *SCN5A* founder mutation with non-nocturnal ventricular tachyarrhythmia and sudden cardiac death. *Heart Rhythm Society*, 2016, San Francisco, US.
3. L.G. Klæboe, I.S. Leren, **R.M.A. ter Bekke**, H. Røsjø, T. Omland, L. Gullestad, K.H. Haugaa, T. Edvardsen. Left ventricular mechanical dispersion predicts outcome in conservatively treated patients with severe aortic valve stenosis. *European Society of Cardiology Congress*, Rome, 2016.



4. L.G. Klæboe, T.F. Haland, I.S. Leren, **R.M.A. ter Bekke**, H. Røsjø, T. Omland, K.H. Haugaa, T. Edvardsen. Left ventricular mechanical dispersion predicts clinical outcome in patients with moderate to severe aortic stenosis. *European Society of Cardiology Congress*, London, 2015.
5. **R.M.A. ter Bekke**, A.M.E. Moers, M.M.J. de Jong, M.J.M. Cluitmans, E. Vanoli, P.G.A. Volders. Torsadogenic proclivity in a canine model of drug-induced long-QT1 syndrome: left- versus right-stellate ganglion stimulation. *37th Meeting of the European Working Group on Cardiac Cellular Electrophysiology*, 2013, Athens, Greece.
6. **R.M.A. ter Bekke**, A.M.E. Moers, M.M.J. de Jong, M.J.M. Cluitmans, E. Vanoli, P.G.A. Volders. Left-stellate ganglion stimulation triggers torsades de pointes in a canine model of drug-induced long-QT1 syndrome. *Heart Rhythm* 2013;10:S403-S404. Heart Rhythm Society, 2013.
7. **R.M.A. ter Bekke**, K.H. Haugaa, A. van den Wijngaard, M.J. Ackerman, T. Edvardsen, P.G.A. Volders. Electromechanical window as arrhythmia risk indicator in genotyped long-QT syndrome. *Neth Heart J* 2013;21:14.
8. M. David, **R.M.A. ter Bekke**, S.R.M. Seyen, I.P.C. Krapels, A. van den Wijngaard, R.L.H.M.G. Spätjens, P.G.A. Volders. Augmented window I_{Na} by the novel *SCN5A* mutation L828F: implications for abnormal ventricular impulse formation and treatment. *Heart Rhythm* 2012;9:S8-S9.
9. **R.M.A. ter Bekke**, K.H. Haugaa, A. van den Wijngaard, T. Edvardsen, Volders P.G.A. Electromechanical window: arrhythmogenic marker in genotyped long-QT syndrome. *Heart Rhythm* 2012;9:S86.
10. **R.M.A. ter Bekke**, K.H. Haugaa, A. van den Wijngaard, T. Edvardsen, Volders P.G.A. Electromechanical window is profoundly negative in genotyped long-QT syndrome patients: relation to arrhythmogenic risk. *75th anniversary of Szent-Györgyi's Nobel Prize Award*, March 23, 2012.
11. **R.M.A. ter Bekke**, P.G.A. Volders. Amiodarone-induced torsades de pointes: importance of genotyping the patient. *Europace*, 2011, Madrid.

